UNIVERSITAT POLITÈCNICA DE VALÈNCIA

HYDRAULIC ENGINEERING AND ENVIRONMENT DEPARTMENT

PhD in Water and Environmental Engineering

PhD Thesis

# FLOOD CONTROL IN URBAN AREAS THROUGH THE REHABILITATION OF DRAINAGE NETWORKS

Author:
**Leonardo Bayas Jiménez**

Thesis supervisors:
**F. Javier Martínez Solano**
**Pedro L. Iglesias Rey**

September 2023, Valencia, Spain

# DEDICATION

*"To my mother, with all my love and gratitude."*

*Ecclesiastes 2:24*

# ACKNOWLEDGMENTS

The realization of this thesis would not have been possible without the support of many people, the following lines are dedicated to them. First of all, I want to thank my mother Elena and my sisters Maggie, Judith and Verónica for their dedicated support not only during the preparation of this thesis but also during all these years of study in Europe. I also want to thank my girlfriend Nicole for her support and her accompaniment in this interesting and uncertain journal of research. To you my gratitude and affection.

Next, I want to thank my tutors, Dr. F. Javier Martínez Solano and Dr. Pedro L. Iglesias Rey for their guidance, advice, comments, suggestions, and observations throughout the development of this thesis, without their valuable contribution. it would not have been possible to finish this work.

I must also thank to the Hydraulic Engineering and Environment Department (DIHMA) of the Polytechnic University of Valencia, especially the director of the department, Dr. Amparo López Jiménez, for the cordial welcome and the total availability for the use of the computer equipment and resources of the department during the entire time of the doctorate.

I cannot fail to mention Dr. Daniel Mora Meliá from the Department of Engineering and Construction Management of the University of Talca, for his valuable contribution to the articles presented in chapters 2 and 3 of this thesis.

I also express my sincere gratitude to the Department of Environment, Land and Infrastructure Engineering (DIATI) of the Polytechnic University of Turin where I did my research stay. I want to give special thanks to Dr. Fulvio Boano with whom I had the opportunity to work on the article presented in the chapter 4 of this thesis.

I want to mention the support for the realization of this thesis from the Program Fondecyt through Project No. 1210410 and Project No. 1180660 of the National Agency for Research and Development (ANID) of Chile. From the program PAID 12-21 of the Polytechnic University of Valencia and the program E+/EU Erasmus+ Traineeship.

Last but not least, I want to mention to professors, students, and fellows who I met and shared time in these years of study at both DIHMA and DIATI.

To all these people and those I have failed to mention, thank you.

# ABSTRACT

Currently, most of the world's population lives in cities and this trend is expected to continue, moving more rural population to urban areas every year. This phenomenon is mainly due to the economic development that is generated in the cities. These conditions pose significant challenges for cities in terms of planning and management. If the growth of urbanization is properly managed, it can contribute to sustainable growth, increasing productivity and people's standard of living. However, it cannot be overlooked that the growth of cities implies an impact on the environment. One of the problems that causes the most concern is the expansion of cities that replace the green and agricultural spaces that surround the cities with streets and impermeable structures. This process decreases the capacity of the soil to absorb water in a rain event, increasing runoff and the risk of flooding. If adding to this problem of cities the undeniable climate change that increases the frequency of extreme rainfall events in certain areas of the planet, the adaptation of the infrastructure of cities to make them safer is an urgent need.

Drainage systems are essential infrastructures, designed to capture and transport water produced by precipitation, their proper functioning generates security and wellness for people, while inadequate functioning is associated with risk and vulnerability. Under climate change scenarios, these structures, which were designed for lower flows, do not guarantee the effective evacuation of water, making cities vulnerable to floods that can generate social and economic losses. To mitigate these impacts, different measures have been developed, such as the so-called Best Management Practices or the installation of Low Impact Development etc. However, these measures are not enough to control the peak flow of extreme rainfall. Adapting the existing network to the new climatic conditions is presented as an ideal alternative for flood control in the urban environment. Expanding the capacity of the network by changing the size of the pipes for others with a larger diameter has been the traditional approach that has been used for many years. The inclusion of storm tanks in the system is a measure that was later adopted to provide it with greater resilience to extreme rainfall peaks. Unfortunately, the construction of these structures in the

environment entails great difficulty due to the size of the intervention, the time, and the cost. In this context, the present work presents a novel way of improving drainage networks combining the replacement of pipes, the installation of storm tanks in the drainage network and also includes elements of hydraulic control in the drainage network. With these actions it is considered that the rehabilitation of the network will be more efficient in technical and economic terms. To achieve this, an optimization model created from a modified genetic algorithm connected to the SWMM model through a toolkit is used. The optimization model focuses on minimizing the cost of the required infrastructure and the costs associated with flooding. Posing the problem in this way, an objective function is defined composed of cost functions that will be evaluated to find the best solutions. The development of different steps to obtain an efficient methodology, the strategies to reduce calculation times and computational effort, the economic analysis of floods and the required structures are detailed in each chapter of this thesis.

# RESUMEN

Actualmente, la mayor parte de la población mundial vive en ciudades y se espera que esta tendencia continue, trasladando cada año más población rural hacia las áreas urbanas. Este fenómeno se debe principalmente al desarrollo económico que se genera en las ciudades. Estas condiciones plantean desafíos importantes para las ciudades en cuanto a su planificación y gestión. Si el crecimiento de la urbanización se gestiona adecuadamente puede contribuir al crecimiento sostenible, aumentando la productividad y el nivel de vida de las personas. Sin embargo, no se puede pasar por alto que el crecimiento de las ciudades implica una afectación al medioambiente. Uno de los problemas que más preocupación causa es la expansión de las ciudades que sustituyen los espacios verdes y agrícolas que rodean a las ciudades por calles y estructuras impermeables. Este proceso disminuye la capacidad del suelo para absorber el agua en un evento de lluvia, incrementando la escorrentía y el riesgo de inundaciones. Si a este problema particular de las ciudades, le sumamos el innegable cambio climático que aumenta la frecuencia de eventos de lluvias extremas en ciertas zonas del planeta, la adaptación de la infraestructura de las ciudades para hacerlas más seguras es una necesidad imperiosa.

Los sistemas de drenaje son infraestructuras esenciales, concebidos para captar y transportar el agua producto de las precipitaciones, su buen funcionamiento genera seguridad y bienestar a las personas mientras que un funcionamiento inadecuado se asocia al riesgo y a la vulnerabilidad. Bajo escenarios de cambio climático estas estructuras que fueron diseñadas para caudales menores no garantizan la efectiva evacuación de las aguas, volviendo a las ciudades vulnerables a las inundaciones que pueden generar pérdidas sociales y económicas. Para mitigar estos impactos se han desarrollado diferentes medidas como las denominadas buenas prácticas de manejo o la instalación de sistemas de drenaje con tecnología de bajo impacto, entre otras. Sin embargo, estas medidas no son suficientes para controlar el caudal pico de una lluvia extrema. Adaptar la red existente a las nuevas condiciones climáticas, se presenta como una alternativa idónea para el control de las inundaciones en el entorno urbano. Ampliar la capacidad de la red cambiando el tamaño de las tuberías por otras de

mayor diámetro ha sido el enfoque tradicional que se ha venido usando desde hace muchos años. La inclusión de tanques de tormenta en el sistema es una medida que se adoptó posteriormente para dotarlo de mayor resiliencia a los picos de lluvias extremas. Desafortunadamente la construcción de estas estructuras en el entorno conlleva una gran dificultad por el tamaño de la intervención, el tiempo y el coste. En este contexto, el presente trabajo, presenta una novedosa forma de mejorar las redes de drenaje combinando el cambio de tuberías, la instalación de tanques de tormenta en la red de drenaje e incluye también elementos de control hidráulico en la red de drenaje. Con estas acciones se considera que la rehabilitación de la red será más eficiente en términos técnicos y económicos. Para lograrlo, se usa un modelo de optimización creado a partir de un algoritmo genético modificado conectado al modelo SWMM mediante una toolkit. El modelo de optimización se enfoca en minimizar el coste de la infraestructura requerida y de los costes asociados a las inundaciones. Planteado así el problema, se define una función objetivo compuesta por funciones de coste que será evaluada para encontrar las mejores soluciones. El desarrollo de diferentes pasos para la obtención de una metodología eficiente, las estrategias para reducir los tiempos de cálculo y el esfuerzo computacional, el análisis económico de las inundaciones y las estructuras requeridas se detalla en cada capítulo de esta tesis.

# RESUM

Actualment, la major part de la població mundial viu en ciutats i s'espera que aquesta tendència continue, traslladant cada any més població rural cap a les àrees urbanes. Aquest fenomen es deu principalment al desenvolupament econòmic que es genera a les ciutats. Aquestes condicions plantegen desafiaments importants per a les ciutats quant a la seua planificació i gestió. Si el creixement de la urbanització es gestiona adequadament pot contribuir al creixement sostenible, augmentant la productivitat i el nivell de vida de les persones. No obstant això, no es pot passar per alt que el creixement de les ciutats implica una afectació al medi ambient. Un dels problemes que més preocupació causa és l'expansió de les ciutats que substitueixen els espais verds i agrícoles que envolten a les ciutats per carrers i estructures impermeables. Aquest procés disminueix la capacitat del sòl per a absorbir l'aigua en un esdeveniment de pluja, incrementant l'escolament i el risc d'inundacions. Si a aquest problema particular de les ciutats, li sumem l'innegable canvi climàtic que augmenta la freqüència d'esdeveniments de pluges extremes en unes certes zones del planeta, l'adaptació de la infraestructura de les ciutats per a fer-les més segures és una necessitat imperiosa.

Els sistemes de drenatge són infraestructures essencials, concebuts per a captar i transportar l'aigua producte de les precipitacions, el seu bon funcionament genera seguretat i benestar a les persones mentre que un funcionament inadequat s'associa al risc i a la vulnerabilitat. Sota escenaris de canvi climàtic aquestes estructures que van ser dissenyades per a cabals menors no garanteixen l'efectiva evacuació de les aigües, tornant a les ciutats vulnerables a les inundacions que poden generar pèrdues socials i econòmiques. Per a mitigar aquests impactes s'han desenvolupat diferents mesures com les denominades bones pràctiques de maneig o la instal·lació de sistemes de drenatge amb tecnologia de baix impacte, entre altres. No obstant això, aquestes mesures no són suficients per a controlar el cabal pique d'una pluja extrema. Adaptar la xarxa existent a les noves condicions climàtiques, es presenta com una alternativa idònia per al control de les inundacions en l'entorn urbà. Ampliar la capacitat de la xarxa canviant la grandària de les canonades per altres de major diàmetre ha sigut

l'enfocament tradicional que s'ha vingut usant des de fa molts anys. La inclusió de tancs de tempesta en el sistema és una mesura que es va adoptar posteriorment per a dotar-lo de major resiliència als pics de pluges extremes. Desafortunadament la construcció d'aquestes estructures en l'entorn comporta una gran dificultat per la grandària de la intervenció, el temps i el cost. En aquest context, el present treball, presenta una nova manera de millorar les xarxes de drenatge combinant el canvi de canonades, la instal·lació de tancs de tempesta en la xarxa de drenatge i inclou també elements de control hidràulic en la xarxa de drenatge. Amb aquestes accions es considera que la rehabilitació de la xarxa serà més eficient en termes tècnics i econòmics. Per a aconseguir-ho, s'usa un model d'optimització creat a partir d'un algorisme genètic modificat connectat al model SWMM mitjançant una toolkit. El model d'optimització s'enfoca a minimitzar el cost de la infraestructura requerida i dels costos associats a les inundacions. Plantejat així el problema, es defineix una funció objectiu composta per funcions de cost que serà avaluada per a trobar les millors solucions. El desenvolupament de diferents passos per a l'obtenció d'una metodologia eficient, les estratègies per a reduir els temps de càlcul i l'esforç computacional, l'anàlisi econòmica de les inundacions i les estructures requerides es detalla en cada capítol d'aquesta tesi.

# CONTENT

# CHAPTER 1.

# INTRODUCTION

## 1.1 MOTIVATION OF THE THESIS

The growth of urban areas in the world has accelerated. More than 50% of the world population lives in cities. This trend increases in developing countries where, although growth is lower, the percentage is high (Figure 1.1). These conditions present important challenges for administrators of the cities who detect that the demand for service and infrastructure increases year by year. This demand for services occurs mainly in slums generally built without planning where an overload to the existing infrastructures and their malfunction is generated. In 2018, 23.5% of the urban population lived in slums [1].

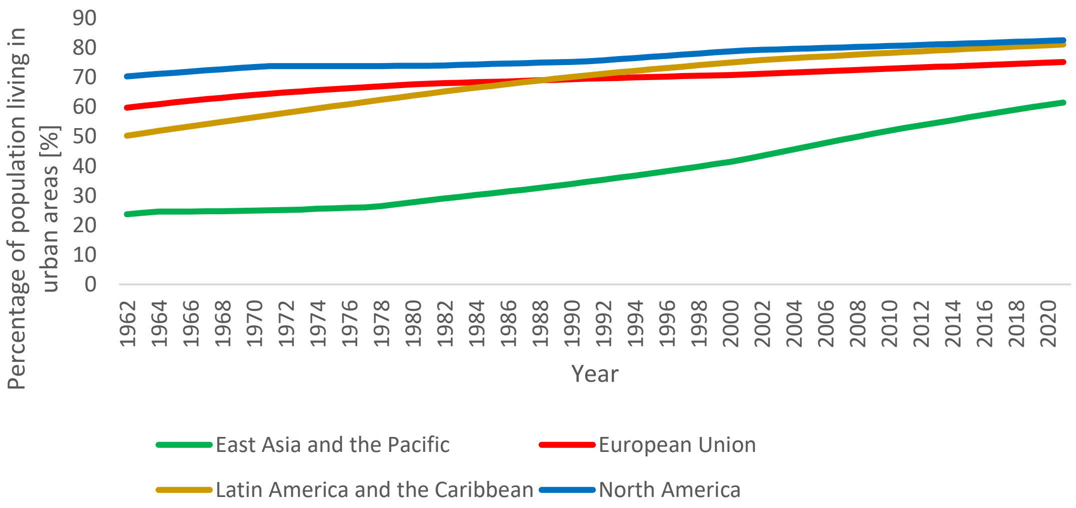


**Figure 1.1.** Percentage of population living in urban areas for region (Data from The World Bank [2])

This growth of cities also reduces the green spaces, increasing the impervious surface, reducing the volume of water that infiltrates and increasing surface runoff. Considering extreme rainfall events have increased in frequency and intensity in different parts of the world, it is undeniable flooding in urban areas will become more common and damage in these densely populated areas will be greater and more dangerous.

The United Nations approved the 2030 agenda for sustainable development in 2015, which includes a series of goals as an opportunity to improve people's lives, combat climate change, and defend the environment. In the Goal 11: Make cities and human settlements inclusive, safe, resilient, and sustainable [3]. On Target 11.1 mentions “By 2030, ensure access for all to adequate, safe and affordable housing and basic services and upgrade slums.” While Target 11.b mentions that “By 2020, substantially increase the number of cities and human settlements adopting and implementing integrated policies and plans towards inclusion, resource efficiency, mitigation and adaptation to climate change, resilience to disasters, and develop and implement, in line with the Sendai Framework for Disaster Risk Reduction 2015-2030, holistic disaster risk management at all levels”. These targets directly imply the management of drainage networks and the need to adapt them to current scenarios offering people safe cities to live. The main motivation of this work is to offer an alternative to achieve flood control in urban environments through the rehabilitation of drainage networks, focused on optimizing available resources. To achieve this purpose, current tools and knowledge are used to propose a robust and reliable methodology for network managers.

## 1.2 GENERAL INTRODUCTION

### 1.2.1 Current problems of drainage systems

Drainage networks are designed to capture and convey surface runoff water, preventing it from accumulating on the surface and causing inconvenience to people in their daily activities. The proper functioning of the drainage network offers the city security and well-being, while a network with problems provokes a feeling of risk and vulnerability to floods [4-6]. Various causes generate the malfunction of the drainage networks, poor planning, the deterioration of the networks over time, poor maintenance of the system, among other problems [7,8]. However, the increase in the intensity of extreme rainfall due mainly to climate change and the waterproofing of the soil due to the growth of cities are considered the most important reasons of this increase [9-11]. The effects of climate change have led to droughts in certain parts of the planet, while in others there is an increase in extreme rainfall. The Intergovernmental Panel on Climate Change in its Sixth Assessment Report reports a global increase in the frequency of extreme rainfall as a result of global warming [12]. Simulations of climate models with future scenarios show that this trend is very likely to continue [13-15].

On the other hand, cities continue to grow unstoppably. The phenomenon of moving rural population to cities continues to increase. Estimates show that this trend will continue, projecting that by 2050 the 60% of the world population will live in urban environments [16,17]. As a result of this population increase the impervious area and pavement rate increase, changing the land use and decreasing the surrounding green areas. Consequently, it generates the increase of runoff and a shorter time of concentration. Thus, there is an increase in flooding events with serious economic and social consequences. Therefore, the problem arises that many networks initially designed in an adequate manner have a lack of capacity and must be rehabilitated.

### 1.2.2 Drainage rehabilitation techniques

There are several different methods to improve the functioning of drainage networks. They can be grouped into two categories:

- Structural measures, which consider designing and constructing infrastructure focused on increasing volume capacity or quality control and are based primarily on rainwater retention or infiltration into the ground.

- Non-structural measures, which include procedures such as modified landscaping practices, pollution prevention, citizen education, street sweeping, management and development practices designed to limit urban runoff.

*1.2.2.1 Traditional rehabilitation techniques*

In this thesis, the structural measure considered is the replacement of pipes with others of greater capacity. It is a traditional method to improve drainage networks. Different methods are used to identify a pipe with problems: Deterioration Point Assignment Schemes; Break even analysis; Regression and failure probability methods; and Mechanistic models [18].

However, the rehabilitation of a drainage system by changing only specific pipes contradicts the methodologies used for the design of the systems. For instance, increasing the diameter of a pipe could imply that downstream the system experiences a narrowing in the diameter of the networks. In this scenario optimization methods are a tool that allows finding solutions to the identified problem. Some methods previously used to optimize drainage networks are: linear programming [19], nonlinear programming [20], dynamic programming [21], metaheuristic approaches [22,23], machine learning techniques [24,25], and, cellular automata [26], among others. These techniques allow giving greater resilience to drainage networks and are a good option that should be considered as a valid and suitable alternative.

However, in current scenarios in which environmental conditions have changed, concerns are focused on the increase of extreme rainfall events that would generate greater surface runoff and aggravate the risk of flooding. It is necessary to consider other types of structures to make drainage systems more robust. Structures such as Storm Tanks (STs), and Low Impact Development (LID) are among the most studied measures to mitigate the effects of increased runoff, not only in terms of flooding that can be generated but also the water quality that can be affected in the first moments of the event [27-29].

*1.2.2.2 Use of storm tanks in rehabilitation*

The use of STs in an urban environment to reduce the risk of flooding has been studied and proven to be one of the most efficient methods to reduce surface runoff [28,30-34]. LID systems, on the contrary, are still mostly at the stage of theoretical analysis and pilot testing, without their extensive use being widely implemented [35-36].

Cimorelli et al. [37] after a literature inspection, deduce the following practical rules regarding the use of STs:

1. The reduction in peak discharge caused by the presence of a ST decreases gradually along the downstream direction. It is not advisable to place tanks too far from the location where the flow attenuation effect is desired.

2. Placing a tank on the downstream side of the network produces no upstream effect.
3. Unwise placement of multiple STs can result in increased peak discharges downstream due to time shifting of the peaks, which may result in their possible overlap.

Some studies delve into the use of algorithmic optimization to find the best location and dimensions of the STs [6,33,38,39]. There have also been works studying the suitability of installing on-line STs instead of traditional STs. Traditional STs receive water that is derived from the drainage system and require pumping systems to evacuate the water after the rain event. The on-line STs base their operation on using the longitudinal slope of the drainage networks for the entry and exit of water from its structure. It is clear then that the objective of these tanks is the momentary detention of water and the control of water peaks in an extreme rainfall event. Studies show the convenience of the use of these tanks to prevent flooding [37,40,41]. The importance of the sizing of the outlet orifice to retain water is another topic that has aroused the interest of researchers [32,42,43].

*1.2.2.3 Modern rehabilitation techniques*

Recent research considers the combined use of STs and pipe replacement [36,38,41,44]. These works show the combination of actions offers very good results. These authors use for their research on-line STs with the objective that water is temporarily stored in the tanks. The authors use evolutionary algorithms and the Storm Water Management Model (SWMM) to perform the hydraulic simulations of the network for the optimization of the drainage networks. In some results, the researchers observe the solutions require a reduction in the diameter of certain pipes, so they conclude that some Hydraulic Control (HC) element should be implemented. The inclusion of HCs in drainage networks has been studied as a way to improve networks especially when considering real-time control techniques [45,46] and to use the drainage network as temporary water storage [47-49].

*1.2.2.4 Green infrastructure*

Green infrastructure is another technique that can be used for flood control, such as LID techniques. LID is a surface element, preferably vegetated and permeable, that is part of the urban-hydrological-landscape structure. They are designed to filter, retain, transport, store, reuse, and infiltrate rainwater into the ground, in order to reduce floods and maintain or even improve the water quality. Among the main types of LID structures are permeable pavements, rain gardens and filtering drains, permeable channels, ecological roofs, vertical gardens, wetlands, etc. LID proves to be an infrastructure that reduces the volume of flooding and, above all, water contamination [27,29]. However, for extreme rainfall events, they cannot be as efficient in containing the flow peak as STs [28].

### 1.2.3 The cost of flood damage

The objectives of the rehabilitation of drainage networks in all the research works are the same: to adapt the drainage network to current conditions in order to achieve optimum performance at minimum cost and to provide greater safety to cities in the face of flood risk. The study of the risks to people, property and infrastructure that a flood would cause should focus on determining the distribution and magnitude of the damage. Studies in this field have divided damage into two groups: intangible damage and tangible damage. Intangible damages are negative impacts whose quantification is subjective and very difficult to quantify [50]. These damages can include mental suffering, environmental degradation, among others. Tangible damages are divided into indirect damages and direct damages. Indirect damages are not caused by the flood directly but by the secondary effects that interrupt economic activities. O'Donnell and Thorne [51] point out that a large proportion of the total economic burden of floods can be attributed to indirect chain effects on goods, services, supply chains and productivity, until the economy fully recovers. Some studies analyze these damages based on the concept of vulnerability and propose alternative ways to estimate them [25,52].

Direct damage, on the other hand, is generally determined using observable data and in economic terms. This type of damage has been analyzed in greater depth by engineers and researchers. To determine these damages, damage-depth curves are generally used to represent the vulnerability of the assets at risk. The parameters used to estimate the damage with these curves are based on statistics and involve high uncertainty [53]. Martínez-Gomariz, et al. [54] express that the actual damage not only depends on water depth but also on other factors such as water velocity, flood duration, time of year, suspended debris, or warning time. So damage-depth approaches carry significant intrinsic uncertainty. Damage-depth curves can be expressed in absolute or relative terms. Absolute curves express damage in economic terms. Relative curves express damage as a percentage of the total value of the property. Depth-damage curves can be classified by the way in which they are obtained as follows: analytical [55,56], empirical [57,58], synthetic [59]; and combined [60,61]. Finally, there are curves determined as a function of land use, type of structures, social stratum, flood duration or warning time.

The damages obtained in economic terms using depth-damage curves are of significant interest in establishing the annual cost to cities. Generally, flood studies focus their attention on large rainfall events produced by high return periods that usually cause substantial damages but may not contribute much to average annual costs due to their low probability [62]. The Expected Annual Damage (EAD) is an index used to measure the annual impact of floods in economic terms. It is determined by integrating the area under the curve of flood damages produced by a series of events with against their corresponding exceedance probabilities of the return periods studied (Figure 1.2).

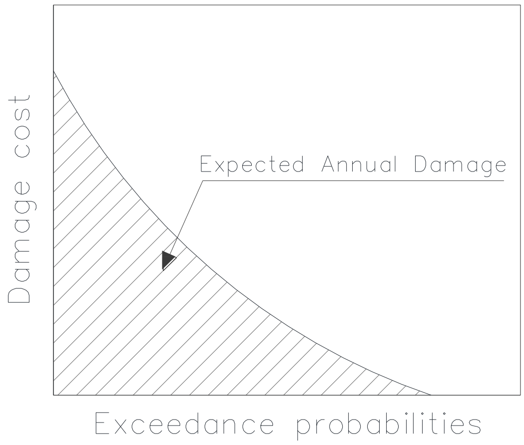


**Figure 1.2** Expected annual damage as area under the curve

Several works on floods have been developed based on the EAD [63-67] and have made this index one of the most widely used to analyze the impact of flood damages in cities. Zhou et. [68] present a framework in which they recommend the use of a log-linear relationship in obtaining the exceedance probability damage curve. This simplification allows to perform few simulations and to extrapolate the damage cost for intermediate return periods. The use of logarithmic-linear models is frequently used in hydrology, which suggests that this approximation is quite reasonable.

Olsen et al [62] conducted a work comparing three ways of calculating the EAD and concluded that there is no substantial difference between the methodologies analyzed. However, they point out that in urban watersheds special attention should be paid to land use in the vulnerability assessment since there may be significant differences in the results. This recommendation is also made by other authors [69,70].

### 1.2.4 Computational advances applied to the rehabilitation of drainage networks

A common feature of all the exhibited works is they are based on optimization techniques and mathematical models. Computational development has given a great boost to research in urban drainage. Computational hydraulic models are used as virtual laboratories to mimic the real sewer network, where scenarios and alternatives can be evaluated to make the better decisions [7].

The extraordinary power of current computer equipment had allowed the consolidation of sophisticated tools for modeling and simulating the hydrological cycle, its transport and final discharge. Simulation results using mathematical models are widely used for planning, design, rehabilitation, and exploitation purposes. A mathematical model of rainwater is composed of three main processes: hydrological modeling, hydraulic modeling, and water quality modeling. Among the best known mathematical models used in urban drainage research the following are available: EPA SWMM 5 [71], SOBEK URBAN [72], MOUSE [73], Infoworks CS [74], ResUrSim [75]. These models are based on the formulation and resolution of the complete Saint-Venant equations.

### 1.2.5 Optimization in the rehabilitation of drainage networks

The mathematical modeling of drainage networks is a powerful tool for network rehabilitation and flood prevention. However, it is joint work with optimization algorithms that has facilitated significant progress in this field of research.

Metaheuristics is a powerful tool used for optimization in the field of water resources for different applications such as design, calibration, rehabilitation, operation, planning, among others. Evolutionary algorithms are the most widely used [76]. These algorithms use various mechanisms of biological evolution for their operation (reproduction, selection, mutation, crossover). The most used algorithms are the Genetic Algorithms (GA) [77-80], Shuffled frog leaping algorithm (SFLA) [81-84], Simulated annealing [85,86], Ant colony [84, 87], and Particle Swarm Optimization (PSO) [88,89].

#### 1.2.6 Use of Genetic Algorithms in rehabilitation of drainage networks

GAs have been gaining popularity in different fields mainly because they have proven to be very robust and do not require the continuity of the objective function. Afshar [90] concludes GAs can be more efficient than other methods to solve large-scale problems. In a work carried out by Mora-Melia [91] different evolutionary algorithms are compared. The author points out that GAs and SFLA are the most powerful techniques to find the minimum solution in complex problems. However, GAs may have an advantage over the other algorithms because they have two tuning parameters while SFLA has five parameters, which makes it easier to implement. They also warns that all these techniques entail a high computational cost.

### 1.2.7 Search Space Reduction

These algorithms search for the solution in a Search Space (SS) formed by the Decision Variables (DVs) and the precision of the values they can take. Computational advances have made it possible to find solutions closer to the optimum. However, the computational effort and time can be considerably large due to the large SS to be explored if the accuracy or refinement of the search is high. Conversely, if the refinement of the search is decreased, the founded solution may be far from the optimal one. Refining the search for the solution can exponentially increase the size of the SS [92]. For these reasons, establishing a method to improve and reduce the SS is a topic of much interest. Research on this topic has determined two groups of techniques to Search Space Reduction (SSR). A first group of techniques are focused on specifically modifying the space to be explored, reducing the search to the prominent areas of containing the best solutions [44,78, 93,94]. Another group of techniques are focused on modifying the algorithm performance by incorporating some heuristics [95-99].

### 1.2.8 Stop criterion

Due to the iterative nature of these techniques, it is important to establish a point where the algorithms terminate the search process. Evolutionary techniques do not have a defined stopping point as do other techniques such as linear programming. So an approximate stopping criterion must be defined. This stopping criterion must guarantee the algorithm does not stop prematurely delivering unsatisfactory solutions, but also it does not generate excessive and unnecessary work. The most frequently used stopping criterion is the one that stops the process after a defined number of generations. While recent approaches prefer a stopping criterion that terminates the process after not finding a significant improvement in the quality of the solutions found.

However, in a study made by Zielinski et al. [100] the authors define six stopping criteria:

1. Reference criteria: the process stops when a set percentage of the population converges.
2. Exhaustion-based criteria: The process stops when a predefined number of generations is reached.
3. Improvement-based criteria: The process stops when no significant improvement is found after a certain number of evaluations.
4. Movement-based criteria: The process stops when the changes in the population with respect to the average value of the solutions found are below a previously defined limit value.
5. Distribution-based criteria: The process stops when the distance of each vector to the best population vector is less than a previously defined limit value.
6. Combined criteria: The process stops when a criterion product of the combinations of the above-mentioned criteria is reached.

Maier et al. [92] mentions that no particular criterion would have an advantage over another for a given problem, so testing different options remains a necessity for researchers.

## 1.3 OBJECTIVES

### 1.3.1 General Objective

The general objective of this thesis is to propose a methodology for flood control in urban areas through the rehabilitation of drainage networks with the inclusion of different structures in the drainage network. To achieve this rehabilitation, the use of an optimization model is considered. This model allows to identify the best solutions for the proposed problem by evaluating an objective function through a Pseudo-Genetic Algorithm (PGA). The objective function is established in economic values through the evaluation of the cost of the installed infrastructure and the cost of the damage caused by floods.

### 1.3.2. Specific Objectives

To achieve the general objective described above, the following specific objectives are established:

- To define an optimization model that considers as rehabilitation actions: the replacement of pipes increasing the water transport capacity, the construction of on-line STs for the temporary storage of water and the inclusion of some element that generates head losses in order to down the flow of water. The utilization of smaller STs in proximity to areas experiencing flooding issues will be prioritized over the option of installing a few larger STs. This approach aligns with the recommendations provided by Cimorelli et al. [37].
- To establish an objective function This function composed of the costs of the infrastructure required to improve the network and the cost of the damage caused by floods.
- To study the impact of including head losses by including HCs in the network to reduce flooding.
- To establish a stop criterion or convergence criterion that improves the efficiency of the search process for the solution closest to the global optimum.
- To propose different SSR methods to improve the efficiency of the optimization process, reducing computational effort and calculation times.
- To analyze the cost of the damage caused by the floods considering the different land uses of the studied area to have a more exact value of the costs and propitiating a better optimization of the network.
- To propose a new optimization approach that allows analyzing the cost of annual flood damage and the annual investment cost of the infrastructure proposed to improve the network.

## 1.4 GENERAL APPROACH

### 1.4.1 Background

The starting point for this work is the research carried out by Ngamalieu-Nengoue et al. [38,41,44]. They propose a way of rehabilitating drainage networks using modern rehabilitation techniques and considering the replacement of pipes and the installation of on-line STs. These types of techniques are presented in section 1.2.2.3 of this thesis. The authors use PGA and Sorting Genetic Algorithm (NSGA-II) to optimize the network and the SWMM model to perform the hydraulic analysis. To find the solutions, an objective function established in economic terms is evaluated to relate the damage costs to the actions to be taken to reduce them.

The researchers also present a process of reduction of the SS. The results obtained are relevant in acceptable computation times. One of the observations made to this work is that in certain results the optimized pipes have smaller diameters than the original ones. Thus it is deduced that introducing head losses in certain pipes of the network allows to improve its operation when they work together with on-line STs. These head losses can be generated by a HC element that allows to reduce the water outflow.

The study of HC elements (valves, orifices, etc.) is presented as an interesting alternative to control floods. But its joint work with pipe replacement and tank installation is a new alternative that could give good results. As mentioned, the work also focuses on reducing of the SS through a process of eliminating DVs by identifying the nodes where STs should be installed. In a second part of the process, identifying the pipes to be replaced. This is an important contribution of his work that is intended to be deepened and expanded in this thesis.

In addition, in their work, the researchers use an average damage-depth curve for the entire area analyzed to determine the cost of flood damage. However, this approach does not discriminate the level of protection required for certain strategic or vulnerable areas from others. Therefore, this approach should be critically analyzed in order to propose alternatives. Having thus introduced the starting scenario, the present work pretends to provide a new rehabilitation methodology based on the research previously carried out and increase its performance.

### 1.4.2 Calculation alternatives

To achieve the objectives set out in this thesis, a rehabilitation methodology will be developed considering the inclusion of HCs in addition to the replacement of pipes and the installation of STs. From this initial approach, an optimization model will be developed to find the best solutions. The PGA is chosen as the search engine, whose benefits are mentioned in the introduction. The SWMM model is used for the hydraulic analysis. The optimization model will evaluate an objective function composed of two types of terms. A first term made up of the costs of the infrastructure needed to upgrade the network (pipes, tanks, and HCs) and a second term made up of the cost of flood damages. The optimization model will try to find the best solution to the problem by minimizing this function.

It should be mentioned that when working with a discrete coding PGA it is necessary to study the discretization to be used, the discretization should be done in such a way that it covers all the options that each DVs can adopt, without falling into an excessive refinement that generates a very large SS that generates unnecessary computational efforts. In this regard, one of the factors to consider is that when including in the analysis the possibility of installing HCs, the number of DVs increases significantly, which may affect the calculation times. Due to this condition, implementing a process that reduces the SS is a priority task in this work. The study will focus on the reduction of the SS by adopting different procedures to identify the best search region thus reducing the computational effort required, it is very important to note that the measures adopted are directly related to the size of the networks so different procedures should be adopted according to the analyzed network. At this point it should be noted that although there are strategies to reduce the SS by modifying the search algorithm, this work does not consider this option.

Besides, a fundamental part of this study is the analysis of the flood damage cost. The ways to determine this cost are mentioned in section 1.2.3 of this work. A prominent alternative is the use of damage-depth curves. These curves can be related to the land uses of the basin analyzed, allowing measures to be taken according to the importance and needs of each urban area.

### 1.4.3 Challenges

This research presents different challenges that will be addressed in the following chapters. The main and most worrying one is the computational time required by the model to find good solutions. It should be considered that the SS depends fundamentally on two factors, the network elements analyzed (nodes and pipes) and the discretization used. In the pipes, two actions are considered, the change of the pipes and the installation of HCs. This makes it clear the study of the SS is essential to reduce computation times. In this sense the actions to reduce the SS can be two. First, to reduce the number of options that each DVs can adopt through a study of the discretization and to reduce the DVs by identifying the most prominent. In this sense, it must be clear that the objective of reducing computation times does not imply a loss of quality in the results obtained, so the study must be sufficiently deep to ensure a balance between the required computation times and the solutions found. Related to this issue, improving the efficiency of the process is another challenge of this work, the computation time should be used in an appropriate way, allocating an important time to reduce the SS but also to the search for the best solutions in the optimal region. Therefore, setting a correct limit of the computational time will be an important aspect of study in this thesis.

Finally, another important challenge in this thesis is to complete certain research lines opened in previous works. In this sense, an important challenge in this thesis is to present a new way of evaluating the costs of rehabilitation. Analyzing the cost of the damage that can be caused by the most unfavorable extreme rainfall event versus the cost of the whole infrastructure can be a good alternative of evaluation. However, this analysis does not consider other rainfall events that will occur during the system design period that are not accounted for when evaluating the objective function. Thus, the challenge in this aspect will be to present a new way of quantifying the damage that overcomes these drawbacks, giving greater accuracy to the results. This new approach could increase computation times, so the relevance of the SSR process once again becomes relevant.

### 1.4.4 Initial Assumptions and limitations

This work uses the SWMM model to carry out the simulations of the studied networks and a PGA algorithm as a search engine. Defined the optimization model in this way, certain premises must be considered:

1. This work does not contemplate the hydrological study of the analyzed area. The available IDF curves are used to obtain the rainfall events used for the hydraulic study of the network. In the same way, the study of runoff, its characteristics, and parameters, exceed the objectives of this work.
2. Rain is considered spatially static for the entire network. There are works that show that for the analysis in small basins typical of urban areas, flash floods are used [101,102]. Flash floods are defined in the work carried out by R. Merz & Blöschl [103].
3. In this doctoral thesis, the SWMM 1D model developed for urban areas is used, which completely solves the Saint-Venant equations. For the execution of the simulations, the Dynamic Wave model is used, which better represents the pressure flow and the floods. The main force equation used is Darcy-Weisbach.
4. It is assumed that flooding occurs due to water stagnation and that 100% of the runoff enters the manholes through the system's gutters.
5. In this work the mathematical model of the network is not questioned. It is assumed that the networks to be rehabilitated were initially well designed and it is considered as starting data.
6. To develop the optimization models, a PGA is used. The algorithm parameters used Population, Crossing and Mutation are those that have traditionally been used in this type of work [104].
7. This work for flood control in urban areas develops some methodologies to rehabilitate drainage networks. The contemplated interventions in the networks that are the following: Replacement of pipes, Installation of STs and inclusion of HCs in the pipes of the network. In this way, the nodes and pipes of the analyzed drainage network are defined as DVs.
8. The used STs have the following features: online configuration; single chamber without outlet control device; depth equal to that of existing manholes.
9. The objective function or fitness evaluated to find the best solutions to the problem s and set in economic terms. Having to establish cost functions for each action analyzing the hydraulic variables of the problem.

Finally, this work has certain limitations that should be considered:

1. This work is focused on gravity feed drainage networks. Drainage networks with pumping systems are outside the objectives of this work.

2. To establish the cost functions, the average excavation depths for both pipes and STs is considered.
3. This work does not contemplate changes in the topology of the network.
4. For the study of the SSR this work focuses on the analysis of the search region. Changes in the algorithm are not considered.

## 1.5 STRUCTURE OF THE THESIS

This thesis is structured according to the current normative for obtaining the title of PhD at the Universitat Politècnica de València by compendium of scientific articles. In order to achieve the planned objectives, different chapters have been developed in which the topics proposed in this thesis are studied in depth. Chapters 2 – 4 correspond to three scientific articles (each of these articles presents different case studies analyzed with the proposed methodology) these chapters include the literal text of the published articles. However, changes have been made in the numbering of figures, tables, equations, and citations to adapt them to a single order within this thesis.

In short, the chapters developed are the following:

- Chapter 1: Introduction. This chapter describes the motivation behind this thesis. Next, a general introduction to the subject is made through a review of the main contributions in the field of study. The general objective and the specific objectives of this thesis are also established. After this, the general approach of this thesis is exposed. Further on, the hypotheses used, and the scope of this work are established. Finally, the structure of this thesis is shown.
- Chapter 2: Inclusion of Hydraulic Controls in Rehabilitation Models of Drainage Networks to Control Floods. This chapter shows a new way to improve drainage systems with minimal investment costs, using for this purpose a novel methodology that considers the inclusion of HCs in the network, the installation of STs and the replacement of pipes. The presented methodology uses the SWMM model for the hydraulic analysis of the network and a PGA to optimize the network. This work evaluates the cost of the required infrastructure and the damage caused by floods to find the optimal solution. The main conclusion of this study is that the inclusion of HCs can reduce the cost of network rehabilitation and decrease flood levels.
- Chapter 3: Search Space Reduction for Genetic Algorithms Applied to Drainage Network Optimization Problems. This work presents a method of SSR applied to the rehabilitation of drainage networks. The method is based on reducing the initially large SS to a smaller one that contains the optimal solution. Through iterative processes, the SSis gradually reduced to define the final region. The rehabilitation methodology contemplates the optimization of networks using the joint work of the installation of STs, replacement of pipes, and implementation of HCs.

Optimization problems consider a large number of DVs and could require a huge computational effort. For this reason, this work focuses on identifying the most promising region of the SS to contain the optimal solution and to improve the efficiency of the process. Finally, this method is applied in real networks to show its validity.

- Chapter 4: Economic Analysis of Flood Risk Applied to the Rehabilitation of Drainage Networks. This chapter focuses on evaluating the flood risk in economic terms. To achieve this, the EAD from floods and the annual investments in infrastructure to control floods are estimated. These two terms are used to form an objective function to be minimized. To evaluate this objective function, an optimization model is presented that incorporates a GA to find the best solutions to the problem; the hydraulic analysis of the network is performed with the SWMM model. This work also presents a strategy to reduce computation times by reducing the SS focused mainly on large networks. This is intended to show a complete and robust methodology that can be used by managers and administrators of drainage networks in cities.
- Chapter 5: General Discussion. This chapter presents a general discussion of the results achieved in Chapters 2 - 4. The discussion focuses on two main aspects, the results obtained in the rehabilitation of drainage networks itself and the results obtained in improving the efficiency of the optimization process.
- Chapter 6: Conclusions. This chapter presents the general conclusions of this work. It also presents the main contributions of this thesis to the study field and the future lines of research resulting from this work. Finally, the publications derived from this research are shown.
- Chapter 7: References.

Appendix. This section contains the following appendices. Appendix I. Notation. Appendix II. Abbreviations. Appendix III. Network data. The data correspond to the networks used as case studies presented in previous chapters. E-Chico network, Ayurá network, Balloon network and ES-N network.

# CHAPTER 2.

# INCLUSION OF HYDRAULIC CONTROLS IN REHABILITATION MODELS OF DRAINAGE NETWORKS TO CONTROL FLOODS

# Preamble

The article presented in this chapter analyzes the advantages of including HCs in the drainage network rehabilitation process. This novel methodology arises from the need to introduce head losses in certain pipes of the rehabilitated drainage networks that have been observed in previous works.

With the study carried out in this chapter, the following objectives are intended to be covered as starting points of this thesis. First, the study of the impact that head losses generated by HCs can have on the system and to analyze the possible advantages of using these elements in conjunction with the installation of on-line STs and the replacement of pipes with other of larger diameters. Second, the development of an optimization model that considers the three actions described in the rehabilitation of networks using a PGA to find the best solutions. Third, establish an objective function in economic terms that considers infrastructure costs and the cost of flood damage that should be minimized by the developed optimization model. Finally, the work carried out proposes a new stopping criterion for the optimization process to improve its efficiency. The purpose of the criterion is to set the number of iterations of the optimization model developed based on the characteristics of the algorithm used.

In this way, this work begins an investigation that aims to provide a methodology for urban flood control using current developments to find solutions at a relatively low cost.

*This article was published as: Bayas-Jiménez, L.; Martínez-Solano, F.J.; Iglesias-Rey, P.L.; Mora-Melia, D.; Fuertes-Miquel, V.S. Inclusion of Hydraulic Controls in Rehabilitation Models of Drainage Networks to Control Floods. Water 2021, 13, 514. Available in open access at: https://doi.org/10.3390/w13040514*

## 2.1 INTRODUCTION

Discussions have been generated about the pressure that climate change can generate on water supply and drainage systems. Recent research has shown that climate change is a preponderant factor and affects the future availability of water resources [105]. Additionally, other studies show that due to anthropogenic climate change, the climate cannot be considered unchanging and presents spatially heterogeneous trends in both mean behavior and variability. [106] This shows that the increase in extreme rains in certain parts of the world is evident, and there is a need to take measures [107]. Floods in urban areas are mainly due to the increase in the impervious surface and the increase in the intensity of extreme rains [108–111]. This increase and the impervious surface due to the urban growth of cities reduces the time of concentration of the water and produces a rapid accumulation of water on the surface that drainage network systems cannot evacuate. All these effects have a consequence: the appearance of increasingly frequent and intense floods.

Floods in urban areas are one of the problems of greatest concern. The damage associated with this type of disaster is expected to increase in the future [112,113]. Although rain floods generate less economic losses than river floods, they are much more frequent, so their accumulated cost could be higher in one year than another [114].

There are different methods or technologies that can be applied to face the consequences of excess runoff in urban areas. A proven measure to control urban runoff is the installation of infrastructure that allows water to be temporarily retained and stored during rain events. One of the best structures to achieve this goal is STs. In this field, one of the first works was developed by Howard [115], who presented a theoretical method to evaluate the storage efficiency of a retention tank in combination with a treatment plant using probabilistic methods based on precipitation data. More recently, Butler et al. [116] studied the effect of climate change on ST performance. They relied on Intergovernmental Panel on Climate Change (IPCC) medium-high emission scenarios for the city of London. The results of their work indicate that significantly larger storage volumes are required to maintain the same level of flood protection. One of the most prominent studies on this topic was conducted by Andrés-Doménech et al. [28], who studied the ability of STs to regain their efficiency. With this objective, they presented a probabilistic analytical model to assess the volumetric efficiency of STs according to the new climatic scenarios and urban catchment.

Later, Wang et al. [33] presented a method of optimizing the location of STs in two modules trying to reduce flooding, cost of tanks and available total solids load. The first module evaluates and classifies flood nodes with the Analytical Hierarchy Process (AHP) [117] using two indicators: flood depth and flood duration. The second is an iterative module that provides the optimal scheme for the location of the tanks through the method of searching for generalized patterns. In addition, Cunha et al. [32] presented an optimization method based on a previous disposition of STs to size them and the outflow orifice. They concluded the importance of a good dimensioning of the orifice since it reduces the output flow of the storage unit that regulates the descending flows, allowing flow control and a reduction of floods in the whole network.

Better results are obtained by the combination of STs and the replacement of pipes with others with higher diameters. Saldarriaga et al. [118] applied two different approaches to determine the optimal location and size of the storage units through the application of Simulated Annealing and GAs. This research validated the use of STs for peak flow reduction in urban areas. It also showed the advantages of considering the replacement of certain pipes and the installation of STs instead of replacing the whole pipe infrastructure. Iglesias et al. [36] presented a methodology to improve stormwater systems using an optimization model that incorporates a PGA [104]. The model includes as DVs the replacement of pipes, the location and sizing of STs and the initial state, and start and stop levels in the case of systems with pumping stations. The study demonstrated the economic benefits of the joint installation of STs and the replacement of pipes with others of greater capacity. Following this line of research, Ngamalieu-Nengoue et al. [44] present a methodology that uses the aforementioned postulates seeking rehabilitation of drainage networks and shortens the calculation time through a process of SSR. Their methodology is divided into two parts. The first one uses a PGA and aims to reduce the SS for solutions. The second one optimizes the multiple objectives of the new scenario generated in the first part using a NSGA-II. Continuing with his research, Ngamalieu-Nengoue et al. [38] present in their work a way to calculate the flood level using the ponded area of the SWMM model [71]. The optimization model assumes the definition of this area in each node to convert flood volume into flood level. The method developed by Ngamalieu-Nengoue et al. [38] considers reducing the diameter of certain pipes and concludes that it is necessary to include resistance elements that generate a head loss equivalent to that which would be caused by the installation of smaller diameters.

The use of HCs in drainage networks is considered by different authors as a tool to limit the flow of water in drainage networks, promoting their retention and storage within the network. An outstanding study is the one prepared by Dziopak [49], who proposed, as an alternative to ST, using the sewerage network as a temporary water storage unit. To achieve this goal, this author designed a retention channel with interior partitions in the form of cameras with an opening at the bottom of the channel acting as an orifice. In this way, the conduit becomes a retention channel.

On the other hand, Leitão et al. [47] presented a model that includes an algorithm for the location of flow limiters in the drainage network with the objective of maximizing storage within the network. They reach two conclusions. The first was that the storage capacity in the networks can be very large. The second was that if the local flow control devices are installed correctly, it can become an interesting solution to mitigate floods. This model also considers the potential impact of the failure of the flow control device. In parallel, Słyś [48] proposed a type of channel to retain runoff within the network. To achieve this, the channel is segmented into compartments. These compartments have two outlets; a hole at the bottom for the passage of wastewater and an opening at the top to allow rainwater to overflow into the next compartment. Later, Ngamalieu-Nengoue et al. [41] obtained optimized diameters smaller than the original in certain pipes as a result of their study in which they use an NSGA-II. These results emphasize the need to include HCs to introduce a head loss in the system. These investigations suggest that HCs can be used as a technique to improve the efficiency of the system by allowing the accumulation of water at certain points in the network. HCs slow down the flow of the water, reducing the time of concentration and therefore the probability of flooding. However, none of the previous authors has considered performing joint optimization of STs and HCs.

For this reason, this methodology proposes including the use of HC in the optimization of drainage networks. In this work, two classes of cost functions have been defined, one associated with the investment cost to improve the network (installation of tanks, replacement of pipes and HCs) and the other related to the cost of the damage that flooding can cause. To find the optimal solution, the model uses a PGA connected to the SWMM hydraulic simulation model through a Toolkit [119]. For this reason, the objective of this work is to include additional energy losses to help retain water in the network, decrease the levels of flooding in the networks and minimize the size of the necessary protection structures.

## 2.2. FORMULATION OF THE PROBLEM

### 2.2.1. Initial Assumptions

The methodology consists of performing the hydraulic analysis of the network using the SWMM model and with the help of a PGA to find the best solutions to adapt the system to extreme rain events. The possibilities to improve the performance of the network are changing pipe diameters, installing STs and including devices for HC of flow. Presented in this way, the following hypotheses are considered:

A spatially static design storm is considered for the entire network. This design storm contemplates the most unfavorable operating scenario. The hydrologic study and the runoff model are beyond the scope of this work. Usually, for design or assessment purposes in small, urban areas, flash floods are used as defined by Merz and Blöschl [103].

The SWMM is used as a network analysis tool. Dynamic wave model was used because it is the model that best represents both the pressurized flow and floods.

The mathematical model of the network must be calibrated and simplified as much as possible without losing accuracy in the results.

The actions considered are the renovation of pipes with others of greater diameter, the installation of STs and the installation of HCs. Changes in the topology of the network are not included in this work.

STs are considered installed on-line, and their depth is the same as that of the existing manhole. Therefore, the cost of STs is proportional to the depth, and the area of STs is defined as a DV.

The optimization problem is analyzed in terms of costs [38]. The objective function must be established based on the hydraulic variables and includes the cost of renovating pipes, the cost of installing STs, the cost of HCs and the damage costs caused by floods.

### 2.2.2. Hydraulic Control

A HC element is a device that allows the control of flow in the network. In this work, the HCs are installed in the pipes that come out of the STs (Figure 2.1). The purpose of including this device is to generate a local loss to slow down the flow of water, inducing it to accumulate upstream and using the network as temporary storage. This alternative is presented as a novel option that can contribute to improving the levels of flooding of the networks and minimizing the size of the necessary protection infrastructure.

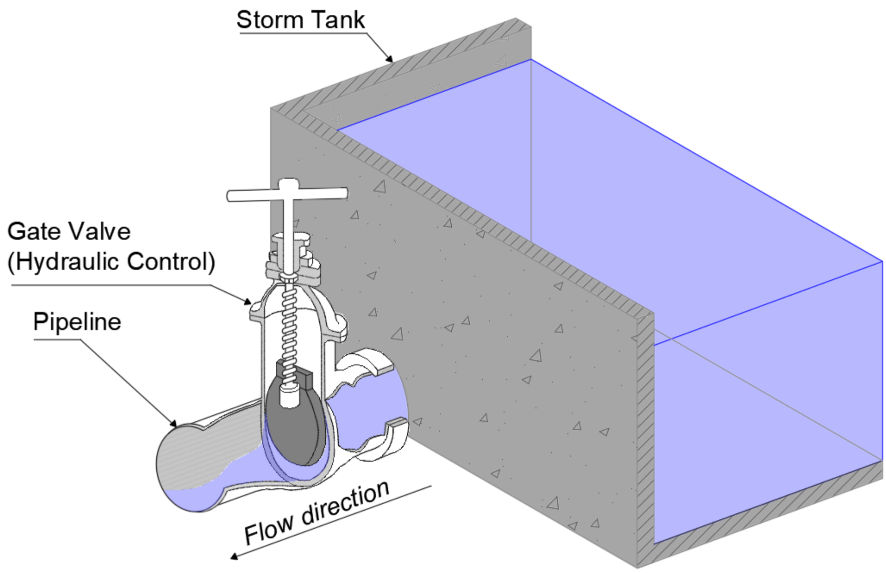


**Figure 2.1.** Gate valve installed as a HC.

In the results obtained in the study carried out by Ngamalieu-Nengoue et al. [38], the reduction of the diameter is observed in certain pipes leaving ST. These smaller diameters act as HC in the system. It would then be thought that the inclusion of a local head loss in the initial part of the pipe that leaves the ST produces similar results to those obtained by these researchers. This statement needed to be proven.

To find the best option for including the HCs, the network used by Ngamalieu-Nengoue et al. [38] was used. In the final solution presented by these authors, it was observed that two pipes of the solution (named as P04 and P10) had smaller diameters than the original ones. Reducing diameters during a rehabilitation program in a sewage network seemed unrealistic. An alternative solution consisted of the use of some type of HC of flow in these pipes. To verify that similar results could be obtained, the network was considered with the optimized solution proposed by the authors but keeping the original diameters of pipes P04 and P10. In these pipes, a HC based on including local head losses was used. This local loss was modeled by installing a valve or a gate in the initial part of the pipes that came out of the ST. The area of the through-hole is variable, allowing setting the opening according to the demands of the system. To represent the head loss generated by the control element, an expression to calculate the coefficient of losses in valves was needed. In this work, the expression defined by Tullis [120] was used (Equation (2.1)):

$$k = \frac{2g\Delta H}{V^2} \tag{2.1}$$

where, g is the acceleration of the gravity, ΔH is the loss of energy in the gate and V is the average flow velocity through the gate. The values of the coefficient k as a function of valve travel are shown in Figure 2.2.

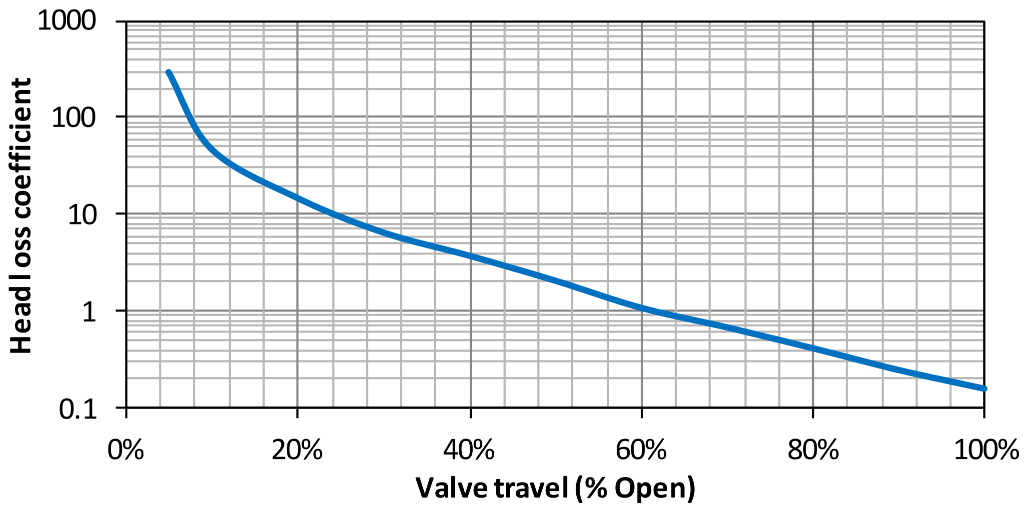


**Figure 2.2.** Head loss coefficient as a function of valve travel.

The head loss coefficient represented in Figure 2.2 can be mathematically adjusted to the following Equation (2.2):

$$k = C_1\theta^{C_2} \tag{2.2}$$

where $C_1$ and $C_2$ represent the adjustment coefficients and θ is the valve opening percentage. For this work, the value used of coefficient $C_1$ was 0.2736 and the value for the exponent $C_2$ was −2.395.

The local head loss defined in Equation (2.1) was calculated based on the flow that the pipes with the smaller diameter would transport. Once these local head losses were obtained, they were included in pipes P04 and P10. Under these conditions, a hydraulic analysis of the network was performed in the SWMM model, obtaining the flow rates in these pipes for the entire simulation period. Figure 2.3 compares the flow rates of the pipes P04 and

P10 in the solution presented by Ngamalieu-Nengoue et al. [38] to the flow rates that were obtained including a local head loss in the pipes.

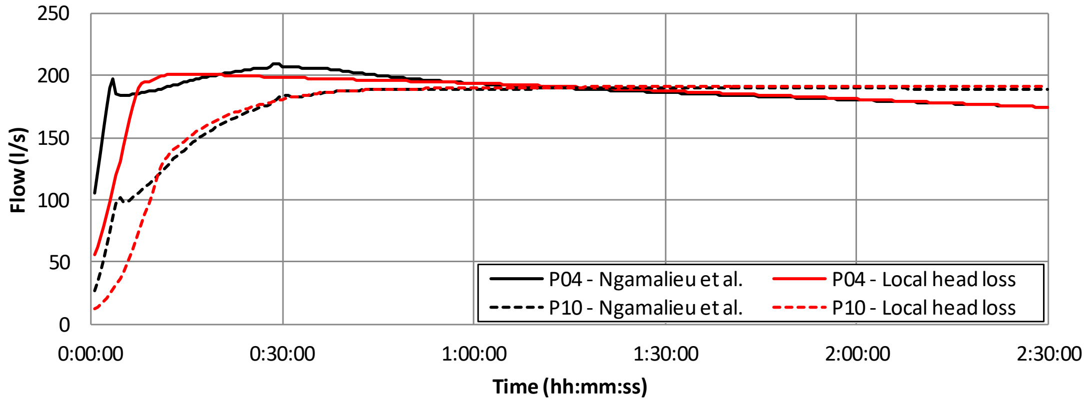


**Figure 2.3.** Evolution over time of the flow in pipes P04 and P10.

The results indicated that both alternatives (a pipe with a reduced diameter and a local head loss) could be used as HC in a network. It is interesting to analyze the use of a local loss since it would be much easier to implement than a pipe change and economically more advantageous. In the work presented in this paper, a modification of the SWMM connection Toolkit was done to allow the modification of the local head loss coefficient within any pipe.

### 2.2.3. Decision Variables

In this investigation, the drainage network optimization problem considers three types of DVs. The first type is the diameter of the pipes; the optimization model searches for the best combination of network diameters to minimize flooding. This DV can range from a value of 0 (the pipe is not replaced) to a maximum established value. The value 0 implies that the capacity of the pipe is enough to carry the analyzed flow, while a different value indicates the need to increase the capacity of the pipe. It is necessary to define the following parameters for the analysis of this DV: $N_C$ represents the number of pipes in the network, and $m_s$ is the number of pipes selected for replacement and can vary from 0 to $N_C$. Each pipe candidate to be replaced can adopt a diameter of a defined range. Therefore, ND is defined as the range of available diameters, and this range can have a reduced number of diameters $ND_0$ or a full range $ND_{max}$.

The second type of DV considered by the optimization model is the storage capacity of the nodes. The optimization model searches for the best location of the STs in the network and their lowest volume to reduce flooding. When considering the problem in an urban environment, the excavation is limited to the current depth of the manholes, defining the cross-section of the ST as a DV. DVs related to STs can take values from 0 (ST is not required in the node) to a previously defined maximum value based on the available space. The model defines the following parameters to analyze this DV: $N_N$ is the number of nodes in the network; $n_s$ is the number of nodes where ST will be installed and whose value can vary from 0 to $N_N$. SWMM defines the cross-section of an ST using Equation (2.3):

$$S = A_S\, y^{B_S} + C_S \qquad (2.3)$$

where $A_S$, $B_S$ and $C_S$ are adjustment coefficients for the tank section and y is the water level of the node. For tanks of constant section, the coefficient $A_S$ represents the cross-section, while the coefficients $B_S$ and $C_S$ are null. This cross-section S must necessarily be discretized. For this purpose, the maximum cross-section $S_{max}$ is divided into a range of partitions N that can take values from $N_0$ to $N_{max}$.

The last group of DVs are those that consider the loss coefficients introduced in certain pipes in the network. A local loss can be caused by a rapid change in magnitude or direction of velocity (bends, contractions or extensions in the pipe geometry). In this work, a gate valve with different opening degrees is installed in the initial part of the pipes that come out of the ST. The action of this local head loss is considered as HC. The number of pipes in which HCs are installed is represented by $p_s$. θ is defined as the opening range that the gate valve can adopt. The range of opening values that the gate valve can take is represented as Nθ.

### 2.2.4. Objective Function

The objective function to be optimized is established in monetary units and is based on the research carried out by Ngamalieu-Nengoue et al. [44]. The main contribution of this work is to consider a new term in the objective function. This term is the cost function of installation of the HC elements at the exit of the selected STs. Equation (2.4) represents the objective function.

$$F = \tau_1 \sum_{i=1}^{m_s} C_D(D_i) + \tau_2 \sum_{i=1}^{n_s} C_V(V_i) + \tau_3 \sum_{i=1}^{p_s} C_v\,(D_i) + \tau_4 \sum_{i=1}^{N_N} C_y(y_i) \qquad (2.4)$$

where $C_D(D_i)$ represents the cost of the renovation of pipes, $C_V(V_i)$ represents the cost of installation of the STs, $C_v(D_i)$ represents the cost of the installation of the HC and $C_y(y_i)$ represents the damage costs caused by the flood.

The cost of the renovation of the pipes was established from actual data supplied by manufacturers. This function represents the cost of changing pipes for others of greater capacity. It is a second-degree polynomial function and is expressed as a function of the diameter $D_i$. Equation (2.5) expresses the cost of each meter of pipe. In this equation, α and β are adjustment coefficients selected for each project.

$$C_D(D_i) = \propto D_i + \beta\, D_i^{\,2} \qquad (2.5)$$

The cost of installing ST is related to the volume required to store water that cannot be evacuated by the network in an event of extreme rain. The cost function (Equation (2.6)) is composed of two terms. The first term,

$C_{min}$, represents a minimum cost established for the ST, while the second term, $V_j$, is variable based on the required storage volume $V_j$ affected by a constant $C_{var}$ and an exponent w.

$$C_V(V_i) = C_{min} + C_{var}\, V_i^{\omega} \tag{2.6}$$

The cost of installing HC was established based on the actual cost of gate valves of different diameters supplied by the manufacturers. It is a second-degree polynomial function and is expressed as a function of the diameter $D_i$. In Equation (2.7), γ and μ are adjustment coefficients specifically defined for each project.

$$C_v(D_i) = \gamma D_i + \mu D_i^{2} \tag{2.7}$$

The cost of flood damage is based on studies by Iglesias-Rey et al. [37] and later by Ngamalieu-Nengoue et al. [44]. The function expresses the cost based on the depth that the water reaches in a flood event. The expression is determined using a vulnerability curve that establishes the percentage of damages based on the water level reached. The authors combined this curve with the flood costs per square meter for different land uses (Equation (2.8)).

$$C_y(y_i) = C_{max}\left(1 - e^{-\lambda \frac{y_i}{y_{max}}}\right)^{r} \tag{2.8}$$

In Equation (2.8), $C_{max}$ represents the maximum cost per square meter that causes a flood. When the maximum flood level $y_{max}$ is reached, the damage is considered irreparable, and the function takes this maximum value. λ and r are adjustment coefficients based on historical flood damage data.

## 2.3. METHODOLOGY

The methodology of this work is to perform the network analysis using the SWMM model. Then, the results of this analysis are analyzed with the help of an algorithm to find the best solutions according to the values of the objective function. This work used a PGA based on an integer coding of the solution instead of traditional binary coding. A PGA solution is represented by a chromosome comprising a series of genes, and each gene is identified with a DV through an integer coding. These algorithms can find many local optimums that can give a final solution far from the optimum.

In this case, every individual has a genome that codes the diameter of selected conduits, the size of the ST and the setting of the HCs installed in the network. In all three cases, if the gene is 0, this is interpreted as there being no tank, conduit or control to be installed or modified in such a location. Then, an evaluation of investment costs is made using Equations (2.5)–(2.7). Finally, a hydraulic analysis is performed, and the results are extracted using a programming library [119] so that the flood cost can also be evaluated using Equation (2.8). More details about the whole process might be found in [104].

To improve the efficiency of the algorithm in the optimization process, a convergence criterion must be defined. This convergence criterion determines the number of iterations that the algorithm must perform when evaluating the objective function to find a satisfactory final solution.

To define this convergence criterion, it is considered that a solution very close to the final solution has been found, in which only one gene on the chromosome has not yet reached its optimal value. This value is reached by mutation, so the probability of occurrence of this change must be calculated. Equation (2.9) shows the expression to calculate this probability.

$$P_O = P_{mut} \times (1 - P_{mut})^{N_{DV}-1} \frac{1}{X_{max}} \qquad (2.9)$$

where, $P_O$ is the probability of occurrence, $P_{mut}$ is the mutation probability, $N_{DV}$ is the number of DVs and $X_{max}$ is the maximum number of discretization options of the DVs.

$P_{mut}$ can be defined with Equation (2.10) presented by Mora-Melia et al. [104]:

$$P_{mut} = \frac{\delta}{N_{DV}} \qquad (2.10)$$

where δ is a constant with a value equal to 1. The authors note that the crossover process in a PGA generates fewer alternatives than a classic GA. For this reason, the probability of mutation in PGA is between 1% and 10%.

If a certain probability of success is established for several iterations, the convergence criterion $G_{max}$ can be determined using Equation (2.11).

$$G_{max} = \frac{\log(1 - P_e)}{\log(1 - P_O)} \qquad (2.11)$$

where $P_e$ is the value of the previously established probability of success. To guarantee that the change by mutation is made, a minimum probability of 80% is established. This convergence criterion increases the computational effort required in the optimization process compared to traditional convergence criteria; however, its use is justified because results closer to the global optimum are obtained.

### 2.3.1. Optimization Process

Optimization problems have challenges due to the large Space of Solutions (SS) they can generate. In this work, the maximum size of each rehabilitation scenario (problem size) can be expressed using Equation (2.12).

$$SS = {ND_{max}}^{N_C} {N_{max}}^{N_N} {N\theta_{max}}^{N_C} \qquad (2.12)$$

To improve the efficiency of the model, an SSR method similar to that proposed by Ngamalieu-Nengoue et al. [44] has been used. This method aims to decrease the calculation time in drainage network rehabilitation models through an interactive process that decreases the SS with the use of a PGA. Specifically, the methodology consists of two stages that are summarized in Figure 2.4.

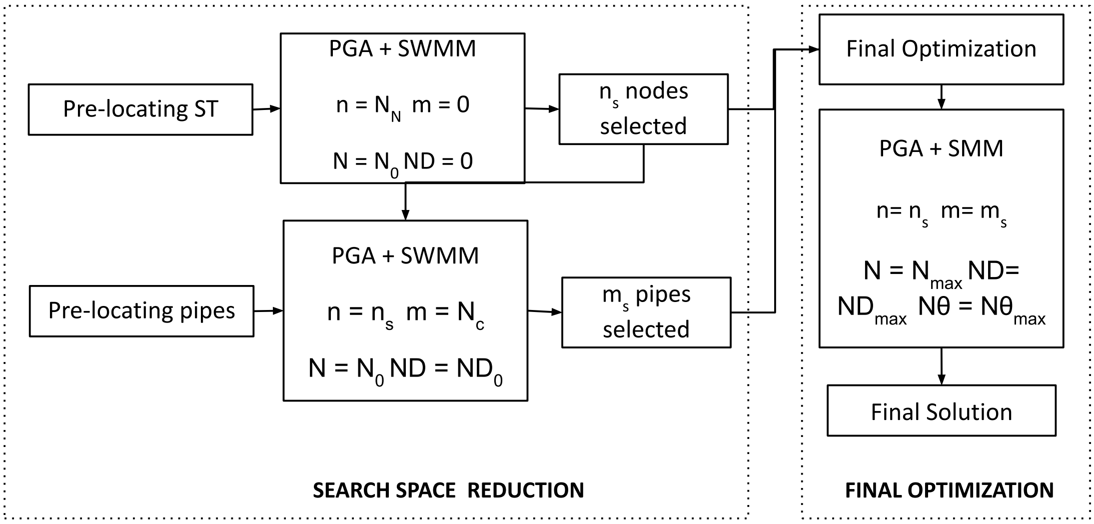


**Figure 2.4.** Optimization process.

As a first stage, the methodology focuses on determining the probable location of the STs. For this, a series of simulations ($N_{it}$) are carried out with the optimization model considering all the nodes of the network as possible ST locations and without considering the change of pipes ($n = N_N$; $m = 0$). Regarding the discretization of the cross-section, a reduced range $N = N_0$ is used. This simplification is valid because the objective is to pre-locate the ST and not to reach an optimization of the ST dimension. The simulations obtained are classified according to the values that the objective function yields. Then, a percentage of the best solutions found ($p_n$) are selected. An analysis of the genomes obtained is performed from this selected group, determining the number of $n_s$ nodes in which it is highly probable that an ST is located.

In the second stage, the goal is to locate the pipes that likely require a pipe change. To achieve this, a new set of $N_{it}$ simulations is run. In this process, the nodes considered are those obtained in the previous stage ($n = n_s$). As for the pipes, they are considered as candidates to change all the pipes in the network ($m = N_c$). The range of pipes used as DV is a reduced range as is the ST cross-section discretization ($ND = ND_0$; $N = N_0$). After the simulations, a classification of the best solutions obtained is made according to the values of the objective function. A percentage of the best solutions $p_n$ is selected, and an analysis of the genomes obtained is carried out to finally determine the number of candidate pipes to be renewed ($m = m_s$). The SSR procedure has been studied previously, giving good results [44]. Its use was deepened in later studies [121], in which the authors showed the results of applying this method in different ways; their results show the suitability of implementing an SSR method in this type of problem.

Once the SS for solutions has been reduced, a final network optimization is carried out, that is, locating and dimensioning the ST, the pipes to be renewed and the HCs. Regarding HCs, since their installation is linked to the installation of an ST, they are not considered in the SS reduction process. In the final optimization, although the number of DVs has been reduced, each of these variables must explored be more in-depth. Consequently, the discretization of the ST cross-section takes a full range ($N = N_{max}$). Likewise, the range of candidate diameters for the pipes will also be a full range ($ND = ND_{max}$). The opening degrees of the HC will be defined as $N\theta$. With these determined parameters, a final simulation is carried out in which the best solution of the process is obtained.

In summary, the optimization process is made up of two parts. In the first part, the DVs are reduced by locating the probable ST locations and conduits to renew. The level of detail of each of the variables is small but valid for the established objectives. In the second part, a final optimization was carried out where the location and final dimensions of ST, pipes and HCs were determined. A smaller number of variables were used in this part, but with a higher level of detail.

# 2.4. CASE STUDY

## 2.4.1. Description of the Network

The proposed methodology was tested for various drainage networks. In order to show its application, E-Chico network located in Bogotá (Colombia) was selected as a case study (Figure 2.5). This network covers an area of 51 hectares and limits with the Andes in its East end. The difference in elevation between the highest and lowest points is 39 m in height. Figure 2.6 shows a digital elevation model of the area. In this figure, it is easy to realize the role that the hills play in the network. Near the hills, the slope of the terrain is very steep. The slopes of the network pipes vary from 7.22% as maximum value (near the Andes) to 0.16% as minimum value, close to the outlet. The area is divided into 35 hydrological sub-basins. The network has a total length of 5000 m. Pipes' diameters have values from 300 mm to 1400 mm. Further details of this network were presented in the work of Ngamalieu-Nengoue et al. [41], and its use allows comparison of results. Data used for the case study is attached to this article as Supplementary Material.

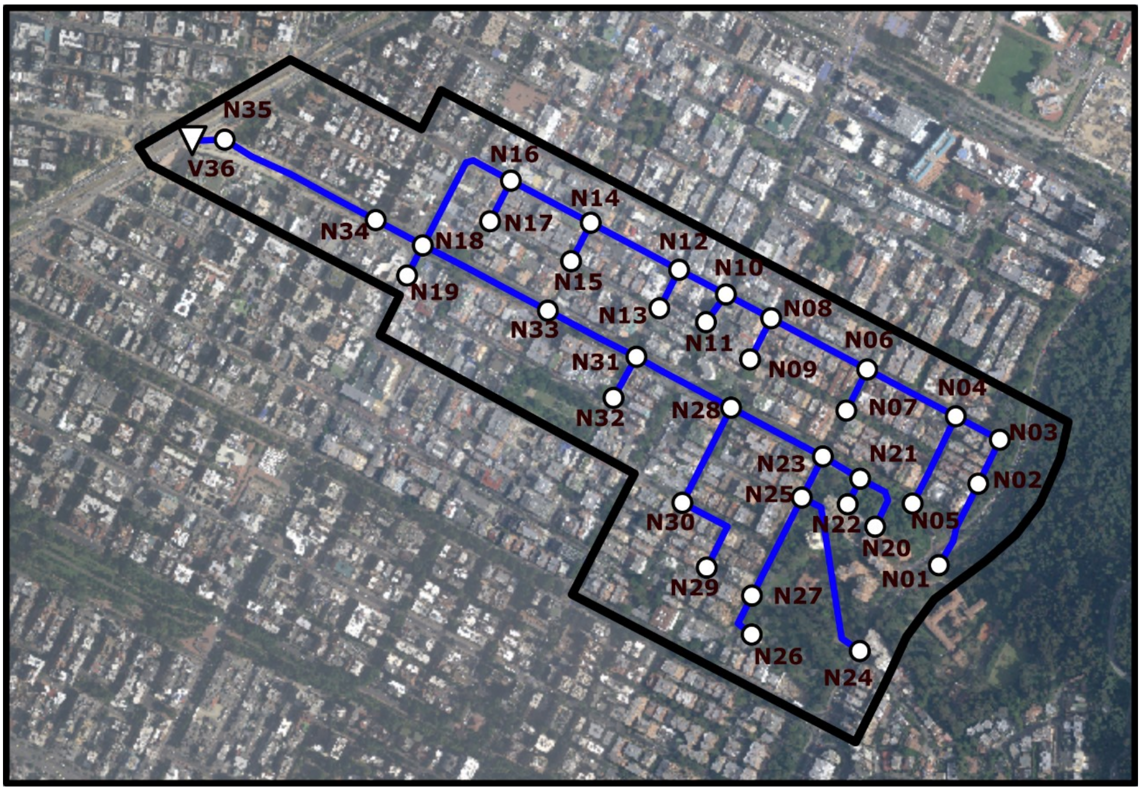


**Figure 2.5.** Representation of the E-Chico network in SWMM model. (Background image taken from [122]).

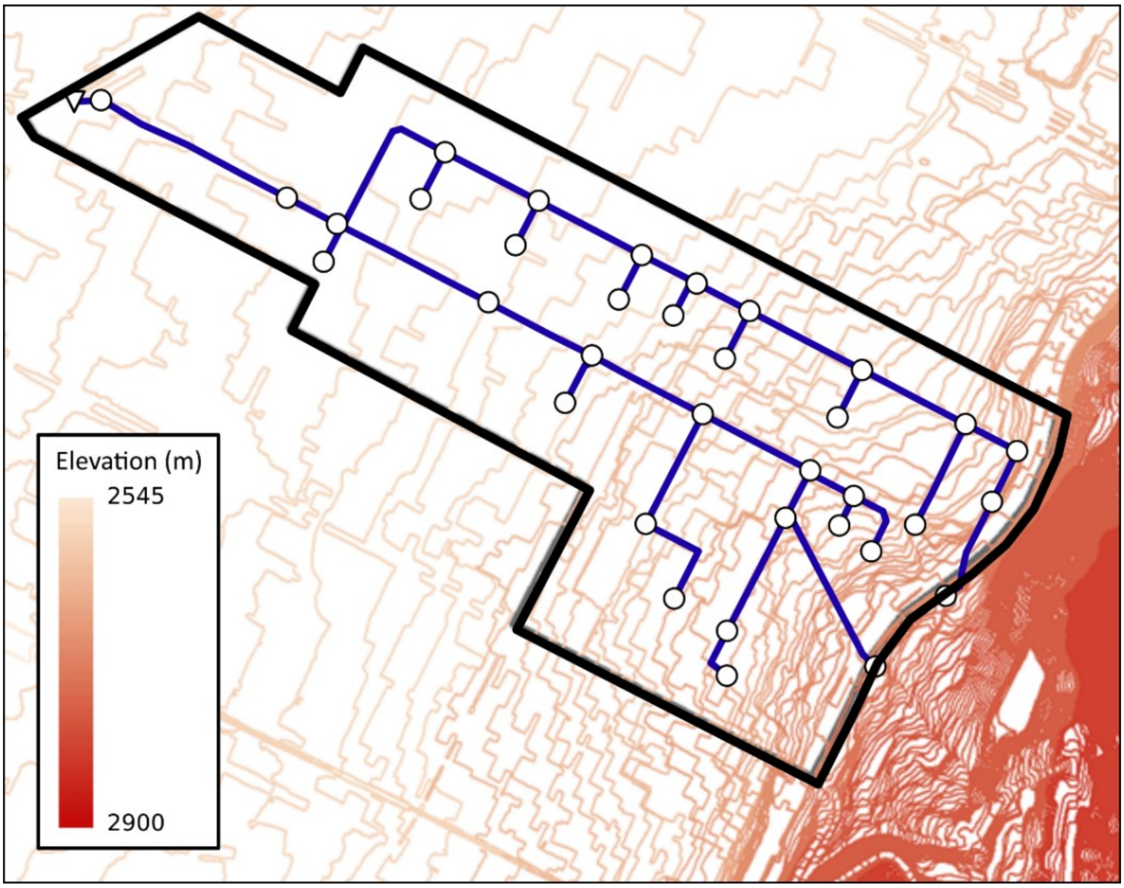


**Figure 2.6.** Digital elevation model of the area for the E-Chico network.

For the evaluation of the problem, a design storm was used (Figure 2.7), calculated by the alternate blocks method with 5 min intervals and previously defined by Ngamalieu-Nengoue et al. [41]. This design storm was calculated from an IDF curve for a return period of 10 years and a duration of 55 min. To avoid extremely high intensities, the intensity was limited to a maximum intensity of 118 mm/h corresponding to a duration of 10 min. The urban basin generates a runoff volume of 20,123 $m^3$ and presents the nodes of the network flooded with a flood volume of 3834 $m^3$, which is 19.07% of the runoff volume.

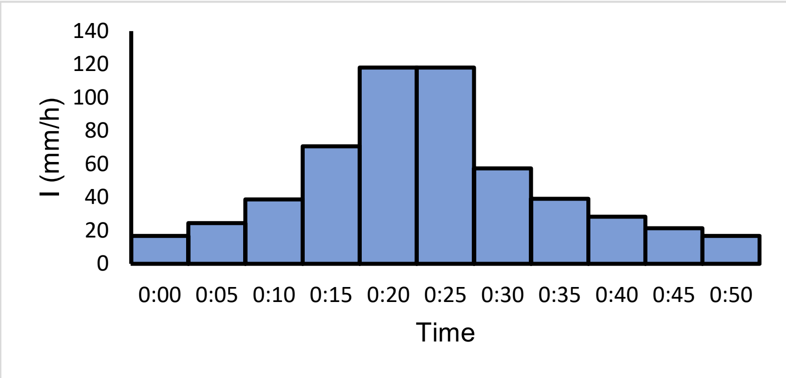


**Figure 2.7.** Design storm for the E-Chico network.

The network in the actual conditions and considering the design storm previously presented for the hydraulic analysis presents flooding problems in many nodes of the network, so it needs to be rehabilitated to recover its benefits and provide the security that cities require. Table 2.1 shows the nodes with flooding problems and the cost of the damages caused by these floods.

**Table 2.1.** Flood on nodes and cost of damage in the current state of the network.

| Node | Flood Volume ($m^3$) | Flood Area ($m^2$) | y (m) | Cost (€) |
|---|---|---|---|---|
| N02 | 123.56 | 1240 | 0.100 | 135,857.00 |
| N04 | 132.56 | 930 | 0.413 | 181,375.00 |
| N06 | 501.79 | 1890 | 0.265 | 875,502.00 |
| N07 | 23.95 | 1250 | 0.019 | 6644.00 |
| N09 | 1.82 | 1130 | 0.002 | 45.00 |
| N10 | 385.12 | 700 | 0.550 | 646,838.00 |
| N11 | 25.83 | 820 | 0.032 | 11,288.00 |
| N23 | 949.54 | 450 | 2.110 | 569,922.00 |
| N32 | 36.65 | 1500 | 0.024 | 12,727.00 |
| N33 | 469.82 | 3030 | 0.155 | 671,908.00 |
| N34 | 1181.87 | 3270 | 0.361 | 2,131,929.00 |
| | TOTAL | | | 5,244,035.00 |

The coefficients used in the cost functions of the installation of the different elements (pipes, tanks and controls) are shown in Table 2.2. These coefficients are used with Equations (2.5)–(2.7). The cost of floods was obtained using Equation (2.8) using the parameters shown in Table 2.3.

For the optimization process, the probability of success was fixed to $P_e$ = 80%. Finally, for every step, one hundred simulations were performed, that is, $N_{it}$ = 100.

**Table 2.2**. Coefficients of the cost terms of Pipes, STs and HC.

| Renovation of Pipes | | Installation of STs | | | Installation of HC | |
|---|---|---|---|---|---|---|
| **α** | **β** | **$C_{min}$** | **$C_{var}$** | **ω** | **γ** | **μ** |
| 40.69 | 208.06 | 169.23 | 318.4 | 0.65 | 4173.70 | −210.82 |

**Table 2.3.** Coefficients of flood damage cost function.

| **λ** | **r** | **$y_{max}$** | **$C_{max}$** |
|---|---|---|---|
| 4.89 | 2.00 | 1.40 | 1268.09 |

## 2.4.2. Application of the Methodology

*2.4.2.1. Reduction of the Space of Solutions Process (SSR).*

In their work, Ngamalieu-Nengoue et al. [41] discretized the ST area in a wide range of $N_{max}$ = 40. In addition, the 25 different diameters were available for the rehabilitation of pipes. Finally, the losses in the HCs are a continuous variable and need to be discretized as well. The valve travel was divided into 10 fractions on a logarithmic scale. Moreover, an additional value of 0 was used to describe ST where HC was not needed. The head loss coefficient was calculated using Equation (2.2). With these data, the size of the problem was calculated using Equation (2.12), giving a problem size of $2.2 \cdot 10^{117}$. This constitutes a very big problem that needs to be reduced.

The first stage of the SSR process is the pre-location of STs. The parameters defined to carry out this process are n = $N_N$ = 35 (that is, all the nodes are considered the pre-location process of ST) and N = $N_0$ = 10 (the discretization of the ST area reduced to this value). In this process, the renewal of pipes is not considered (m = 0).

With these defined parameters, the $N_{it}$ simulations are carried out. From these simulations, a percentage of the best solutions $p_n$ = 5% is selected. In each of the simulations of the selected percentage, the nodes where ST has been installed are analyzed, generating a list of nodes where an ST is possibly installed.

The second stage of the SSR process considers the previously selected nodes n = ns. The discretization of the ST is kept in a narrow range (N = $N_0$ = 10). In this stage, it is considered that all the pipes in the network can be candidates to be replaced (m = NC), and the range of diameters that pipes can take is reduced (ND = $ND_0$ = 10). Table 2.4 shows the values of the nine diameters considered in this reduced range. The option of not changing the diameter of the pipe is also considered if its capacity is sufficient. An additional restriction is to prevent one of the pipes from being replaced by another of smaller diameter.

**Table 2.4.** Reduced range of diameters.

| **Diameter (mm)** | 300 | 400 | 600 | 800 | 1000 | 1200 | 1500 | 1800 | 2000 |
|---|---|---|---|---|---|---|---|---|---|

The PGA parameters are the same defined for stage one $P_e$ = 80%, $N_{it}$ = 100. Once the $N_{it}$ simulations have been carried out, a percentage of the best solutions is selected ($p_n$ = 5%). From this selected percentage, the pipes that have been changed are analyzed and a list of probable pipes that must be renewed is generated. After the SSR process, the size of the problem was reduced to SS = $3.6 \cdot 10^{82}$. Figure 2.8 shows the preselected nodes and pipes in the SSR process.

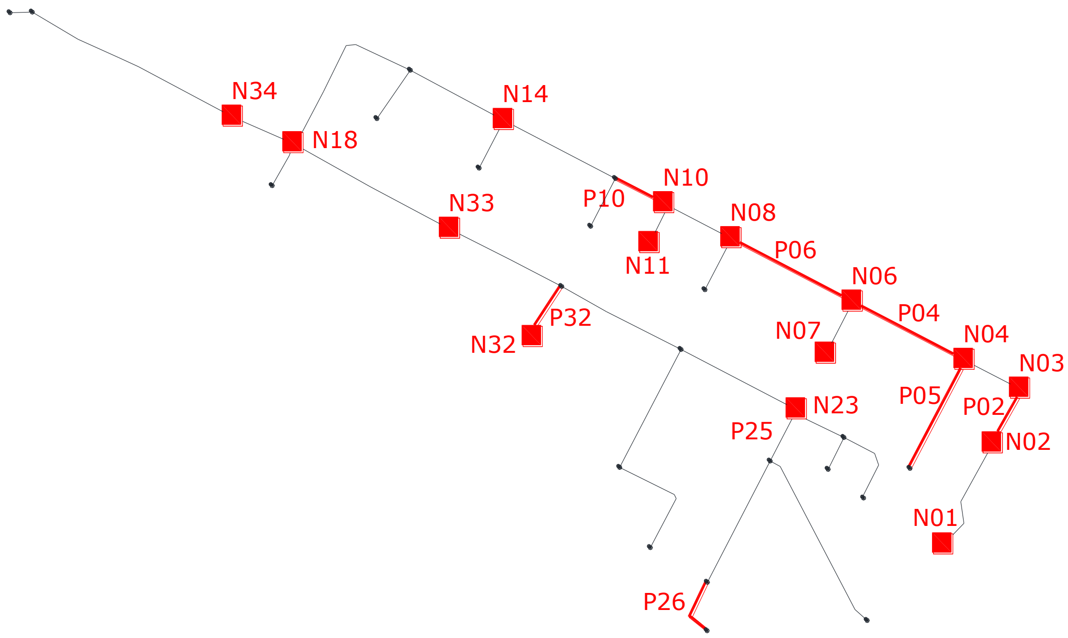


**Figure 2.8.** Nodes and pipes preselected in the SSR process.

### *2.4.2.2. Final Optimization*

For the final optimization, the previously located nodes and pipes n = $n_s$, m = $m_s$ are considered, but in this stage, the discretization of the ST area takes a wide range: N = $N_{max}$ = 40. In the same way, pipe diameter values are selected from the full range of available diameters (Table 2.5). Thus, the range of variation of these DVs is ND = $ND_{max}$ = 25.

**Table 2.5.** Complete range of diameters (mm).

| **Diameters (mm)** | | | | | | | | | | | |
|---|---|---|---|---|---|---|---|---|---|---|---|
| 300 | 350 | 400 | 450 | 500 | 600 | 700 | 800 | 900 | 1000 | 1100 | 1200 |
| 1300 | 1400 | 1500 | 1600 | 1800 | 1900 | 2000 | 2200 | 2400 | 2600 | 2800 | 3000 |

This stage also includes the option of installing HCs at the outlet of the STs. The discretization of the opening range of the gate valve is $N\theta$ = $N\theta_{max}$ =

10. With all these values (n, m, N, ND and Nθ), an optimization is carried out that generates the final solution of the process.

## 2.5. RESULTS

The results of the final optimization are as follows. It is required to replace the current P02 pipe with a diameter of 400 mm with another with a diameter of 500 mm. Three STs must be installed in the nodes N04, N10 and N23. Table 2.6 shows the required volume of the STs. Finally, it is required to install three HC elements must be installed in pipes P04, P10 and P23. The local head loss that these elements must generate is detailed in Table 2.7. Figure 2.9 shows the elements to be installed and their location. With these actions, the objective function has a value of 203,859.69 € made up of the following terms: cost of pipe renovation 6583.81 €, cost of installation of STs 181,540.69 €, cost of installation of HC elements 7671.75 € and the cost of flood damages 8063.44 €.

**Table 2.6.** Area and volume required in STs.

| Node | Area ($m^2$) | Volume ($m^3$) |
|---|---|---|
| N04 | 550.00 | 946.00 |
| N10 | 1050.00 | 2299.50 |
| N23 | 1050.00 | 274.50 |

**Table 2.7.** Loss coefficient k required in hydraulics control elements.

| ID | Location | k | θ |
|---|---|---|---|
| HC04 | P04 | 14.73 | 18.93% |
| HC10 | P10 | 6.64 | 26.41% |
| HC23 | P23 | 161.01 | 6.97% |

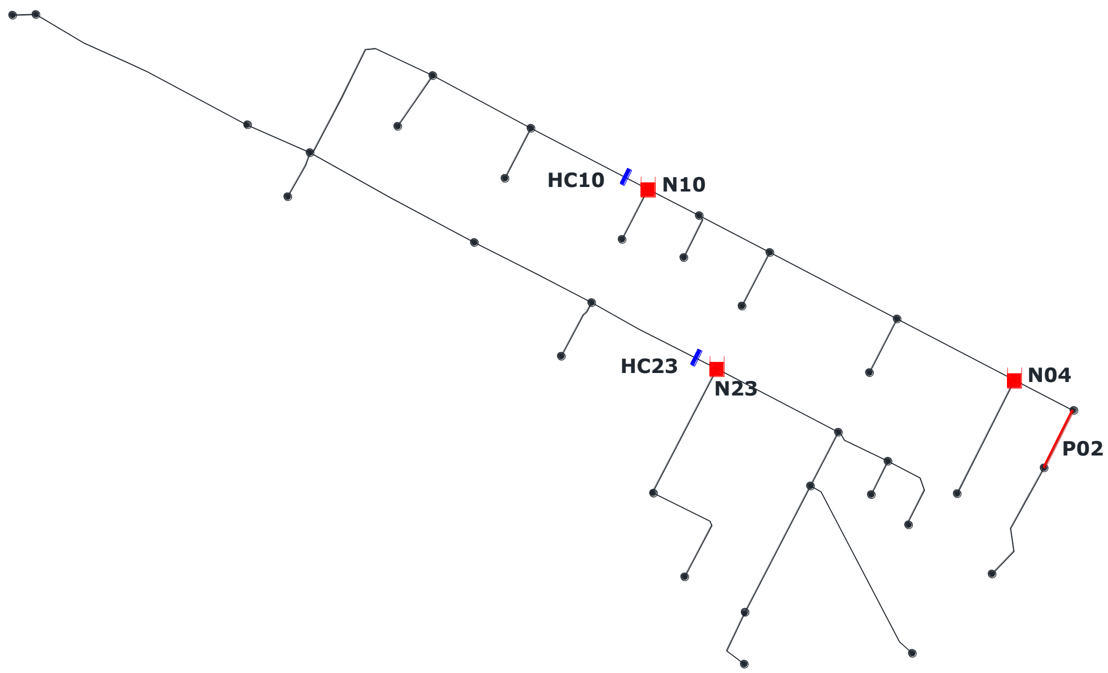

**Figure 2.9.** Infrastructure to be implemented in the network after final optimization.

These results considerably improve those obtained by Ngamalieu-Nengoue et al. [38]. Table 2.8 compares the rehabilitation costs of different methodologies:

Case a). Ngamalieu-Nengoue et al. method, changing only pipe diameters.

Case b). Ngamalieu-Nengoue et al. method, only installing STs.

Case c). Ngamalieu-Nengoue et al. method, combining both options.

Case d). Proposed methodology, including the SSR and the use of HCs.

**Table 2.8.** Comparison of the objective functions.

| **Method.** | | **Terms of the Objective Function** | | | |
|---|---|---|---|---|---|
| | | **Pipe cost** | **ST cost** | **HC Cost** | **Flood Damage cost** |
| Case a) | | 766,761.00 € | 0.00 € | - | 24,753.00 € |
| | Total | 791,214.00 € | | | |
| | SS | $4.0 \cdot 10^{38}$ | | | |
| Case b) | | - | 268,063.00 € | - | 5,392.00 € |
| | Total | 273,455.00 € | | | |
| | SS | $5.8 \cdot 10^{61}$ | | | |
| Case c) | | 14,927.00 € | 186,353.00 € | - | 12,701.00 € |
| | Total | 213,981.00 € | | | |
| | SS | $4.2 \cdot 10^{69}$ | | | |
| Case d) | | 6,583.81 € | 181,540.69 € | 7,671.75 € | 8,063.44 € |
| | Total | 203,859.69 € | | | |
| | SS | $3.6 \cdot 10^{82}$ | | | |

There is an improvement both in the total value of the objective function and in the value of flood damage. The results indicate that when implementing a HC element, a slowdown of the water flow is generated. This reduction of the flow downwards induces the system to use the volume of the network more efficiently, reducing both the costs of the rehabilitation of the network and flood levels. In other words, the introduction of HC allows finding better solutions for the rehabilitation of drainage networks.

It is important to highlight that the inclusion of HCs allows reducing the cost in every term. That is, in comparison with previous results, pipe cost, ST cost and flood damage cost using the proposed methodology are reduced with respect to the works by Ngamalieu-Nengoue et al. [38].

Including HCs increase the size of the problem. This might be the main drawback of the methodology. However, this problem was solved using an SSR process that reduced considerably the problem.

## 2.6. CONCLUSIONS

Extreme rains and impermeable ground due to population growth have caused many cities to experience flooding. Drainage networks were not designed for these new conditions, so adaptation is necessary. Implementing tanks to retain flow peaks is a well-studied alternative that has proven to have advantages over other methods in extreme rain events. In the literature, there are many techniques to rehabilitate drainage networks and reduce damage caused by floods. However, none of them were based on hydraulic simulation and considered at the same time the replacement of pipes, the installation of STs and the introduction of HC.

One of the main contributions of this work is the inclusion of HC as a complementary rehabilitation strategy to the replacement of pipes and the STs installation. For this, it has been necessary to represent in economic terms all the parameters involved in the process, including investment costs and costs associated with flood damage. In this sense, another contribution has been the inclusion of HC and its valuation in economic terms. The participation of HC has been possible to make it compatible with the part of the objective function previously defined. This formulation of the objective functions in monetary units is very useful for decision-makers in the development of a rehabilitation project.

The proposed method also includes improvements in the solution space exploration capabilities. In this way, the SSR methodology has been generalized to be compatible with the presence of potential HC devices. Likewise, the specific convergence criterion $G_{max}$ of the optimization model has been formulated explicitly in terms of the probability of success.

The applicability of the method has been shown through the case study presented. Given that the study network is located in Colombia, the prices used as a reference have been those of that country, although the numerical values have been translated into Euros to facilitate understanding. As can be seen, the application of the proposed methodology, which includes HC, leads to solutions for the rehabilitation of the drainage networks that are cheaper and with lower flood costs. In summary, implementing HCs reduces flood levels and the size of the necessary structures. Therefore, we can achieve the conclusion that hydraulics controls are valid and effective elements in the rehabilitation of drainage networks.

One of the main limitations of the method, derived from the initial working hypotheses, is the impossibility of modifying the topology of the network. This means that it is not possible to add new pipes. Indirectly, this means that all the STs added to the network must be installed in on-line mode. Undoubtedly, one of the improvements of this work lies in allowing the installation of off-line STs with new pipes that connect these tanks to the network and included in the methodology the determination of the devices that must be activated for the filling and emptying these tanks. In any case, obtaining this improvement is something that seems a natural consequence of the results obtained in this work.

Finally, the results obtained comprise a feasible solution for a defined problem with a defined rainfall. Depending on this rainfall, different solutions will be obtained. Hence, there is no optimal solution, and any problem must be solved in accordance with budget availability, design criteria, etc. This an open field for future investigations.

**Supplementary Materials:** The following supplementary materials are available in Appendix III of this thesis. Figure A3.1.1. Representation of E-Chico drainage network; Figure A3.1.2. Design storm based on the Alternating Blocks Method; Table A3.1.1. Data for nodes and subcatchments in E-Chico network; Table A3.1.2. Data for conduits in E-Chico network; Table A3.1.3. Time series for the design storm used in E-Chico network; Table A3.1.4. Series of valve travel and head loss coefficients.

This supplementary material is part of the scientific article presented in this Chapter and is also available online at: https://www.mdpi.com/2073-4441/13/4/514/s1

# CHAPTER 3.

# SEARCH SPACE REDUCTION FOR GENETIC ALGORITHMS APPLIED TO DRAINAGE NETWORK OPTIMIZATION PROBLEMS

# Preamble

Once the rehabilitation methodology that provides promising results has been established, the next step in this research is to improve the efficiency of the optimization process. Since the methodology as it is conceived operates a significant number of DVs, resulting in significantly longer calculation times. The aim of the study is to identify the regions of the SS that contain the best solutions.

The analysis of the discretization of the DVs and the reduction of the number of DVs themselves form the basis of the proposed procedure. The SSR procedure also proposes a hydraulic sector reduction for large networks, which allows for a faster identification of the best search regions.

This procedure achieves the objective of reducing calculation times without losing the quality of the solutions found. Establishing this procedure is key to the development of the rehabilitation methodology, as the computational effort required is a significant limitation in optimization processes.

*This article was published as: Bayas-Jiménez, L.; Martínez-Solano, F.J.; Iglesias-Rey, P.L.; Mora-Meliá, D. Search Space Reduction for Genetic Algorithms Applied to Drainage Network Optimization Problems. Water 2021, 13, 2008. Available in open access at: https://doi.org/10.3390/w13152008*

## 3.1. INTRODUCTION

Drainage systems around the world have experienced an increase in operating pressure in recent years. This is mainly due to the increase in the intensity of rains and urban growth. According to many authors, extreme rains occur with increasing frequency around the world, mainly due to climate change, and are the main factor of flooding in urban basins [123–125]. On the other hand, anthropological action has altered the composition of the world atmosphere; one of the most evident is produced by the development of urban space. During the last few decades, cities have experienced a constant process of growth, which has reduced the green areas that surround them, replacing them with highly impermeable surfaces. These factors have led many cities to appreciate the increase in surface runoff, and in many cases, the collapse of their drainage systems [126–128]. These problems make it necessary to improve the functioning of the drainage networks to restore security to the cities. Floods in urban areas generate significant economic impacts in cities. Concern increases as cities are increasingly exposed to flood risk [129,130]. To face this problem, different options for optimizing drainage networks have been developed.

One of the most prominent approaches is called low impact development (LID). LID approaches have been widely used to minimize the flow of water produced by urban runoff, retaining the water and enhancing its infiltration. This type of approach also attempts to improve water quality by removing pollutants in vegetation and restoring urban ecosystems. Among the most used types of these systems are permeable paving, infiltration trenches, vegetated swales, bio retention basins, and infiltration basins. However, although LID are a valid solution to reduce runoff, these approaches do not have great resilience in extreme rain events [36,131–133]. The use of STs in an urban environment to reduce the risk of flooding has been studied and proven as one of the most efficient methods to reduce surface runoff [28,32,33]. Better results have been given by using the combination of STs installation and pipe renewal [38,41]. The inclusion of HC elements [134] appear as an improvement of these works and turns out to be an alternative that improves the results obtained.

To face the problem of floods, some authors improved the networks by taking as a criterion the avoidance of floods in the study area [37], while other authors improved the networks based on the flood volume [38,135]. Different methodologies have been developed to address this problem. However, the need to find minimal cost designs has led researchers to optimization algorithms. Different evolutionary techniques have been tested for the optimization of drainage networks, highlighting an ant colony optimization algorithm [136,137], simulated annealing [6,33], harmony search algorithm [108,138], and taboo search algorithm [139]. All of these techniques show good results in different cases studied. However, GAs that do not require continuity of the objective function stand out in this field due to their robustness, and their use has gained popularity in drainage network optimization work [36,38,41,44,118,140,141].

GAs are stochastic search strategies based on natural selection mechanisms, which involve aspects of biological evolution to solve optimization problems. One characteristic of these types of algorithms is the way that they explore the space solution. While other algorithms follow a single search direction, GAs perform parallel searches in different directions. This characteristic adds to their ability to explore complex adaptive landscapes and has made these algorithms a widely used tool in water resources research.

However, one of the problems that most worries researchers is the difficulty that GAs can present in finding solutions close to the global optimum. Kadu et al. [96] mentions that GAs are efficient and effective in finding low-cost solutions in drainage system optimization problems. The efficiency and effectiveness depend on several parameters, some that contemplate the parameters of the algorithm and others of the space where the GA seeks the optimal solutions. The problem with the SS occurs because of the large number of DVs that the algorithm must analyze in a real-life problem. Handling a significant number of DVs causes the SS to grow exponentially. This problem turns into a considerable computational demand to find a satisfactory solution to the problem proposed. Although the computational advance can compensate the time required in this operation, in reality, there are problems in which the SS is so large that it becomes unapproachable. For this reason, the need arises to reduce the SS. This reduction, however, must be done in such a way that the most promising region that contains the best solutions is clearly identified. Maier et al. [92] mention that a reduction in the size of the SS generally results in its approximation, either because a series of DVs have to be fixed before optimization or because the nature of the interactions between the DVs excludes the effective size reduction. This could potentially exclude the region containing the global optimum, and thus reduce the quality of the solutions found. For this reason, the reduction method must guarantee that the selected region is truly the best, and that the best solutions to the problem are not excluded from it. To solve this situation, different works have been carried out to effectively reduce the SS.

One of the first works was carried out by Schraudolph and Belew [142]. These authors presented an approach based on dynamic parameter coding to adaptively control the mapping of fixed-length chromosomes to real values, so that, at each iteration, the algorithm searches a smaller SS. Ndiritu and T.M. Daniell [143] presented a modified GA combining a fine-tuning strategy to reduce the SS with a hill climbing strategy to move to more promising regions. In recent research, Sophocleous, Savić, and Kapelan [78] presented a model to detect and locate leaks in water distribution networks. The model employs two stages: SSR and leak detection and location. In the first stage, they reduce the number of DVs and the range of values that they can take through an analysis of the characteristics of the network. For the second stage, they used a GA to find the solution to the problem. Simultaneously, Ngamalieu-Nengoue, Iglesias-Rey, and Martínez-Solano [44] presented a methodology to SSR applied to a drainage network rehabilitation model. The reduction of the SS is based on locating the possible nodes in which STs will be installed and subsequently identifying the possible pipes that should be renewed. The process is carried out by reducing the number of DVs and the range of values that they can adopt. In a later work Bayas-Jiménez et al. [134], they used the same methodology to optimize drainage networks. The authors included in the optimization process the use of HCs that certainly improved the results obtained, but that considerably increased the SS. The proposed methodology continues and complements these works with the aim of improving the efficiency of the optimization process. Specifically, the method reduces the SS using the sectorization criteria to improve calculation times and reduce the computational effort required. To achieve this, an SSR method is applied in each hydraulic sector, decreasing the DVs and defining a final search region. Once the region that is presumed to have the best solutions is delimited, a final optimization is carried out to find the best possible solution. The method is applied to different drainage networks to prove its benefits.

# 3.2. MATERIALS AND METHODS

## 3.2.1. Problem Statement

This work consists of the rehabilitation of networks that present flood problems due to lack of capacity. To improve the network, the renovation of pipes for others of greater capacity, the installation of STs, and the installation of HCs were considered. In the optimization model, the possible diameters of the pipes to be renewed, the volume of the storage of the STs, and the degrees of opening of the control element were defined as DVs. For use in the optimization model, they must be fully defined. The first type of DV consists of all pipes in the network $N_C$; each of these pipes can take a diameter value from a previously defined list of options ND. If a DV takes the value of 0, it indicates that this pipe does not need to increase its diameter, while a different value indicates that this pipe was optimized by the optimization model. The group of optimized DVs is represented by the notation $m_s$. A second group of DVs consist of all nodes of the $N_N$ network where STs can be installed. As these DVs represent the volume required by each ST, for the analysis, the maximum height of the tank equal to the current height of the manhole is considered, leaving the cross-sectional area of the tank as a variable. This DV can take values within an options list NS defined in the discretization of the cross-sectional area of the tank. If, in the optimization process, the value 0 is obtained for a DV, it must be understood that this node does not require an ST to be installed. The set of nodes that requires STs to be installed is represented by the notation $n_s$. Finally, the third group of DVs consists of the DVs that determine the installation of HCs in the pipes. This group of DVs can take values from a list of options Nθ that results from discretizing the degree of opening. The value 0 indicates that the installation of an HC is not necessary. The group of optimized DVs is represented by the notation $p_s$.

### 3.2.2. Optimization Model

The optimization model in this article considered the methodology presented in a previous work [134]. The model used as an optimization engine a modified genetic algorithm called the PGA [104]. GAs are inspired by the theory of evolution and natural selection. GAs work on a set of potential solutions called the population. This population is composed of a series of solutions called individuals, and an individual is made up of a series of positions that represent each of the DVs involved in the optimization processes, which are called chromosomes. These chromosomes are made up of a string of numbers called coding. A traditional GA has a binary coding. In contrast, the PGA used in this work has an integer coding. This coding has the advantage that each gene represents a DV that gives good results in optimization of hydraulic problems. In a GA, each individual is defined as a data structure that represents a possible solution of the SS of the problem. Evolution strategies work on individuals, who represent solutions to the problem, so they evolve through generations. Within the population, each individual is differentiated according to their value of the objective function. To obtain the next generations, new individuals are created using two basic evolution strategies, such as the crossover operator and the mutation operator.

The PGA connects to the SWMM model [71] using a toolkit [119] to carry out a series of simulations in order to find an optimal solution to the problem. To achieve this, the PGA evaluates an objective function composed of four cost functions [134] that are determined based on the results provided by the SWMM model in the simulations carried out. This process is carried out iteratively until a defined stop criterion is reached. Figure 3.1 summarizes the operation of the optimization model.

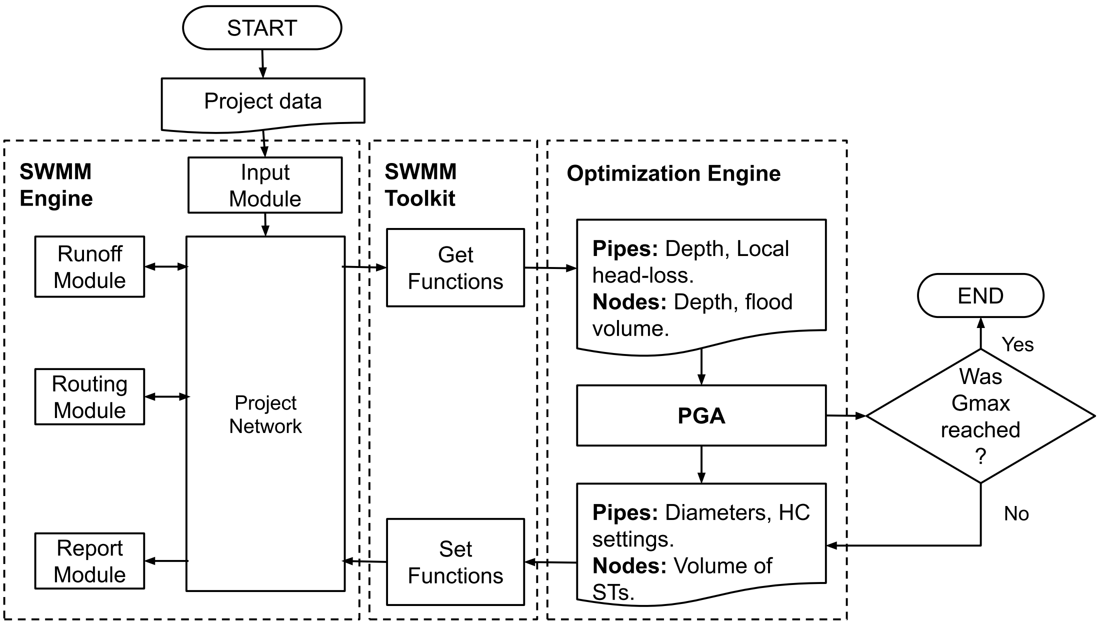


**Figure 3.1.** Operation scheme of the optimization model.

This optimization process is iterative and requires establishing an end point to the process. GAs end the process when a high percentage of the population converges to a value or a fixed number of evaluations that is determined by criteria, such as a maximum number of generations or a maximum resolution time. In this work, the termination criterion was based on the value of the objective function. When, after a certain number of generations ($G_{max}$), the OF does not decrease, the algorithm stops. At that time, it is understood that the solution will not improve, and the process ends.

*3.2.2.1. Objective Function*

The optimization problem aims to minimize the costs associated with flood damage with as little investment as possible. According to this, an objective function is established that evaluates the problem in economic terms. This objective function consists of four cost functions. The first function corresponds to the cost of the renewal of pipes that must be replaced due to the lack of capacity. This function is established from actual cost data provided by pipe manufacturers. The function relates the cost of the pipe to its diameter. In addition, it includes the coefficients α and β to adjust the cost according to the place where the methodology is applied.

$$C_D(D_i) = \left(\propto D_i + \beta D_i^{\,2}\right)L_i \qquad (3.1)$$

In Equation (3.1), $D_i$ is the diameter of the pipe, $L_i$ is the length of the pipe, and the coefficients α and β are adjustment coefficients selected for a specific project.

The second term corresponds to the cost of installing STs that would be required to temporarily store the water that the network is not able to evacuate in the event of extreme rain.

$$C_V(V_i) = C_{min} + C_{var}\, V_i^{\,\omega} \qquad (3.2)$$

The first term of Equation (3.2) represents a minimum cost ($C_{min}$) established for the construction of the STs, while the second term is a variable as a function of the required storage volume ($V_i$) affected by a constant $C_{var}$ and an exponent ω.

The third term of the objective function represents the cost of installing HC elements in certain pipes at the outlet of STs. This function is established from actual gate valve cost data.

$$C_C(D_i) = \gamma D_i + \mu D_i^{\,2} \qquad (3.3)$$

In Equation (3.3), $D_i$ is the diameter of the pipe, and the coefficients γ and μ are used to adjust the cost of the HC elements to the place where the methodology is applied.

Finally, an equation must be defined that presents the cost of flood damage; this function depends on the level reached by the water $y_i$. The definition of this cost is based on the work done by Ngamalieu-Nengoue et al. [38]. The authors combined this curve with the costs of flooding per square meter for different land uses. In Equation (3.4), from 1.40 m of flooding, the damage is considered irreparable and, therefore, the function stops growing, and the cost will reach its maximum ($C_{max}$). Then, a constant $y_{max}$ equal to 1.40 m is established.

$$C_y(y_i) = C_{max}\left(1 - e^{-\lambda \frac{y_i}{y_{max}}}\right)^{\upsilon} \tag{3.4}$$

These four cost functions define the objective function (Equation (3.5)) that the optimization model will seek to decrease to reach the best solution.

$$OF = \sum_{i=1}^{m_s} C_D(D_i) + \sum_{i=1}^{n_s} C_V(V_i) + \sum_{i=1}^{p_s} C_{Cv}(D_i) + \sum_{i=1}^{N_N} C_y(y_i) \tag{3.5}$$

*3.2.2.2. PGA Parameters*

For an adequate work of the algorithm, a suitable population size must be defined, so that, on the one hand, the SS of the analyzed scenario is adequately covered and, on the other hand, it does not demand excessive computational effort. An expression (Equation (3.6)) is defined to face the problem efficiently. The equation was presented in a work developed by Mora-Melia et al. [104].

$$Л = \varphi\, N_{DV} \tag{3.6}$$

where Л represents the population, $N_{DV}$ represents the number of DVs, and $\varphi$ is a constant with a value equal to 2. To give the model an element of diversity, a mutation probability is defined, which is established in Equation (3.7) by Mora-Melia et al. in a previous work [39].

$$P_{mut} = \frac{\delta}{N_{DV}} \tag{3.7}$$

where δ is a constant with a value equal to 1.

The optimization model uses a stop criterion $G_{max}$ presented by Bayas-Jiménez et al. [134] and shown in Equation (3.8).

$$G_{max} = \frac{\log(1 - P_e)}{\log(1 - P_O)} \tag{3.8}$$

where $P_e$ is called the probability of success, which is defined according to the requirement of the calculation to be performed. After several runs, the authors have concluded that a value of $P_e$ of 80% is needed to guarantee a change due to mutation, however, in this work, different percentages were used according to the different scenarios proposed. Finally, $P_O$ is the probability of occurrence that is determined using Equation (3.9).

$$P_O = P_{mut}\,(1 - P_{mut})^{N_{DV}-1}\,\frac{1}{X_{max}} \tag{3.9}$$

where $N_{DV}$ is the number of DVs that have been analyzed, $X_{max}$ is the maximum number of discretization options for the DVs, and $P_{mut}$ is the mutation probability.

### 3.2.3. Search Space Reduction Process

Transforming the SS from continuous to discrete inherently leads to a problem. If the discretization is small, that is, the number of options that the DV can take is small, then the space exploration may not be efficient, and the algorithm may not be able to identify an optimal solution. On the other hand, if the discretization is very refined, the list of options that the DV can take would notably increase the SS, and the computational effort required would be considerable. The SS is defined considering the DVs and the values that these can adopt; an expression is then defined (Equation (3.10)) that allows us to know the size of SS that the algorithm must explore in each proposed scenario.

$$\mathrm{SS} = \mathrm{n_i}\,(\log \mathrm{ND}) + \mathrm{m_i}\,(\log \mathrm{NS}) + \mathrm{p_i}\,(\log \mathrm{N\theta}) \qquad (3.10)$$

where ni represents the candidate pipes to be renewed, mi represents the candidate nodes to install STs, and pi represents the candidate pipes to install HCs in a defined scenario. The equation is presented in logarithmic form with the aim that the SS can be appreciated in a better way.

*3.2.3.1. Reduction by Hydraulic Sectors*

Equations (3.6)–(3.9) show the importance of the problem size to define the genetic operators. This is one of the main reasons why the SSR is a useful tool when facing problems from a heuristic approach. In the case of large drainage networks, the large number of DVs becomes an important problem. This high number of DVs demands significant computational effort. The drainage networks consist of branches that serve different sub-catchments, and their runoff flows are added to the network, discharging their waters to a bigger pipe. In other words, the network can be seen as a set of hydraulic sectors (HSs). If these sectors can be identified, a particular analysis of them can be carried out to reduce the number of DVs within the sector and consequently reduce the SS. The optimization process begins by identifying the HSs that composed the network. The optimization model is configured to include the DVs that composed the HS to be optimized. The SSR method is applied to each HS, thereby defining a smaller search region in each HS. Once the SSR process has been carried out for every HS, a new scenario of the network is assembled, where the least prominent regions containing the best solutions have been eliminated. The SSR method is applied to this new scenario to eliminate the least interesting sectors of the new network scenario. Figure 3.2 illustrates how the application of the sectorized SSR method would work.

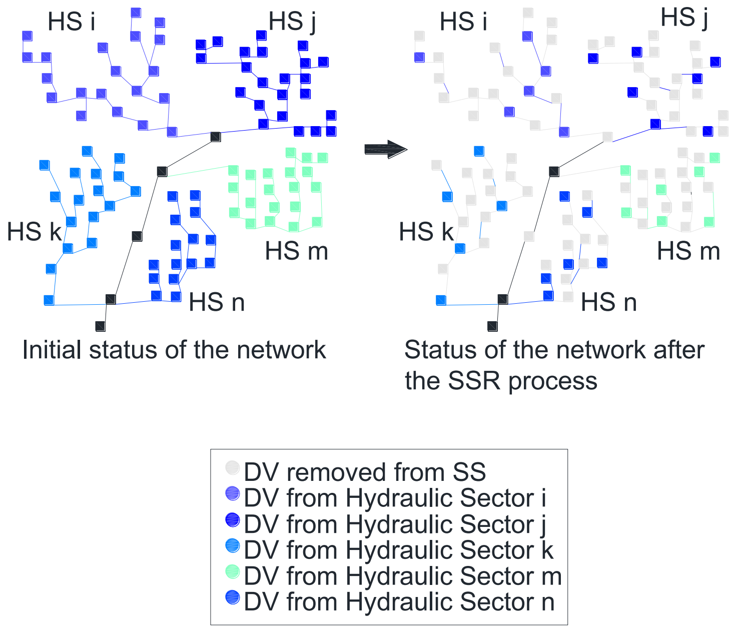


**Figure 3.2.** SSR process using reduction by hydraulic sectors.

With the reduced problem, a final optimization of the network is carried out to obtain the best solution to the problem posed. The sectorized optimization process is shown in Figure 3.3.

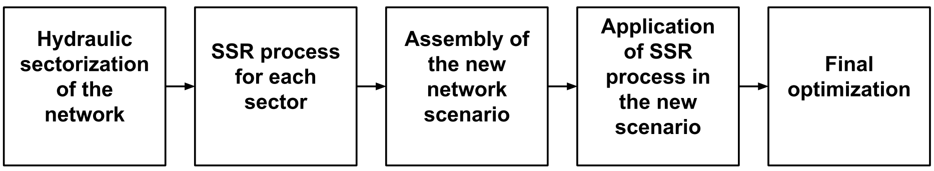


**Figure 3.3.** Reduction process by HS.

*3.2.3.2. Reduction in the Number of Options*

This implies that the quality of a determined solution depends on the time available. If the quality of the solution is not significant for a particular problem, calculation times can be minimized by defining a short list of options. In contrast, a higher quality solution requires a list of options where the separation interval in the discretization is short. It is evident, then, that the value of this separation in the discretization has a preponderant importance in obtaining the result. It can be said that, in an iterative process, such as optimization with GAs, the quality of the solution will improve if the size of separation used to discretize the DVs is progressively decreased. In this work, two lists of discretization options were determined for each type of DV, one called coarse and the other much refined (Figure 3.4). These two types of discretization have been determined ensuring that the separation interval allows a good exploration of the SS. Certainly, the coarse options list has a large separation, and it includes separate points, but these points cover the entire SS.

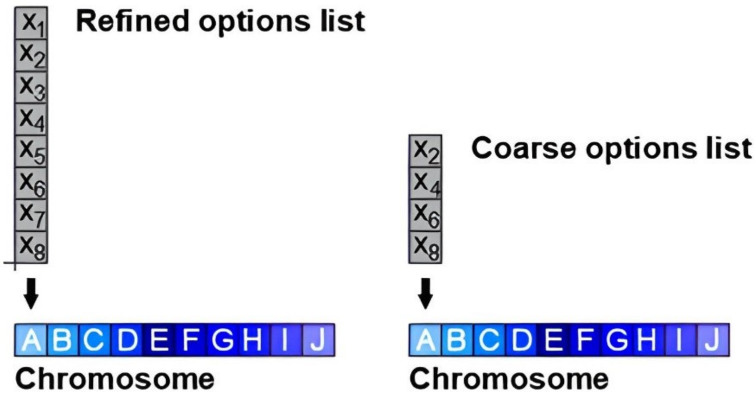


**Figure 3.4.** Representation of course and refined options lists.

In the case of pipes, as it is a type of discrete variable, the refined options list $ND_{max}$ corresponded to all pipe diameters available on the market. On the other hand, the coarse options list $ND_0$ was set in such a way that it considered the diameters differentiated and conveniently separated to cover different available ranges that allowed the PGA to make the change of diameter values in the optimization process.

In the case of the DVs that analyzed the nodes where the installation of STs was required, the discretization was performed by dividing the maximum surface into equal intervals. The spacing fixed to discretize the area is called ΔS. Equation (3.11) was used to calculated ΔS.

$$\Delta S = \frac{S_{max}}{NS} \tag{3.11}$$

where $S_{max}$ is the maximum area available. In this way, the refined options list $NS_{max}$ consisted of 40 values, and the coarse options list $NS_0$ consisted of 10 values. The area of each ST is calculated by Equation (3.12).

$$S_i = \Delta S \cdot X_i \tag{3.12}$$

where $S_i$ is the area of each ST and $X_i$ is the value that the DV takes from the options list.

The volume of each ST is calculated by Equation (3.13).

$$V_i = h_i \cdot S_i \tag{3.13}$$

where $V_i$ is the volume of the ST and $h_i$ is the invert elevation of the ST.

The discretization of the HC opening positions was set according to the valve travel curve presented in Figure 3.5 and defined in a previous work [134].

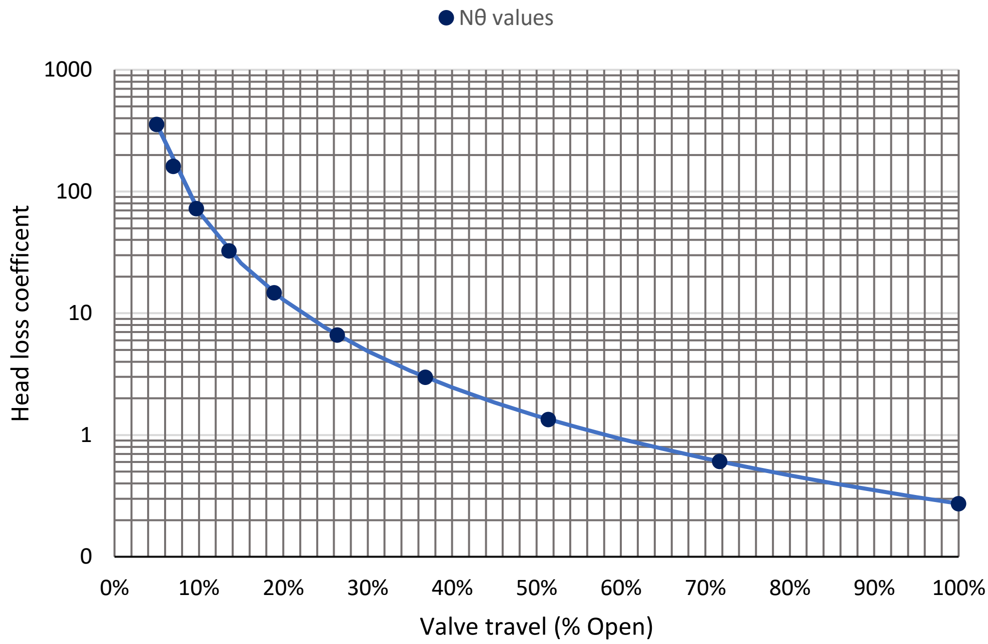


**Figure 3.5.** Valve travel of a gate valve and Nθ values for HCs.

To determine the separation interval in the discretization that covers the entire SS, the head loss coefficients (k) are expressed on a logarithmic scale. Consequently, 10 opening positions have been set that allow a good diversity of opening options that composed the options list Nθ for this type of DV. HC is not part of the SSR process, so a coarse options list was not defined for its analysis. Figure 3.5 shows the Nθ values with the value that each gene represents.

Using a coarse options list obtained a lower quality solution, but the time spent searching for the solution was less. If the chromosome obtained in a low-quality solution is analyzed, it would be observed that it is composed of a chain of genes; each gene represents a value designated to a DV. If a gene has the value 0, it indicates that, in the optimization process, this DV does not require changing its initial condition. If this scenario is repeated in a new calculation, it may be thought that this DV does not need to be optimized, and excluding it from the analysis could be considered, reducing the number of DVs and consequently reducing the SS. This procedure is the base of the SS reduction methodology, where sequentially it is sought to eliminate DVs that do not require optimization, keeping the DVs that compose the region that contains the best solutions.

#### *3.2.3.3. Reduction in the Number of Decision Variables*

The process of SSR has as a first step a mapping with the optimization model of the entire SS and the DVs of STs, and pipes are analyzed by the algorithm using a list of options with coarse discretization. The use of a coarse options list allows the identification of the DVs that may be included in the most promising region of the algorithm's exploration space. For this, a certain number of evaluations $N_{it}$ is established, and from the results obtained the ninety-fifth percentile ($P_{95}$) of the solutions is selected. In the selected $P_{95}$, each chromosome is analyzed, quantifying how many genes different from 0, called valid genes, have been obtained for each DV. If a DV does not have at least 20% valid genes, it is assumed that this DV is not part of the promising region of the SS, and it is eliminated from the new SS. If, on the contrary, a DV presents a high repeatability of valid genes, it is considered a candidate to be contained in the most promising search region. The percentage of 20% is then established as the criterion for the selection of variables to be considered in the SS. Figure 3.6 shows an example of how the selection criteria work in the SSR.

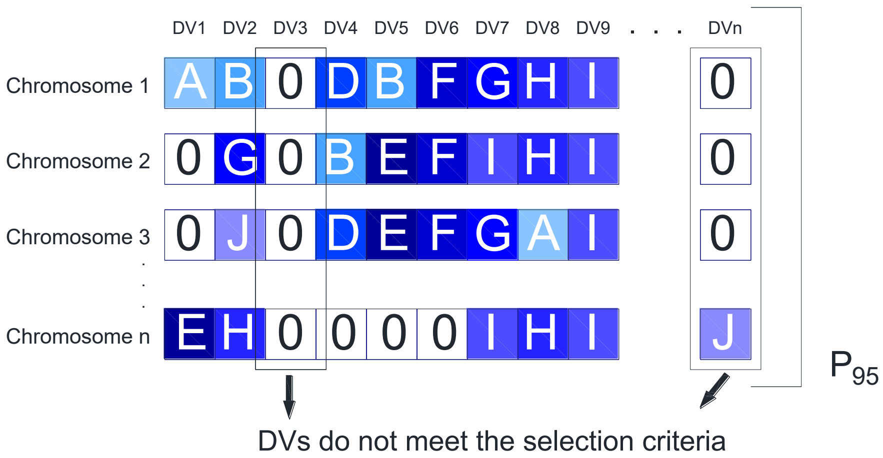


**Figure 3.6.** Representation of the selection criteria of the SSR.

The process is repeated in the new defined region, eliminating the DVs that do not meet the selection criteria. In each iteration of the process, the convergence of the results towards certain DVs whose repeatability in the sampling increases, each time defining the region with the best solutions. The process ends when all variables meet the selection criteria, and the SS cannot be further reduced. In the SSR process, $P_e$ is set at 20%. This percentage is used to find solutions without demanding a lot of calculation time. The reason why a Pe of 20% is used is because, in this process, it is not a goal to find the final solution, but to eliminate DVs to reduce the SS.

### 3.2.4. Final Optimization

Once the final search region is defined, the final optimization is performed in this new scenario. The refined options list for pipes, $ND_{max}$, and the refined options list for STs, $NS_{max}$, are used in this optimization. At this stage, the HCs are also included in the optimization model, so the options list Nθ is also used. With the optimization model configured in this way, a much finer exploration of the reduced space is intended, since it is assumed that the global optimum is found in this region. With this objective in addition, a much more demanding stopping criterion is used with a $P_e$ equal to 80%. It should also be noted that the value of $X_{max}$ in Equation (3.8) increases because the refined discretization is used. With the $G_{max}$ defined in this way, the model is expected to demand a higher computational effort. However, with the objective of finding the closest solution to the optimal solution, this effort is justified. The proposed optimization process is summarized in Figure 3.7.

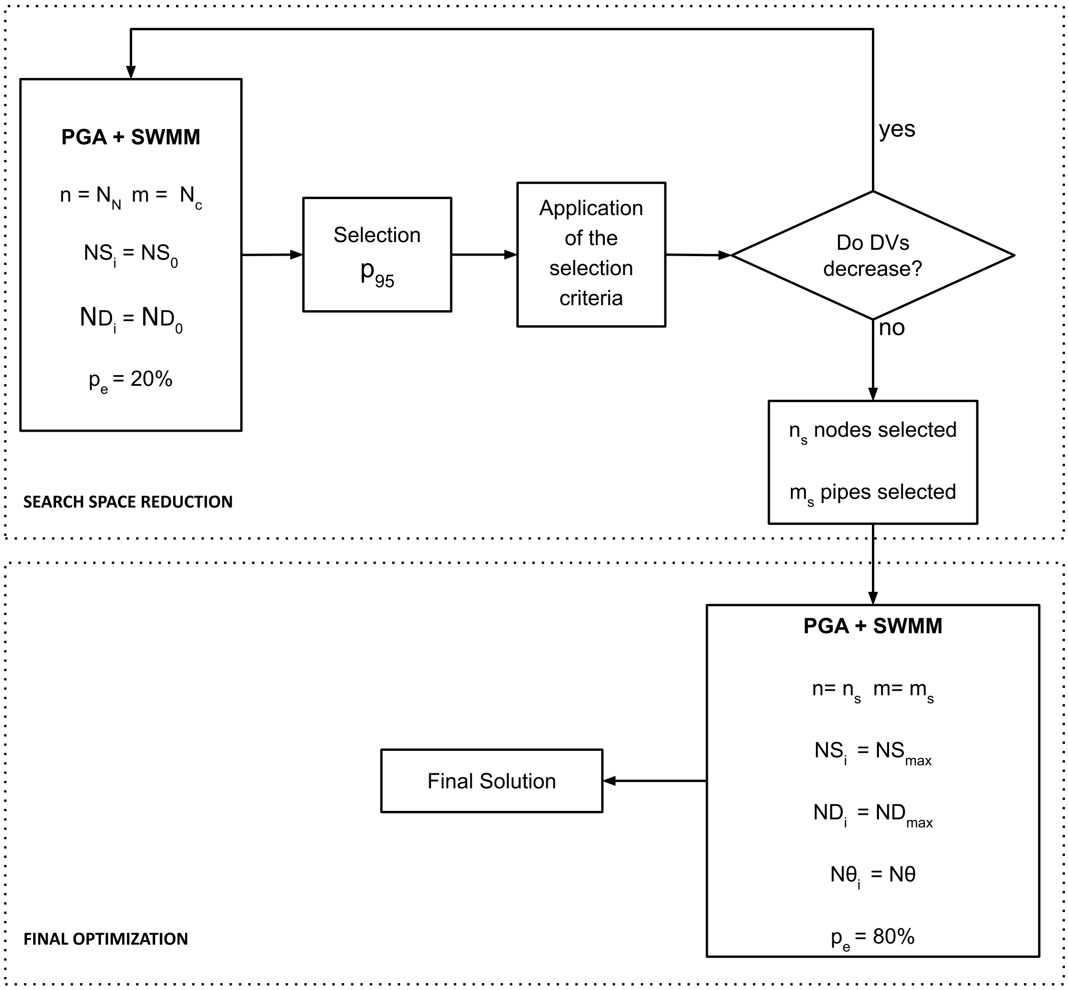


**Figure 3.7.** Flow chart of the optimization process.

## 3.2.5. Application of the Model

### *3.2.5.1. E-Chico Network*

To apply the methodology, the E-Chico network located in the city of Bogotá, Colombia was selected. This network has 35 hydrological sub-basins that occupy an area of 51 hectares, 35 conduits, and 35 connection nodes. All pipes are circular, and their diameters range from 300 mm to 1400 mm. The network is approximately 5000 m long. This network has the particularity of being in the foothills of the Andes Mountain Range, which makes it have steep slopes with a difference in level of 39 m between the lowest and highest point of the network; these characteristics make the operation of this network totally dependent on gravity. The hydraulic model of the network was made by Saldarriaga et al. in a previous work [118]. In an actual state and for a design storm with a return period of 10 years, the urban basin generates a runoff of 20,123 m3, and has a flood volume of

3834 m3, which represents 19.07% of the runoff volume and concentrates in 11 nodes of the network.

For the analysis of the network, a design storm was used based on an intensity-duration-frequency curve, previously defined by Ngamalieu-Nengoue et al. [41]. This design storm was calculated using the alternate block method with 5-min intervals from an IDF curve for a return period of 10 years and a calculated duration of 55 min. The maximum intensity was limited to 118 mm/h, corresponding to a duration of 10 min to avoid very high intensities.

According to its configuration, two hydraulic sectors, HS-1 and HS-2, could be identified in the network (Figure 3.8). HS-1 composed the upper part of the network with 17 pipes and 17 nodes, while HS-2 composed the lower part of the network with 14 pipes and 14 nodes. Although smaller sectors might be identified, the number of DVs of these branches was too small to be interesting enough to analyze them separately. Therefore, separating the network into two sectors was considered a more advantageous option. The nodes and pipes excluded from both sectors were added to the optimization process in the assembly of the new scenario that was generated after reducing the SSR process of the SHs.

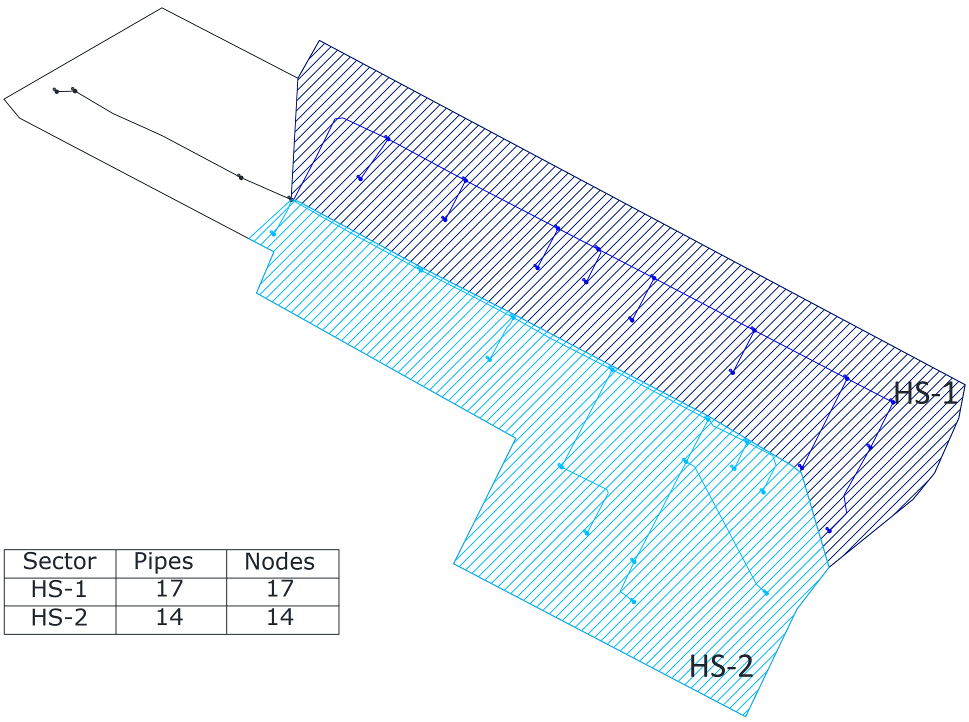


| Sector | Pipes | Nodes |
|---|---|---|
| HS-1 | 17 | 17 |
| HS-2 | 14 | 14 |

**Figure 3.8.** Hydraulic sectors of the E-Chico network.

The PGA parameters that were applied to the optimization model to start the SSR process are those shown in Table 3.1. Once the SS was reduced, the final optimization was applied to the resulting region. The parameters used in this stage are those shown in Table 3.1. To carry out the optimization, Nit = 250 was defined for each proposed iteration. With this value, it was expected to have enough iterations to achieve convergence towards a satisfactory solution.

**Table 3.1.** Algorithm parameters for the SSR process.

| Scenario | $N_{DV}$ | N | $P_{mut}$ | $P_e$ | $X_{max}$ | $G_{max}$ |
|---|---|---|---|---|---|---|
| SH-1 | 34 | 68 | 2.94% | 20% | 10 | 203 |
| SH-2 | 28 | 56 | 3.57% | 20% | 10 | 167 |
| New scenario | 16 | 32 | 6.25% | 20% | 10 | 94 |
| Final optimization | 9 | 18 | 11.11% | 80% | 40 | 1486 |

For the calculation of the objective function, the coefficients of the cost functions defined in Equations (3.1)–(3.4) were determined. These coefficients were defined for the case study according to the costs of the Colombian economy. Table 3.2 shows the coefficients for the infrastructure cost functions. Equation (3.14) shows the coefficients for calculating the cost of flood damage.

$$C_y(y_i) = 1268.09\left(1 - e^{-4.89\frac{y_i}{1.4}}\right)^2 \tag{3.14}$$

**Table 3.2.** Coefficients of the cost terms of pipes, STs, and HCs.

| Cost of Pipes | | Cost of STs | | | Cost of HC | |
|---|---|---|---|---|---|---|
| α | β | $C_{min}$ | $C_{var}$ | ω | Y | μ |
| 40.69 | 208.06 | 169.23 | 318.4 | 0.65 | 4173.7 | -210.82 |

*3.2.5.2. Ayurá Network*

The method was applied to a second network of larger dimensions. This second network corresponded to a neighborhood in the city of Medellín, Colombia called Ayurá. The network crosses the city from south to north, and covers an area of 22.5 ha divided into 96 sub-basins. The network is composed of 86 nodes and 86 circular ducts, with a diameter ranging from 200 mm to 1050 mm. The difference in levels between the highest point of the network and the lowest is 14.61 m. These characteristics make the operation of the network entirely dependent on gravity. The average slope of the pipes that compose the network has a value of 1.81%.

For the analysis of the network, a design storm calculated by the method of alternate blocks was used. The total runoff from the network in the scenario studied is 13,970 $m^3$. The flooding in different nodes of the network has a total value of 4012 $m^3$, which represents 28.72% of the total runoff.

The network topology does not allow for differentiation of specific HSs. The network is composed of different branches that are connected to a principal line. To face the optimization problem, it was decided to divide the network into two sectors (Figure 3.9). A sector called HS-1 considered the upper part of the network with 49 nodes and 49 pipes where the SSR methodology was applied. Once the optimal region of HS-1 was defined, a new scenario was formed in which the SSR process was applied again, defining a final reduced region. Lastly, a final optimization was performed in the determined region to find the best solution to the optimization problem. Table 3.3 shows the parameters initially used by the PGA for each scenario proposed. To divide the network into two sectors, it was considered that the network was composed of 258 DVs corresponding to pipes, STs, and HCs, so analyzing it completely would increase the SS that the PGA must explore. For this reason, optimizing the network by sectors would mean reducing the calculation times. On the other hand, analyzing the network in sectors allows reducing the DVs considered in the optimization process, which would determine a stop criterion defined by Equation (3.8) to decrease considerably. Specifically, when analyzing HS-1 in the first part, the stopping criterion was reduced by 24% when applying the SSR methodology compared to if it were applied throughout the network.

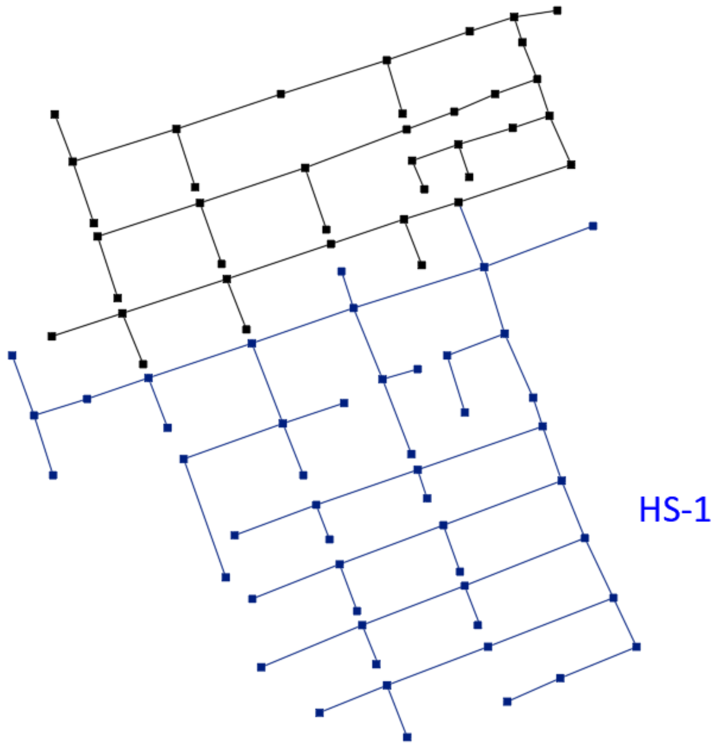


**Figure 3.9.** Ayurá network sectorization.

**Table 3.3.** PGA initial parameters for each scenario.

| Scenario | $N_{DV}$ | N | $P_{mut}$ | $P_e$ | $X_{max}$ | $G_{max}$ |
|---|---|---|---|---|---|---|
| SH-1 | 98 | 196 | 1.02% | 20% | 10 | 294 |
| New scenario | 65 | 130 | 1.54% | 20% | 10 | 391 |
| Final optimization | 60 | 120 | 1.67% | 80.00% | 40 | 10411 |

To determine the value of the objective function and its cost terms, the coefficients shown in Table 3.2 and Table 3.3 are used. As in the E-Chico network, for the Ayurá network, $N_{it}$ = 250 was established for each iteration in the SSR process and in the final optimization.

# 3.3. RESULTS

## 3.3.1. E-Chico Network

Figure 3.10 summarizes the SSR process in the E-Chico network. In the first step, HS-1 and HS-2 were processed separately. Once the number of variables was reduced, a new scenario was set up with the remaining DV from HS-1, HS-2, and the elements not included in any HS (conduits C18, C34, and C35, and the corresponding tanks ST18, ST34, and ST35). The results showed that certain DVs had a higher repeatability. By applying the selection criteria, the areas of the SS that were less interesting to explore were eliminated, thus defining a new SS. While the SS was reduced, the repeatability increased in the most promising DVs to be considered in the final analysis region. With the SS reduced in the HSs, the new search scenario was assembled that included the nodes and pipes obtained in the previous process and elements of the network that had not been analyzed. To perform the final optimization, the DVs of the HCs must be added to this region.

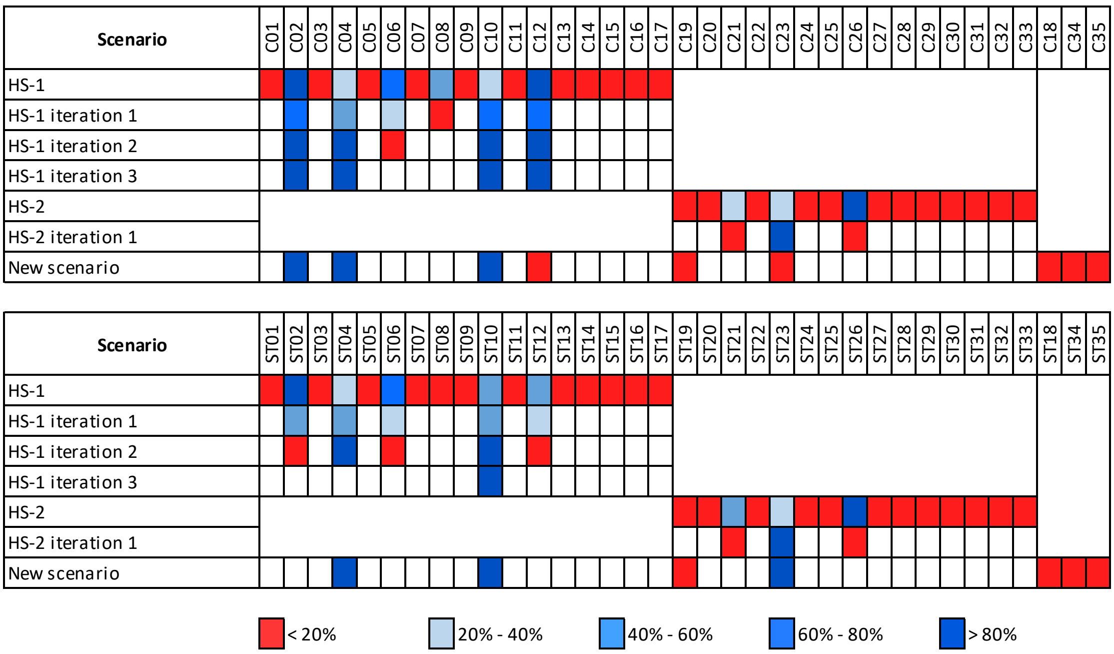


**Figure 3.10.** SSR process in the E-Chico network.

Table 3.4 shows the reduction of the SS in each iteration of the optimization model; the SS was reduced from a magnitude of 140, which would be obtained when optimizing the network without any type of SSR strategy, to a magnitude of 12 once the proposed method was applied. In the final scenario, the DVs corresponding to the HCs were added.

**Table 3.4.** Size of the SS in each resulting scenario.

| Scenario | DVs | SS | OF min | Nsim |
|---|---|---|---|---|
| HS-1 | 34 | 34 | 765,329.71 € | 581 |

| | | | | |
|---|---|---|---|---|
| HS-1 iteration 1 | 11 | 11 | 750,980.89 € | 178 |
| HS-1 iteration 2 | 10 | 10 | 750,980.89 € | 156 |
| HS-1 iteration 3 | 6 | 6 | 750,980.89 € | 87 |
| HS-2 | 28 | 28 | 1,926,507.19 € | 504 |
| HS-2 iteration 1 | 6 | 6 | 3,199,277.55 € | 83 |
| New scenario | 16 | 16 | 227,984.83 € | 272 |
| Final optimization | 9 | 12 | 199,813.79 € | 2634 |
| Full network E-Chico | 105 | 140 | 251,711.79 € | 1367 |

The final solution required the renewal of a pipe (C02) that increased its diameter from 0.4 m to 0.5 m. The installation of STs was in nodes N04, N10, and N23 with volumes of 1462 $m^3$, 2300 $m^3$, and 1958 $m^3$, respectively. The installation of HCs in the pipes C04, C10, and C23 had k values of 72.55, 14.73, and 14.73, respectively. Figure 3.11 illustrates the elements to be installed in the network. The costs of the final solution found by the optimization model are shown in Table 3.4. With these actions, we had the necessary infrastructure costs to optimize the network as follows: cost of pipes = 6583.81 €, cost of STs = 179,757.70 €, and cost of HCs = 7671.78 €. The cost of flood damage was 5800.66 €. Thus, the objective function took the value of 199,713.95 €. This value contrasted with the cost obtained when applying a standard GA optimization without SSR. In the latter case, the optimal value found after 250 runs of the algorithm was 251,711.79 € (26% more expensive).

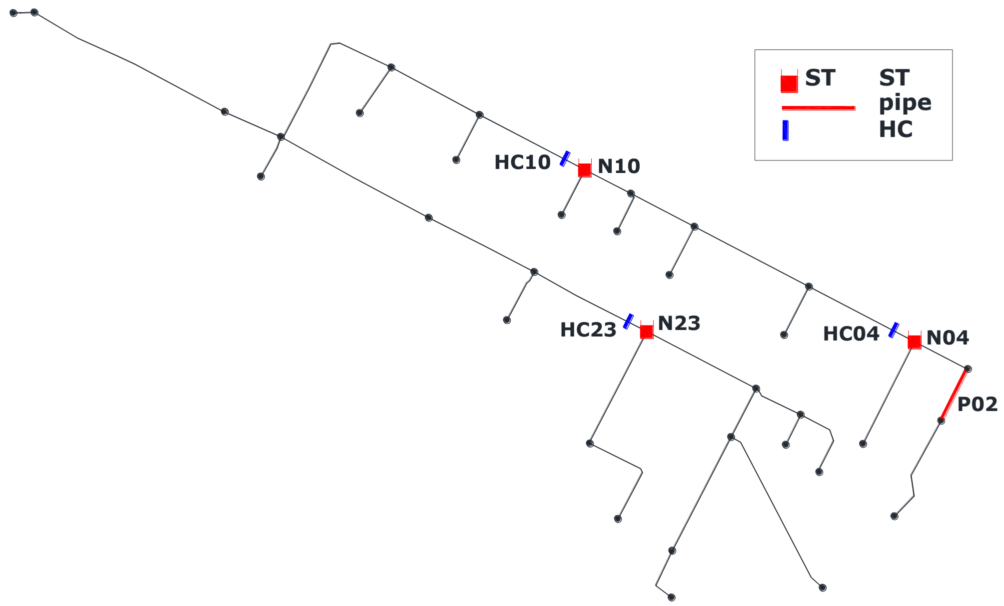


**Figure 3.11.** Final solution reached after the full optimization process in the E-Chico network.

Figure 3.12 shows the comparison between the different scenarios when reducing the SS and optimizing the E-Chico network without the application of a previous SSR process. The value of the minimum objective function in each simulation carried out is represented on the *x*-axis, and the accumulated frequency with which this value appears in the $N_{sim}$ is on the *y*-

axis. This figure is used to see the degree of dispersion of the results obtained in the simulation. The optimization process is more efficient if the curve has a greater slope. The final optimization curve shows the advantages of applying the SSR method in a first stage. This figure also shows that the dispersion of the results obtained for the objective function was reduced as the number of DVs decreased.

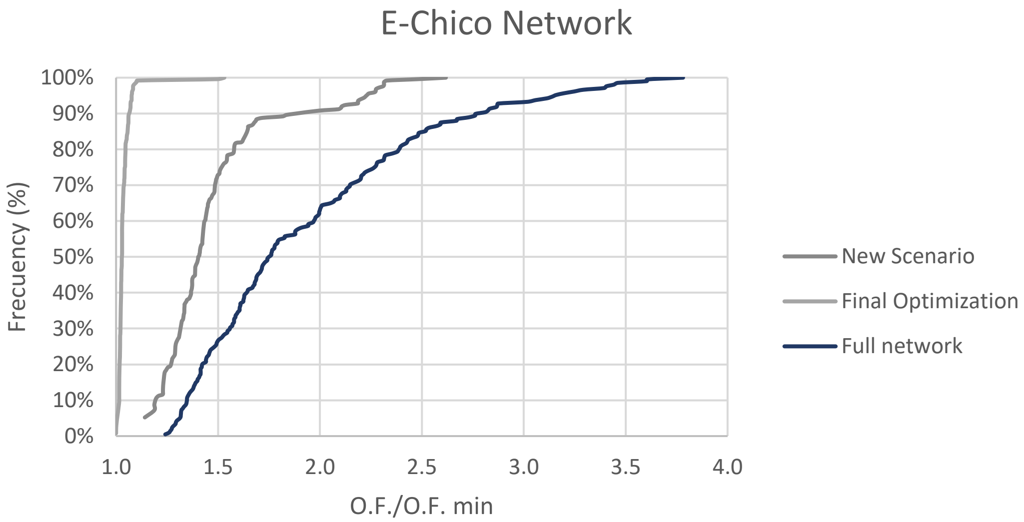


**Figure 3.12.** Comparison between the results of E-Chico (Table 3.4) of different scenarios in the SSR process and the optimization of the whole network without the application of SSR.

### 3.3.2. Ayurá Network

Figures 3.13 and 3.14 show the application of SSR to the tanks and conduits of the Ayurá network, respectively. As it can be easily observed, the search region was noticeably reduced in only two iterations in the HS-1, mainly in the case of tanks (Figure 3.13). After reducing the number of DVs in HS-1, a new scenario was defined. The SSR process was then applied to this new scenario. Finally, the DVs corresponding to the HCs were added to this new scenario for the final optimization of the network.

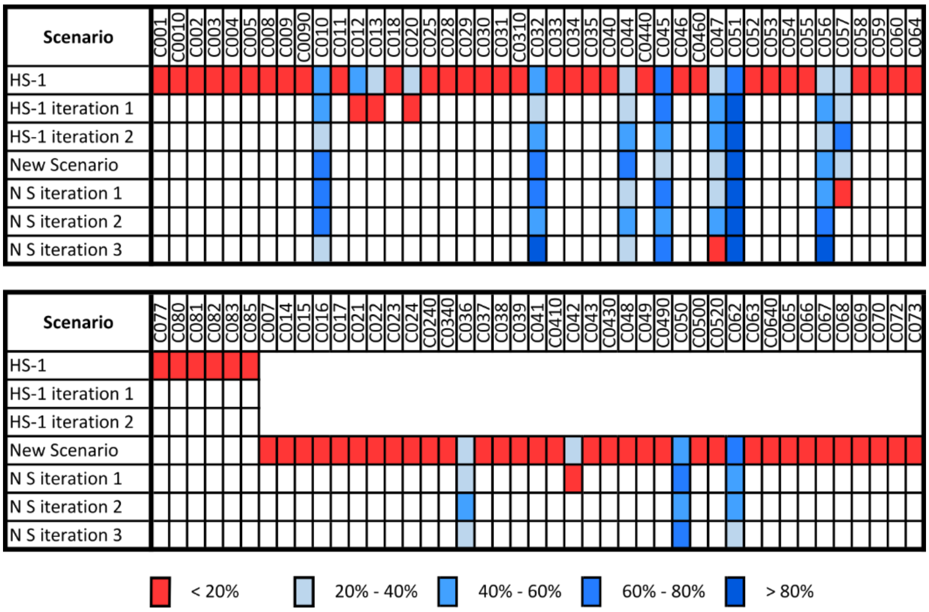


**Figure 3.13.** SSR process in the nodes of the Ayurá network.

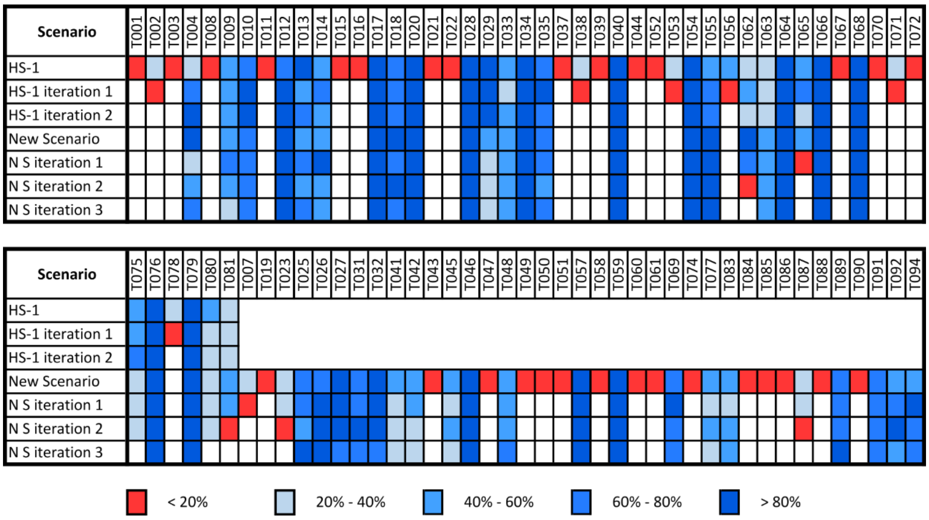


**Figure 3.14.** SSR process in the conduits of the Ayurá network.

Table 3.5 summarizes the SS for the entire network and for each scenario in the Ayurá network SSR process.

**Table 3.5.** Size of the SS in each resulting scenario of the Ayurá network.

| Scenario | DVs | SS | OF min | $N_{sim}$ |
|---|---|---|---|---|
| HS-1 | 98 | 98 | 1,858,940.08 € | 2576 |
| HS-1 iteration 1 | 45 | 45 | 1,792,735.25 € | 997 |
| HS-1 iteration 2 | 36 | 36 | 1,790,516.01 € | 723 |
| New Scenario (NS) | 110 | 110 | 413,071.97 € | 3127 |
| N S iteration 1 | 62 | 62 | 402,043.79 € | 1435 |
| N S iteration 2 | 58 | 58 | 386,612.41 € | 1269 |
| N S iteration 3 | 52 | 52 | 376,739.30 € | 967 |
| Final Optimization | 60 | 82 | 328,049.63 € | 21068 |
| Full network Ayurá | 258 | 344 | 456,820.42 € | 3553 |

The final solution required the renovation of 25 pipes, the installation of five STs, and the inclusion of two elements of HCs at the outlet of the STs. Table 3.6 shows the diameters of the network in an initial state and the optimized diameters of the pipes to be installed. Table 3.7 shows the characteristics of the STs and HCs that must be installed according to the results obtained. Figure 3.15 illustrates the elements to be installed in the network. Specifically, the final solution has an objective function of 328,049.63 €. The cost of the renewal of the pipes had a value of 112,297.59 €, the cost of the installation of STs had a value of 201,454.17 €, and the cost of the installation of HCs had a value of 2768.62 €. The cost of the damage caused by the floods had a value of 1529.25 €.

**Table 3.6.** Results of the pipes in the final optimization.

| Pipe | Original Diameter (m) | Optimized Diameter (m) |
|---|---|---|
| T004 | 0.375 | 0.45 |
| T010 | 0.6 | 0.8 |
| T012 | 0.4 | 0.5 |
| T017 | 0.2 | 0.3 |
| T020 | 0.3 | 0.35 |
| T026 | 0.5 | 0.7 |
| T028 | 0.2 | 0.3 |
| T031 | 0.25 | 0.3 |
| T032 | 0.5 | 1.6 |
| T034 | 0.2 | 0.35 |
| T040 | 0.25 | 0.35 |
| T041 | 0.525 | 0.6 |
| T042 | 0.525 | 0.7 |
| T046 | 0.3 | 0.45 |
| T048 | 0.3 | 0.5 |
| T054 | 0.25 | 0.45 |
| T057 | 0.3 | 0.4 |
| T059 | 0.2 | 0.3 |
| T064 | 0.375 | 0.6 |
| T066 | 0.3 | 0.4 |
| T068 | 0.25 | 0.3 |
| T069 | 0.5 | 0.7 |
| T076 | 0.2 | 0.3 |
| T079 | 0.375 | 0.45 |
| T083 | 1.05 | 1.3 |

**Table 3.7.** Results of STs and HCs in the final optimization.

| Element | ST Volume | k in HC | Diameter in HC |
|---|---|---|---|
| C032 | 428 | - | - |
| C044 | 507.5 | - | - |
| C050 | 600 | - | - |
| C051 | 2310 | - | - |
| C056 | 300 | - | - |
| T045 | - | 2.99 | 0.30 |
| T055 | - | 6.64 | 0.375 |

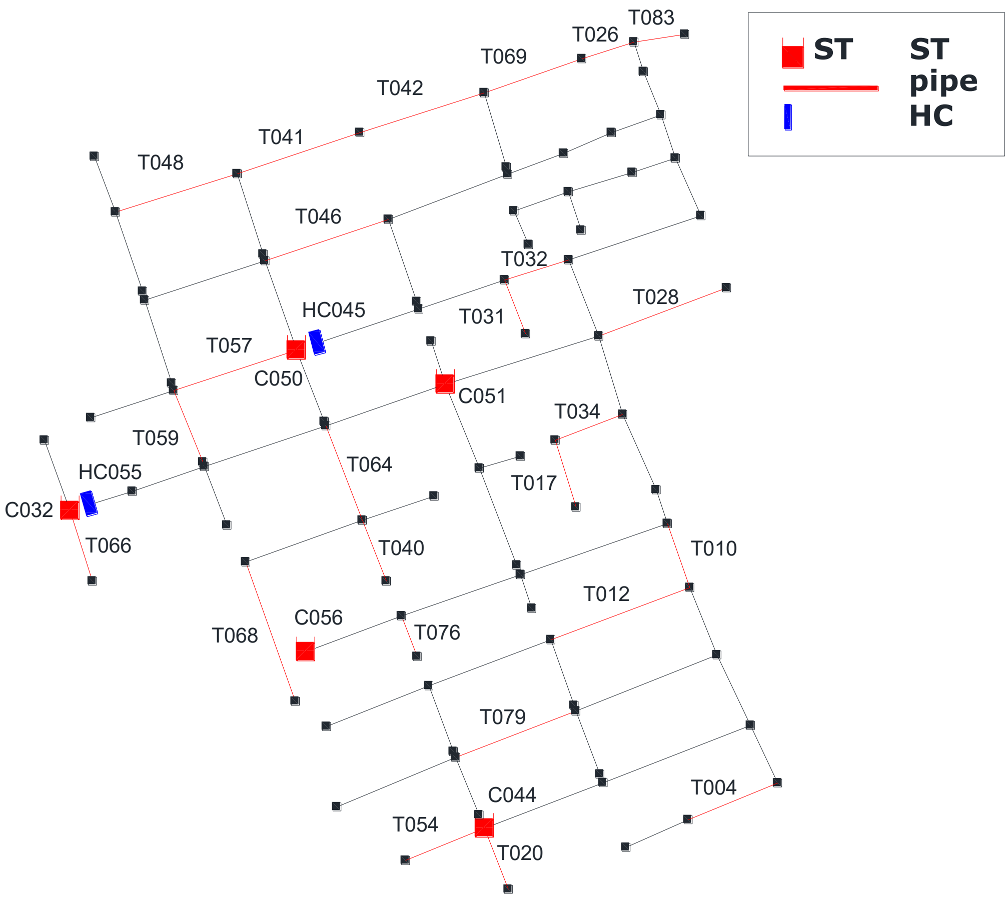


**Figure 3.15.** Final solution proposed for the Ayurá network.

Figure 3.16 compares the results when optimizing the full network without applying the SSR method (blue line) and the different iterations carried out until optimization is achieved with the proposed method (set of gray-scaled lines). Both methodologies were repeated 250 times. The figure shows on the *x*-axis the relationship of the objective function of each result with the minimum objective function found. The *y*-axis represents the accumulated frequency. The values represented correspond to the established $N_{sim}$ (250 in this case). As can be seen, the optimization process improved remarkably by applying the SSR method iteratively. Finally, the curve corresponding to the final optimization was obtained with a greater slope of the curve, which indicated that, in this scenario, the dispersion of solutions was lower. To better appreciate how the dispersion of the results decreased with the proposed methodology, the comparison of these results with the optimization without previously applying the SSR process is shown in Figure 3.17.

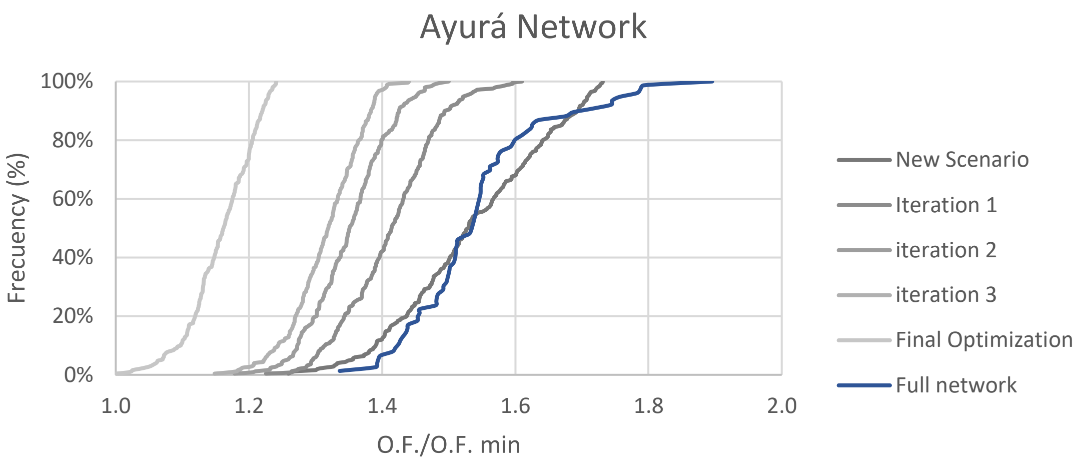


**Figure 3.16.** Comparison between the results of Ayurá (Table 3.5) of different scenarios in the SSR process and the optimization of the whole network without the application of SSR.

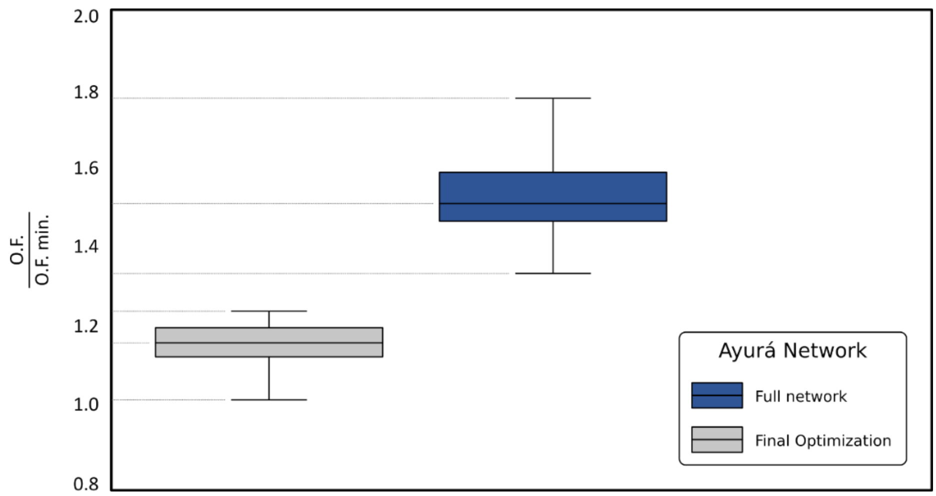


**Figure 3.17.** Comparison of the results obtained in the Ayurá (Table 3.5) network between the proposed method and optimizing without an SSR process.

## 3.4. DISCUSSION

The methodology presented in this work considers different types of DVs: pipes, STs, and HCs. Consequently, there is a large search space. To solve this problem, a process is presented to reduce this search space. The analysis of this discretization has been made considering that the sampling points cover the entire SS and that the process is applicable to any type of network. However, a previous detailed study showed that the characteristics of the network, maximum and minimum diameters installed, and available flood area can shorten the size of the options list for each DV by reducing the initial SS and decreasing the definition time of the final search region. This is one of the fields that can be explored in future work. On the other hand, to discretize the continuous DVs, two spacing values are adopted that generate two lists of options, one called rough and the other called refined. One limitation of the presented method is that the spacing has been established according to the criteria of the authors, and although it is true that covering the SS in the best way has been tried, future works should consider the establishment of this spacing by analyzing the influence of the algorithm parameters.

Another aspect to discuss in this work is the different percentages used as the probability of success when establishing the stopping criteria. The use of a low probability of success ($P_e$ = 20%) in the SSR process aims to eliminate DVs. This elimination assumes that if, with a loose value of $P_e$, the repeatability of a DV is low, it is assumed that this DV will not be part of the region of best solutions. In the figures (repeatability figures), it can be observed how the repeatability in the most promising DVs increases as the SS decreases, while the DVs that present a low repeatability disappear in subsequent iterations. These facts emphasize the value of the presented method to identify the region with the best solutions within the SS. However, the use of more demanding values of $P_e$ as the search region is reduced is presented as an interesting option to improve the efficiency of the process. This is undoubtedly an aspect that should be analyzed in depth in future work. In this work, the concept of reducing the SS by hydraulic sectors has also been introduced. This way of applying the SSR method is presented as an interesting option that allows the optimization model to work in parallel, able to define the search region faster than when analyzing the entire network, although it is true, in the optimization of the Ayurá network, that the hydraulic sectors are not clearly differentiated. Dividing the network into two parts allows us to have a manageable number of DVs by optimizing the network. Applying the SSR process at the top of the network at first and incorporating the selected DVs at the bottom part of the network reduces significantly the computational effort required. In the case of the E-Chico network, two sectors, called HS-1 and HS-2, are clearly differentiated. In this network, it can be seen how the repeatability increases in each iteration until presenting a repeatability of 100% in the selected DVs. Additionally, Figure 3.17 compares the dispersion of the solutions of the results when applying the proposed methodology in the studied networks and when optimizing the networks without applying any SSR process. In Figure 3.17, it is clearly observed that, when optimizing the complete network, the dispersion of the results is greater, having values of the objective function up to 3.7 times greater than the minimum value, while, when applying the proposed methodology, the dispersion of the results decreases significantly. The curve obtained in the final optimization has a greater slope, and the variation of the results found is reduced by about 1.50 times. In the Ayurá network (Figure 3.16), there are similar results; the optimized network without any SSR process has a greater dispersion of results, having objective function values of up to 1.90 times greater than the minimum value found. This shows us that optimizing networks with a large number of DVs increases the dispersion of the solutions. Therefore, applying the SSR process not only reduces calculation time, but also improves efficiency in optimization. These particularities were already observed by Ngamalieu et al. [38] in a previous work.

On the other hand, the results show that, when optimizing the network by sectors, the values of Л and $G_{max}$ decrease; this is because their value depends on the number of DVs analyzed by the PGA. Therefore, the calculation times and the computational effort are going to be much less than when optimizing the entire network. This shows us that the methodology can be indicated to optimize large networks. In another order of things, the results obtained from $N_{sim}$ in Table 3.5 show that the number of iterations that each simulation requires to find the solution decreases in each application of the SSR process. These results are presented in the two networks studied, so it can be said that the methodology presented improves the efficiency of the optimization. For the final optimization, using a refined optimization and a more demanding Pe, the number of simulations increases. Considering that the objective is to find the best solution in a reduced SS, this increase is fully justified. In the Ayurá network (Table 3.6), it is observed that, in each iteration, the iterations decrease, having a $N_{sim}$ = 3127 in the new scenario until $N_{sim}$ = 967 in the third iteration. Optimizing the network by sectors has clear benefits. The decrease in the objective function is clearly observed in Figure 3.17 when compared to the optimization of the network without applying the SSR process. The figure shows that the largest dispersion of the optimized network without an SSR process is found in the first quartile. On the other hand, it can be observed that the best result of the optimized network without applying the SSR process has a higher value than the worst value of the final optimization of the proposed methodology. In the Ayurá network (Figure 3.17), there are similar results, and it is observed that the highest number of results in the final optimization is in the last quartile, which reflects the suitability of the methodology.

The final optimization shows the suitability of applying the optimization methodology with the installation of STs, renewal of pipes, and installation of HCs. The use of a more demanding stopping criterion can guarantee us that the search for the best solutions in the final search region is carried out intensively. For these reasons, this form of optimization should be investigated in greater depth, as it could provide interesting results in terms of reducing calculation times in the face of this type of problem.

Lastly, technological advancement and limited resources have motivated the development of new research strategies to optimize time and economic resources. Algorithms have been consolidated as a valid tool to facilitate this task. Their use in different fields of research has been popularized in recent years. In problems of water resources, GAs have had a relevant use [76,92,144]. GAs have been applied in subjects such as water distribution systems and closely related applications, urban drainage and sewer system applications, water supply and wastewater treatment applications, applications in hydrologic and fluvial modeling, groundwater system applications, groundwater remediation, groundwater monitoring, and evolutionary computation in hydrologic parameter identification. The proposed SSR methodology considers the iterative elimination of DVs from a problem, and can be applied to other types of problems with a similar approach. This may be a contribution of the present work for future developments in the field of optimization through evolutionary strategies.

## 3.5. CONCLUSIONS

The increase in flood events in different cities of the world makes it necessary to develop methodologies to face them, considering the improvement of the systems with the lowest possible cost. The use of heuristic approaches is a good alternative to solve this type of problem. The methodology based on the optimization of the network considering the replacement of pipes, installation of STs, and inclusion of HCs has proven to be a valid alternative to solve these types of problems. To improve the efficiency of the optimization model, this work focuses on presenting a methodology for reducing the SS for solutions to improve the working efficiency of the optimization model. The application of this methodology significantly reduces the number of total iterations when compared to the initial scenario, that is, if it will perform the optimization with all of the DVs.

In the E-Chico network in particular, the SS is reduced from a magnitude of 140 to a magnitude of 12, while, in the Ayurá network, much larger than E-Chico, the SS is reduced from a magnitude of 344 to one of 82. If it is considered that the size of the SS is measured in a logarithmic scale, it can be seen that a significant reduction has been made. These results show that the SSR method is valid and advantageous to apply in optimization problems with drainage networks. For the Ayurá network, the improvement of the results can be observed more greatly when applying the proposed method than in the complete network without any previous reduction of the SS. On the other hand, if the results obtained from the E-Chico network are compared with the results obtained in a previous study [134], it can be seen that the objective function of the problem has been reduced, including the cost of flood damage. Therefore, it can be concluded that by using the method of SSR based on the use of a coarse discretization of the DVs and a lax stop criterion in the first stage, as well as a refined discretization and a demanding stop criterion in the second stage, the efficiency of the optimization model is improved. The two cases presented have been applied to drainage networks located in Colombia, and thus were expressed in terms of the local Colombian economy, the investment costs in infrastructure, and the costs associated with flood damage. In this way, formulating cost functions in monetary units is very useful for decision makers in the development of a rehabilitation project.

New trends are focused on source control by means of LID techniques. Future works must address the possibility of combining the strategy presented in this work with another focused on the reduction of runoff using components such as green roofs, pervious pavement, or infiltration structures.

Finally, the results obtained show a good solution for a previously defined rain. Different results will be obtained for other design storms. Therefore, there is no single solution to the problem, and the initial approaches to the problem will be made in accordance with design criteria and local regulations.

**Supplementary Materials:** The following supplementary materials are part of this Chapter and are available in Appendix III of this thesis. Figure A3.1.1. Representation of E-Chico drainage network; Figure A3.1.2. Design storm based on the Alternating Blocks Method used in E-Chico network; Figure A3.2.1. Representation of Ayurá drainage network; Figure A3.2.2. Design storm based on the alternating blocks method used in Ayurá network; Table A3.1.1. Data for nodes and subcatchments in E-Chico network; Table A3.1.2. Data for conduits in E-Chico network; Table A3.1.3. Time series for the design storm used in E-Chico network; Table A3.2.1. Data for nodes in Ayurá network; Table A3.2.2. Data for subcatchments in Ayurá network; Table A3.2.3. Data for conduits in Ayurá network; Table A3.2.4. Time series for the design storm used in Ayurá network.

# CHAPTER 4.

# ECONOMIC ANALYSIS OF FLOOD RISK APPLIED TO THE REHABILITATION OF DRAINAGE NETWORKS

# Preamble

The article shown in Chapter 4 presents a different form of economic analysis than those used in previous chapters. The analysis established for the first two articles considers two types of costs, on the one hand infrastructure costs and on the other hand the costs resulting from the flooding generated by the rain studied. These two types of costs form an objective function that is minimized by the optimization model to find the best result. To calculate the costs of flood damage, a rain is used to perform the hydraulic analysis of the network, determining the level of flooding in each node of the network. Then, using an equation obtained from an average damage – depth curve for the study area, the cost of flood damage is determined. While the infrastructure costs are the total costs required in the design period, thus defining the objective function to be minimized.

The methodology is good and allows us to improve taking the most unfavorable situation as a reference. However, it does not consider damage that may occur with minor rainfall that will appear in the design period and that its damage is not accounted for when evaluating the objective function. For this reason, a new way of accounting for this damage is presented in the article, based on the estimation of the annual risk of floods and the annualized investment in infrastructure. The estimation is made by relating the exceedance radius for different return periods and the cost of the associated damage for the rain of each return period. On the other hand, to improve the precision of the results in this work, a discrimination of the cost of the damages caused by floods is carried out according to the different land uses in the study area. With these actions it is intended to take an important step in the presented methodology that generates results closer to real world problems and that is a tool that helps the management of drainage networks.

*This article was published as: Bayas-Jiménez, L.; Martínez-Solano, F.J.; Iglesias-Rey, P.L.; Boano, F. Economic Analysis of Flood Risk Applied to the Rehabilitation of Drainage Networks. Water 2022, 14, 2901. Available in open access at: https://doi.org/10.3390/w14182901*

## 4.1. INTRODUCTION

Urban drainage infrastructure is built at high cost and represents an important asset of cities that is expected to have a long service life. However, the occurrence of floods in cities is becoming more and more evident, generating concern for engineers and managers of city drainage systems. The increase in the frequency of extreme rainfall events is notorious; many studies have delved into the causes of this increase [145,146] and are able to conclude that it is due to an increase in rainfall intensity, mainly due to climate change. In addition to this fact, the growth of cities has decreased the number of green spaces, replacing them with impervious surfaces that increase runoff, aggravating the flooding problem [11,147-149]. These conditions have generated frequent floods that generate heavy losses in cities [111,150,151]. O'Donnell and Thorne [130] mention that, by 2050, 68% of the world's population will live in urban areas, so taking measures against flood risk is of primary importance. Rehabilitating drainage networks is a topic of growing interest for researchers; the use of STs to mitigate runoff peaks in extreme rainfall events has proven to be an efficient alternative [28,134]. For this reason, their use has been considered in the present work in conjunction with the classical approach of renovating pipes. Furthermore, the inclusion of CHs to rehabilitate networks is considered. For the optimization process of drainage networks, researchers have used different methodologies, highlighting the use of evolutionary algorithms that give good results in water resource research [92]; of these, GAs show great performance in the search for the best solutions due to their adaptation to complex landscapes [152,153]. The PGA used in this work has shown robustness and efficiency in finding solutions, and is easier to implement in optimization models [91]. However, computation times can be very long due to the large SS that the algorithm must explore. To improve the performance of the algorithms, some strategy must be implemented to optimize the search. One way to do this is to decrease the SS by identifying the best regions containing the best solutions and discarding the less attractive ones. Different works have been carried out with this method [78,142], demonstrating that these strategies can improve the efficiency of optimization models. In this way, in a previously performed work, Bayas-Jiménez et al. [152] present a methodology for SSR focusing on the recursive reduction of DVs with the use of reduced option lists to identify the best search regions. In this work, an SSR method based on the method of Bayas-Jiménez et al. [152] is used, focusing on reducing the SS in large networks to improve the efficiency of the rehabilitation methodology.

On the other hand, in the work carried out by Bayas-Jiménez et al. [134], the authors present a methodology to rehabilitate drainage networks and improve the efficiency of the optimization model. However, one of the drawbacks of this methodology is the joint evaluation of total investment costs and damage costs for a single rainfall. Although it is a valid methodology, which shows in monetary amounts the advantages of rehabilitating the network using the highest intensity rainfall that the drainage system will face, it does not show us the cost of flood damages with rainfall lower than the return period (T) used. These lower intensity rains can present significant damages in the study area, as rightly mentioned by Freni et al. [154]. For this reason, and with the objective of improving the methodology, this work focuses on determining the annual damage cost that can be caused by floods and annualizing the cost of the required investment. To determine the annual cost of flood damage, we have reviewed the work done by Zhou et al. [68] and Olsen et al. [62], who present models to identify low-cost adaptation measures that mitigate events with high annual risk. In this way, the cost of flood risk is calculated by integrating the area under the curve generated by flood damage in the return periods considered. Finally, a solution is obtained that integrates the annual cost of the flood risk and the annual investment that would be required to face it. This work also emphasizes the need to implement a SSR strategy in the methodology so that a method that significantly reduces calculation times is used. It is important to mention that the optimization model uses the SWMM model to analyze the network; this model completely solves the Saint-Venant equations. For the hydraulic analysis with SWMM, the dynamic wave model is used with the Darcy–Weisbach as the main force equation. The methodology also assumes that flooding occurs by water stagnation, i.e., that the total volume of runoff enters the manholes through the gutters of the system. However, this methodology has certain limitations that must be considered:

- The hydrologic study and the runoff model are beyond the scope of this work.
- No changes in the network topology are considered. The actions allowed to improve the network are the replacement of pipes, the installation of STs and the inclusion of HC elements in the network.
- The networks in which this methodology can be applied must be gravity-fed. Networks with pumping systems are not considered in this study.
- The hydraulic model is considered as a datum; its parameters and initial conditions are not questioned.

With this work, the authors intend to show a robust methodology that encompasses solutions to the difficulties that may arise in the rehabilitation of drainage networks, providing different alternatives to reduce calculation times and ensure that the optimization criterion satisfies the expectations of network managers.

## 4.2. MATERIALS AND METHODS

The methodology considered carrying out different actions in the drainage network to reduce the risk of flooding in the studied area. These actions were: the replacement of pipes by others of larger diameter; the construction of small STs to replace the existing wells; and the installation of HC elements to slow down the flow of water in the network. To determine where these elements would be implemented and what characteristics they would have, an optimization model was used. The model used a PGA as an optimization engine [104]. The hydraulic analysis of the model was performed with the SWMM model [71] connected to the PGA through a toolkit developed by Martínez-Solano et al. [119]. This way of rehabilitating drainage networks was presented in a previous work by Bayas-Jiménez et al. [134], demonstrating its advantages by decreasing the cost of flood damage. However, this methodology analyzes flood costs for a single design rainfall. Although it is true that this rainfall event is the one that is going to demand the most from the system, the methodology does not consider other rain events of lesser intensity that may occur with greater probability in the design period and could generate floods. To solve this problem, this work modified the way of quantifying flood damage by focusing on the analysis of flood risk. Land use and rainfall magnitude are the most important characteristics in flood risk analysis. The study of these characteristics in urban areas and the relationship between them has resulted in the so-called damage–depth curves (Figure 4.1a) that relate the damage in monetary units or percentage and the depth of flooding. These curves are intended to represent the vulnerability of cities to flood risk [66].

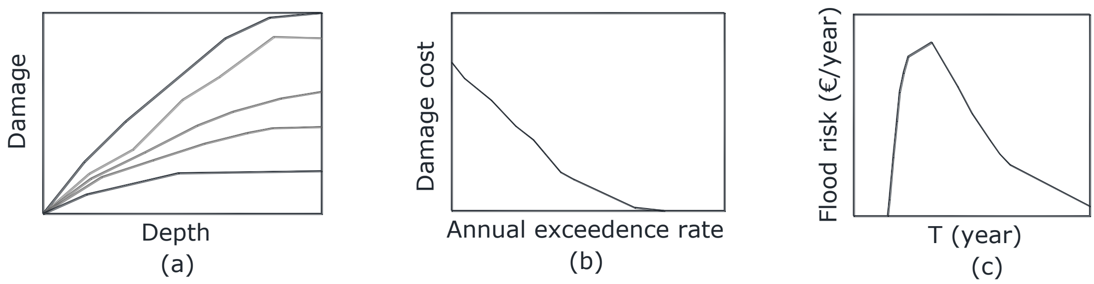


**Figure 4.1.** Damage–Depth curve (a), Damage–annual exceedance rate curve (b) and Flood risk density curve (c).

One tool used as an indicator of vulnerability is the EAD [155]. This method estimates the average flood damage calculated for a series of events. The method considers that if the annual exceedance rate can be expressed as the inverse of T and the damages in monetary units, different values of flood damages can be calculated for different return periods, thus defining a curve (Figure 4.1.b). In this way, the average annual flood risk can be calculated by integrating the area under this curve [156]. In the work carried out by Olsen et al. [62], the authors compared different methods for estimating flood risk in urban drainage systems. In addition to these comparisons, the authors emphasize that, as return periods increase, flood damage costs also increase, but the annual exceedance rate also decreases, as can be seen in the flood risk density curve (Figure 4.1.c). It was necessary to integrate this way of evaluating flooding into the methodology by relating it to the annualized infrastructure investment costs. With this objective in mind, an optimization model was developed that could find the best solution to the raised issue.

### 4.2.1. Optimization model

The optimization model used a PGA as a search engine; this type of algorithm, unlike traditional GAs, uses an integer encoding. The PGA was connected to the SWMM model through a toolkit to perform a series of simulations to find an optimal solution to the problem. To achieve this, the PGA evaluated an objective function composed of two types of cost functions: the annualized costs of infrastructure investment and the costs of the annual cost of flood risk. This implied that design rainfalls must be defined in advance for different return periods. The rainfall was constructed by means of a design hyetograph obtained through the analysis of intensity–duration–frequency (IDF) curves. These rainfalls were introduced into the network to be analyzed by the model. Figure 4.2 summarizes the operation of the optimization model. The optimization process was iterative and required establishing an end point for a process called the convergence criterion ($G_{max}$). This criterion considers that when the value of the objective function does not change during a certain number of generations, the objective function has reached its minimum and the process ends. $G_{max}$ is explained in depth in the work presented by Bayas-Jiménez et al. [152].

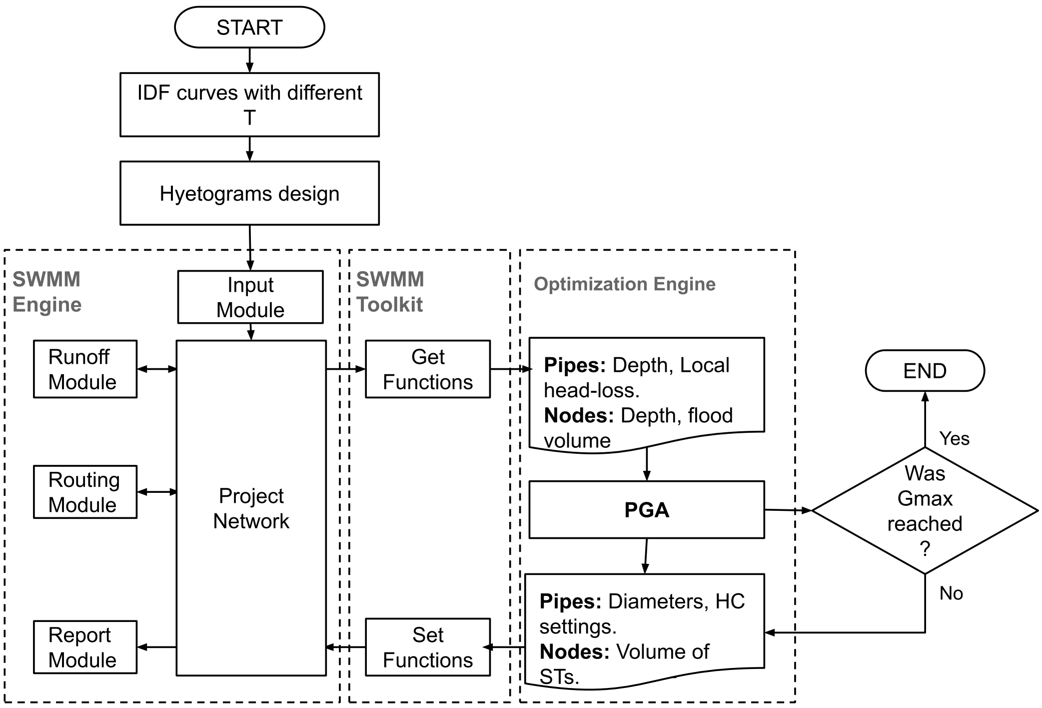


**Figure 4.2.** Schematic diagram of the optimization model.

#### *4.2.1.1. Decision variables*

Since this methodology used a PGA for optimization, the DVs were required to take values from lists of options with discrete values. In order to perform the network optimization, it was necessary to clearly define the DVs used in this methodology. The methodology considered three types of DVs. The first type of DVs considered was pipe diameter. In the optimization process, the pipes selected to be optimized could take values from the existing diameter range $ND_{max}$. The previously defined list of options for optimization, called ΔND, was composed of a small number of diameters immediately larger than the analyzed pipe diameter. This decision was taken because pipes in the optimization process would only take values larger than the current diameter, so defining lists using the whole range of pipes would only increase the computational effort unnecessarily; with this action, the size of the problem was considerably decreased.

The second type of DVs considered was the storage capacity of the STs. This work considered the depth of the STs to be the same as the existing manholes, so the cross section of the STs was defined as a DV. In the optimization process, the nodes selected to be optimized ns could take values from a previously defined list of options. As shown in Section 2.2, the methodology was composed of two stages. In the first stage, a coarse option list $NS_0$ was used and for the second stage, a refined option list $NS_{max}$ was used. Finally, the third type of DVs considered the head loss values that the HC element installed in the pipes could generate. In the optimization process, the selected pipes $v_s$ could have HCs with a degree of openness from a previously defined option list Nθ.

*4.2.1.2. Cost Functions*

In order to define the objective function that the optimization model would evaluate, the first step was to establish the cost functions of the investments in infrastructure and the cost of the flood risk.

The first infrastructure investment cost function was the replacement of pipes. To determine this cost, the cost of acquisition and installation of pipes was analyzed for different diameters.

According to the values obtained, an equation was defined that fits a second-degree polygonal curve and is presented as Equation (4.1).

$$\mathrm{C_p(D_i)} = \left(\alpha\, \mathrm{D_i}^2 + \beta\, \mathrm{D_i} - \gamma\right) \mathrm{L_i} \tag{4.1}$$

In the equation, $C_p$ ($D_i$) represents the pipe replacement cost in euros, $D_i$ is the pipe diameter and $L_i$ represents the pipe length in meters. The coefficients α, β and γ are adjustment coefficients corresponding to each project.

The second infrastructure investment cost function was the cost of STs. To define this function, the cost of building tanks of different sizes was analyzed. With these data, a cost function composed of two terms was determined and is shown in Equation (4.2).

$$\mathrm{C_T(V_i)} = \mathrm{C_{min}} + \mathrm{C_{var}}\mathrm{V_i}^{\omega} \tag{4.2}$$

where $C_T$ ($V_i$) represents the cost in euros of the construction of a ST. $C_{min}$ represents the minimum cost of building a ST. $V_i$ is the flood volume that the tank must store in cubic meters. $C_{var}$ and ω are coefficients corresponding to the analyzed project. The third structural investment cost function determined for this work was the cost of HC. To define this function, the cost of purchasing and installing valves of different diameters was analyzed. This analysis determined a second-degree polynomial function, shown in Equation (4.3).

$$C_v(D_i) = \sigma {D_i}^2 + \mu\, D_i + \varphi \tag{4.3}$$

where $C_v$ $(D_i)$ is the cost of the HC in euros, $D_i$ is the diameter of the pipe where the HC would be installed, in meters, and σ, μ and φ are adjustment coefficients of the analyzed project.

On the other hand, to account for the reduction in investment in infrastructure, an annual amortization factor Λ was required that affects each cost function. In this work, the expression shown by Steiner [159] was used and is shown in Equation (4.4).

$$\Lambda = \frac{r}{1 - (1 + r)^{-t}} \tag{4.4}$$

In the equation, r is the annual interest and t is the time in years in which the investment is expected to be recovered.

Determining flood costs is a complicated task, since there are many aspects to be considered and they are commonly divided into two categories: intangible damages and tangible damages. Tangible damages are those that can be expressed in monetary terms and are those that have been widely used in the analysis of flood damages in urban areas. One of the most widely used techniques for flood damage analysis is to use flood depth or flood level as a reference. The analysis based on the flood level allows the reduction of flooding and the cost of flooding, depending on the flood zone. An expression that calculates the cost of flood damage as a function of flood depth and land use is the damage–depth curve; thus, an expression that allows this calculation is presented in Equation (4.5).

$$C_y(y_i) = C_{max}\, A_i \left(1 - e^{-\lambda \frac{y_i}{y_{max}}}\right)^{\upsilon} \tag{4.5}$$

In Equation (4.5), $C_y$ $(y_i)$ represents the damage cost in euros and $y_{max}$ is the maximum depth at which the flooding reaches the maximum damage in meters. $C_{max}$ is the maximum flood damage cost obtained when $y_{max}$ is reached, Ai is the flood area of the analyzed subcatchment in square meters, $y_i$ is the reached depth of the analyzed node in meters and λ and υ are adjustment coefficients based on historical flood damage data.

Once the cost of flooding had been defined, to proceed in analyzing the flood risk, we started from the work presented by Arnbjerg-Nielsen and Fleischer [64], who proposed a way of estimating the annual damage by relating the cost of flood damage from rainfall of various return periods. The authors conclude that the annual damage can be obtained by integrating the area under the curve obtained from plotting the flood cost ($C_y$ $(D_i)$) as a function of its annual exceedance rate (p). In a more recent work, Olsen et al. [62] mention that a good approximation of the curve can be obtained with a log-linear relationship and that, when integrated, it can show the average annual cost of flood risk; Figure 4.3 shows this relationship.

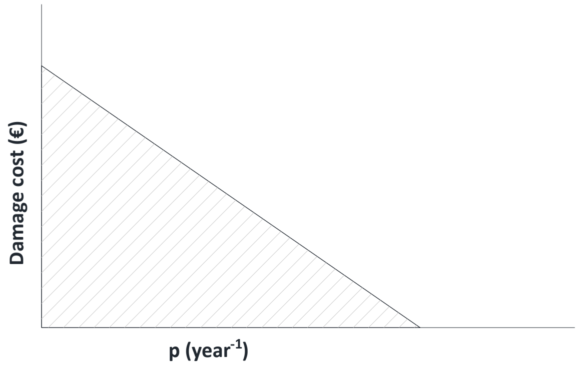


**Figure 4.3.** Annual cost of flood risk as the area under the curve in a log-linear relationship.

The equation of the line obtained from this assumption takes the form of the expression shown in Equation (4.6), where a and b are the coefficients of the line.

$$C_y(y_i) = a\ln[p] + b \tag{4.6}$$

To integrate Equation (4.6), the lower limit 0 was defined as representing the annual exceedance rate associated with an event, with an infinite value of T and $p_0$ representing the annual exceedance rate for which flood damage begins to occur (Equation (4.7)). Equation (4.8) shows how to calculate the annual flood risk cost $C_F(p)$.

$$C_F(p) = \int_0^{p_0} (a\ln[p] + b)\ dp \tag{4.7}$$

$$C_F(p) = a\,(p_0\ln[p_0] - p_0) + b\,p_0 \tag{4.8}$$

Finally, with all the costs defined, an objective function that the optimization model sought to minimize was proposed. Equation (4.9) shows the objective function.

$$OF = \Lambda\left[C_p(D_i) + C_T(V_i) + C_v(D_i)\right] + C_F(p) \tag{4.9}$$

## 4.2.2. Optimization Process

### *4.2.2.1. Search space reduction*

The SS basically depends on two elements: the DVs and each of the values that these DVs can adopt. When using a PGA, it is mandatory to discretize the SS, i.e., the values that the DVs take must be chosen from a list of options composed of a finite number of values. In this way, the discretization must be carried out carefully. Bayas-Jiménez et al. [152] mentions that an excessive refinement of the SS would greatly increase the SS and would require a very large computational effort. However, if the discretization is coarse, the precision of the results is diminished. The authors also propose an expression to determine the size of the SS, presented in Equation (4.10).

$$\mathrm{SS} = \mathrm{m_s}\,(\log \Delta\mathrm{ND}) + \mathrm{n_s}\,(\log \mathrm{NS}) + \mathrm{v_s}\,(\log \mathrm{N}\theta) \tag{4.10}$$

where ΔND, NS and Nθ represent the options lists used for pipes, STs and HCs, respectively. Some work has been done with the objective of identifying the areas of the SS that contain the best solutions. The works focus on two ways to reduce the SS, some focusing on the change of the search region [78,157] and others focusing on changing the algorithm's operation [96,99]. In this work, a method based on the change of the search region was used. In summary, the method reduced the SS by identifying and eliminating DVs that were not part of the optimal search region.

Due to the fact that, in networks of large sizes, the computational effort can be important and consume significant computational time, the SSR method called clustering is presented based on the work presented by Bayas et al. [152]. This method allows a reduction in the search region based on the identification of the most promising regions in a parallel way in the drainage network.

Drainage networks are generally made up of branches that collect rainwater from specific areas previously defined in the design stage of the drainage network. The water carried by these branches is discharged into a main network that collects the water from all the branches and transports it to treatment plants. Figure 4.4 shows an example of this network configuration.

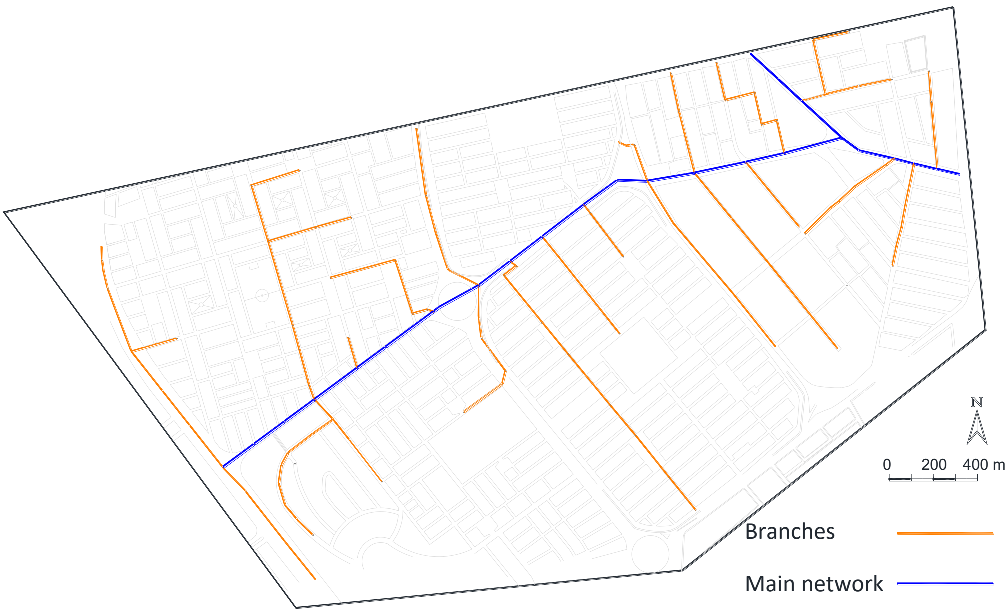


**Figure 4.4.** Drainage network with identification of branches and main network.

It can be said that the network can be viewed as a set of sectors. If these sectors can be identified, a particular analysis of them can be performed to reduce the number of DVs within the sector and, consequently, reduce the overall SS. To perform the network analysis, it was necessary to make changes in the optimization model to analyze each sector that made up the drainage network in parallel. Once the sectors were fully defined, a series of evaluations were performed independently and in parallel with coarse option lists $NS_0$ for nodes. In the case of pipes, and in order to optimize the process, a ΔND list of diameters immediately larger than analyzed pipe was used.

The results obtained were analyzed and the selection criterion proposed by Bayas-Jiménez et al. [152] was applied. In the same way, a lax $G_{max}$ was used because the objective was to eliminate DVs quickly and not to optimize the network. This process is applied iteratively until DVs could not be reduced further. Once the best regions of each sector were defined, a new search was made in the complete network, with the $n_s$ and $m_s$ selected in the sectors to finally delimit the optimal search region. It should be noted that the clustering method required significant computational use, so the method required the use of a cluster server to take advantage of its characteristics. Thus, despite the fact that several analyses were carried out, when they were carried out at the same time, and when working with sectors with fewer DVs, results were achieved in less time.

*4.2.2.2. Final Optimization*

Finally, after applying the SSR method, a final optimization was performed to find the solution closest to the optimum. HCs were included in this stage; since their installation was linked to the installation of an ST, they were not considered in the SSR process. Likewise, at this stage, each of the DVs that made up the final search region were required to be explored in depth. Consequently, a refined (or full option) list $NS_{max}$ was used for STs. In the case of pipes, the same ΔND range of diameters immediately larger than the analyzed pipes was used. Finally, for the HCs, a list of options Nθ was used that defined the degrees of opening that the element could adopt. At this stage, a more demanding $G_{max}$ was also used to find the closest solution to the optimum. This is the process that was followed to obtain the solution to the problem analyzed with the proposed methodology.

### 4.2.3. Case Studies

*4.2.3.1. Balloon Network*

The Balloon network is part of a drainage network located in a city in northern Italy. The network covers an area of 40.88 hectares. With a length of 1.85 km, the network is in a flat area whose highest point has an elevation of 229 m above sea level and the lowest point of 221 m above sea level. The network is made up of 71 pipes and 70 nodes. A total of 75 drainage sub-basins discharge their waters into the network. Figure 4.5 shows a schematic of the Balloon network. The entire network is gravity-fed. One problem with the network is the low slope of some of the pipes due to the topographical conditions of the area. To improve network circulation, the network has been designed with deep manholes reaching depths of more than 10 m. Despite this, the network has frequent flooding problems and needs to be rehabilitated. With the methodology and parameters used in this work, the network would present costs associated with the risk of flooding of 733,282 euros per year.

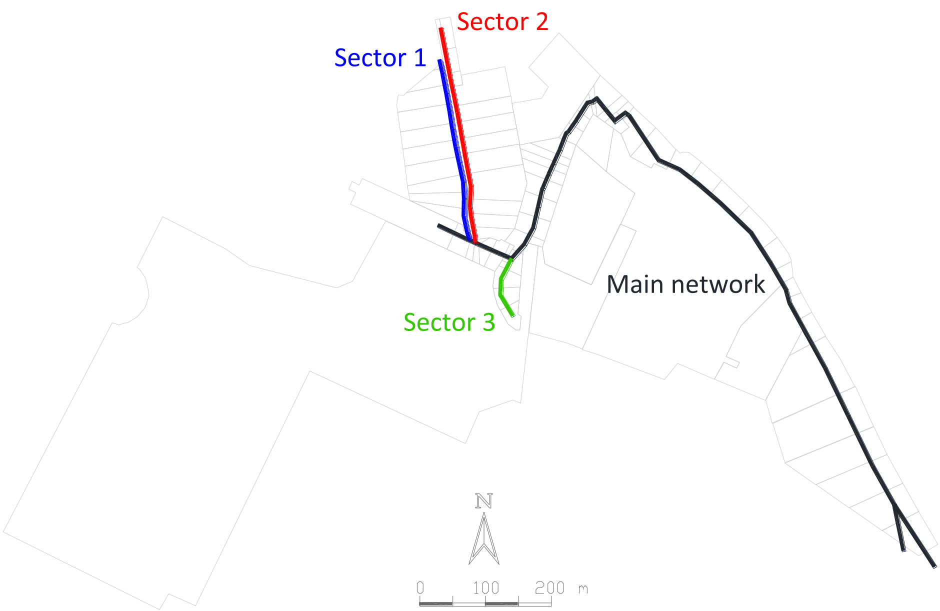


**Figure 4.5.** Balloon Network.

For the analysis of the network, design rainfalls were constructed using the alternating block method for return periods of 2, 5, 10, 20, 50 and 100 years. The IDF curves for the return periods studied are shown in Figure 4.6. Similarly, the land uses and the percentage they occupy in the study area are shown in Table S3 of the supplementary material of this work.

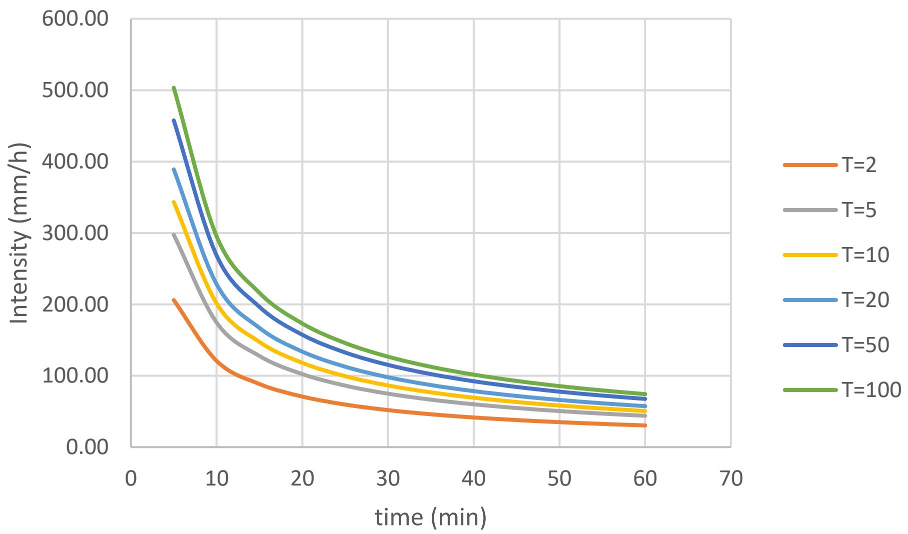


**Figure 4.6.** IDF Curves studied for Balloon network.

*4.2.3.2.ES-N Network*

The ES-N network is located in the city of Bogotá, Colombia. The network is made up of 385 nodes, 385 conduits and 385 hydrological sub-basins covering an area of 123.24 ha (Figure 4.7). The network has a total length of 20.11 km. The topography of the area is relatively flat with an average slope of 0.39%. However, the network has been designed to operate entirely by gravity, with pipes located more than 4 m deep. The network is made up of circular pipes with diameters ranging from 0.20 m to 1.40 m. Considering the methodology presented in this work, the network would present costs associated with the risk of flooding of 118,955 euros per year.

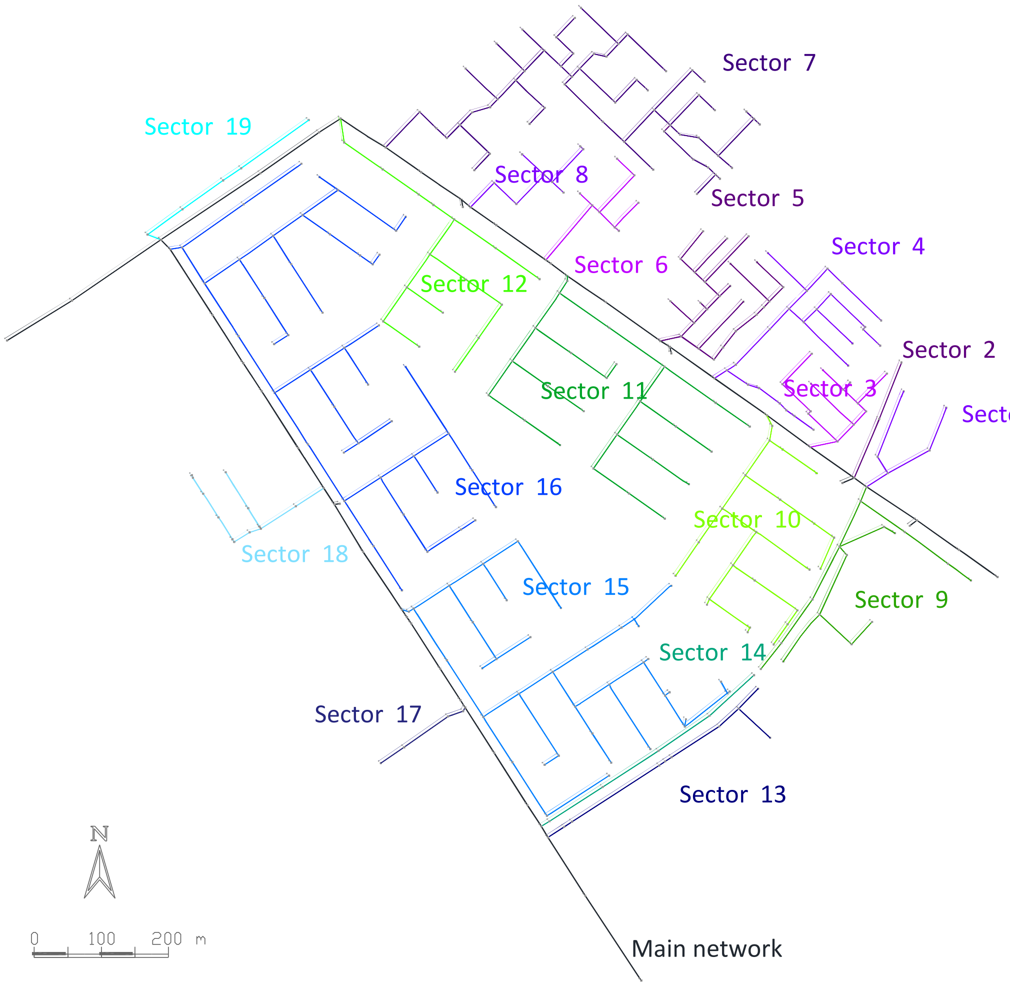


**Figure 4.7.** ES-N Network.

For the case study, two rainfalls were defined, designed with two return periods of 50 and 100 years and calculated by the method of alternating blocks with 10-minute intervals. Rainfall was calculated from previously defined IDF curves. The curves obtained are shown in Figure 4.8. On the other hand, for the network study, the percentage of different land uses in the study area were established. Table S6 of the supplementary material shows these land uses.

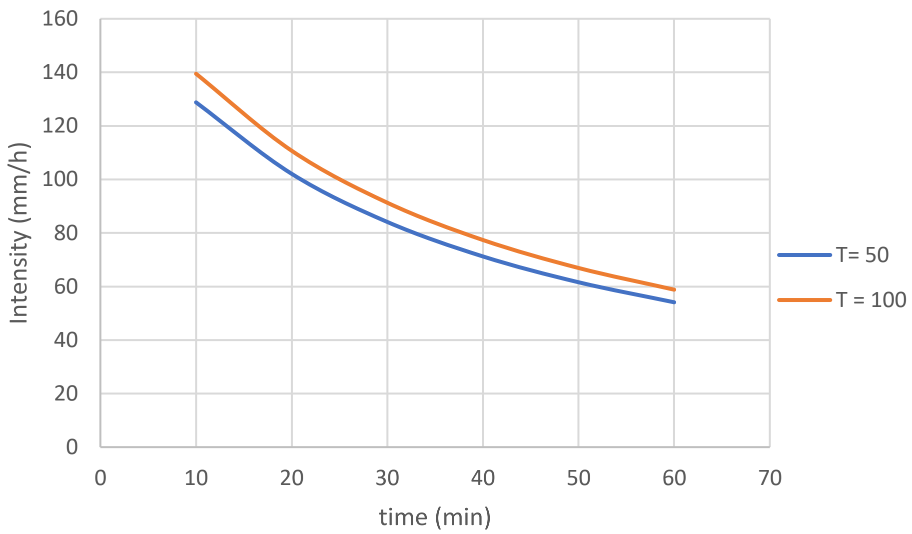


**Figure 4.8.** IDF curves studied for ES-N network.

*4.2.3.3 Investment costs*

To define the coefficients of the cost function, a study was conducted on the prices of pipes of different commercially available diameters, as well as the cost of their installation. Figure 4.9 shows the cost curve of the pipes of the existing diameters per linear meter and the adjustment of the curve produced by these values. The same graph shows the equation with the coefficients obtained.

To determine the cost function of the STs, a study was conducted on the cost of the construction of these tanks of different sizes, including the excavation and removal of the excavated material. According to these costs, the curve shown in Figure 4.9 was determined, as well as the expression with the coefficients obtained.

Similarly, a study was conducted on the cost of gate valves, accessories and complementary installations necessary for the installation of HCs in pipelines. Figure 4.9 shows the costs of different HCs with commercially available diameters. The equation with the coefficients obtained is also shown.

As for the annual amortization factor, considering the design period and the type of construction, an interest rate of 3% and an investment return time of 20 years was fixed.

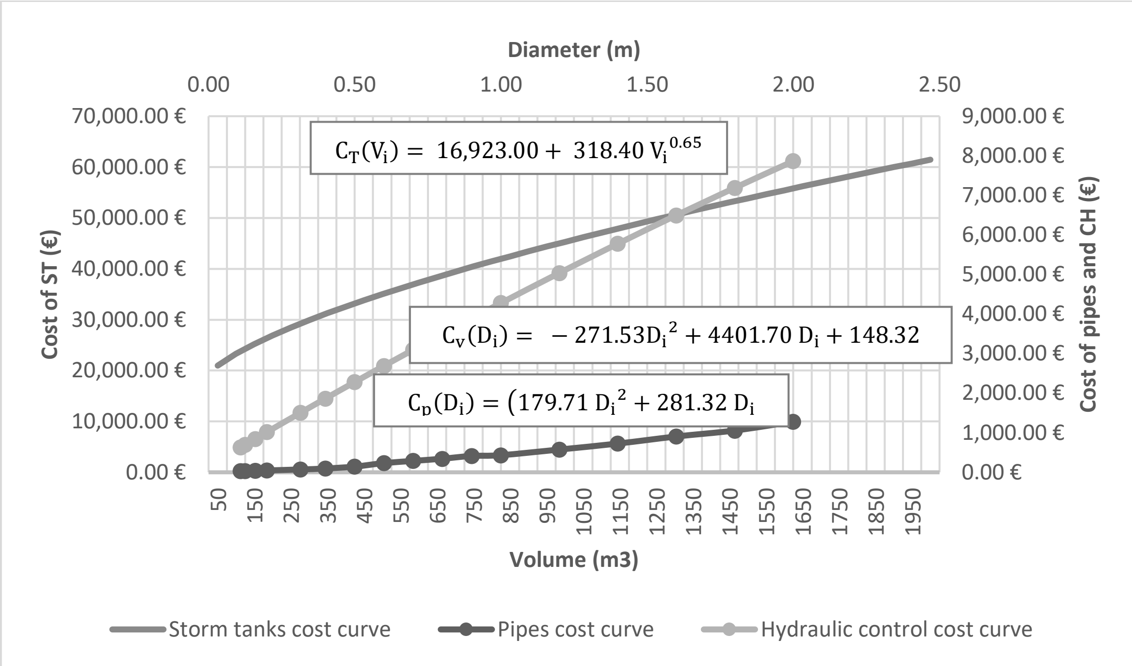


**Figure 4.9.** Cost curves of pipelines, STs and HCs for the case study.

### *4.2.3.4. Flood Costs*

For the study of flood costs, the damage–depth curves presented by Martínez-Gomariz et al. [158] were analyzed. The authors present a series of curves for different types of buildings. Taking these curves as a reference, Equation (4.5) was used to determine the flood damage cost for different land uses. The expression adjusted quite well to the values that the authors present. Table 4.1 shows the goodness of fit. Figure 4.10 shows the damage–depth curves obtained. Thus, all the cost functions required for the study of risk in economic terms for the developed model were defined. The coefficients used to define the curves for the different land uses analyzed are shown in Table 4.2.

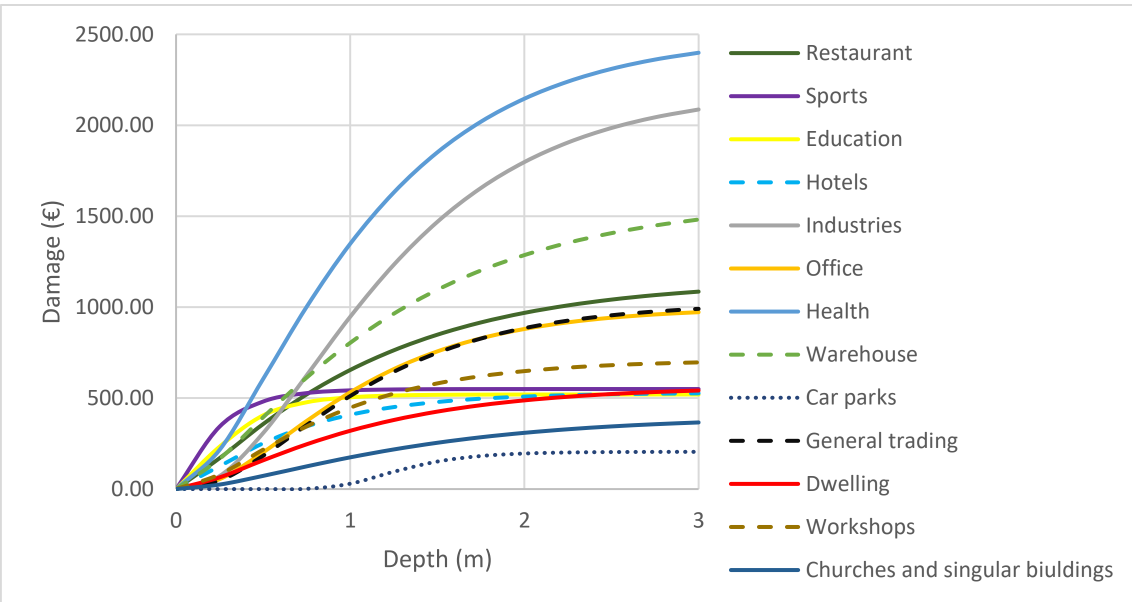


**Figure 4.10.** Damage–depth curve for the case study.

**Table 4.1.** Goodness of fit for the different land uses with Equation (4.5).

| Type | SSE | R-square | Adjusted R-square | RMSE |
|---|---|---|---|---|
| Restaurant | 1.01E+04 | 0.99 | 0.99 | 44.97 |
| Sports | 2.07E+03 | 0.99 | 0.99 | 18.59 |
| Education | 5.40E+01 | 1.00 | 1.00 | 3.00 |
| Hotels | 8.46E+02 | 1.00 | 1.00 | 13.01 |
| Industries | 1.25E+05 | 0.97 | 0.97 | 157.90 |
| Office | 1.95E+04 | 0.98 | 0.97 | 62.49 |
| Health | 5.40E+04 | 0.99 | 0.99 | 103.90 |
| Warehouse | 1.94E+04 | 0.99 | 0.99 | 62.31 |
| Car parks | 4.58E+02 | 0.99 | 0.99 | 9.57 |
| General trading | 4.34E+03 | 1.00 | 0.99 | 29.44 |
| Dwelling | 9.02E+03 | 0.97 | 0.96 | 42.48 |
| Workshops | 2.47E+03 | 0.99 | 0.99 | 22.24 |
| Churches and singular buildings | 2.63E+03 | 0.98 | 0.97 | 22.93 |

**Table 4.2.** Coefficients of equation (4.5) for different land uses.

| Land Uses | $C_{max}$ | $y_{max}$ | $\lambda$ | $\upsilon$ |
|---|---|---|---|---|
| Restaurant | 1150 | 2.20 | 2.30 | 1.30 |
| Sports | 550 | 1.00 | 4.50 | 1.20 |
| Education | 520 | 1.10 | 4.50 | 1.80 |
| Hotels | 530 | 2.20 | 3.90 | 1.40 |
| Industries | 2200 | 2.20 | 2.89 | 2.69 |
| Office | 1000 | 2.00 | 3.00 | 2.50 |
| Health | 2500 | 2.30 | 2.94 | 1.89 |
| Warehouse | 1600 | 1.80 | 1.80 | 1.50 |
| Car_parks | 205 | 2.00 | 7.38 | 76.74 |
| General_trading | 1025 | 2.00 | 2.90 | 2.60 |
| Dwelling | 565 | 2.00 | 2.45 | 1.63 |
| Workshops | 710 | 1.50 | 2.30 | 1.90 |
| Churches | 400 | 2.70 | 2.77 | 1.87 |

## 4.3. RESULTS

### 4.3.1. Balloon Network

Before applying the SSR method, the sectors that make up the Balloon network and the size of SS are identified. The total network has a magnitude of SS of 233 and 3 sectors are identified that discharge their waters to the main network. Table 4.3 summarizes the elements that make up each sector, the DVs and the magnitude of SS. Figure 4.5 shows the sectors and the main network that make up the Balloon network. First, to each of the sectors, the parallel SSR method is applied to decrease the number of DVs. Table 4.3 also shows the reduction in the magnitude of SS in each of the sectors when applying the clustering method.

**Table 4.3.** Elements, magnitude of SS and percentage of reduction of the sectors that make up the Balloon network.

| **Sector** | **Number of Pipes** | **Number of Nodes** | **DV** | **SS** | **Reduction of SS in clustering process** |
|---|---|---|---|---|---|
| Sector 1 | 11 | 11 | 33 | 36 | 100% |
| Sector 2 | 12 | 12 | 36 | 40 | 96% |
| Sector 3 | 4 | 4 | 12 | 13 | 100% |
| Main network | 44 | 43 | 130 | 144 | |
| Total | 71 | 70 | 211 | 233 | |

After the initial reduction by sectors, the SSR method is applied to the network iteratively until the final search region is defined. Once the SS is reduced, we proceed to the final optimization, performing a series of simulations to obtain the best possible solution. Figure 4.11 shows the stages of the SSR in the Balloon network, the number of DVs and the magnitude of SS at each stage of the SSR process, as well as the final solution. Table 4.4 shows the terms that compose the objective function of the solution found and the characteristics of the elements to be installed. Figure 4.12 illustrates the elements to be installed in the network.

| | | | | | | | | | | | |
|---|---|---|---|---|---|---|---|---|---|---|---|
| C1 | C2 | C3 | C4 | C5 | C6 | C7 | C8 | C9 | C10 | C11 | C12 |
| C13 | C14 | C15 | C16 | C17 | C18 | C19 | C21 | C22 | C23 | C24 | C25 |
| C26 | C27 | C28 | C29 | C30 | C31 | C32 | C33 | C34 | C35 | C36 | C37 |
| C38 | C39 | C41 | C42 | C45 | C46 | C58 | C59 | C60 | C61 | C62 | C63 |
| C64 | C65 | C66 | C67 | C68 | C69 | C70 | C71 | C72 | C73 | C74 | C75 |
| C76 | C77 | C78 | C79 | C80 | C81 | C82 | C83 | C84 | C85 | C86 | N1 |
| N2 | N3 | N4 | N5 | N6 | N7 | N8 | N9 | N10 | N11 | N12 | N13 |
| N14 | N15 | N16 | N17 | N18 | N19 | N20 | N21 | N22 | N23 | N24 | N25 |
| N26 | N27 | N28 | N29 | N30 | N31 | N32 | N33 | N34 | N35 | N36 | N37 |
| N38 | N39 | N41 | N43 | N45 | N46 | N47 | N48 | N49 | N50 | N51 | N52 |
| N53 | N54 | N55 | N56 | N57 | N58 | N59 | N60 | N61 | N62 | N63 | N64 |
| N65 | N66 | N67 | N68 | N69 | N70 | N71 | N72 | N73 | HC75 | | |

| Color Key | Description | Pipes | Nodes | HC | DVs | S |
|---|---|---|---|---|---|---|
| | DVs eliminated in the analysis by sectors | 27 | 22 | 22 | 71 | 76 |
| | DVs in the first iteration | 41 | 44 | 44 | 129 | 143 |
| | DVs selected in the first iteration | 8 | 8 | 8 | 24 | 26 |
| | DVs selected in the second iteration | 4 | 4 | 4 | 12 | 13 |
| | DVs in the final Solution | 4 | 3 | 1 | 8 | - |

**Figure 4.11.** SSR in Balloon network.

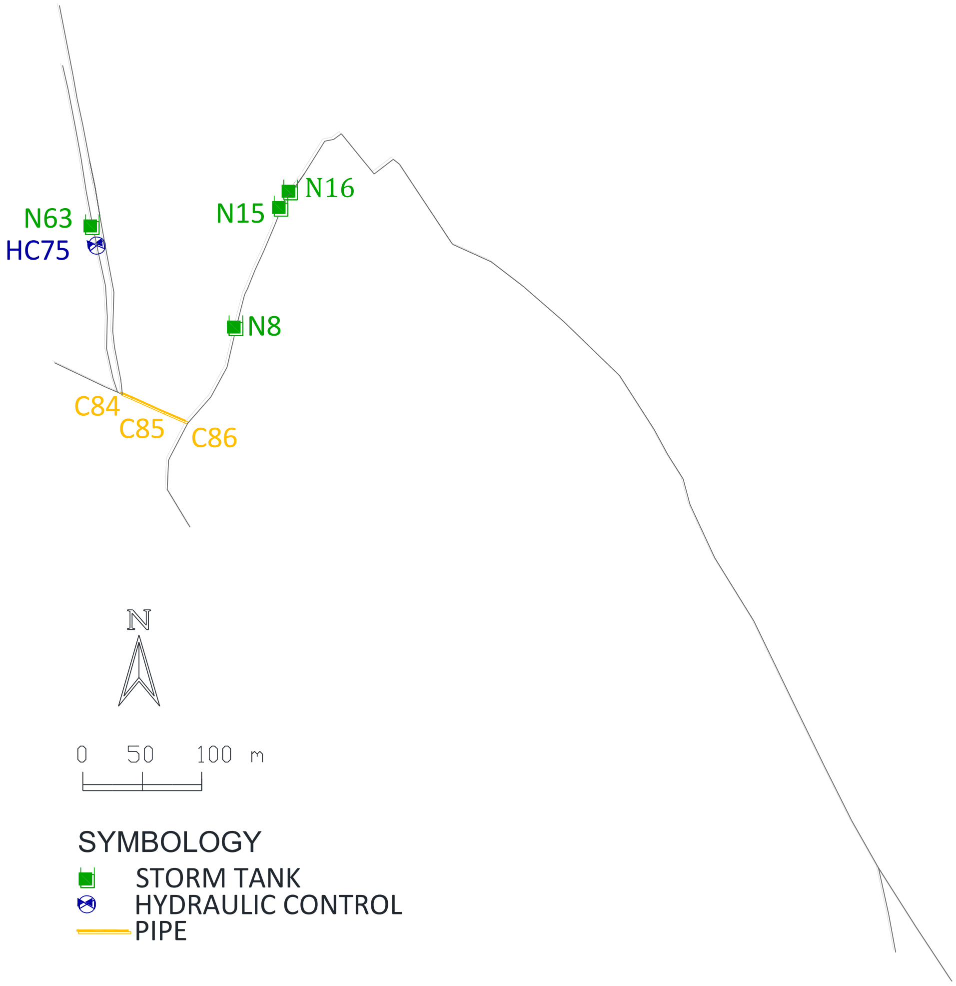


**Figure 4.12.** Location of infrastructure needed to rehabilitate the Balloon network

**Table 4.4.** Results of the final optimization in the Balloon network

| Terms in OF | Characteristics | | | | | Cost per year |
|---|---|---|---|---|---|---|
| Pipes | Elements | C5 | C84 | C85 | C86 | 2,739 € |
| | Present diam. (m) | 0.7 | 0.7 | 0.7 | 0.7 | |
| | Optimized diam. (m) | 1 | 1.1 | 1 | 1 | |
| STs | Elements | N8 | N15 | N16 | N63 | 19,727 € |
| | Volume (m$^3$) | 2496 | 4284 | 5031 | 594 | |
| | Elements | C75 | | | | 153 € |
| HCs | Head loss (m) | 72.55 | | | | |
| Flood | | | | | | 5,608 € |
| Total | | | | | | 28,227 € |

### 4.3.2. ES-N Network

The complete network has an SS magnitude of 1271. Analyzing the problem with the recursive method would demand a very high computational time. For this reason, the SSR clustering method has been considered for the study of the network. As a first step, all the sectors that make up the drainage network are defined. Nineteen sectors have been identified and will be optimized in parallel. Table 4.5 shows the elements of which the network is composed, the number of DVs and the magnitude of SS. By analyzing the network by sectors and in parallel, it is possible to appreciate the decrease in the magnitude of SS that the algorithm must explore in each scenario. If, in addition to this, it is considered that, in the SSR process, the coarse option lists are used, the computational effort is notably reduced.

For better visualization, the sectors of the drainage network and the main network are differentiated in Figure 4.7. Applying the SSR method to each sector reduces the number of DVs considerably. The method is applied iteratively until SS cannot be reduced. Table 4.5 shows the percentage reduction in SS magnitude.

**Table 4.5.** Elements, magnitude of SS and percentage of reduction in the clustering stage of the sectors that make up the ES-N network.

| Sector | Number of Pipes | Number of Nodes | DVs | SS | Reduction of SS in clustering process |
|---|---|---|---|---|---|
| Sector 1 | 5 | 5 | 15 | 17 | 100% |
| Sector 2 | 2 | 2 | 6 | 7 | 100% |
| Sector 3 | 13 | 13 | 39 | 43 | 100% |
| Sector 4 | 23 | 23 | 69 | 76 | 98% |
| Sector 5 | 24 | 24 | 72 | 79 | 91% |
| Sector 6 | 8 | 8 | 24 | 26 | 100% |
| Sector 7 | 55 | 55 | 165 | 182 | 99% |
| Sector 8 | 8 | 8 | 24 | 26 | 100% |
| Sector 9 | 15 | 15 | 45 | 50 | 100% |
| Sector 10 | 23 | 23 | 69 | 76 | 100% |
| Sector 11 | 25 | 25 | 75 | 83 | 100% |
| Sector 12 | 16 | 16 | 48 | 53 | 97% |
| Sector 13 | 9 | 9 | 27 | 30 | 100% |
| Sector 14 | 5 | 5 | 15 | 17 | 100% |
| Sector 15 | 39 | 39 | 117 | 129 | 97% |
| Sector 16 | 45 | 45 | 135 | 149 | 97% |
| Sector 17 | 4 | 4 | 12 | 13 | 100% |
| Sector 18 | 12 | 12 | 36 | 40 | 75% |
| Sector 19 | 5 | 5 | 15 | 17 | 100% |
| Main network | 49 | 49 | 147 | 162 | |
| Total | 385 | 385 | 1155 | 1271 | |

After the application of the SSR in each sector, a new scenario is configured for the optimization of the network that includes the selected DVs in each sector and in the main network. Applying the method in this scenario iteratively defines the final search region. Later, for the final optimization, a refined list of options for the STs is used and the HC elements are included in the search. At this stage, a much more demanding stopping criterion for the algorithm is also used to find the solution close to the optimal value. After performing a series of simulations, the best possible solution is obtained. Figure 4.13 shows the SSR until the final solution is found. Table 4.6 shows the terms that compose the objective function of the solution found and the characteristics of the elements to be implemented. Figure 4.14 illustrates the elements to be installed in the network. Finally, the dispersion of the different results obtained from the objective function in each iteration and the number of DVs in the case study networks are shown in Figure 4.15.

| | | | | | | | | | | | | | | | |
|---|---|---|---|---|---|---|---|---|---|---|---|---|---|---|---|
| P71 | P93 | P217 | P231 | P246 | P332 | P342 | P343 | P344 | P345 | P346 | P347 | P348 | P349 | P350 | P351 |
| P352 | P353 | P354 | P355 | P356 | P357 | P358 | P359 | P360 | P361 | P362 | P363 | P364 | P365 | P366 | P367 |
| P372 | P373 | P368 | P369 | P370 | P371 | P374 | P375 | P376 | P377 | P378 | P379 | P380 | P381 | P382 | P384 |
| P385 | P200 | P34 | P53 | P87 | P326 | P253 | P266 | P293 | P294 | P328 | P335 | | | | |
| N01 | N02 | N03 | N04 | N05 | N06 | N41 | N78 | N82 | N110 | N116 | N117 | N119 | N127 | N129 | N133 |
| N139 | N142 | N149 | N161 | N163 | N170 | N178 | N183 | N189 | N191 | N206 | N216 | N227 | N232 | N241 | N252 |
| N255 | N257 | N259 | N260 | N268 | N269 | N275 | N280 | N282 | N284 | N297 | N304 | N376 | N378 | N382 | N383 |
| N385 | N343 | N131 | N276 | N71 | N215 | N308 | N126 | HC25 | | | | | | | |

| Color Key | Description | Pipes | Nodes | HC | DVs | S |
|---|---|---|---|---|---|---|
| | DVs eliminated in the analysis by sectors | 325 | 329 | 329 | 983 | 1083 |
| | DVs in the first iteration | 60 | 56 | 56 | 172 | 188 |
| | DVs selected in the first iteration | 8 | 15 | 15 | 38 | 45 |
| | DVs selected in the second iteration | 5 | 9 | 9 | 23 | 27 |
| | DVs in the final Solution | 4 | 9 | 1 | 14 | - |

**Figure 4.13.** SSR in the ES-N network.

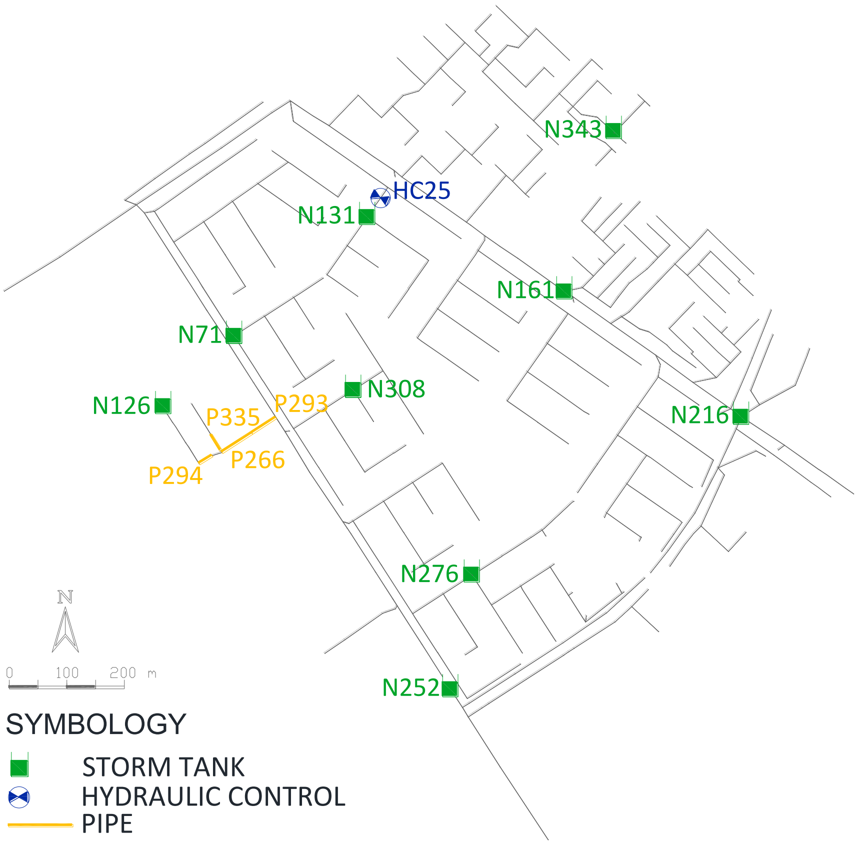


**Figure 4.14.** Location of infrastructure needed to rehabilitate the ES-N network.

**Table 4.6.** Objective function of the best solution found for the ES-N network

| Terms in OF | Characteristics | | | | Cost per year |
|---|---|---|---|---|---|
| **Pipes** | Elements | P266<br>P335 | P293 | P294 | 2,672.00 € |
| | Present diameter (m) | 0.4<br>0.3 | 0.4 | 0.25 | |
| | Optimized diameter (m) | 0.7<br>0.5 | 0.7 | 0.45 | |
| **STs** | Elements | N71<br>N161<br>N276 | N126<br>N216<br>N308 | N131<br>N252<br>N343 | 41,930.00 € |
| | Volume ($m^3$) | 1700<br>1950<br>1250 | 500<br>1950<br>1050 | 750<br>1100<br>800 | |
| **HCs** | Elements | P25 | | | 125.00 € |
| | Head loss (m) | 72.55 | | | |
| **Flood** | | | | | 27,722.00 € |
| **Total** | | | | | 72,449.00 € |

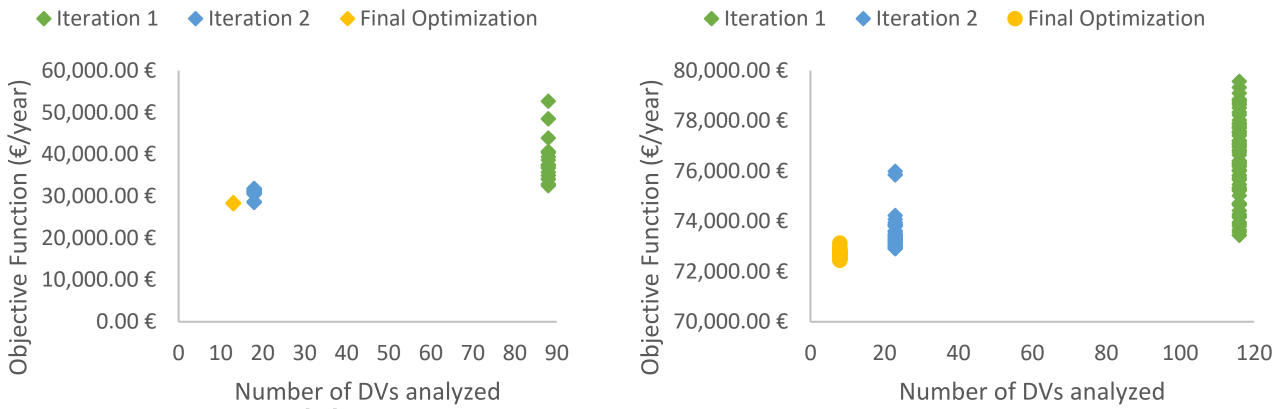


(a) (b)

**Figure 4.15.** Results of the Objective Function in each iteration analyzed. (a) Balloon network. (b) ES-N network.

## 4.4. DISCUSSION

In the optimization process, it is desirable to have a strategy that reduces calculation times, especially when large networks are analyzed. The SSR method used is applied in two networks presented as case studies. In the case of the Balloon network, the network does not have many sectors that make up the drainage network, identifying three sectors. In the process of reduction by sectors, the SS is reduced by 37%. Then, in the iterative analysis with the complete network, it is possible to reduce the SS up to 94%. On the other hand, the ES-N network has the characteristic of being made up of 19 sectors that discharge water to the main network of the drainage network. In this network, the clustering method is applied for the parallel reduction of SS in the analysis stage by sectors; SS is reduced by 85%, this being the great advantage of this methodology: that when analyzing in parallel, a smaller number of DVs are obtained faster. Finally, the SS is reduced to 97.88% in two subsequent iterations. These results show us that the method is particularly beneficial when networks composed of several sectors are analyzed, this being a characteristic of large networks. The process of reducing the SS must prioritize the identification of the best areas of the SS. Figure 4.15 shows how, when reducing the search region to the most prominent areas, the values of the objective function obtained decrease. It can also be observed how the dispersion of results decreases in each iteration. This can show us that the procedure meets its objective. The results of the final optimization, in economic terms, show the cost of the annual investment prorated throughout the design period and the expected cost that the flood may generate annually. In the Balloon network, losses of 733,282 euros per year are currently generated. When the optimization is carried out, the expected cost of these damages is reduced to 5,608 euros per year. On the other hand, in the ES-N network, without making any improvements to the network, rains can be expected to generate damages of 118,955 euros per year. With the implementation of the infrastructure according to the solution found, these damages can be reduced to 27,722 euros per year. If it is considered that the required investment in infrastructure is 3% and 38%, respectively, of the current flood risk costs, it can be said that these investments are relatively low and allow us to verify the advantages of this type of rehabilitation in drainage networks.

## 4.5. CONCLUSIONS

There are different methods to improve drainage networks. In this work, a methodology based on the substitution of drainage networks combined with the installation of STs and HCs is proposed. The case studies analyzed show the benefits of the method over the traditional pipe replacement technique, since when combined with the installation of STs in line and with the use of HCs, the slowing down of the water is encouraged, reducing the peak of the water flow. In relation to the use of STs in line, it can be said that they have an advantage over traditional STs that are designed to contain a larger volume of water and then require pumping systems to dislodge the water from the tank. With the STs in line, what is sought is a temporary storage of the water to reduce the speed of accumulation downstream. These advantages are explained in detail by Bayas-Jiménez et al. [134]. The use of GAs is presented as one of the most suitable alternatives to find solutions to this type of problem. Although it is true that its use entails a significant use of resources, there are techniques that can reduce the calculation time. The method presented in this work was previously presented by Bayas-Jiménez et al. [152]. The results obtained in the analyzed case studies show us the suitability of this method. Although the method does not allow a direct reduction of the SS and requires its application in an iterative way, it allows us to address a problem that, without this reduction, would require enormous computational efforts. It should be noted that this method allows rapid convergence towards the best search region. If the results of the first iteration of the SRR process are analyzed, it can be seen how a large amount of the SS is quickly eliminated.

The analysis of the problem focused on evaluating the problem in economic terms, quantifying the cost that the flood would produce in the cities. The analysis fundamentally depends on the volume of flood water that is generated. Analyzing the problem using a design rainfall for the return period used for the design of the network may, at first sight, be the best alternative to the problem. By using this design rainfall, the situation that makes the greatest demands on the operation of the network can be analyzed. However, this form of analysis does not analyze other minor rains that may appear during the period of operation of the network and that can generate floods in the network that, although minor, are not accounted for in the analyzed objective function. The approach used in this work has tried to solve this problem. By analyzing the costs on an annualized basis based on an annual estimate of the damage, it is possible to have a clearer idea of the cost of the damages that the risk of flooding implies. In any case, it must be taken into account that this method is approximate, and that the results will depend greatly on the number of storms analyzed. It is noteworthy to mention that this work does not contemplate in its objectives the realization of projections of increased rainfall due to the effects of climate change. However, if you wanted to analyze a network under this scenario, the methodology could be applied without problems.

On the other hand, identifying different land uses in the studied areas allows for a better optimization of the networks compared to the use of an average curve for the entire study area, as has been done in previous works; this is undoubtedly an improvement that this work presents to the developed methodology. However, this additional action demands longer calculation times, so the use of an SSR method becomes unavoidable.

Finally, distinguishing different zones within the study area and the cost that a flood would entail in that place allows greater protection to be given to particularly sensitive zones or strategies in the functioning of the city. In contrast, in areas where a flood would not cause serious problems, for example, in green areas, a greater volume of flooding can be allowed. This would allow linking the present study to the joint analysis with low-impact developments (LIDs) techniques in specific areas of the cities in which these techniques can be included. This study is proposed as a future development in this line of research.

**Supplementary Materials:** The following supplementary materials are available in Appendix III of this thesis. Figure A3.3.1. Representation of Balloon drainage network; Figure A3.4.1. Representation of ES-N drainage network; Table A3.3.1. Data for nodes and subcatchments of Balloon network.; Table A3.3.2. Data for conduits in Balloon network; Table A3.3.3. Land uses in the study area of Balloon network; Table A3.4.1. Data for nodes and subcatchments in the ES-N network.; Table A3.4.2. Data for conduits in ES-N network; Table A3.4.3. Land uses in the study area of ES-N network. This supplementary material is part of the scientific article presented in this Chapter and is also available online at: https://www.mdpi.com/article/10.3390/w14182901/s1.

# CHAPTER 5.

# GENERAL DISCUSSION

## 5.1 REHABILITATION METHODOLOGY

### 5.1.1 Optimization model

To rehabilitate the drainage networks, an optimization model was developed to find the best combination of the three actions considered to solve the flooding problem, pipe renewal, construction of STs and installation of HCs. The model is based on heuristic search by using a PGA that evaluates an objective function the algorithm seeks to minimize. This function established in economic terms is composed of two classes of terms, one consisting of the cost of the infrastructure and the other one consisting of the cost of the damage caused by floods. Some modifications were made to this function in the chapters developed due to the improvements made to the optimization model in each chapter. However, its fundamental concept is maintained. The algorithm uses the data from the hydraulic analysis performed with the SWMM model to evaluate the objective function. The obtaining and modification of network data is performed with the help of a Toolkit developed by Martinez et al. [119]. The operation of the optimization model used in Chapters 2 and 3 is illustrated in Figure 3.1. Figure 4.2 shows the model used in that chapter with a small modification to the model used previously. This modification is due to the change in the flood assessment from an analyzed rainfall to the analysis of rainfall with different return periods for estimating annual damage.

Finally, it should be said that the drawbacks of the model are related to the characteristics of GAs and more specifically to integer coding algorithms. The main problem is the time required to converge to the best solution due to the large size of the SS to be explored. Another aspect that should be considered is the premature convergence to solutions not close to the optimal one that must be avoided by means of some strategy. For this reason, this thesis proposes two fundamental actions to overcome these drawbacks: an SSR procedure that improves the efficiency of the optimization process, and a stopping criterion that enhances the efficacy of the search for the best solutions.

### 5.1.2 Use of hydraulic control

The need for HCs was already introduced in the work done by Ngamalieu-Nengoue et al. [38]. These authors obtain smaller diameters in certain optimized pipes. This fact suggests some elements generating local head losses at certain points in the network were required. This work continues this line of research and develops a methodology to include these HCs in an optimization model. The methodology considers the joint work of these HCs with the replacement of pipes and the installation of on-line STs.

In this work, for the mathematical and economic analyzes, a gate valve is selected as the HC. Valves was chosen because they are easy to install and to represent in terms of their opening degree, as shown in Figure 2.2. This characteristic is very important since using a discrete discretization PGA can develop an options list for this type of DVs. The options list used is shown in Table A3.1.4 and in graphical form in Figure 3.5. For the hydraulic analysis, the optimization model introduces the loss coefficient associated with each opening degree as *Entry loss coefficient* in the SWMM model. In this way, loss of energy that the valve would generate in the pipe is simulated.

As mentioned in previous paragraphs, the work carried out by Ngamalieu-Nengoue et al. [38] found a solution that reduces the diameter of the pipes to slow down the water. If this action is replaced by the installation of a valve, a similar hydraulic behavior of the networks was obtained as shown in Figure 2.3. This fact demonstrates the economic suitability of this new way of rehabilitating networks.

Chapter 2 presents a case study where the E-Chico network is analyzed, which has serious flooding problems that generate flood damage costs of 5,244,035 €. When applying the methodology, a solution that requires the installation of HCs is found. The solution obtained effectively addresses the problem by significantly reducing flooding costs to 8063.44 €. Furthermore, the expense associated with implementing HCs accounts for just 4% of the total infrastructure investment. To demonstrate the advantages of using HCs, the results obtained are compared with those presented by Ngamalieu-Nengoue et al. [38] shown in Table 2.8, specifically case c). Also summarized in Table 5.1 of this section. In these results, it can be observed that all the terms of the objective function are reduced. Thus, pipe costs are reduced by 56% because it is no longer necessary to replace pipes P04, P10, P23 with others of smaller diameter. The STs costs are reduced by 3% which are the most expensive infrastructures. Flood damage cost is reduced by 37%, which is the most important benefit obtained. Finally, it is observed that the value of the final solution found is reduced by around 5%, from 213,981€ to 203,859.69€. These results demonstrates that the use of HCs is advantageous in reducing flood volume and the investment cost required to control them.

**Table 5.1.** Comparison of results. Ngamalieu-Nengoue et al. methodology and Proposed methodology.

| Case | Investment cost (€) | | | Flood Cost (€) | Objective Function (€) |
|---|---|---|---|---|---|
| | Pipe | ST | HC | | |
| Ngamalieu-Nengoue et al. | 14,927.00 | 186,353.00 | - | 12,701.00 | 213,981.00 |
| Proposed | 6,583.81 | 181,540.69 | 7,671.75 | 8,063.44 | 203,859.69 |

In Chapter 3 two case studies are presented, E-Chico and Ayurá. Although this chapter focuses on SSR, since the same methodology is applied, it is worth making some observations on the use of HCs. In the solutions obtained, it is observed that HCs appear. In the case of E-Chico network, the objective function improves by 2%. possibly due to the application of a new process of SSR. It is also observed that the installation of HCs is required in the same pipes and with the same degrees of opening, which shows the best solution with this methodology could have been reached. In Ayurá network, it is also seen how HCs contribute to the solution of the problem with a low investment cost. Something similar happens with the case studies of Chapter 4 where two networks, Balloon and ES-N are analyzed. In this chapter, floods costs are analyzed in a different way than in the two previous chapters. However, under these new conditions, HCs are still required in the solutions found. In this way, it can be said that one of the first aspects derived from the developments obtained is the need to install HCs to control the flooding problem.

Despite these benefits, certain problems have arisen regarding the incorporation of these elements. One of them and the most complex to deal with is the increase of the SS due to the increase of the number of DVs. Specifically, all the exit pipes from the nodes where STs are possibly installed are included in the SS. This problem becomes more evident when working with large networks as in the case of the ES-N network of Chapter 4.

Other minor drawback encountered in developing this methodology was defining a cost function for the HCs. This was resolved by establishing a mathematical expression based on the curve obtained by relating gate valve prices to the different diameters available. The procedure is simple and can be adjusted to the costs of different places without major inconvenience. Finally, another minor drawback was establishing an adequate discretization of the valve opening degrees to define a correct options list. A list corresponding to 10 valve positions was chosen, which in several simulations performed to test this discretization yielded favorable results.

### 5.1.3. Discretization of decision variables

To develop the optimization model, a GA was chosen. The advantages of using this type of algorithms are explained in sections 1.2.6 and 3.1 of this thesis highlighting its robustness and its great capacity to explore complex regions. The PGA specifically has an integer coding that allows each DV to be assigned a specific value. This characteristic implies that the analyzed DVs must be discretized. Achieving this discretization has been one of the most difficult issues in the development of this work. If a very refined discretization is performed, the size of the SS will increase significantly. On the contrary, if a coarse discretization is performed, important regions of the SS can be left out of the analysis. Therefore, this process involved testing different sampling points to comprehensively cover SS, while avoiding excessive refinement and defining appropriate intervals between the points.

Accordingly, the DVs studied are discretized. In the case of pipes, the work is simplified since the commercial diameters are values determined by standardized norms, so they are already discrete values. Commercial diameters were established from a minimum of 100 mm up to 3000 mm in order to cover the majority of cases. Thus, there is a list of 25 options including the DV with value 0 (no pipe change required).

In the case of tanks, a list of options was drawn up with a range from a minimum area of 0 $m^2$ (no ST required) to a maximum area of 2000 $m^2$ with intervals of 50 $m^2$ defining an option list of 50 values. This refinement seeks to provide a good diversity of options without increasing the SS too much. It should be noted that the methodology is unaffected by the minimum and maximum values considered, but rather by the number of options defined. Finally, for the case of HCs, a list of options consisting of 10 different positions was established. These 10 positions are assumed to be sufficient for the analysis. This assumption is based on a large number of simulations carried out as tests that indicate that maintaining these jumps or discretization intervals for both STs and HCs are effective.

For the SSR process, reduced option lists were used. As explained in Chapter 3, this is justified because the purpose is to identify the DVs that are most likely to be part of the optimal SS. This is under the hypothesis that, if a DV requires improvements, the corresponding gene in the obtained chromosome will take a value different from 0 even if the discretization is coarse. It is then evident that determining a list of coarse choices must be done with great care. In this work, these lists were determined after performing multiple simulations with different discretization and observing experiences in previous works. In short, coarse options list was defined for the SSR process. For pipes, 10 options are defined with 9 diameters ranging from 300 to 2000 mm and the option of not changing the pipe. For the STs, 10 options are defined with values ranging from 0 to 2000 $m^2$, with intervals of 200$m^2$.

As previously stated, the coarse options lists are used in the SSR process. In this process the possible pipes that require larger diameter and the nodes where STs would be installed are identified. In the case of HCs, since they are linked to the appearance of an upstream ST, it is not considered in the SSR process. For this reason, a single discretization is used in the final optimization stage.

The results in Chapter 2 and Chapter 3 show these lists can be suitable for this type of analysis. In Chapter 4, in order to improve the efficiency of the process, the use of coarse and refined option lists in the pipe analysis were changed and a short option list with 5 diameters is fixed for the whole process. This option list takes into account the 5 diameters that are larger than the diameter of the analyzed pipe, so the option list is different for each DV. This change implies a reduction in the SS in the case studies analyzed, specifically the initial SS is reduced by 17%. This reduction extends to the different scenarios studied. Taking into account that this reduction in the SS is solely due to the new list of options, prior to applying the SSR process, it can be concluded that it is a advantageous decision.

The proposed list is based on the fact that the methodology analyzes networks without serious design problems and that would not require major changes. The methodology focuses on networks that present lack of capacity due to increased rainfall. This could be a limitation of this new optimization criterion. If a network has these problems, more adequate diameters could be left out of the analysis to solve the problem. In any case, these types of problems are not the objective of this study, so it can be said that this discretization is suitable and advantageous.

### 5.1.3 Analysis of the cost of floods

The analysis in economic terms involves delivering to the drainage network managers a tool to make decisions about the necessary interventions in the drainage network. Some works address the rehabilitation problem in economic terms showing its convenience [6,109,138]. For this thesis, two approaches to quantifying flood damage costs are considered.

The first approach considers the cost generated by the design rainfall in the study area. To establish this cost, the model collects flood volume data for the network nodes identified in the hydraulic analysis. These data are then used to determine the flooding depth for each corresponding node, which is subsequently used to calculate the cost of flooding using Equation (2.8). This expression is obtained from a damage-depth curve that relates the damage cost to the flood depth. The expression also sets a maximum damage cost, which is reached when the flood depth is sufficient to cause total damage. The cost of flood damage is calculated for each node experiencing flooding. The total flood damage for the study area is determined by summing these individual node costs.

Chapters 2 and 3 utilize this approach. The coefficients used in the equation to obtain the cost of flooding are shown in Table 2.3. These values were obtained from previous work by Ngamalieu-Nengoue et al. [38]. In Chapter 2 this analysis is used in the E-Chico network examined as a case study. Table 2.1 shows the flood conditions and the cost they generate in the studied network, which has a value of €5,244,035. After applying the methodology, the cost of flood damage is reduced to 1% of the initial damage, which demonstrates the validity of the methodology. In Chapter 3, the same way of accounting for flood damage is used in the case studies. Similar results are obtained, showing a slight improvement in the case of the E-Chico network due to the improvements in the SSR process developed in this chapter.

This is undoubtedly a remarkable way to analyze the cost of flooding. However, comparing the total infrastructure investment costs to the effects of a single rainfall in the network design period may leave some concern regarding other major rainfall events that may occur in this period and are not considered. To overcome this problem, a second approach to calculating these costs by estimating the annual flood risk is proposed in Chapter 4. The approach is based on the method developed by Arnell [155] to estimate the annual cost of damage by analyzing the behavior of a rainfall with different return periods T. The proposed method relates the flood cost (obtained in the same way as in the previous method) to the annual exceedance rate corresponding to each T. For this work, previous research is used that suggests expressing this relationship in log-linear form. Expressed in this way, a straight line is obtained, which has advantages in defining its mathematical expression. The way to obtain the expression for estimating the annual flood risk is presented in section 4.2.1.2. Put it this way, there are certain changes in the methodology that should be mentioned. On the one hand, the model must analyze the network for more than one rain, which requires a greater computational effort. On the other hand, once the cost of annualized flood damage has been obtained, it is necessary also to annualize the infrastructure costs so that they are evaluated by the model in the same circumstances. To do so, the annual amortization factor of Steiner [159] is used. The interest rate and the time of return on investment are those used for this type of structure.

This new approach also proposes the use of different Damage - Depth curves of the different land uses that can be found in a city. This delivers results closer to the real ones, although they imply, again, a longer calculation time.

In Chapter 4, this approach is put into practice and applied to two case studies: Balloon network and ES-N network. Regarding the hydrological part, in the Balloon network, rainfall is used for 6 return periods (Figure 4.6) and in the ES-N network, 2 return periods (Figure 4.8). Using more rains in the analysis could improve the accuracy of the results. However, increasing the amount of rainfall unnecessarily should be avoided, especially for large networks, as it would increase the computational time. Regarding land uses, 13 types have been defined. These types are based on the results obtained by Martínez-Gomariz et al. [158] adjusted to equation (4.5) used in this thesis. The results of fitting these curves to the equation (Table 4.1) show the suitability of using this expression. Subsequently, the required coefficients are obtained (Table 4.2) to carry out the analysis of the cost of flooding and finally the estimate of the annual risk.

It should be noted that, although the use of the annual flood risk estimation presented here demands an increase in terms of calculation time. This is fully justified since it makes it possible to overcome certain gaps of the previous analysis. In this way, the rigor of the results offered by the methodology is increased.

# 5.2. EFFICIENCY OF THE OPTIMIZATION PROCESS

## 5.2.1 Methodologies of search space reduction

Problems using GAs, by their nature, tend to involve a significant number of DVs. If this intrinsic condition of GAs is added to the characteristic of the PGA that evaluates integer values from a list of options, a large SS to be explored is formed. The exploration must be strategic to identify the regions that possibly contain the best solutions. In this way, the required calculation time would be reduced, and networks that would otherwise be unapproachable could be studied. For these reasons implementing an SSR method is necessary and is one of the main objectives of this work.

This thesis develops two SSR methods that are presented and studied in the case studies of Chapters 3 and 4. Chapter 3 presents the recursive method which consists of the iterative elimination of two types of DVs nodes and pipes by applying a selection criterion shown in section 3.2.3.3 which is applied to $P_{95}$ of the best solutions. This criterion defines the best search regions leaving some diversity in the solutions found in the following evaluations. As explained above the discretization used at this stage is a very important aspect, using for this purpose the so-called coarse option lists and presented in an extended form in section 3.2.3.2. This chapter also introduces the convenience of reducing the DVs for large networks by sectors or branches of the network, providing the procedure with an alternative for analyzing networks of important sizes. The results obtained in the two networks studied in the Chapter 3 show the criterion complies with identifying the best search region. The analyses of Figure 3.10 and Figure 3.13 show that in each iteration the DVs that are not part of the optimal region are eliminated. These results are summarized in Figures 5.1 and 5.2, respectively.

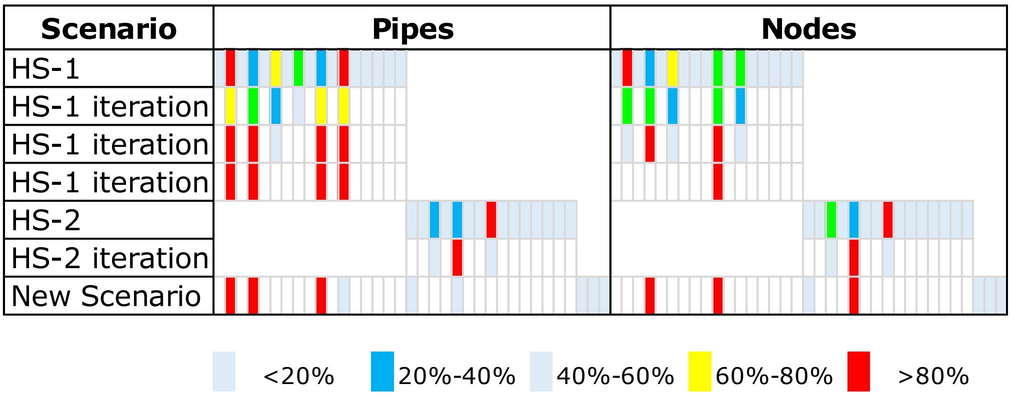


**Figure 5.1.** Summary of the SSR process in the E-Chico network

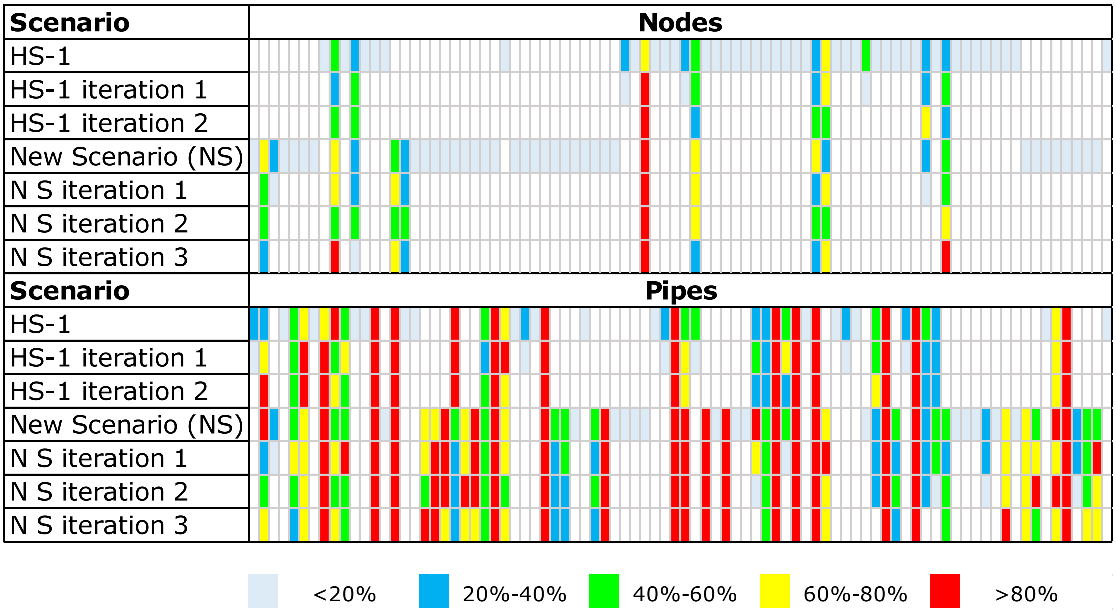


**Figure 5.2.** Summary of the SSR process in the Ayurá network

At the same time, the DVs that form the promising region increase their repeatability in each iteration. This shows convergence towards the best solutions occurs in the process. The above mentioned is reinforced by the results shown in Table 3.4 and Table 3.5 where it is seen how the minimum objective function obtained in each iteration decreases. The improvements in each iteration of the SSR are evidenced in the graphs: Frequency – O.F./O.F.$_{min}$ presented in Figure 3.12 and Figure 3.16. and are summarized in Figure 5.3 of this section. These figures show that not only the minimum objective function found decreases, but in general the set of solutions improve in each iteration. The procedure also modifies the $G_{max}$ used by adopting a much lax criterion for this stage in order to reduce calculation times. All these results can indicate that the assumptions of setting a laxer $G_{max}$ in the SSR process and analyzing the networks by sectors to improve the process are adequate.

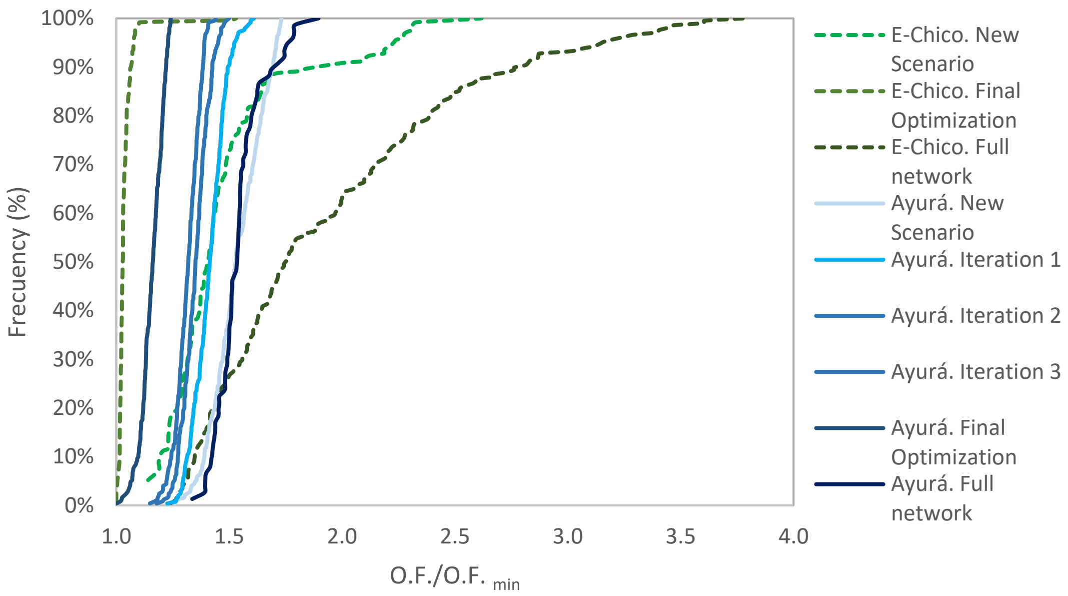


**Figure 5.3.** Frequency – O.F./O.F.$_{min}$ graphs, for E-Chico and Ayurá networks

It should also be mentioned that the SSR method presented in Chapter 3 shows better results than the one proposed by Ngamalieu-Nengoue et al. [38] used in Chapter 2 by finding a solution with a lower value of the objective function when analyzing the same network. The benefits of using an SSR process in each sector are shown in Chapter 4, where the so-called clustering method is studied in two drainage networks of different sizes. In the case of the Balloon network of smaller dimensions and with three small sectors the method may not give an obvious advantage over the recursive method. But in the ES-N network is where the power of this method is really evident. It is possible to optimize a network of 19 sectors that was not possible to optimize with the recursive method in reasonable times. Table 4.3 and Table 4.5 show the advantages of the process by reducing the DVs in each sector with percentages higher than 75%. In the subsequent stages, a similar procedure to the recursive one is followed, where again the advantages of the methodology are evident. These results are also summarized in Table 5.2 of this section. Finally, Figure 4.15 show how in each iteration, the number of DVs and the dispersion of the solutions found are reduced.

Table 5.2. Summary of the SSR in the Balloon and ES-N networks by applying the clustering methodology

| **Sector** | **DV** | **SS** | **SSR clustering process** |
|---|---|---|---|
| Balloon network | | | |
| Sector 1 | 33 | 36 | 100% |
| Sector 2 | 36 | 40 | 96% |
| Sector 3 | 12 | 13 | 100% |
| ES-N network | | | |
| Sector 1 | 15 | 17 | 100% |
| Sector 2 | 6 | 7 | 100% |
| Sector 3 | 39 | 43 | 100% |
| Sector 4 | 69 | 76 | 98% |
| Sector 5 | 72 | 79 | 91% |
| Sector 6 | 24 | 26 | 100% |
| Sector 7 | 165 | 182 | 99% |
| Sector 8 | 24 | 26 | 100% |
| Sector 9 | 45 | 50 | 100% |
| Sector 10 | 69 | 76 | 100% |
| Sector 11 | 75 | 83 | 100% |
| Sector 12 | 48 | 53 | 97% |
| Sector 13 | 27 | 30 | 100% |
| Sector 14 | 15 | 17 | 100% |
| Sector 15 | 117 | 129 | 97% |
| Sector 16 | 135 | 149 | 97% |
| Sector 17 | 12 | 13 | 100% |
| Sector 18 | 36 | 40 | 75% |
| Sector 19 | 15 | 17 | 100% |

The procedure is valid, although it has some limitations that should be described. While it is true that the method of elimination by hydraulic sectors or clustering is valid for large networks, it can be more complex in networks that do not have fully identifiable branches or sectors. This is experienced in the second case study of Chapter 3 where it is observed that Ayurá network does not present identifiable sectors. To optimize the network, it is decided to divide the network at a point near the middle of the network. Then, the SSR process is applied in the upper half of the network to eliminate DVs. Next, the whole network is analyzed considering only the DVs identified as good in the upper half of the network to finally find the best search region. This process adds an additional task (dividing the network) that must be considered. Beyond these particular problems, a limitation of these methods is their iterative character. The procedure demands high computational efforts in the first iteration that considers all the DVs of the network or the sector. However, according to the results obtained, it is in this iteration where the DVs are considerably reduced. Despite these limitations, its advantages are greater, and it is a procedure that should be considered in this type of problems.

### 5.2.2 Stopping criteria

GA have an important characteristic. At the beginning of the search for the solution they progress rapidly, i.e., the value of the objective function improves rapidly from one evaluation to the next but then in subsequent evaluations this tendency tends to diminish, with small improvements being observed. Finding a stopping criterion that allows to finish the process close to the optimal solution should be the objective of this type of analysis.

To achieve this goal, a new stopping criterion has been developed and is presented in Chapter 2. The proposed criterion is based on the study of a solution (chromosome) obtained in the optimization process that is very close to the optimal solution and in which only one DV (gene) has not reached its optimal value and would only reach it by mutation. Thus, by defining a high probability of reaching this change by mutation, the best solution would be obtained. The probability of success of reaching this mutation has been set at 80%, presuming that it is high enough to reach the mutation. While this value may be debatable, the test simulations performed gave favorable results. The development of the new criterion is fully explained in section 2.3 of Chapter 2 and the final expression obtained in Equation (2.11).

To demonstrate the benefits of this criterion, it has been applied in the case study of Chapter 2 where the E-Chico network is studied. This network has been previously analyzed in a previous work [160] under the same conditions, but with a traditional shutdown criterion of 100 generations without change before shutdown, obtaining an objective function with a value of 209,150.40.

The results with the proposed criterion are presented in case d) of Table 2.8 of Chapter 2, obtaining an objective function of 203,859.69 €, i.e. an improvement of 3% in the results obtained. This improvement becomes more relevant if it is considered that the results are compared in a small network. If this criterion is applied to a larger network, the reduction in costs would be significant. However, it must be said that the increase in computational effort is significant, so it is debatable whether this stopping criterion should be used throughout the optimization process.

Based on the above, in Chapter 3 where an SSR procedure is proposed, it is proposed to use a lax stopping criterion while reducing the DVs. By lax criterion it is meant assigning a low success probability (20% in the proposed procedure) that allows reducing the computational times. As mentioned in Chapter 3, this is justified because at this stage of the methodology the aim is not to find the best solutions but to eliminate areas of the SS that are not interesting to study. Thus, if a DV is not selected under these conditions it will be much less likely to be selected with more demanding selection criteria. Then, for the final optimization in the most promising SS the proposed procedure does use the 80% success probability increasing the number of iterations required to find the best solution. In the E-Chico network studied in Chapter 3, these aforementioned criteria are applied obtaining an objective function of 199,813.79 € reducing by 2% the best solution found in Chapter 2 with a lower computational effort. Here it can be discussed if the improvement is due to a better identification of the optimal search region when applying the proposed SSR procedure, but since the stopping criterion is part of the procedure, it is understood that it contributes to the improvement of the methodology. What is not under discussion is the reduction of the calculation times by choosing lax criteria for the SSR and more demanding only in the final part. These criteria are also applied in the second case study of Chapter 3 and in the case studies of Chapter 4 because of the benefits shown.

Finally, this chapter has discussed the developments in this thesis. Establishing a methodology to rehabilitate drainage networks for flood control is the main objective of this work. The main contribution is to propose an optimization model based on a PGA that includes the use of HCs. This model evaluates the problem in economic terms of both infrastructure and flood damage. To achieve this, not only the hydraulic behavior under these proposed actions has been studied. It has also been studied to improve the efficiency of the optimization process. From this, the SSR process and the stopping criteria proposed above are derived. These developments are an important contribution not only for the rehabilitation of drainage networks but also for the optimization processes based on GAs. In summary, all the developments made in this thesis aim to meet the objectives set at the beginning, and based on the results achieved, it can be said that they have been reached.

# CHAPTER 6.

# CONCLUSIONS

## 6.1 GENERAL CONCLUSIONS

From the results of the research carried out in this thesis, the following conclusions can be inferred:

1. Implementing STs in the drainage network is widely studied as a good alternative to buffer water peaks during an extreme rainfall event. Their use on-line in the drainage network allows temporary storage without the need to include pumping equipment. Some works have been carried out using this type of tanks trying to define their optimal size and location within the network, but the problem has not been addressed in conjunction with the change of pipes and the installation of HCs, which, as shown in this thesis, offer very promising results.

2. The inclusion of HCs in the proposed methodology proves to be a suitable alternative for the rehabilitation of drainage networks. The HC used is a gate valve that slows down the flow of water by reducing the accumulation of water in the lower part of the network. The HC is a new concept that has been developed with the purpose of meeting the need that has been detected in previous works, improving the solutions obtained. The advantage of its use is introduced and studied in Chapter 2 where the methodology is compared with previous works that do not implement this control element. The results discussed show there is a reduction in the value of the objective function with the use of this relatively low-cost element. The results also show the proposed configuration methodology provides better solutions that considering only pipe replacement or tank installation. In all the solutions found in the case studies of Chapter 2, Chapter 3, and Chapter 4, the appearance of HCs is observed, which reinforces the idea that including this element to improve the network is an advantageous alternative.

3. A stopping or convergence criterion based on the Improvement-based criteria is also presented in this work. It allows to terminate the optimization process after a defined number of generations without improvement. The criterion is based on guaranteeing change by mutation. Thus, the criterion adopted would generate a large number of evaluations that the optimization model must perform to find the best possible solution. This may be a disadvantage due to the nature of the algorithm used, which already involves a high computational time. However, the results show the solutions found are improved. Therefore, it should be studied whether it is convenient to use this criterion in the analysis of large networks with a high number of DVs or to look for new ways to improve the efficiency of the optimization process. The aforementioned is evident in the SSR processes presented, where the $G_{max}$ used is reduced, sacrificing the finding of better solutions, but reducing the calculation times, which in this stage is most important.

4. A notable contribution of this thesis is the developed and applied SSR methods in the case studies. Specifically, two SSR methods have been presented. One is called the recursive method, which iteratively reduces the SS until defining an optimal search region. The second one, named clustering, is a variation of the first. This method applies the recursive approach to each hydraulic sector of the network to reduce the SS. Thus, the clustering method is focused on large-scale networks. This contribution provides an alternative for optimizing such problems where multiple DVs are involved, using evolutionary algorithms.

5. In order to apply this SSR procedure in large networks, a variant of this methodology is also presented to reduce the SS by sectors or branches. This methodology called, clustering and used extensively in Chapter 4, is a valid alternative after being applied in a network of considerable dimensions that could not be optimized with the iterative method initially proposed. This analysis can be criticized at first because it studies each sector of the network separately without considering the effects on the downstream network. However, the analysis only seeks to identify the DVs sensitive to be optimized and not to make a change in the network. Once these DVs that are presumed to form the optimal SS are identified, the optimization of the network is initiated. The results of both the reduction of the objective function and the dispersion of the solutions found show there is convergence towards the best solution. So it can be concluded that the methodology is valid. The benefits of this method are more evident because it allows the optimization of networks that could not be optimized with previous methods due to the large number of DVs.

6. It should also be mentioned that the analysis in economic terms of the cost of floods can be an interesting alternative for network managers to know the benefit of rehabilitation. Chapter 2 and Chapter 3 present these analyses based on the network design storm. This analysis can be extended to a climate change scenario considering the increase in rainfall intensity that the predictive model yields. This can be a good methodology for analyzing a network and search for improvement alternatives. However, this approach would not consider certain minor rainfall events that may occur during the design period of the drainage network. These events could generate minor flooding, but that are not considered in the analysis, leading a lower cost-benefit value than the real one. To overcome this drawback in Chapter 4 a new approach is presented considering the EAD which is popularly used to quantify the annual cost of flood damage. Certainly, a limitation of this approach is that it will deliver approximate results and that the accuracy will depend on the number of rainfalls and the design periods selected to determine those rainfalls. Nevertheless, it is a remarkable advance. It allows us to know the benefits in a more realistic way of the actions carried out.

Above all, it can show the cost of the annual investment required in infrastructure to face floods.

7. Another improvement is the use of flood cost functions for different land uses presented in Chapter 4. In Chapter 2 and Chapter 3 a cost function is used that uses an average damage-depth curve which generates approximate results. This is not the case in Chapter 4 where different damage-depth curves related to the land use of each urban watershed analyzed in the study area are established. The use of different curves allows, in certain areas such as parks or green areas a greater volume of flooding that can reduce the size of the required structures and anticipate the use of green infrastructure in certain parts of the cities. Despite all these advantages, it is important to keep in mind that this new analysis requires an initial processing time that includes the identification of the different land uses and their percentage in the study area.

## 6.2 MAIN CONTRIBUTIONS OF THE THESIS

The main contribution of this work is the presentation of a methodology to optimize drainage networks that has considered to rehabilitate drainage networks the change of pipes, the installation of on-line STs, and the inclusion of HC elements. These actions seek to offer an improvement in the drainage networks to reduce flooding with relatively low investment costs. To achieve this, optimization techniques using a modified GA are employed to develop an optimization model. The resulting model has been provided with two methodologies for reducing the SS to improve efficiency, one of these methodologies is focused on networks of large sizes. This work also presents two ways of analyzing flood damage. The first one analyzes the damage produced by a design rainfall for the return period that is the most demanding on the system. The other analyzes the cost of flood risk considering the EAD from rainfall for a given design period. This last form of analysis offers the possibility of quantifying the annual investment required to improve the network.

In addition to the main contribution of this thesis, this work makes contributions both in the field of drainage network rehabilitation and in the field of optimization, which are detailed below.

### 6.2.1 Contributions to flood control through the rehabilitation of drainage networks

*6.2.1.1 Hydraulic control*

One of the main contributions of this thesis is the inclusion of HCs as an additional element to improve drainage networks. Its use is amply justified in the case studies presented that show how this relatively low-cost element can reduce flood levels in the drainage network. For the present work, a gate valve with different degrees of opening that make up the list of options used by the algorithm is used as HC. The methodology could consider other types of elements that generate a head loss. However, the ease of modifying the opening degree of a valve gives this option a visible advantage. Like the other actions considered for the rehabilitation of the networks, the HC defines a cost function to be evaluated with the optimization model.

*6.2.1.2. Economic analysis of flood risk*

An important contribution of this thesis is the evaluation of the annual cost of flood risk. This novel approach enables the estimation of the impact of floods on the studied network and comparison with the investment cost in infrastructure to mitigate them. To assess these flood costs, rainfall events with varying return periods are analyzed. Although this may result in longer calculation times, it substantially enhances the presented methodology and offers a fresh alternative for analyzing such problems.

Furthermore, this method encompasses the analysis of flood costs for different sub-basins, which represents another noteworthy contribution of this research. This analysis makes it possible to consider the cost of the damage that a flood would generate according to the activities carried out in a certain area. Indirectly, the analysis proposed in this way would give greater protection to some areas over others according to the cost of the expected damage. This differentiation is beneficial since it allows economic resources to be used to protect areas that are essential for the normal functioning of cities or that require more protection such as hospitals, dwellings, or schools. This is an important contribution that substantially improves the methodology compared to previous works where the average cost of flood damage was used.

### 6.2.2 Contributions in the field of optimization

*6.2.2.1 SSR methods*

A notable contribution of this thesis is the developed and applied SSR methods in the case studies. Specifically, two SSR methods have been presented. One is called the recursive method, which iteratively reduces the SS until defining an optimal search region. The second one, named clustering, is a variation of the first. This method applies the recursive approach to each hydraulic sector of the network to reduce the SS. Thus, the clustering method is focused on large-scale networks. This contribution provides an alternative for optimizing such problems where multiple decision variables are involved, using evolutionary algorithms.

6.2.2.2. Stopping criteria

Another important contribution of this work is the stopping criteria defined for its use in the optimization model. The criterion based on guaranteeing a certain probability of success in the change by mutation of the genes of a resulting chromosome provides good results when compared with traditional stopping criteria. Although the increase in computational effort is considerable. Using a low probability of success in the SSR process is an alternative that is offered to somewhat reduce calculation times. This reduction is fully justified in the methodology and results of Chapter 3 where the reduction of the SS is correctly reduced. Then, to find the final solution in the reduced region, a higher probability of success is used.

## 6.3 FUTURE LINES OF RESEARCH

Although the work presented here exhaustively addresses the issue of rehabilitation of drainage networks to deal with flooding, since it is such a broad field of study, it leaves open some lines of future development that can certainly be deepened.

1. The study was carried out focused on drainage networks that are gravity-fed, under this scenario solutions have been proposed that can be considered close to optimal to reduce the effects of flooding. However, this study does not consider drainage networks that require pumping systems for their operation. This is a field of study that should be deepened since many cities with flat topography have this type of system. It is important to mention that in the proposed analysis, the optimization of the starting and stopping periods of the pumps, as well as the possibility of adding new pumping stations can be a field of interesting deepening. Studying the incidence of these actions on the network and the impact it may have on the sizing of other infrastructures is very attractive to investigate.

2. The methodology presented here focuses on improving drainage networks for economic flood control. For this reason it is chosen to use on-line control tanks whose main objective is to mitigate the effects of water peaks in extreme rain events. However, studying the behavior of the drainage system considering the use of off-line STs could be an interesting future research direction. These STs divert water out of the system during extreme rainfall events, thus preventing the entry of poor-quality water and contaminants washed from the surface, which could affect the functioning of the wastewater treatment plants located at the end of the system. Exploring the possibility of incorporating such STs at specific points in the network and assessing their compatibility with the proposed actions in this thesis would be appealing for future investigations.

3. The results obtained in Chapter 4 of this thesis show a promising future line of research. This involves the incorporation of sustainable drainage systems or green infrastructure in specific zones within the urban area, where a controlled level of flooding can be tolerated during extreme rainfall events. Thus, by identifying suitable areas for incorporating infiltration structures beforehand, it is possible to reduce the volume of water that the drainage system needs to handle. This, in turn, leads to a reduction in the dimensions of the structures required for rehabilitating the drainage networks. In this way, incorporating LID into the methodology becomes a relevant line of research. This becomes more attractive if you consider that the new versions of the SWMM model (version 5.2) already incorporate LID systems into their analysis.

4. Another line of research that can be deepened is in the study of discretization. In this study, certain parameters have been established to achieve a proper discretization of the DVs. The crude and refined lists, as well as the jumps or intervals have been adopted after having carried out an extensive number of simulations. However, it is still a criterion of its own that can be deeply studied to achieve an optimal discretization interval supported by other mathematical disciplines.

5. One field where the study can certainly be deepened is the SSR. In this work, a reduction in the size of the SS has been carried out, identifying the DVs that can be eliminated from the optimal search region. The process is iterative and although very effective, it can be improved, especially if it is taken into account that high computational resources are required, especially in the clustering method. An advantage of this methodology is that it can be applied to any type of heuristic optimization problem. However, the convenience of carrying out a previous study of the analyzed drainage network could be studied to detect DVs that can be eliminated before applying the optimization methods. It may also be thought that carrying out a pre-conditioning of the drainage network can reduce the SS. Finally, in this work it is not considered to make changes in the search algorithm to reduce the size of the SS. That may be an interesting line of research that may lead to promising results.

6. Another line of research that this work leaves started is about improving the efficiency of the model. To achieve this, a stopping criterion has been established which defines a high number of evaluations without improvement in the solutions found to stop the search algorithm. In this field, the study could be expanded in order to reduce the computational effort the proposed criterion requires. On the other hand, this work has not delved into the study of the algorithm parameters using the values traditionally used in this type of algorithms. An exhaustive study of the genetic operators (mutation, crossroads, and population size) for this type of problem could improve the calculation times to find the best solutions.

7. Another research area that should be included in this line of investigation is the study of water quality. While this work primarily focuses on flood prevention and its impacts in urban areas, water quality is a crucial aspect that is influenced during such events. Exploring the changes in water quality within the network and examining the effects of STs and HCs on water quality represent a promising avenue for future research.

8. Finally, this work presents a methodology based on the SSR to optimize drainage networks of large sizes. It is called the clustering method. This introduces a new line of research that can be initiated for this type of networks, with focus on the network schematization that allows reducing the size of the problem.

## 6.4 PUBLICATIONS RESULTING FROM THE DOCTORAL THESIS

As a result of the research carried out in this doctoral thesis, the following scientific publications have been produced.

**Scientific articles**

- Bayas-Jiménez, L.; Martínez-Solano, F. J.; Iglesias-Rey, P. L.; Mora-Melia, D. and Fuertes-Miquel, V. S. "Inclusion of Hydraulic Controls in Rehabilitation Models of Drainage Networks to Control Floods," Water, vol. 13, no. 4, p. 514, Feb. 2021. Available in:
- Bayas-Jiménez, L.; Martínez-Solano, F. J.; Iglesias-Rey, P. L. and Mora-Meliá, D. "Search space reduction for genetic algorithms applied to drainage network optimization problems," Water, vol. 13, no. 15, p. 2008, Jul. 2021. Available in:
- Bayas-Jiménez, L.; Martínez-Solano, F. J.; Iglesias-Rey, P. L. and Boano, F. "Economic Analysis of Flood Risk Applied to the Rehabilitation of Drainage Networks," Water 2022, Vol. 14, Page 2901, vol. 14, no. 18, p. 2901, Sep. 2022. Available in:

**Academic conference**

- Bayas-Jiménez, L.; Iglesias-Rey, P. L. and Martínez-Solano, F. J. Multi-Objective Optimization of Drainage Networks for Flood Control in Urban Area Due to Climate Change, Proceedings, vol. 48, no. 1, p. 27, Nov. 2019. Available in: https://doi.org/10.3390/ECWS-4-06451
- Bayas-Jiménez, L.; Martínez-Solano, F. J. and Iglesias-Rey, P. L. A Method to optimize Urban Drainage Networks Based on the Reduction of The Search Space of Genetic Algorithms. In Proceedings of 5th International Electronic Conference on Water Sciences. 16–30 Nov 2020. Available in: https://sciforum.net/manuscripts/8282/manuscript.pdf
- Bayas-Jiménez, L.; Iglesias-Rey, P. L. and Martínez-Solano, F. J. Optimización de redes de drenaje para el control de inundaciones en medios urbanos. In Proceedings of IV seminario UPMWATER, Madrid, Spain, 21 Jan 2021. ISBN: 978-84-09-32952-6. Available in: https://blogs.upm.es/upm-water/wp-content/uploads/sites/481/2021/10/IV-Seminario-UPMWater_Libro-de-Abstracts.pdf
- Bayas-Jiménez, L.; Martínez-Solano, F. J.; Iglesias-Rey, P. L. and Boano F. An approach to improve drainage networks based on the study of flood risk. In Proceedings of 2nd International Joint Conference on Water Distribution Systems Analysis & Computing and Control in the Water Industry. Valencia, Spain, 18-22 July 2022. Available in: https://doi.org/10.4995/WDSA-CCWI2022.2022.14186

**Chapters of books**

- Bayas-Jiménez, L.; Martínez-Solano, F. J. and Iglesias-Rey, P.L. Metodología de rehabilitación de redes de drenaje mediante la inclusión de elementos de control hidráulico. In Riesgo de inundación en España: análisis y soluciones para la generación de territorios resilientes. 1st ed.; López Ortiz, M. I.; Melgarejo Moreno, J. Universitat d'Alacant: Alicante, Spain, 2020; Vol. 1, 863-872. ISBN: 978-84-1302-091-4. Available in: http://rua.ua.es/dspace/handle/10045/109017
- Bayas-Jiménez, L.; Deño Nuñez, F.A.; Martínez-Solano¸F.J. and Iglesias-Rey P.L. Reducción del espacio de búsqueda en la optimización de redes de drenaje basada en el análisis de riesgo inundación. In Fenómenos extremos: sequías e inundaciones. Melgarejo Moreno J.; López Ortiz; J.M. Fernández Aracil, P. Universitat d'Alacant: Alicante, Spain,2021; Vol. 1, 809-820. ISBN: 978-84-1302-138-6. Available in: http://rua.ua.es/dspace/handle/10045/118411

# Chapter 7

# REFERENCES

1. United Nations - Department of Economic and Social Affairs - Statistics Division. SDG Indicators. Available online: https://unstats.un.org/sdgs/report/2022/Goal-11/. (Accessed: 17 November 2022).
2. The World Bank - Data. Urban population - Data. Available online: https://data.worldbank.org/indicator/SP.URB.TOTL. (Accessed: 17 November 2022)
3. United Nations - Development Programme. Sustainable Development Goals. Available online: https://www.undp.org/sustainable-development-goals#sustainable-cities-and-communities. (Accessed: 17 November 2022]
4. Yazdi, J. Lee, E. H.; and Kim, J. H. "Stochastic multiobjective optimization model for urban drainage network rehabilitation, *J. Water Resour. Plan. Manag*. **2015**, *141*, 8.
5. Gaudio, R.; Penna, N. and Viteritti, V. A combined methodology for the hydraulic rehabilitation of urban drainage networks, *Urban Water J*. **2016**, *13*, 644–656.
6. Cunha, M.C.; Zeferino, J.A.; Simões, N.E.; Santos, G.L.; Saldarriaga, J.G. A decision support model for the optimal siting and sizing of storage units in stormwater drainage systems. *Int. J. Sustain. Dev. Plan.* **2017**, *12*, 122–132.
7. Barreto Cordero, W. J.; Multi-objective optimization for urban drainage rehabilitation. PhD Thesis, Delft University of Technology, Delft - The Netherlands, March 2012.
8. Abass, K. Rising incidence of urban floods: understanding the causes for flood risk reduction in Kumasi, Ghana, *GeoJournal* **2022**, *87*, 1367–1384.
9. Leal, M.; Boavida-Portugal, I.; Fragoso, M.; Ramos, C. How much does an extreme rainfall event cost? Material damage and relationships between insurance, rainfall, land cover and urban flooding. *Hydrol. Sci. J.* **2019**, *64*, 673–689.
10. Maiolo, M. et al., On the Use of a Real-Time Control Approach for Urban Stormwater Management, *Water* **2020**, *12*, 2842.
11. Szeląg, B.; Suligowski, R.; De Paola, F.; Siwicki, P.; Majerek, D.; Łagód, G. Influence of urban catchment characteristics and rainfall origins on the phenomenon of stormwater flooding: Case study. *Environ. Model. Softw*. **2022**, *150*, 105335.
12. Lee, A.; Marotzke, J.-Y., J.; Bala, G.; Cao, L.; Corti, S.; Dunne, J.P.; Engelbrecht, F.; Fischer, E.; Fyfe, J.C.; Jones C.; Maycock, T. Z.; Mutemi, J.; Ndiaye, O. and Panickal, S. *IPCC AR6 Chapter 4. Future global climate: scenario-based projections and near-term information*, August. 2021.
13. Dunning, C. M.; Black, E. and Allan, R. P. Later Wet Seasons with More Intense Rainfall over Africa under Future Climate Change, *J. Clim*. **2018**, *31*, 9719–9738.
14. Tang, K. H. D. Climate change in Malaysia: Trends, contributors, impacts, mitigation and adaptations, *Sci. Total Environ*. **2019**, *650*, 1858–1871.
15. Tabari, H. Climate change impact on flood and extreme precipitation increases with water availability, *Sci. Reports 2020*, *10*, 1–10.
16. United Nations, Department of Economic and Social Affairs, Population Division (2018). *The World's Cities in 2018—Data Booklet* (ST/ESA/ SER.A/417). Available online: www.unpopulation.org.
17. Hernantes, J.; Maraña, P. Gimenez, R.; Sarriegi, J. M. and Labaka, L. Towards resilient cities: A maturity model for operationalizing resilience, *Cities* **2019**, *84*, 96–103.
18. Loganathan, G. V; Park, S. and Sherali, H. D. Threshold break rate for pipeline replacement in water distribution systems, *J. Water Resour. Plan. Manag*. **2002**, *128*, 271–279.
19. Gotsis, D.; Spiliotis, M. and Giakoumakis, S. Reuse of drainage water in irrigation with the aid of 0-1 linear programming, *Irrig. Drain. Syst*. **2011**, *25*, 385–394.
20. Rep, K. R.; Kompare, B. Roš, M. and Kravanja, S. Cost Optimization of Integrated Wastewater Drainage and Treatment Systems, *Water Environ. Res*. **2008**, *80*, 581–595.
21. Rashid, M. M.; Hayes, D. F. and Asce, M. Dynamic Programming Methodology for Prioritizing Sewerage Projects, *J. Water Resour. Plan. Manag*. **2010**, *137*, 193–204.
22. Afshar, M. H. A parameter free Continuous Ant Colony Optimization Algorithm for the optimal design of storm sewer networks: Constrained and unconstrained approach, *Adv. Eng. Softw*. **2010**, *41*, 188–195.
23. Vasudevan B. and Sinha, A. K. Reliability improvement of reconfigurable distribution system using GA and PSO, *Electr. Eng*. **2018**, *100*, 1263–1275.
24. Hosseini, S. M. and Ghasemi, A. Hydraulic performance analysis of sewer systems with uncertain parameters, *J. Hydroinformatics* **2012**, *14*, 682–696.
25. Zhang, D.; Martinez, N.; Lindholm, G. and Ratnaweera, H. Manage Sewer In-Line Storage Control Using Hydraulic Model and Recurrent Neural Network, *Water Resour. Manag*. **2018**, *32*, 2079–2098.
26. Afshar, M. H.; Shahidi, M.; Rohani, M. and Sargolzaei, M. Application of cellular automata to sewer network optimization problems, *Sci. Iran*. **2011**, *18*, 304–312.
27. Li, F.; Yan, X.-F. and Duan, H.-F. Sustainable Design of Urban Stormwater Drainage Systems by Implementing Detention Tank and LID Measures for Flooding Risk Control and Water Quality Management, *Water Resour. Manag.* **2019**, *33*, 3271-3288.

28. Andrés-Doménech, I.; Montanari, A.; Marco, J.B. Efficiency of storm detention tanks for urban drainage systems under climate variability. *J. Water Resour. Plan. Manag.* **2012**, *138*, 36–46.
29. Duan, H. F.; Li, F. and Yan, H. Multi-Objective Optimal Design of Detention Tanks in the Urban Stormwater Drainage System: LID Implementation and Analysis, *Water Resour. Manag*. **2016**, *30*, 4635–4648.
30. Woods, B. B.; Kellagher, R.; Martin, P.; Jefferies, C.; Bray, R. and Shaffer, P. *The SUDS manual (C697)*; CIRIA, London, United Kingdom, 2007, 600, 2007.
31. Todeschini, S.; Papiri, S. and Ciaponi, C. Performance of stormwater detention tanks for urban drainage systems in northern Italy, *J. Environ. Manage*. **2012**, *101*, 33–45.
32. Cunha, M.C.; Zeferino, J.A.; Simões, N.E.; Saldarriaga, J.G. Optimal location and sizing of storage units in a drainage system. *Environ. Model. Softw*. **2016**, *83*, 155–166.
33. Wang, M.; Sun, Y.; Sweetapple, C. Optimization of storage tank locations in an urban stormwater drainage system using a two-stage approach. *J. Environ. Manag*. **2017**, *204*, 31–38.
34. Zhang, P.; Cai, Y.; and Wang, J. A simulation-based real-time control system for reducing urban runoff pollution through a stormwater storage tank, *J. Clean. Prod*. **2018**, *183*, 641–652.
35. J. R. Vogel et al., “Critical Review of Technical Questions Facing Low Impact Development and Green Infrastructure: A Perspective from the Great Plains,” Water Environ. Res., vol. 87, no. 9, pp. 849–862, Sep. 2015.
36. Iglesias-Rey, P.L.; Martínez-Solano, F.J.; Saldarriaga, J.G.; Navarro-Planas, V.R. Pseudo-genetic Model Optimization for Rehabilitation of Urban Storm-water Drainage Networks. *Procedia Eng.* **2017**, *186*, 617–625.
37. Cimorelli, L.; Morlando, F.; Cozzolino, L.; Covelli, C.; Della Morte, R.; Pianese, D. Optimal positioning and sizing of detention tanks within urban drainage networks. *J. Irrig. Drain. Eng.* **2016**, *142*, 1.
38. Ngamalieu-Nengoue, U.A.; Iglesias-Rey, P.L.; Martínez-Solano, F.J.; Mora-Meliá, D.; Valderrama, J.G.S. Urban drainage network rehabilitation considering storm tank installation and pipe substitution. *Water* **2019**, *11*, 515.
39. Li, X. et al., Multisurrogate Assisted Evolutionary Algorithm–Based Optimal Operation of Drainage Facilities in Urban Storm Drainage Systems for Flood Mitigation, *J. Hydrol. Eng*. **2022**, *27*, 11.
40. Lee, E. H.; Lee, Y. S.; Joo, J. G.; Jung, D. and Kim, J. H. Investigating the Impact of Proactive Pump Operation and Capacity Expansion on Urban Drainage System Resilience, *J. Water Resour. Plan. Manag*. **2017**, *143*, 04017024.
41. Ngamalieu-Nengoue, U.A.; Martínez-Solano, F.J.; Iglesias-Rey, P.L.; Mora-Meliá, D. Multi-objective optimization for urban drainage or sewer networks rehabilitation through pipes substitution and storage tanks installation. *Water* **2019**, *11*, 935.
42. Di Matteo, M. et al., Controlling rainwater storage as a system: An opportunity to reduce urban flood peaks for rare, long duration storms, *Environ. Model. Softw*. **2019**, *111*, 34–41.
43. Schellin, L. M., Dziedzic R. M., and Dziedzic M., “private lot flood peak attenuation by stormwater detention tanks,” wit trans. Built environ. **2022**, vol. 208, pp. 53–64.
44. Ngamalieu-Nengoue, U.A.; Iglesias-Rey, P.L.; Martínez-Solano, F.J. Urban Drainage Networks Rehabilitation Using Multi-Objective Model and Search Space Reduction Methodology. *Infrastructures* **2019**, *4*, 35.
45. F. Jafari, S. J. Mousavi, J. Yazdi, and J. H. Kim, Long-term versus Real-time Optimal Operation for Gate Regulation during Flood in Urban Drainage Systems, Urban Water Journal 2018, *15*, 750–759.
46. Kändler, N.; Annus, I. and Vassiljev, A. Controlling peak runoff from plots by coupling street storage with distributed real time control, *Urban Water Journal* **2021**, *19*, 97–108.
47. Leitão, J.P.; Carbajal, J.P.; Rieckermann, J.; Simões, N.E.; Sá Marques, A.; de Sousa, L.M. Identifying the best locations to install flow control devices in sewer networks to enable in-sewer storage, *J. Hydrol.* **2018**, *556*, 371–383.
48. Słyś, D. An innovative retention canal-a case study. *E3S Web Conf.* **2018**, 45,*84*, doi:10.1051/e3sconf/20184500084.
49. Dziopak, J. A wastewater retention canal as a sewage network and accumulation reservoir. *E3S Web Conf.* **2018**, *45*, 16.
50. Lekuthai, A. and Vongvisessomjai, S. Intangible flood damage quantification, *Water Resour. Manag*. **2001**, *15*, 343–362.
51. O’Donnell, E.C.; Thorne, C.R. Drivers of future urban flood risk, Philosophical Transactions of the Royal Society A: Mathematical. *Phys. Eng. Sci.* **2020**, *378*, 2168.
52. Kashyap, S. and Mahanta, R. Socioeconomic Vulnerability to Urban Floods in Guwahati, Northeast India: An Indicator-Based Approach, *Economic Effects of Natural Disasters*, **2021**, 457–475.

53. Morita, M. and Tung, Y. K. Uncertainty quantification of flood damage estimation for urban drainage risk management, *Water Sci. Technol*. **2019**, *80*, 478–486.
54. Martínez-Gomariz, E.; Forero-Ortiz, E.; Guerrero-Hidalga, M.; Castán, S. and Gómez, M. Flood depth-damage curves for Spanish urban areas, *Sustain*. **2020**, 12, 2666.
55. Pistrika, A.; Tsakiris, G. and Nalbantis, I. Flood Depth-Damage Functions for Built Environment, *Environ. Process*. **2014**, *1*, 553–572.
56. Tariq, M. A. U. R.; Hoes, O. A. C.; Van De Giesen, N. C.; Muhammad, C.; Ur, A. and Tariq, R. Development of a risk-based framework to integrate flood insurance, *J. Flood Risk Manag.***2014**, *7*, 291–307.
57. Cammerer, H.; Thieken, A. H. and Lammel, J. Adaptability and transferability of flood loss functions in residential areas, *Nat. Hazards Earth Syst. Sci*. **2013**, *13*, 3063–3081.
58. Nafari, R. H.; Ngo, T. and Mendis, P. An Assessment of the Effectiveness of Tree-Based Models for Multi-Variate Flood Damage Assessment in Australia, *Water* **2016**, *8*, 282.
59. Carisi, F.; Schröter, K.; Domeneghetti, A. ¸ Kreibich, H. and Castellarin, A. Development and assessment of uni- and multivariable flood loss models for Emilia-Romagna (Italy), *Nat. Hazards Earth Syst. Sci*. **2018**, *18*, 2057–2079.
60. Karamouz, M.; Fereshtehpour, M.; Ahmadvand, F. and Zahmatkesh, Z. Coastal Flood Damage Estimator: An Alternative to FEMA's HAZUS Platform, *J. Irrig. Drain. Eng*. **2016**, *142*, 04016016.
61. Budiyono, Y.; Aerts, J.; Brinkman, J. J.; Marfai, M. A. and Ward, P. Flood risk assessment for delta mega-cities: a case study of Jakarta, *Nat. Hazards* **2015**, *75*, 389–413.
62. Olsen, A.S.; Zhou, Q.; Linde, J.J.; Arnbjerg-Nielsen, K. Comparing methods of calculating expected annual damage in urban pluvial flood risk assessments. *Water* **2015**, *7*, 255–270.
63. Merz, B.; Elmer, F. and Thieken, A. H. Significance of 'high probability/low damage' versus 'low probability/high damage' flood events, *Nat. Hazards Earth Syst. Sci*. **2009**, *9*, 1033–1046.
64. Arnbjerg-Nielsen, K.; Fleischer, H.S. Feasible adaptation strategies for increased risk of flooding in cities due to climate change. *Water Sci. Technol*. **2009**, *60*, 273–281.
65. Jamali, B.; Bach, P. M. and Deletic, A. Rainwater harvesting for urban flood management – An integrated modelling framework, *Water Res*. **2020**, *171*, 115372.
66. Locatelli, L.; Guerrero, M.; Russo, B.; Martínez-Gomariz, E.; Sunyer, D.; Martínez, M. Socio-Economic Assessment of Green Infrastructure for Climate Change Adaptation in the Context of Urban Drainage Planning. *Sustainability* **2020**, *12*, 3792.
67. Liu, H.; Wang, Y.; Zhang, C.; Chen, A. S., and Fu, G. Assessing real options in urban surface water flood risk management under climate change, *Nat. Hazards* **2018**, *94*, 1–18.
68. Zhou, Q.; Mikkelsen, P.S.; Halsnæs, K.; Arnbjerg-Nielsen, K. Framework for economic pluvial flood risk assessment considering climate change effects and adaptation benefits. *J. Hydrol*. **2012**, *414*, 539–549.
69. Ward, P. J.; De Moel, H. and Aerts, J. C. J. H. How are flood risk estimates affected by the choice of return-periods? *Nat. Hazards Earth Syst. Sci*. **2011**, *11*, 3181–3195.
70. Merz, B.; Kreibich, H.; Schwarze, R. and Thieken, A. Assessment of economic flood damage, *Natural Hazards and Earth System Science* **2010**, *10*, 1697–1724.
71. Rossman, L.A. *Storm Water Management Model (SWMM) User's Manual Version 5.0*; U.S. EPA; Cincinnati, OH, USA, 2009.
72. Deltares Hydraulics, *SOBEK: user's manual*; Delft, the Netherlands, 2004.
73. DHI, *MOUSE pipe flow reference manual*; DHI Software Horsolm, Denmark, 2002.
74. Rubinato, M.; Shucksmith, J.; Saul, A. J. and Shepherd, W. Comparison between InfoWorks hydraulic results and a physical model of an urban drainage system, *Water Sci. Technol*. **2013**, *68*, 372–379.
75. Schmitt, T. G.; Thomas, M. and Ettrich, N. Analysis and modeling of flooding in urban drainage systems, *J. Hydrol*. **2004**, *299*, 300–311.
76. Nicklow, J.; Reed, P.; Savic, D.; Dessalegne, T. State of the Art for Genetic Algorithms and Beyond in Water Resources Planning and Management. *J. Water Resour. Plan. Manag.* **2009**, *136*, 412–432.
77. Park, M.; Chung, G.; Yoo, C. and Kim, J. H. Optimal design of stormwater detention basin using the genetic algorithm, *KSCE J. Civ. Eng*. **2012**, *16*, 660–666.
78. Sophocleous, S.; Savić, D.; Kapelan, Z. Leak Localization in a Real Water Distribution Network Based on Search-Space Reduction. *J. Water Resour. Plan. Manag.* **2019**, *145*, 04019024.
79. Cimorelli, L.; Cozzolino, L.; Covelli, C.; Mucherino, C.; Palumbo, A. and Pianese, D. Optimal Design of Rural Drainage Networks, *J. Irrig. Drain. Eng*. **2013**, 139, 137–144.
80. Sebti, A.; Bennis, S. and Fuamba, M. Cost optimization of hydraulic and structural rehabilitation of urban drainage network, *J. Infrastruct. Syst*. **2014**, *20*, 3.

81. Eusuff M. M. and Lansey, K. E. Optimization of Water Distribution Network Design Using the Shuffled Frog Leaping Algorithm, *J. Water Resour. Plan. Manag*. **2003**, *129*, 210–225.
82. Chung, G.; Lansey, K.; Chung, G. and Lansey K., Application of the Shuffled Frog Leaping Algorithm for the Optimization of a General Large-Scale Water Supply System, *Water Resour. Manag*. **2008** *23*, 797–823.
83. Kumar, S.; Kaushal, D. R., and Gosain, A. K. Study of Parameters Optimization Using SFLA for the Stormwater Drainage Network of Extremely Urbanized Settlements. In Proceedings of *Urbanization Challenges in Emerging Economies*, New Delhi, India, December 12-14, 2017.
84. Kumar, S.; Kaushal, D. R. and Gosain, A. K. Evaluation of evolutionary algorithms for the optimization of storm water drainage network for an urbanized area, *Acta Geophys*. **2019**, *67*, 149–165.
85. Sousa, J.; Ribeiro, L.; Muranho, J. and Sá Marques, A. Locating Leaks in Water Distribution Networks with Simulated Annealing and Graph Theory, *Procedia Eng*. **2015**, *119*, 63–71.
86. Wang, Z.; Tian, J. and Feng, K. Optimal allocation of regional water resources based on simulated annealing particle swarm optimization algorithm, *Energy Reports* **2022**, *8*, 9119–9126.
87. Moeini, R. Different hydraulic analysis conditions for sewer network design optimisation problem using three different evolutionary algorithms, *Int. J. Oper. Res*. **2018**, *33*, 512–537.
88. Ahmadi, A.; Zolfagharipoor, M. A. and Nafisi, M. Development of a Hybrid Algorithm for the Optimal Design of Sewer Networks, *J. Water Resour. Plan. Manag*. **2018**, *144*, 04018045.
89. Kaddoura, K. Performance Modeling for Sewer Networks, PhD Thesis, Concordia University, Montreal, Quebec, Canada, June 2018.
90. Afshar, M. H. Application of a genetic algorithm to storm sewer network optimization, *Sci. Iran*. **2006**, *13*, 234–244.
91. Mora, D. Design of Water Distribution Networks Using Evolutionary Algorithms. Efficiency Analysis. Ph.D. Thesis, Universitat Politècnica de València, Valencia, Spain, July 2012. (In Spanish)
92. Maier, H.R.; Kapelan, Z.; Kasprzyk, J.; Kollat, J.; Matott, L.S.; Cunha, M.C.; Reed, P.M. Evolutionary algorithms and other metaheuristics in water resources: Current status, research challenges and future directions. *Environ. Model. Softw*. **2014**, *62*, 271–299.
93. Afshar, M. H. Rebirthing genetic algorithm for storm sewer network design, *Sci. Iran.***2011**, *19*, 11–19, 2011.
94. Reca, J.; Martínez, J.; López, R. A Hybrid Water Distribution Networks Design Optimization Method Based on a Search Space Reduction Approach and a Genetic Algorithm. *Water* **2017**, *9*, 845.
95. Guo, Y.; Keedwell, E. C.; Walters, G. A. and Khu, S. T. Hybridizing cellular automata principles and NSGAII for multi-objective design of urban water networks, *Lect. Notes Comput. Sci.***2007**, *4403 LNCS*, 546–559.
96. Kadu, M.S.; Gupta, R.; Bhave, P.R. Optimal Design of Water Networks Using a Modified Genetic Algorithm with Reduction in Search Space. *J. Water Resour. Plan. Manag*. **2008**, *134*, 147–160.
97. Zheng, F.; Simpson, A. R. and Zecchin, A. C. Dynamically Expanding Choice-Table Approach to Genetic Algorithm Optimization of Water Distribution Systems, *J. Water Resour. Plan. Manag*. **2011**, *137*, 547–551.
98. Zheng, F.; Simpson, A. R. and Zecchin, A. C. Coupled Binary Linear Programming–Differential Evolution Algorithm Approach for Water Distribution System Optimization, *J. Water Resour. Plan. Manag*. **2014**, *140*, 585–597.
99. Creaco, E.; Pezzinga, G. Embedding linear programming in multi objective genetic algorithms for reducing the size of the search space with application to leakage minimization in water distribution networks. *Environ. Model. Softw*. **2015**, *69*, 308–318.
100. Zielinski, K.; Peters, D. and Laur, R. Stopping Criteria for Single-Objective Optimization. Chakraborty, In *Advances in Differential Evolution. Studies in Computational Intelligence*, Springer, Heidelberg, Berlin, Germany, 2008; Volume 143.
101. Testa, G.; Zuccalà, D.; Alcrudo, F.; Mulet, J. and Soares-Frazão, S. Flash flood flow experiment in a simplified urban district, Journal of Hydraulic Research **2010**, *45*, 37–44.
102. Xia, J.; Falconer, R. A.; Lin, B. and Tan, G. Modelling flash flood risk in urban areas, *Proc. Inst. Civ. Eng. Water Manag*. **2011**, *164*, 267–282.
103. Merz, R.; Blöschl, G. A process typology of regional floods. *Water Resour. Res*. **2003**, *39*, 12.

104. Mora-Melia, D.; Iglesias-Rey, P.L.; Martinez-Solano, F.J.; Fuertes-Miquel, V.S. Design of Water Distribution Networks using a Pseudo-Genetic Algorithm and Sensitivity of Genetic Operators. *Water Resour. Manag*. **2013**, *27*, 4149–4162.
105. Gosling, S.N.; Arnell, N.W. A global assessment of the impact of climate change on water scarcity. *Clim. Change* **2016**, *134*, 371–385.
106. Döll, P.; Jiménez-Cisneros, B.; Oki, T.; Arnell, N.; Benito, G.; Cogley, J.G.; Jiang, T.; Kundzewicz, Z.; Mwakalila, S.; Nishijima, A. Integrating risks of climate change into water management. *Hydrol. Sci. J*. **2014**, *60*, 4–13.
107. Field, C.B. Managing the risks of extreme events and disasters to advance climate change adaption: Special report of the Intergovernmental Panel on Climate Change. *Choice Rev. Online* **2013**, *50*, 4454.
108. Kwon, S.H.; Jung, D.; Kim, J.H. Urban drainage system design minimizing system cost constrained to failure depth and duration under flooding events. *Adv. Intell. Syst. Comput.* **2019**, *741*, 153–158.
109. Alves, A.; Vojinovic, Z.; Kapelan, Z.; Sanchez, A.; Gersonius, B. Exploring trade-offs among the multiple benefits of green-blue-grey infrastructure for urban flood mitigation. *Sci. Total Environ.* **2020**, *703*, 134980.
110. Dawson, R.J.; Speight, L.; Hall, J.W.; Djordjevic, S.; Savic, D.; Leandro, J. Attribution of flood risk in urban areas, *J. Hydroinform.* **2008**, *10*, 275–288.
111. Nicklin, H.; Leicher, A.M.; Dieperink, C.; Van Leeuwen, K. Understanding the Costs of Inaction—An Assessment of Pluvial Flood Damages in Two European Cities. *Water* **2019**, *11*, 801.
112. Simões, N.E.; Ochoa-Rodríguez, S.; Wang, L.P.; Pina, R.D.; Marques, A.A.S.; Onof, C.; Leitão, J.P. Stochastic Urban Pluvial Flood Hazard Maps Based upon a Spatial-Temporal Rainfall Generator. *Water* **2015**, *7*, 3396–3406.
113. Rözer, V.; Müller, M.; Bubeck, P.; Kienzler, S.; Thieken, A.; Pech, I.; Schröter, K.; Buchholz, O.; Kreibich, H. Coping with pluvial floods by private households. *Water* **2016**, *8*, 304.
114. Van Ootegem, L.; Verhofstadt, E.; Van Herck, K.; Creten, T. Multivariate pluvial flood damage models. *Environ. Impact Assess. Rev*. **2015**, *54*, 91–100.
115. Howard, C.D.D. Theory of storage and treatment-plant overflows. *J. Environ. Eng. Div.* **1976**, *102*, 709–722.
116. Butler, D.; McEntee, B.; Onof, C.; Hagger, A. Sewer storage tank performance under climate change. *Water Sci. Technol.* **2007**, *56*, 29–35.
117. Saaty, T.L. *The Analytic Hierarchy Process*; Mcgraw Hill: New York, NY, USA, 1980.
118. Saldarriaga, J.; Salcedo, C.; Solarte, L.; Pulgarín, L.; Rivera, M.L.; Camacho, M.; Iglesias-Rey, P.L.; Martínez-Solano, F.J.; Cunha, M. Reducing Flood Risk in Changing Environments: Optimal Location and Sizing of Stormwater Tanks Considering Climate Change. *Water* **2020**, *12*, 2491.
119. Martínez-Solano, F.J.; Iglesias-Rey, P.L.; Saldarriaga, J.G.; Vallejo, D. Creation of an SWMM toolkit for its application in urban drainage networks optimization. *Water* **2016**, *8*, 259.
120. Tullis, J.P. *Hydraulics of Pipelines: Pumps, Valves, Cavitation, Transients*; John Wiley & Sons: New York, NY, USA, 1989; p. 91.
121. Guaya-Caraguay, C.I.; Bayas-Jiménez, L.; Iglesias-Rey, P.L.; Martínez-Solano, F.J.; Briceño-León, C.X. Rehabilitation of Drainage Networks Using Optimization Algorithms and Solution Space Reduction Methodologies. In Proceedings of the 24th International Congress on Project Management and Engineering, Alcoy, Spain, 7–10 July 2020.
122. IDECA (Infraestructura de Datos Espaciales para el Distrito Capital). Available online: https://mapas.bogota.gov.co (accesed on 5 February 2021).
123. Kaykhosravi, S.; Khan, U.T.; Jadidi, M.A. The effect of climate change and urbanization on the demand for low impact development for three Canadian cities. *Water* **2020**, *12*, 1280.
124. Ma, B.; Wu, Z.; Wang, H.; Guo, Y. Study on the Classification of Urban Waterlogging Rainstorms and Rainfall Thresholds in Cities Lacking Actual Data. *Water* **2020**, *12*, 3328.
125. Zhuang, Q.; Liu, S.; Zhou, Z. Spatial Heterogeneity Analysis of Short-Duration Extreme Rainfall Events in Megacities in China. *Water* **2020**, *12*, 3364.
126. Agarwal, S.; Kumar, S. Applicability of SWMM for semi urban catchment flood modeling using extreme rainfall events. *Int. J. Recent Technol. Eng.* **2020**, *8*, 245–251.
127. Ciupa, T.; Suligowski, R. Impact of the City on the Rapid Increase in the Runoff and Transport of Suspended and Dissolved Solids During Rainfall—The Example of the Silnica River (Kielce, Poland). *Water* **2020**, *12*, 2693.
128. Jha, M.; Afreen, S. Flooding Urban Landscapes: Analysis Using Combined Hydrodynamic and Hydrologic Modeling Approaches. *Water* **2020**, *12*, 1986.

129. Leal, M.; Boavida-Portugal, I.; Fragoso, M.; Ramos, C. How much does an extreme rainfall event cost? Material damage and relationships between insurance, rainfall, land cover and urban flooding. *Hydrol. Sci. J.* **2019**, *64*, 673–689.
130. O'Donnell, E.C.; Thorne, C.R. Drivers of future urban flood risk, Philosophical Transactions of the Royal Society A: Mathematical. *Phys. Eng. Sci.* **2020**, *378*, 2168.
131. Mora-Melià, D.; López-Aburto, C.S.; Ballesteros-Pérez, P.; Muñoz-Velasco, P. Viability of Green Roofs as a Flood Mitigation Element in the Central Region of Chile. *Sustainability* **2018**, *10*, 1130.
132. Carter, T.; Jackson, C.R. Vegetated roofs for stormwater management at multiple spatial scales. *Landsc. Urban Plan.* **2007**, *80*, 84–94.
133. Mentens, J.; Raes, D.; Hermy, M. Green roofs as a tool for solving the rainwater runoff problem in the urbanized 21st century? *Landsc. Urban Plan.* **2006**, *77*, 217–226.
134. Bayas-Jiménez, L.; Martínez-Solano, F.J.; Iglesias-Rey, P.L.; Mora-Melia, D.; Fuertes-Miquel, V.S. Inclusion of Hydraulic Controls in Rehabilitation Models of Drainage Networks to Control Floods. *Water* **2021**, *13*, 514.
135. Lee, E.H.; Kim, J.H. Development of a Reliability Index Considering Flood Damage for Urban Drainage Systems. *KSCE J. Civ. Eng.* **2019**, *23*, 1872–1880.
136. Yin, H.; Zheng, F.; Duan, H.F.; Zhang, Q.; Bi, W. Enhancing the effectiveness of urban drainage system design with an improved ACO-based method. *J. Hydro-Environment Res.* **2020**.
137. Apte, S.; Kshirsagar, M.; Khare, K. Optimization of storm water drainage network using ant colony system. In Proceedings of the 1st International Conference on Data Science and Analytics, Pune, India, 30 Nov.-2 Dec. 2018, Publisher: 2018.
138. Kwon, S.H.; Jung, D.; Kim, J.H. Development of a Multiscenario Planning Approach for Urban Drainage Systems. *Appl. Sci.* **2020**, *10*, 1834.
139. Liao, H.-Y.; Pan, T.-Y.; Chang, H.-K.; Hsieh, C.-T.; Lai, J.-S.; Tan, Y.-C.; Su, M.-D. Using Tabu Search Adjusted with Urban Sewer Flood Simulation to Improve Pluvial Flood Warning via Rainfall Thresholds. *Water* **2019**, *11*, 348.
140. Yazdi, J.; Sadollah, A.; Lee, E.H.; Yoo, D.G.; Kim, J.H. Application of multi-objective evolutionary algorithms for the rehabilitation of storm sewer pipe networks. *J. Flood Risk Manag.* **2017**, *10*, 326–338.
141. Yazdi, J.; Mohammadiun, S.; Sadiq, R.; Salehi Neyshabouri, S.A.A.; Alavi Gharahbagh, A. Assessment of different MOEAs for rehabilitation evaluation of Urban Stormwater Drainage Systems–Case study: Eastern catchment of Tehran. *J. Hydro-Environ. Res.* **2018**, *21*, 76–85.
142. Schraudolph, N.N.; Belew, R.K. Dynamic Parameter Encoding for Genetic Algorithms. *Mach. Learn.* **1992**, *9*, 9–21.
143. Ndiritu, J.G.; Daniell, T.M. An improved genetic algorithm for rainfall-runoff model calibration and function optimization. *Math. Comput. Model.* **2001**, *33*, 695–706.
144. Mala-Jetmarova, H.; Sultanova, N.; Savic, D. Lost in optimisation of water distribution systems? A literature review of system operation. *Environ. Model. Softw.* **2017**, *93*, 209–254.
145. Xiong, L.; Yan, L.; Du, T.; Yan, P.; Li, L.; Xu, W. Impacts of Climate Change on Urban Extreme Rainfall and Drainage Infrastructure Performance: A Case Study in Wuhan City, China. *Irrig. Drain*. **2019**, *68*, 152–164.
146. Salinas-Rodriguez, C.; Gersonius, B.; Zevenbergen, C.; Serrano, D.; Ashley, R. A Semi Risk-Based Approach for Managing Urban Drainage Systems under Extreme Rainfall. *Water* **2018**, *10*, 384.
147. Szewrański, S.; Chruściński, J.; Kazak, J.; Świąder, M.; Tokarczyk-Dorociak, K.; Żmuda, R. Pluvial Flood Risk Assessment Tool (PFRA) for Rainwater Management and Adaptation to Climate Change in Newly Urbanised Areas. *Water* **2018**, *10*, 386.
148. Oberascher, M.; Kinzel, C.; Kastlunger, U.; Kleidorfer, M.; Zingerle, C.; Rauch, W.; Sitzenfrei, R. Integrated urban water management with micro storages developed as an IoT-based solution—The smart rain barrel. *Environ. Model. Softw*. **2021**, *139*, 105028.
149. Olcina, J.; Hernández, M.; Morote, Á.-F.; Eslamian, S. Reducing Flood Risk in Spain: The Role of Spatial Planning. In *Flood Handbook*, 1st ed.; Eslamian, S., Eslamian, F.A., Eds.; CRC Press: Boca Raton, FL, USA, 2022; pp. 217–226.
150. Meyer, V.; Becker, N.; Markantonis, V.; Schwarze, R.; Van der Bergh, J.C.J.M.; Bouwer, L.M.; Viavattene, C. Review article: Assessing the costs of natural hazards—State of the art and knowledge gaps. *Nat. Hazards Earth Syst. Sci*. **2013**, *13*, 1351–1373.
151. Mobini, S.; Nilsson, E.; Persson, A.; Becker, P.; Larsson, R. Analysis of pluvial flood damage costs in residential buildings—A case study in Malmö. *Int. J. Disaster Risk Reduct*. **2021**, *62*, 102407.
152. Bayas-Jiménez, L.; Martínez-Solano, F.J.; Iglesias-Rey, P.L.; Mora-Meliá, D. Search space reduction for genetic algorithms applied to drainage network optimization problems. *Water* **2021**, *13*, 2008.

153. Marchi, A.; Salomons, E.; Ostfeld, A.; Kapelan, Z.; Simpson, A.; Zecchin, A.; Maier, H.; Wu, Z.; Elsayed, S.M.; Song, Y.; et al. Battle of the Water Networks II. *J. Water Resour. Plan. Manag*. **2014**, *140*, 04014009.
154. Freni, G.; La Loggia, G.; Notaro, V. Uncertainty in urban flood damage assessment due to urban drainage modelling and depth-damage curve estimation. *Water Sci. Technol.* **2010**, *61*, 2979–2993.
155. Arnell, N.W. Expected Annual Damages and Uncertainties in Flood Frequency Estimation. *J. Water Resour. Plan. Manag*. **1989**, *115*, 94–107.
156. Butler, D.; Digman, C.J.; Makropoulos, C.; Davies, J.W. *Urban Drainage*, 4th ed.; CRC Press, Taylor & Francis Group: Boca Raton, FL, USA, 2018.
157. Reca, J.; Martínez, J.; López, R. A Hybrid Water Distribution Networks Design Optimization Method Based on a Search Space Reduction Approach and a Genetic Algorithm. *Water* **2017**, *9*, 845.
158. Martínez-Gomariz, E.; Gómez, M.; Russo, B.; Sánchez, P.; Montes, J.-A. Methodology for the damage assessment of vehicles exposed to flooding in urban areas. *J. Flood Risk Manag*. **2019**, *12*, e12475.
159. Steiner, H. M. *A review of engineering economic principles*. Mcgraw-hill New York, USA, 2007; 264–265.
160. Bayas-Jiménez, L.; Iglesias-Rey, P. L. and Martínez-Solano, F. J. Multi-Objective Optimization of Drainage Networks for Flood Control in Urban Area Due to Climate Change, *Multidisciplinary Digital Publishing Institute Proceedings* **2019**,*48,* 27.
161. IDEAM (Instituto de Hidrología, Meteorología y Estudios Ambientales). Available online: http://dhime.ideam.gov.co/atencionciudadano/ (accessed on 5 de February 2021)
162. ARPA (L’Agenzia Regionale per la Protezione Ambientale del Piemonte). Available online: https://geoportale.arpa.piemonte.it/app/public/ (accesed on 10 January 2022)

# APPENDIX

# APPENDIX I. NOTATION

| | |
|---|---|
| $a$ | coefficient of the line of the flood cost |
| $A_i$ | flood área [$m^2$] |
| $A_s$ | adjustment coefficient for the tank section |
| $b$ | coefficient of the line of the flood cost |
| $B_s$ | adjustment coefficient for the tank section |
| $C_1$ | adjustment coefficient in the equation of losses in valves |
| $C_2$ | adjustment coefficient in the equation of losses in valves |
| $C_C(D_i)$ | cost of the installation of the hydraulic control |
| $C_D(D_i)$ | cost of the renovation of pipes |
| $C_{max}$ | maximus cost per square meter that cause a flood |
| $C_{min}$ | minimum cost established for the storm tank |
| $C_P(D_i)$ | cost of pipe replacement |
| $C_s$ | adjustment coefficient for the tank section |
| $C_T(V_i)$ | cost of building a storm tank |
| $C_v(D_i)$ | cost of the installation of the hydraulic control |
| $C_V(V_i)$ | cost of installation of the storm tank |
| $C_{var}$ | constant in the cost function of storm tanks |
| $C_y$ (yi) | damage costs caused by the flood |
| $D_i$ | diameter of pipe [m] |
| $F$ | objective function |
| $g$ | acceleration of the gravity [m/s2] |
| $G_{max}$ | stop criterion |
| $h_i$ | invert elevation of storm tank [m] |
| $k$ | coefficient of losses in valves |
| $L_i$ | pipe length (m) |
| $m$ | Pipes |
| $m_i$ | pipes considered in a defined scenario |
| $m_s$ | pipes selected to be optimized |
| $N$ | partition range of cross section |
| $n$ | nodes |
| $N_0$ | reduced number of cross section partitions |
| $N_C$ | number of pipes in the network |
| $ND$ | options list for pipes |
| $ND_0$ | coarse options list for pipes |
| $ND_{max}$ | refined options list for pipes |
| $N_{DV}$ | number of decision variables |
| $n_i$ | nodes considered in a defined scenario |
| $N_{it}$ | number of evaluations |
| $N_{max}$ | maximum number of cross-section partitions |
| $N_N$ | number of nodes in the network |
| $NS$ | options list used for nodes |
| $n_s$ | nodes selected to be optimized |
| $NS_0$ | coarse option list for nodes |

| | |
|---|---|
| $N_{sim}$ | number of simulations in each evaluation |
| $NS_{max}$ | refined option list for nodes |
| $N\theta$ | options list for hydraulic controls |
| $p$ | annual exceedance rate |
| $p_0$ | annual exceedance rate for which flood damage begins to occur |
| $P_{95}$ | ninety-five percentile |
| $P_e$ | success probability |
| $p_i$ | pipes considered to install hydraulic controls in a defined scenario |
| $P_{mut}$ | mutation probability |
| $p_n$ | percentage of the best solutions |
| $P_O$ | occurrence probability |
| $p_s$ | pipes selected to install hydraulic controls |
| $r$ | annual interest |
| $S$ | cross-section of the tank [m$^2$] |
| $S_i$ | area of storm tank [m$^{2]}$ |
| $S_{max}$ | maximum cross-section of the tank [m$^2$] |
| $t$ | years to recover the investment |
| $T$ | return period |
| $V$ | average speed of flow through the gate [m/s] |
| $V_i$ | storage volume [m$^3$] |
| $v_s$ | pipes selected to install hydraulic controls in the optimization process |
| $w$ | exponent in the cost function of storm tanks |
| $X_i$ | value of decision variable taken from the options list for storm tanks |
| $X_{max}$ | maximum number of discretization options of the decision variables |
| $y_i$ | water level of the node [m] |
| $y_{max}$ | maximus flood level [m$^3$] |
| $\alpha$ | adjustment coefficient for calculating the cost of replacing pipes |
| $\beta$ | adjustment coefficient for calculating the cost of replacing pipes |
| $\gamma$ | adjustment coefficient for calculating the cost of replacing pipes |
| $\delta$ | constant for the calculation of the mutation probability |
| $\Delta H$ | loss of energy in the gate [m] |
| $\Delta ND$ | range of diameters immediately larger than the analyzed pipe |
| $\Delta S$ | spacing interval in the discretization of area of storm tank |
| $\theta$ | valve opening percentage |
| $\Lambda$ | annual amortization factor |
| $\lambda$ | adjustment coefficient for calculation of flood damage |
| $\mu$ | adjustment coefficient for calculating the cost of installing hydraulic controls |
| $\sigma$ | adjustment coefficient for calculating the cost of installing hydraulic controls |
| $\upsilon$ | adjustment coefficient for calculation of flood damage |
| $\varphi$ | adjustment coefficient for calculating the cost of installing hydraulic controls |
| $\phi$ | constant for calculation of population |
| $\omega$ | adjustment constant for the calculation of the cost of the construction of storm tanks |
| Л | population size |
| $\tau_1$ | adjustment coefficient of objective function |
| $\tau_2$ | adjustment coefficient of objective function |
| $\tau_3$ | adjustment coefficient of objective function |

| | |
|---|---|
| $\tau_4$ | adjustment coefficient of objective function |

# APPENDIX II. ABBREVIATIONS

| | |
|---|---|
| AHP | Analytical Hierarchy Process |
| DV | Decision Variable |
| EAD | Estimated Annual Damage |
| GA | Genetic Algorithm |
| HC | Hydraulic Control |
| HS | Hydraulic Sector |
| IDF | Intensity–Duration–Frequency |
| IPCC | Intergovernmental Panel on Climate Change |
| LID | Low Impact Development |
| NSGA-II | Non-dominated Sorting Genetic Algorithm |
| OF | Objective Function |
| PGA | Pseudo-Genetic Algorithm |
| SFLA | Shuffled frog leaping algorithm |
| PSO | Particle Swarm Optimization |
| SS | Search Space |
| SSR | Search Space Reduction |
| ST | Storm Tank |
| SWMM | Storm Water Management Model |

# APPENDIX III. NETWORKS DATA

## A3.1 Case Study Data of E-Chico network

The data of this network was obtained from the following sources. The geographic and topographic information was provided by The Spatial Data Infrastructure of Bogotá (IDECA, acronym in Spanish) [122]. The hydraulic information of the network was provided by The Aqueduct, Sewerage and Cleaning Company of Bogotá (EAAB, acronym in Spanish). The hydrological and meteorological information was provided by The Institute of Hydrology, Meteorology and Environmental Studies of Colombia (IDEAM, acronym in Spanish) [161]. The mathematical model of the network was developed as part of the project *Drenaje Urbano y Cambio Climático: hacia los sistemas de alcantarillado del future* financed by COLCIENCIAS.

The E-Chico network is presented in the Figure A3.1.1 below.

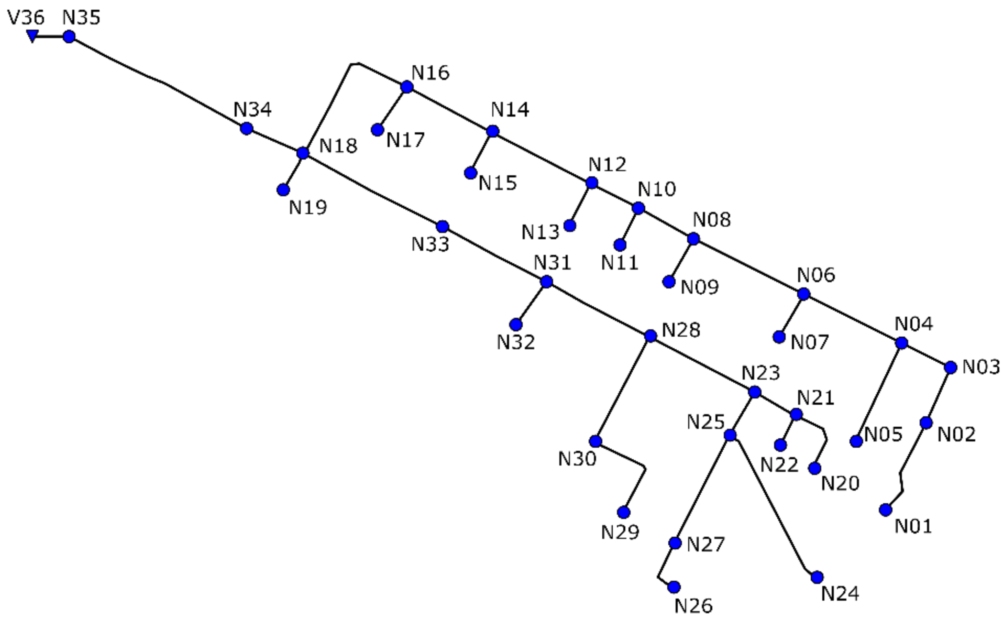


**Figure A3.1.1.** Representation of E-Chico drainage network.

**Table A3.1.1.** Data for nodes and subcatchments in E-Chico network.

| Node ID | Invert Elevation [m] | Max. Depth [m] | Flooding Area [m2] | Sub-catchment Area [ha] | Impervious Area [%] | Width [m] | Slope [%] |
|---|---|---|---|---|---|---|---|
| N01 | 2585.94 | 1.40 | 1380 | 1.38 | 73.6 | 44 | 16.9 |
| N02 | 2574.53 | 2.25 | 1240 | 1.24 | 80.9 | 25 | 12.3 |

| Node ID | Invert Elevation [m] | Max. Depth [m] | Flooding Area [m2] | Sub-catchment Area [ha] | Impervious Area [%] | Width [m] | Slope [%] |
|---|---|---|---|---|---|---|---|
| N03 | 2573.25 | 2.25 | 1080 | 1.08 | 29.2 | 84 | 27.7 |
| N04 | 2567.97 | 1.72 | 930 | 0.93 | 100 | 46 | 4.8 |
| N05 | 2575.26 | 2.06 | 1530 | 1.53 | 82.8 | 38 | 7.0 |
| N06 | 2563.08 | 1.83 | 1890 | 1.89 | 100 | 43 | 3.1 |
| N07 | 2563.67 | 2.45 | 1250 | 1.25 | 100 | 43 | 3.9 |
| N08 | 2558.57 | 2.49 | 1930 | 1.93 | 100 | 45 | 3.1 |
| N09 | 2560.66 | 1.32 | 1130 | 1.13 | 100 | 43 | 3.8 |
| N10 | 2556.14 | 2.19 | 700 | 0.70 | 100 | 16 | 2.0 |
| N11 | 2556.62 | 3.35 | 820 | 0.82 | 100 | 42 | 2.6 |
| N12 | 2555.55 | 2.43 | 1730 | 1.73 | 100 | 42 | 1.1 |
| N13 | 2555.97 | 2.74 | 1000 | 1.00 | 100 | 45 | 1.1 |
| N14 | 2553.85 | 1.97 | 1530 | 1.53 | 100 | 40 | 0.9 |
| N15 | 2555.04 | 1.38 | 1160 | 1.16 | 100 | 42 | 0.8 |
| N16 | 2553.02 | 2.29 | 1480 | 1.48 | 100 | 28 | 0.7 |
| N17 | 2553.31 | 2.10 | 1000 | 1.00 | 100 | 45 | 0.9 |
| N18 | 2551.24 | 2.81 | 2520 | 2.52 | 100 | 27 | 0.9 |
| N19 | 2552.88 | 1.38 | 470 | 0.47 | 100 | 22 | 0.8 |
| N20 | 2575.59 | 1.25 | 1450 | 1.45 | 52.6 | 26 | 7.5 |
| N21 | 2570.06 | 1.57 | 990 | 0.99 | 86.2 | 25 | 4.7 |
| N22 | 2572.07 | 1.90 | 620 | 0.62 | 64.7 | 29 | 4.7 |
| N23 | 2564.59 | 2.61 | 450 | 0.45 | 100 | 22 | 3.4 |
| N24 | 2587.65 | 2.60 | 1280 | 1.28 | 61.5 | 110 | 24.4 |
| N25 | 2568.14 | 2.26 | 2190 | 2.19 | 90.3 | 44 | 4.8 |
| N26 | 2571.98 | 1.48 | 1250 | 1.25 | 94.8 | 29 | 3.3 |
| N27 | 2571.38 | 2.42 | 1120 | 1.12 | 85.3 | 42 | 4.3 |
| N28 | 2561.86 | 2.63 | 2420 | 2.42 | 100 | 48 | 3.6 |
| N29 | 2569.21 | 1.53 | 1530 | 1.53 | 100 | 55 | 3.6 |
| N30 | 2565.41 | 1.28 | 1950 | 1.95 | 100 | 49 | 3.8 |
| N31 | 2556.50 | 3.49 | 2710 | 2.71 | 100 | 21 | 2.2 |
| N32 | 2559.00 | 0.91 | 1500 | 1.50 | 90.6 | 25 | 1.9 |
| N33 | 2553.39 | 1.94 | 3030 | 3.03 | 100 | 24 | 1.1 |
| N34 | 2548.97 | 3.07 | 3270 | 3.27 | 100 | 44 | 0.5 |
| N35 | 2548.43 | 3.07 | 1210 | 1.21 | 90.6 | 20 | 0.7 |

**Table A3.1.2.** Data for conduits in E-Chico network.

| Link ID | Node 1 | Node 2 | Length [m] | Manning Roughness | Diameter [m] |
|---|---|---|---|---|---|
| P01 | N01 | N02 | 172.65 | 0.011 | 0.40 |
| P02 | N02 | N03 | 90.99 | 0.011 | 0.40 |
| P03 | N03 | N04 | 93.17 | 0.011 | 0.40 |
| P04 | N04 | N06 | 187.94 | 0.011 | 0.55 |
| P05 | N05 | N04 | 180.27 | 0.011 | 0.40 |
| P06 | N06 | N08 | 203.82 | 0.011 | 0.60 |
| P07 | N07 | N06 | 85.55 | 0.011 | 0.40 |
| P08 | N08 | N10 | 113.02 | 0.011 | 0.75 |

| Link ID | Node 1 | Node 2 | Length [m] | Manning Roughness | Diameter [m] |
|---|---|---|---|---|---|
| P09 | N09 | N08 | 85.62 | 0.011 | 0.40 |
| P10 | N10 | N12 | 81.80 | 0.011 | 0.75 |
| P11 | N11 | N10 | 68.24 | 0.011 | 0.30 |
| P12 | N12 | N14 | 187.31 | 0.011 | 0.90 |
| P13 | N13 | N12 | 80.08 | 0.011 | 0.40 |
| P14 | N14 | N16 | 169.06 | 0.011 | 1.10 |
| P15 | N15 | N14 | 79.98 | 0.011 | 0.50 |
| P16 | N16 | N18 | 270.92 | 0.011 | 1.20 |
| P17 | N17 | N16 | 84.81 | 0.011 | 0.40 |
| P18 | N18 | N34 | 90.38 | 0.011 | 1.30 |
| P19 | N19 | N18 | 66.74 | 0.011 | 0.40 |
| P20 | N20 | N21 | 124.22 | 0.011 | 0.45 |
| P21 | N21 | N23 | 79.16 | 0.011 | 0.45 |
| P22 | N22 | N21 | 52.91 | 0.011 | 0.30 |
| P23 | N23 | N28 | 194.54 | 0.011 | 0.60 |
| P24 | N24 | N25 | 270.94 | 0.011 | 0.56 |
| P25 | N25 | N23 | 85.78 | 0.011 | 0.60 |
| P26 | N26 | N27 | 91.21 | 0.011 | 0.40 |
| P27 | N27 | N25 | 203.14 | 0.011 | 0.55 |
| P28 | N28 | N31 | 201.07 | 0.011 | 0.75 |
| P29 | N29 | N30 | 180.09 | 0.011 | 0.50 |
| P30 | N30 | N28 | 197.82 | 0.011 | 0.60 |
| P31 | N31 | N33 | 187.12 | 0.011 | 0.85 |
| P32 | N32 | N31 | 88.46 | 0.011 | 0.40 |
| P33 | N33 | N18 | 273.72 | 0.011 | 1.00 |
| P34 | N34 | N35 | 337.56 | 0.011 | 1.40 |
| P35 | N35 | V36 | 33.19 | 0.011 | 1.40 |

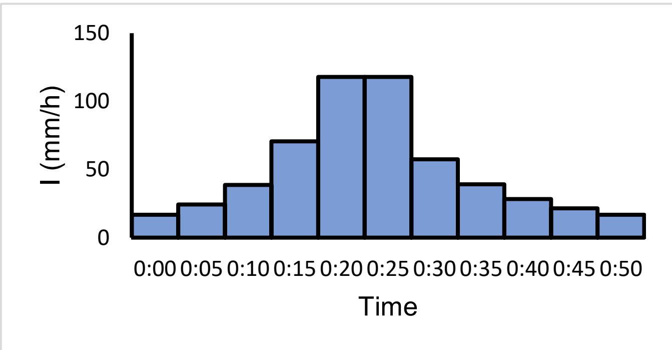


**Figure A3.1.2.** Design storm based on the Alternating Blocks Method used in E-Chico network.

**Table A3.1.3.** Time series for the design storm used in E-Chico network.

| Time | Value |
|---|---|
| 0:00 | 16.73 |
| 0:05 | 24.4 |
| 0:10 | 38.78 |

| Time | Value |
|---|---|
| 0:15 | 70.61 |
| 0:20 | 118 |
| 0:25 | 118 |
| 0:30 | 57.48 |
| 0:35 | 39.12 |
| 0:40 | 28.3 |
| 0:45 | 21.39 |
| 0:50 | 16.73 |

**Table A3.1.4.** Series of valve travel and head loss coefficients.

| Value | t= A/A0 | K(Eqn. 2.2) |
|---|---|---|
| 0(*) | 100 | 0 |
| 1 | 100 | 0.27 |
| 2 | 71.69 | 0.61 |
| 3 | 51.39 | 1.35 |
| 4 | 36.84 | 2.99 |
| 5 | 26.41 | 6.664 |
| 6 | 18.93 | 14.73 |
| 7 | 13.57 | 32.69 |
| 8 | 9.73 | 72.55 |
| 9 | 6.97 | 161.01 |
| 10 | 5 | 357.34 |

(*) Corresponding to not install HCs.

## A3.2 Case Study Data of Ayurá network

The data of this network was obtained from the following sources. The geographic and topographic information was provided by The Spatial Data Infrastructure of Bogotá (IDECA, acronym in Spanish) [122]. The hydraulic information of the network was provided by The Aqueduct, Sewerage and Cleaning Company of Bogotá (EAAB, acronym in Spanish). The hydrological and meteorological information was provided by The Institute of Hydrology, Meteorology and Environmental Studies of Colombia (IDEAM, acronym in Spanish) [161]. The mathematical model of the network was developed as part of the project *Drenaje Urbano y Cambio Climático: hacia los sistemas de alcantarillado del future* financed by COLCIENCIAS.

Ayurá network is presented in the Figure A3.2.1 below.

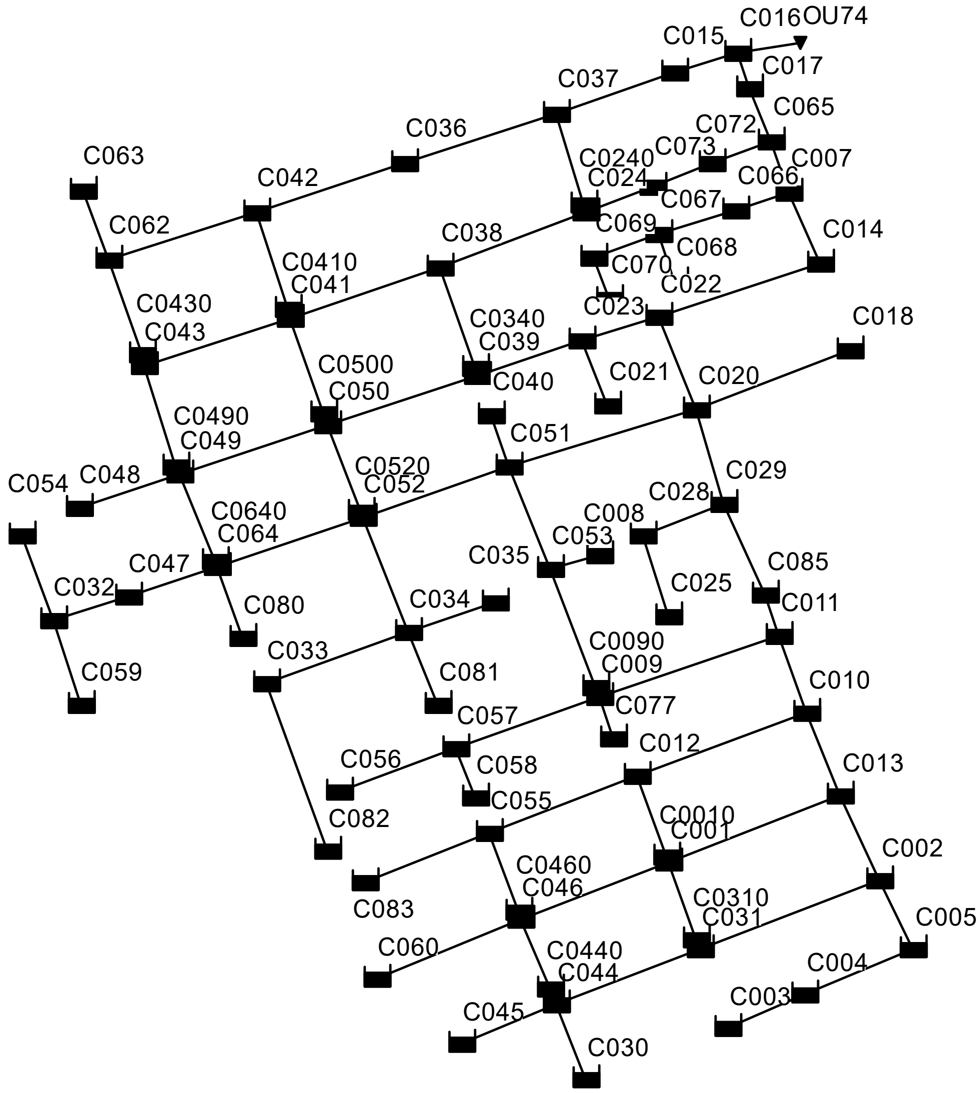


**Figure A3.2.1.** Representation of Ayurá drainage network

**Table A3.2.1.** Data for nodes in Ayurá network.

| Node ID | Invert Elevation [m] | Max. Depth [m] | Flooding Area [m2] |
|---|---|---|---|
| C063 | 1551.47 | 1.90 | 283.30 |
| C062 | 1551.00 | 1.82 | 245.77 |
| C042 | 1549.47 | 2.66 | 567.96 |
| C043 | 1552.45 | 2.02 | 514.02 |
| C041 | 1550.73 | 2.10 | 276.14 |
| C049 | 1552.97 | 1.26 | 173.74 |
| C048 | 1553.56 | 1.40 | 277.81 |
| C054 | 1555.80 | 1.50 | 344.51 |
| C032 | 1554.71 | 2.14 | 215.58 |
| C059 | 1556.66 | 1.60 | 711.06 |
| C047 | 1554.16 | 1.90 | 230.61 |
| C064 | 1553.68 | 2.10 | 188.76 |
| C080 | 1555.14 | 1.60 | 246.10 |
| C052 | 1552.31 | 2.20 | 243.69 |
| C050 | 1551.21 | 1.50 | 261.69 |
| C036 | 1547.71 | 2.30 | 475.89 |
| C016 | 1545.17 | 2.71 | 89.02 |
| C017 | 1545.57 | 2.82 | 128.01 |
| C065 | 1546.39 | 2.97 | 105.62 |
| C007 | 1546.54 | 2.91 | 101.23 |
| C015 | 1545.70 | 2.55 | 233.51 |
| C037 | 1546.23 | 2.29 | 400.19 |
| C014 | 1547.05 | 2.60 | 71.90 |
| C072 | 1547.73 | 3.07 | 60.42 |
| C066 | 1546.75 | 2.46 | 138.82 |
| C018 | 1550.82 | 1.42 | 171.67 |
| C073 | 1548.15 | 3.14 | 117.05 |
| C067 | 1548.20 | 2.38 | 54.63 |
| C068 | 1549.05 | 1.81 | 135.41 |
| C022 | 1548.68 | 2.75 | 141.02 |
| C070 | 1549.15 | 1.77 | 137.79 |
| C069 | 1548.42 | 1.90 | 182.53 |
| C024 | 1548.23 | 3.10 | 66.07 |
| C038 | 1548.95 | 2.21 | 545.50 |
| C039 | 1549.45 | 2.75 | 370.87 |
| C023 | 1548.78 | 2.30 | 135.40 |
| C021 | 1549.38 | 2.20 | 240.22 |
| C020 | 1549.59 | 2.75 | 55.65 |
| C040 | 1550.61 | 1.70 | 242.18 |
| C051 | 1550.24 | 2.20 | 352.12 |
| C029 | 1550.90 | 4.50 | 32.27 |
| C005 | 1556.30 | 2.75 | 71.29 |

| Node ID | Invert Elevation [m] | Max. Depth [m] | Flooding Area [m2] |
|---|---|---|---|
| C002 | 1555.38 | 2.30 | 263.18 |
| C013 | 1554.35 | 2.16 | 365.18 |
| C010 | 1553.33 | 2.30 | 377.68 |
| C011 | 1552.73 | 2.95 | 273.32 |
| C085 | 1551.91 | 2.75 | 10.09 |
| C028 | 1551.76 | 1.85 | 159.45 |
| C025 | 1552.20 | 2.00 | 267.83 |
| C008 | 1551.80 | 1.70 | 134.68 |
| C053 | 1551.14 | 1.75 | 224.97 |
| C004 | 1557.23 | 1.97 | 134.49 |
| C003 | 1557.54 | 2.50 | 406.74 |
| C030 | 1559.00 | 1.45 | 511.97 |
| C031 | 1557.08 | 1.88 | 198.47 |
| C001 | 1556.11 | 1.65 | 226.12 |
| C044 | 1558.11 | 1.45 | 175.03 |
| C045 | 1558.49 | 1.50 | 751.41 |
| C060 | 1559.61 | 1.40 | 512.15 |
| C046 | 1557.86 | 1.45 | 219.60 |
| C055 | 1557.29 | 1.80 | 297.16 |
| C012 | 1555.07 | 1.75 | 237.97 |
| C077 | 1555.56 | 1.65 | 223.25 |
| C009 | 1553.48 | 1.90 | 202.34 |
| C035 | 1554.38 | 1.40 | 343.46 |
| C034 | 1554.00 | 1.38 | 222.75 |
| C081 | 1554.60 | 1.58 | 333.28 |
| C057 | 1554.43 | 1.55 | 173.62 |
| C058 | 1555.22 | 1.50 | 218.47 |
| C056 | 1554.83 | 1.50 | 567.59 |
| C083 | 1558.79 | 1.30 | 283.21 |
| C082 | 1557.48 | 1.32 | 258.56 |
| C033 | 1555.06 | 1.82 | 398.39 |
| C0440 | 1558.11 | 1.45 | 175.03 |
| C0310 | 1557.08 | 1.88 | 198.47 |
| C0460 | 1557.86 | 1.45 | 219.60 |
| C0010 | 1556.11 | 1.65 | 226.12 |
| C0640 | 1553.68 | 2.10 | 188.76 |
| C0520 | 1552.31 | 2.20 | 243.69 |
| C0490 | 1552.97 | 1.26 | 173.74 |
| C0500 | 1551.21 | 1.50 | 261.69 |
| C0340 | 1554.00 | 1.38 | 222.75 |
| C0430 | 1552.45 | 2.02 | 257.01 |
| C0410 | 1550.73 | 2.10 | 276.14 |
| C0240 | 1548.23 | 3.10 | 66.07 |

| Node ID | Invert Elevation [m] | Max. Depth [m] | Flooding Area [m2] |
|---|---|---|---|
| C0090 | 1553.48 | 1.90 | 202.34 |

**Table A3.2.2** Data for subcatchments in Ayurá network.

| Sub-catchment ID | Sub-catchment Area [m2] | Impervious Area [m2] | Width [m] | Slope [%] |
|---|---|---|---|---|
| S001 | 0.23 | 85.00 | 16.38 | 8.54 |
| S002 | 0.26 | 77.93 | 12.96 | 6.03 |
| S003 | 0.41 | 85.00 | 16.04 | 8.77 |
| S004 | 0.13 | 79.34 | 7.38 | 6.90 |
| S005 | 0.07 | 75.00 | 6.60 | 7.68 |
| S006 | 0.03 | 75.00 | 3.57 | 6.51 |
| S007 | 0.10 | 75.00 | 7.40 | 6.30 |
| S008 | 0.13 | 85.00 | 7.87 | 3.07 |
| S009 | 0.20 | 85.00 | 15.72 | 8.08 |
| S010 | 0.38 | 77.70 | 15.12 | 4.40 |
| S011 | 0.27 | 76.39 | 12.78 | 9.60 |
| S012 | 0.24 | 85.00 | 10.43 | 7.81 |
| S013 | 0.37 | 78.06 | 14.94 | 4.58 |
| S014 | 0.07 | 75.00 | 5.39 | 8.73 |
| S015 | 0.23 | 82.03 | 12.43 | 4.87 |
| S016 | 0.09 | 75.00 | 7.38 | 4.91 |
| S017 | 0.13 | 75.00 | 8.43 | 6.07 |
| S018 | 0.17 | 75.65 | 9.29 | 5.49 |
| S019 | 0.10 | 76.22 | 6.70 | 12.04 |
| S020 | 0.06 | 84.99 | 4.04 | 7.44 |
| S021 | 0.24 | 84.99 | 12.48 | 3.47 |
| S022 | 0.14 | 84.98 | 9.57 | 1.28 |
| S023 | 0.14 | 85.00 | 9.15 | 7.37 |
| S024 | 0.07 | 85.00 | 8.86 | 3.22 |
| S025 | 0.27 | 84.29 | 12.74 | 8.03 |
| S026 | 0.03 | 75.00 | 3.42 | 8.11 |
| S028 | 0.16 | 83.72 | 9.17 | 8.93 |
| S029 | 0.15 | 75.12 | 9.21 | 10.22 |
| S030 | 0.51 | 85.00 | 16.80 | 7.73 |
| S031 | 0.20 | 85.00 | 15.52 | 4.67 |
| S032 | 0.22 | 85.00 | 11.58 | 8.28 |
| S033 | 0.40 | 85.00 | 14.90 | 4.03 |
| S034 | 0.22 | 85.00 | 16.71 | 3.74 |
| S035 | 0.34 | 85.00 | 14.63 | 4.63 |
| S036 | 0.48 | 85.00 | 16.42 | 4.25 |
| S037 | 0.40 | 85.00 | 15.79 | 6.31 |

| Sub-catchment ID | Sub-catchment Area [m2] | Impervious Area [m2] | Width [m] | Slope [%] |
|---|---|---|---|---|
| S038 | 0.55 | 85.00 | 18.37 | 3.48 |
| S039 | 0.37 | 85.00 | 14.50 | 7.25 |
| S040 | 0.24 | 85.00 | 10.65 | 4.32 |
| S041 | 0.28 | 85.00 | 18.47 | 5.21 |
| S042 | 0.57 | 85.00 | 18.98 | 4.47 |
| S043 | 0.26 | 85.00 | 17.89 | 7.43 |
| S044 | 0.18 | 85.00 | 14.52 | 3.82 |
| S045 | 0.75 | 85.00 | 22.40 | 9.31 |
| S046 | 0.22 | 85.00 | 16.59 | 2.24 |
| S047 | 0.23 | 85.00 | 12.37 | 3.10 |
| S048 | 0.28 | 85.00 | 12.45 | 6.56 |
| S049 | 0.17 | 85.00 | 14.75 | 8.45 |
| S050 | 0.26 | 85.00 | 18.04 | 5.59 |
| S051 | 0.35 | 85.00 | 14.67 | 4.07 |
| S052 | 0.24 | 85.00 | 17.79 | 4.52 |
| S053 | 0.22 | 85.00 | 11.34 | 6.59 |
| S054 | 0.34 | 85.00 | 15.15 | 6.55 |
| S055 | 0.30 | 85.00 | 12.65 | 1.56 |
| S056 | 0.57 | 85.00 | 16.94 | 7.69 |
| S057 | 0.17 | 85.00 | 8.26 | 3.48 |
| S058 | 0.22 | 85.00 | 10.01 | 2.31 |
| S059 | 0.71 | 85.00 | 21.63 | 6.31 |
| S060 | 0.51 | 85.00 | 17.16 | 7.70 |
| S061 | 0.25 | 85.00 | 12.40 | 7.71 |
| S062 | 0.24 | 85.00 | 12.38 | 3.94 |
| S063 | 0.28 | 85.00 | 11.25 | 6.45 |
| S064 | 0.19 | 85.00 | 15.52 | 3.85 |
| S065 | 0.11 | 75.00 | 7.38 | 6.90 |
| S066 | 0.14 | 75.00 | 8.81 | 7.76 |
| S067 | 0.05 | 85.00 | 5.47 | 4.91 |
| S068 | 0.14 | 85.00 | 9.43 | 3.36 |
| S069 | 0.18 | 85.00 | 10.11 | 1.80 |
| S070 | 0.14 | 85.00 | 8.99 | 7.44 |
| S071 | 0.06 | 75.00 | 6.23 | 6.90 |
| S072 | 0.25 | 84.00 | 12.32 | 2.87 |
| S073 | 0.12 | 85.00 | 7.60 | 2.66 |
| S074 | 0.12 | 75.00 | 7.96 | 4.15 |
| S076 | 0.17 | 84.14 | 8.46 | 4.91 |
| S077 | 0.22 | 85.00 | 10.01 | 6.53 |
| S078 | 0.02 | 75.00 | 2.41 | 2.91 |
| S079 | 0.22 | 77.11 | 12.10 | 2.63 |
| S080 | 0.25 | 85.00 | 11.12 | 2.03 |
| S081 | 0.33 | 85.00 | 13.60 | 6.79 |

| Sub-catchment ID | Sub-catchment Area [m2] | Impervious Area [m2] | Width [m] | Slope [%] |
|---|---|---|---|---|
| S082 | 0.26 | 85.00 | 11.54 | 7.96 |
| S083 | 0.28 | 85.00 | 12.62 | 5.83 |
| S084 | 0.01 | 75.00 | 1.43 | 4.60 |
| S085 | 0.11 | 75.00 | 7.96 | 8.56 |
| S0440 | 0.18 | 85.00 | 14.52 | 3.82 |
| S0310 | 0.20 | 85.00 | 15.52 | 4.67 |
| S0460 | 0.22 | 85.00 | 16.59 | 2.24 |
| S0010 | 0.23 | 85.00 | 16.38 | 8.54 |
| S0640 | 0.19 | 85.00 | 15.52 | 3.85 |
| S0520 | 0.24 | 85.00 | 17.79 | 4.52 |
| S0490 | 0.17 | 85.00 | 14.75 | 8.45 |
| S0500 | 0.26 | 85.00 | 18.04 | 5.59 |
| S0340 | 0.22 | 85.00 | 16.71 | 3.74 |
| S0430 | 0.26 | 85.00 | 17.89 | 7.43 |
| S0410 | 0.28 | 85.00 | 18.47 | 5.21 |
| S0240 | 0.07 | 85.00 | 8.86 | 3.22 |
| S0090 | 0.20 | 85.00 | 15.72 | 8.08 |

**Table A3.2.3.** Data for conduits in Ayurá network.

| Link ID | Node 1 | Node 2 | Length [m] | Manning Roughness | Diameter [m] |
|---|---|---|---|---|---|
| T002 | C005 | C002 | 53.84 | 0.013 | 0.40 |
| T004 | C004 | C005 | 40.02 | 0.013 | 0.38 |
| T007 | C014 | C007 | 65.28 | 0.013 | 0.90 |
| T008 | C077 | C009 | 49.10 | 0.013 | 0.45 |
| T009 | C009 | C011 | 87.51 | 0.013 | 0.40 |
| T010 | C010 | C011 | 52.51 | 0.013 | 0.60 |
| T011 | C0010 | C012 | 52.24 | 0.013 | 0.40 |
| T012 | C012 | C010 | 87.41 | 0.013 | 0.40 |
| T013 | C013 | C010 | 50.82 | 0.013 | 0.60 |
| T014 | C002 | C013 | 51.62 | 0.013 | 0.50 |
| T015 | C031 | C002 | 84.90 | 0.013 | 0.38 |
| T016 | C0310 | C001 | 52.17 | 0.013 | 0.25 |
| T017 | C025 | C028 | 45.30 | 0.013 | 0.20 |
| T019 | C0240 | C037 | 61.01 | 0.013 | 0.30 |
| T020 | C030 | C044 | 44.61 | 0.013 | 0.30 |
| T021 | C0090 | C053 | 73.75 | 0.013 | 0.30 |
| T022 | C008 | C053 | 33.27 | 0.013 | 0.30 |
| T025 | C017 | C016 | 19.86 | 0.013 | 1.00 |
| T026 | C015 | C016 | 37.31 | 0.013 | 0.50 |
| T027 | C007 | C065 | 7.14 | 0.013 | 0.90 |
| T029 | C020 | C022 | 55.61 | 0.013 | 0.90 |

| Link ID | Node 1 | Node 2 | Length [m] | Manning Roughness | Diameter [m] |
|---|---|---|---|---|---|
| T031 | C021 | C023 | 54.13 | 0.013 | 0.25 |
| T032 | C023 | C022 | 10.19 | 0.013 | 0.50 |
| T033 | C029 | C020 | 55.57 | 0.013 | 0.90 |
| T034 | C028 | C029 | 42.97 | 0.013 | 0.20 |
| T035 | C011 | C085 | 46.28 | 0.013 | 0.90 |
| T037 | C080 | C064 | 53.25 | 0.013 | 0.30 |
| T038 | C033 | C034 | 86.57 | 0.013 | 0.38 |
| T039 | C035 | C034 | 53.00 | 0.013 | 0.38 |
| T040 | C081 | C034 | 67.26 | 0.013 | 0.25 |
| T041 | C042 | C036 | 88.22 | 0.013 | 0.53 |
| T042 | C036 | C037 | 88.95 | 0.013 | 0.53 |
| T043 | C0340 | C038 | 64.28 | 0.013 | 0.30 |
| T044 | C040 | C051 | 30.83 | 0.013 | 0.25 |
| T045 | C050 | C039 | 88.05 | 0.013 | 0.30 |
| T046 | C041 | C038 | 88.69 | 0.013 | 0.30 |
| T047 | C0410 | C042 | 62.13 | 0.013 | 0.30 |
| T049 | C0430 | C062 | 59.74 | 0.013 | 0.30 |
| T050 | C043 | C041 | 86.22 | 0.013 | 0.30 |
| T051 | C0490 | C043 | 64.48 | 0.013 | 0.53 |
| T052 | C0440 | C046 | 51.89 | 0.013 | 0.25 |
| T053 | C0460 | C055 | 51.97 | 0.013 | 0.25 |
| T054 | C045 | C044 | 58.10 | 0.013 | 0.25 |
| T055 | C032 | C047 | 27.69 | 0.013 | 0.38 |
| T056 | C047 | C064 | 51.93 | 0.013 | 0.38 |
| T057 | C049 | C050 | 87.96 | 0.013 | 0.30 |
| T058 | C0500 | C041 | 64.32 | 0.013 | 0.30 |
| T059 | C0640 | C049 | 55.65 | 0.013 | 0.20 |
| T060 | C048 | C049 | 29.71 | 0.013 | 0.30 |
| T061 | C0520 | C050 | 55.18 | 0.013 | 0.30 |
| T062 | C053 | C051 | 61.58 | 0.013 | 0.45 |
| T063 | C052 | C051 | 86.12 | 0.013 | 0.60 |
| T064 | C034 | C052 | 60.40 | 0.013 | 0.38 |
| T065 | C064 | C052 | 87.30 | 0.013 | 0.53 |
| T066 | C059 | C032 | 50.17 | 0.013 | 0.30 |
| T067 | C054 | C032 | 35.01 | 0.013 | 0.30 |
| T068 | C082 | C033 | 121.02 | 0.013 | 0.25 |
| T069 | C037 | C015 | 70.33 | 0.013 | 0.50 |
| T070 | C051 | C020 | 91.19 | 0.013 | 0.68 |
| T071 | C060 | C046 | 87.56 | 0.013 | 0.38 |
| T072 | C083 | C055 | 75.09 | 0.013 | 0.38 |
| T074 | C063 | C062 | 43.74 | 0.013 | 0.30 |
| T075 | C056 | C057 | 82.84 | 0.013 | 0.38 |
| T076 | C058 | C057 | 29.58 | 0.013 | 0.20 |
| T077 | C039 | C023 | 81.85 | 0.013 | 0.30 |

| Link ID | Node 1 | Node 2 | Length [m] | Manning Roughness | Diameter [m] |
|---|---|---|---|---|---|
| T078 | C044 | C031 | 86.60 | 0.013 | 0.38 |
| T079 | C046 | C001 | 87.83 | 0.013 | 0.38 |
| T080 | C057 | C009 | 86.38 | 0.013 | 0.38 |
| T081 | C055 | C012 | 86.66 | 0.013 | 0.45 |
| T083 | C016 | OU74 | 35.00 | 0.013 | 1.05 |
| T084 | C070 | C069 | 42.40 | 0.013 | 0.30 |
| T085 | C068 | C067 | 47.15 | 0.013 | 0.30 |
| T086 | C069 | C067 | 11.52 | 0.013 | 0.30 |
| T087 | C067 | C066 | 83.25 | 0.013 | 0.40 |
| T088 | C066 | C007 | 11.35 | 0.013 | 0.40 |
| T089 | C065 | C017 | 35.32 | 0.013 | 0.90 |
| T090 | C038 | C024 | 88.00 | 0.013 | 0.70 |
| T091 | C024 | C073 | 15.50 | 0.013 | 0.70 |
| T092 | C073 | C072 | 31.87 | 0.013 | 0.70 |
| T003 | C003 | C004 | 46.31 | 0.013 | 0.38 |
| T018 | C085 | C029 | 25.89 | 0.013 | 0.90 |
| T028 | C018 | C020 | 39.42 | 0.013 | 0.20 |
| T023 | C022 | C014 | 81.96 | 0.013 | 0.90 |
| T048 | C062 | C042 | 87.74 | 0.013 | 0.30 |
| T094 | C072 | C065 | 53.03 | 0.013 | 0.70 |
| T001 | C001 | C013 | 400.00 | 0.013 | 1.00 |

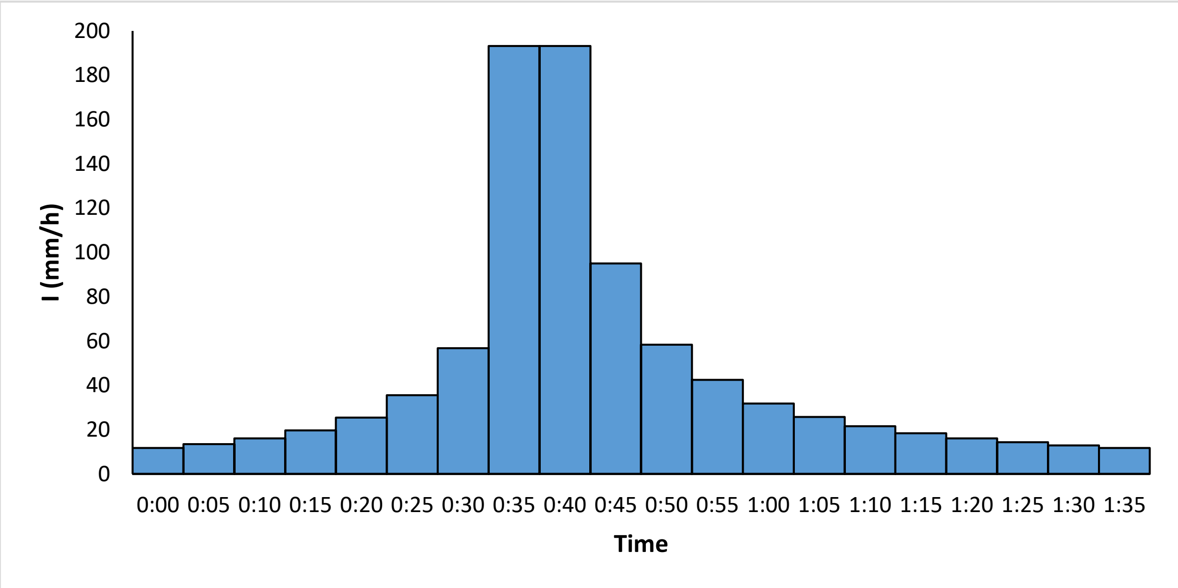


**Figure A3.2.2.** Design storm based on the alternating blocks method used in Ayurá network.

**Table A3.2.4.** Time series for design storm used in Ayurá network.

| Time | Value |
|---|---|

| Time | Value |
|---|---|
| 0:00 | 11.67 |
| 0:05 | 13.52 |
| 0:10 | 16.06 |
| 0:15 | 19.73 |
| 0:20 | 25.46 |
| 0:25 | 35.47 |
| 0:30 | 56.73 |
| 0:35 | 193.13 |
| 0:40 | 193.13 |
| 0:45 | 95.00 |
| 0:50 | 58.42 |
| 0:55 | 42.45 |
| 1:00 | 31.83 |
| 1:05 | 25.70 |
| 1:10 | 21.49 |
| 1:15 | 18.43 |
| 1:20 | 16.11 |
| 1:25 | 14.30 |
| 1:30 | 12.86 |
| 1:35 | 11.67 |

## A3.3 Case Study Data of Balloon network

Data for this network was obtained from the following sources. The geographic and topographic information, as well as the hydraulic information and the mathematical model of the network were provided by the Department of Environment, Land and Infrastructure Engineering of the Polytechnic of Turin (DIATI, acronym in italian). Hydrological and meteorological information was provided by the Regional Agency for Environmental Protection (ARPA, acronym in italian) [162]

Balloon network is presented in the Figure A3.3.1 below.

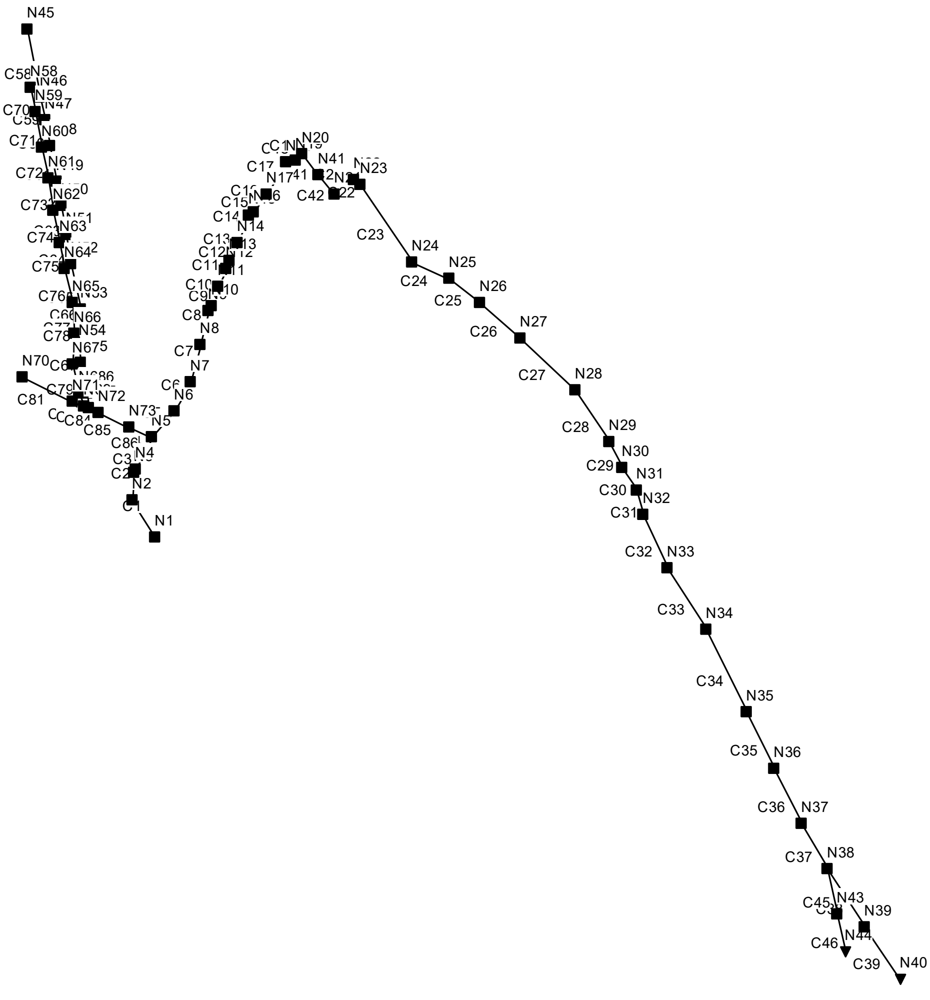


**Figure A3.3.1.** Representation of Balloon drainage network.

**Table A3.3.1.** Data for nodes and subcatchments of Balloon network.

| Node ID | Invert Elevation [m] | Max. Depth [m] | Flooding Area [m2] | Sub-catchment Area [ha] | Impervious Area [%] | Width [m] | Slope [%] |
|---|---|---|---|---|---|---|---|
| N1 | 225.914 | 1.46 | 86.09 | 0.08609 | 85 | 31.89 | 86.00 |
| N2 | 225.395 | 1.73 | 67.87 | 0.06787 | 85 | 31.81 | 75.00 |
| N3 | 225.017 | 1.98 | 10 | 0 | 85 | 0.00 | 0.00 |

| Node ID | Invert Elevation [m] | Max. Depth [m] | Flooding Area [m2] | Sub-catchment Area [ha] | Impervious Area [%] | Width [m] | Slope [%] |
|---|---|---|---|---|---|---|---|
| N4 | 225.003 | 1.97 | 100.7 | 0.1007 | 85 | 32.84 | 61.00 |
| N5 | 224.648 | 2.1 | 66.84 | 0.08684 | 85 | 31.83 | 58.00 |
| N6 | 224.628 | 2.1 | 1211 | 1.30363 | 85 | 37.20 | 265.00 |
| N7 | 223.493 | 2.54 | 136.1 | 0.1361 | 85 | 49.94 | 257.00 |
| N8 | 223.328 | 1.92 | 145.1 | 0.1451 | 85 | 51.82 | 224.00 |
| N9 | 223.202 | 1.86 | 10 | 0 | 85 | 0.00 | 0.00 |
| N10 | 223.223 | 1.81 | 138 | 0.138 | 85 | 44.52 | 67.00 |
| N11 | 223.153 | 1.81 | 116 | 0.116 | 85 | 34.12 | 41.00 |
| N12 | 223.077 | 1.82 | 87 | 0.087 | 85 | 23.36 | 39.00 |
| N13 | 223.015 | 1.86 | 88 | 0.088 | 85 | 21.46 | 44.00 |
| N14 | 223.081 | 1.94 | 121 | 0.121 | 85 | 40.33 | 122.00 |
| N15 | 222.934 | 2.52 | 10 | 0 | 85 | 0.00 | 0.00 |
| N16 | 222.844 | 2.58 | 20659.8 | 22.2588 | 85 | 195.79 | 185.00 |
| N17 | 222.833 | 2.7 | 48 | 0.048 | 85 | 29.54 | 73.00 |
| N18 | 222.895 | 3.4 | 40 | 0.04 | 85 | 24.24 | 218.00 |
| N19 | 222.778 | 3.63 | 23 | 0.023 | 85 | 12.96 | 226.00 |
| N20 | 222.751 | 3.53 | 1060 | 1.398 | 85 | 94.43 | 295.00 |
| N21 | 222.94 | 3.53 | 70 | 0.07 | 85 | 33.73 | 0.36 |
| N22 | 222.867 | 3.7 | 35 | 0.035 | 85 | 24.14 | 295.50 |
| N23 | 222.48 | 5.05 | 184 | 0.184 | 85 | 63.45 | 295.50 |
| N24 | 222.4 | 10.14 | 213 | 0.213 | 85 | 52.38 | 977.00 |
| N25 | 222.35 | 9.92 | 90 | 0.09 | 85 | 34.29 | 57.00 |
| N26 | 222.31 | 7.96 | 95 | 0.095 | 85 | 35.19 | 606.00 |
| N27 | 222.24 | 5.29 | 136 | 0.136 | 85 | 42.17 | 583.00 |
| N28 | 222.18 | 4.21 | 137 | 0.137 | 85 | 41.52 | 209.00 |
| N29 | 222.12 | 4.16 | 103 | 0.103 | 85 | 40.39 | 21.00 |
| N30 | 222 | 4.08 | 5630 | 5.676 | 85 | 139.13 | 200.00 |
| N31 | 221.95 | 3.82 | 41 | 0.041 | 85 | 22.69 | 129.00 |
| N32 | 221.88 | 3.78 | 61 | 1.081 | 85 | 30.12 | 55.00 |
| N33 | 221.87 | 3.05 | 138 | 0.138 | 85 | 47.18 | 140.00 |
| N34 | 221.8 | 2.76 | 579 | 0.579 | 85 | 98.55 | 89.00 |
| N35 | 221.78 | 2.62 | 473 | 0.473 | 85 | 72.49 | 40.00 |
| N36 | 221.69 | 2.63 | 306 | 0.306 | 85 | 51.21 | 24.00 |
| N37 | 221.66 | 2.6 | 253 | 0.253 | 85 | 50.85 | 23.00 |
| N38 | 221 | 3.35 | 255 | 0.255 | 85 | 61.45 | 31.00 |
| N39 | 220.9 | 3.4 | 183 | 0.183 | 85 | 58.56 | 12.00 |
| N41 | 222.805 | 3.48 | 65 | 0.065 | 85 | 26.80 | 3.00 |
| N43 | 220.95 | 3.2 | 10 | 0 | 85 | 0.00 | 0.00 |
| N45 | 228.833 | 1.33 | 71 | 0.071 | 85 | 20.88 | 433.00 |
| N46 | 227.046 | 1.38 | 56 | 0.056 | 85 | 20.74 | 319.00 |
| N47 | 226.66 | 1.016 | 30 | 0.03 | 85 | 16.22 | 117.00 |
| N48 | 226.28 | 1.14 | 314 | 0.314 | 85 | 38.06 | 25.00 |

| Node ID | Invert Elevation [m] | Max. Depth [m] | Flooding Area [m2] | Sub-catchment Area [ha] | Impervious Area [%] | Width [m] | Slope [%] |
|---|---|---|---|---|---|---|---|
| N49 | 226.216 | 1.14 | 185 | 0.185 | 85 | 23.13 | 68.00 |
| N50 | 226.103 | 1.08 | 186 | 0.186 | 85 | 23.40 | 45.00 |
| N51 | 226.013 | 1.04 | 169 | 0.169 | 85 | 21.26 | 47.00 |
| N52 | 225.984 | 0.95 | 226 | 0.226 | 85 | 28.25 | 27.00 |
| N53 | 225.869 | 0.914 | 341 | 0.341 | 85 | 43.35 | 15.00 |
| N54 | 225.73 | 1.016 | 158 | 0.158 | 85 | 22.25 | 284.00 |
| N55 | 225.685 | 1.57 | 123 | 0.123 | 85 | 18.36 | 46.00 |
| N56 | 225.591 | 1.8 | 89 | 0.089 | 85 | 17.28 | 154.00 |
| N57 | 225.269 | 2.12 | 8 | 0.028 | 85 | 4.21 | 84.00 |
| N58 | 227.264 | 1.47 | 50 | 0.05 | 85 | 8.33 | 346.00 |
| N59 | 226.369 | 1.38 | 106 | 0.106 | 85 | 17.10 | 116.00 |
| N60 | 226.161 | 1.24 | 217 | 0.217 | 85 | 29.17 | 31.00 |
| N61 | 226.092 | 1.23 | 235 | 0.235 | 85 | 28.83 | 52.00 |
| N62 | 226.008 | 1.18 | 214 | 0.214 | 85 | 25.94 | 47.00 |
| N63 | 225.989 | 1.08 | 201 | 0.201 | 85 | 24.07 | 62.00 |
| N64 | 225.924 | 0.99 | 256 | 0.256 | 85 | 29.94 | 36.00 |
| N65 | 225.776 | 1.06 | 90 | 0.09 | 85 | 20.69 | 9.00 |
| N66 | 225.67 | 1.191 | 149 | 0.149 | 85 | 17.84 | 143.00 |
| N67 | 225.584 | 1.65 | 121 | 0.121 | 85 | 14.07 | 75.00 |
| N68 | 225.396 | 2.06 | 21 | 0.021 | 85 | 16.15 | 84.00 |
| N69 | 225.297 | 2.12 | 22 | 0.022 | 85 | 9.36 | 120.00 |
| N70 | 226.795 | 1.3 | 640 | 0.64 | 85 | 46.97 | 120.00 |
| N71 | 225.399 | 2.119 | 100 | 0.1 | 85 | 34.48 | 120.00 |
| N72 | 225.195 | 2.14 | 60 | 0.06 | 85 | 24.32 | 125.00 |
| N73 | 224.979 | 2.03 | 70 | 0.07 | 85 | 32.18 | 97.00 |

**Table A3.3.2.** Data for conduits in Balloon network.

| Link ID | Node 1 | Node 2 | Length [m] | Manning Roughness | Diameter [m] |
|---|---|---|---|---|---|
| C1 | N1 | N2 | 29.00 | 0.017 | 0.7 |
| C2 | N2 | N3 | 17.00 | 0.017 | 0.7 |
| C3 | N3 | N4 | 2.00 | 0.017 | 0.7 |
| C4 | N4 | N5 | 39.00 | 0.017 | 0.7 |
| C5 | N5 | N6 | 29.00 | 0.017 | 0.7 |
| C6 | N6 | N7 | 26.50 | 0.017 | 0.95 |
| C7 | N7 | N8 | 35.00 | 0.017 | 0.95 |
| C8 | N8 | N9 | 28.00 | 0.017 | 0.95 |
| C9 | N9 | N10 | 3.00 | 0.017 | 0.95 |
| C10 | N10 | N11 | 17.00 | 0.017 | 0.95 |
| C11 | N11 | N12 | 17.00 | 0.017 | 0.95 |
| C12 | N12 | N13 | 5.00 | 0.017 | 0.95 |

| Link ID | Node 1 | Node 2 | Length [m] | Manning Roughness | Diameter [m] |
|---|---|---|---|---|---|
| C13 | N13 | N14 | 12.00 | 0.017 | 0.95 |
| C14 | N14 | N15 | 25.50 | 0.017 | 0.95 |
| C15 | N15 | N16 | 2.00 | 0.017 | 0.95 |
| C16 | N16 | N17 | 15.00 | 0.017 | 0.95 |
| C17 | N17 | N18 | 34.50 | 0.017 | 0.95 |
| C18 | N18 | N19 | 5.00 | 0.017 | 0.95 |
| C19 | N19 | N20 | 7.00 | 0.017 | 0.95 |
| C21 | N21 | N22 | 15.00 | 0.017 | 2.39 |
| C22 | N22 | N23 | 4.00 | 0.017 | 1.06 |
| C23 | N23 | N24 | 58.00 | 0.017 | 1.06 |
| C24 | N24 | N25 | 47.50 | 0.017 | 1.06 |
| C25 | N25 | N26 | 33.00 | 0.017 | 1.06 |
| C26 | N26 | N27 | 47.00 | 0.017 | 1.06 |
| C27 | N27 | N28 | 54.50 | 0.017 | 1.06 |
| C28 | N28 | N29 | 52.50 | 0.017 | 1.06 |
| C29 | N29 | N30 | 29.50 | 0.017 | 1.06 |
| C30 | N30 | N31 | 24.00 | 0.017 | 1.06 |
| C31 | N31 | N32 | 20.00 | 0.017 | 1.06 |
| C32 | N32 | N33 | 53.00 | 0.017 | 1.11 |
| C33 | N33 | N34 | 40.50 | 0.017 | 1.11 |
| C34 | N34 | N35 | 40.50 | 0.017 | 1.11 |
| C35 | N35 | N36 | 33.50 | 0.017 | 1.11 |
| C36 | N36 | N37 | 26.00 | 0.017 | 1.11 |
| C37 | N37 | N38 | 30.00 | 0.017 | 1.11 |
| C38 | N38 | N39 | 42.00 | 0.017 | 1.06 |
| C39 | N39 | N40 | 36.00 | 0.017 | 1.06 |
| C41 | N20 | N41 | 15.00 | 0.017 | 0.95 |
| C42 | N41 | N21 | 28.00 | 0.017 | 0.95 |
| C45 | N38 | N43 | 32.50 | 0.017 | 0.84 |
| C46 | N43 | N44 | 30.00 | 0.017 | 0.84 |
| C58 | N45 | N46 | 40.10 | 0.0143 | 0.5 |
| C59 | N46 | N47 | 23.51 | 0.0143 | 0.5 |
| C60 | N47 | N48 | 21.94 | 0.0143 | 0.5 |
| C61 | N48 | N49 | 25.40 | 0.0143 | 0.5 |
| C62 | N49 | N50 | 25.30 | 0.0143 | 0.5 |
| C63 | N50 | N51 | 28.87 | 0.0143 | 0.5 |
| C64 | N51 | N52 | 25.40 | 0.0143 | 0.5 |
| C65 | N52 | N53 | 31.30 | 0.0143 | 0.5 |
| C66 | N53 | N54 | 37.87 | 0.0143 | 0.5 |
| C67 | N54 | N55 | 12.31 | 0.0143 | 0.5 |
| C68 | N55 | N56 | 29.85 | 0.0143 | 0.5 |
| C69 | N56 | N57 | 9.54 | 0.0143 | 0.5 |
| C70 | N58 | N59 | 28.50 | 0.0143 | 0.5 |
| C71 | N59 | N60 | 29.90 | 0.0143 | 0.5 |

| Link ID | Node 1 | Node 2 | Length [m] | Manning Roughness | Diameter [m] |
|---|---|---|---|---|---|
| C72 | N60 | N61 | 25.50 | 0.0143 | 0.5 |
| C73 | N61 | N62 | 25.60 | 0.0143 | 0.5 |
| C74 | N62 | N63 | 25.27 | 0.0143 | 0.5 |
| C75 | N63 | N64 | 25.11 | 0.0143 | 0.5 |
| C76 | N64 | N65 | 21.62 | 0.0143 | 0.5 |
| C77 | N65 | N66 | 28.50 | 0.0143 | 0.5 |
| C78 | N66 | N67 | 26.00 | 0.0143 | 0.5 |
| C79 | N67 | N68 | 29.50 | 0.0143 | 0.5 |
| C80 | N68 | N69 | 8.21 | 0.0143 | 0.5 |
| C81 | N70 | N71 | 48.00 | 0.017 | 0.7 |
| C82 | N71 | N69 | 11.00 | 0.017 | 0.7 |
| C83 | N69 | N57 | 3.00 | 0.017 | 0.7 |
| C84 | N57 | N72 | 8.00 | 0.017 | 0.7 |
| C85 | N72 | N73 | 26.00 | 0.017 | 0.7 |
| C86 | N73 | N5 | 27.00 | 0.017 | 0.7 |

**Table A3.3.3.** Land uses in the study area of Balloon network

| Land uses | Percentage |
|---|---|
| Streets and roads | 28.97% |
| General trading | 18.91% |
| Green zones | 10.10% |
| Education | 7.87% |
| Restaurants | 7.56% |
| Hotels | 7.50% |
| Offices | 6.71% |
| Car parks | 3.47% |
| Churches | 2.27% |
| Museums | 1.75% |
| Health | 1.70% |
| Warehouses | 1.68% |
| Dwellings | 1.51% |

## A3.4 Case Study Data of ES-N network

The data of this network was obtained from the following sources. The geographic and topographic information was provided by The Spatial Data Infrastructure of Bogotá (IDECA, acronym in Spanish) [122]. The hydraulic information of the network was provided by The Aqueduct, Sewerage and Cleaning Company of Bogotá (EAAB, acronym in Spanish). The hydrological and meteorological information was provided by The Institute of Hydrology, Meteorology and Environmental Studies of Colombia (IDEAM, acronym in Spanish) [161]. The mathematical model of the network was developed as part of the project *Drenaje Urbano y Cambio Climático: hacia los sistemas de alcantarillado del future* financed by COLCIENCIAS.

ES-N network is presented in the Figure A3.4.1 below.

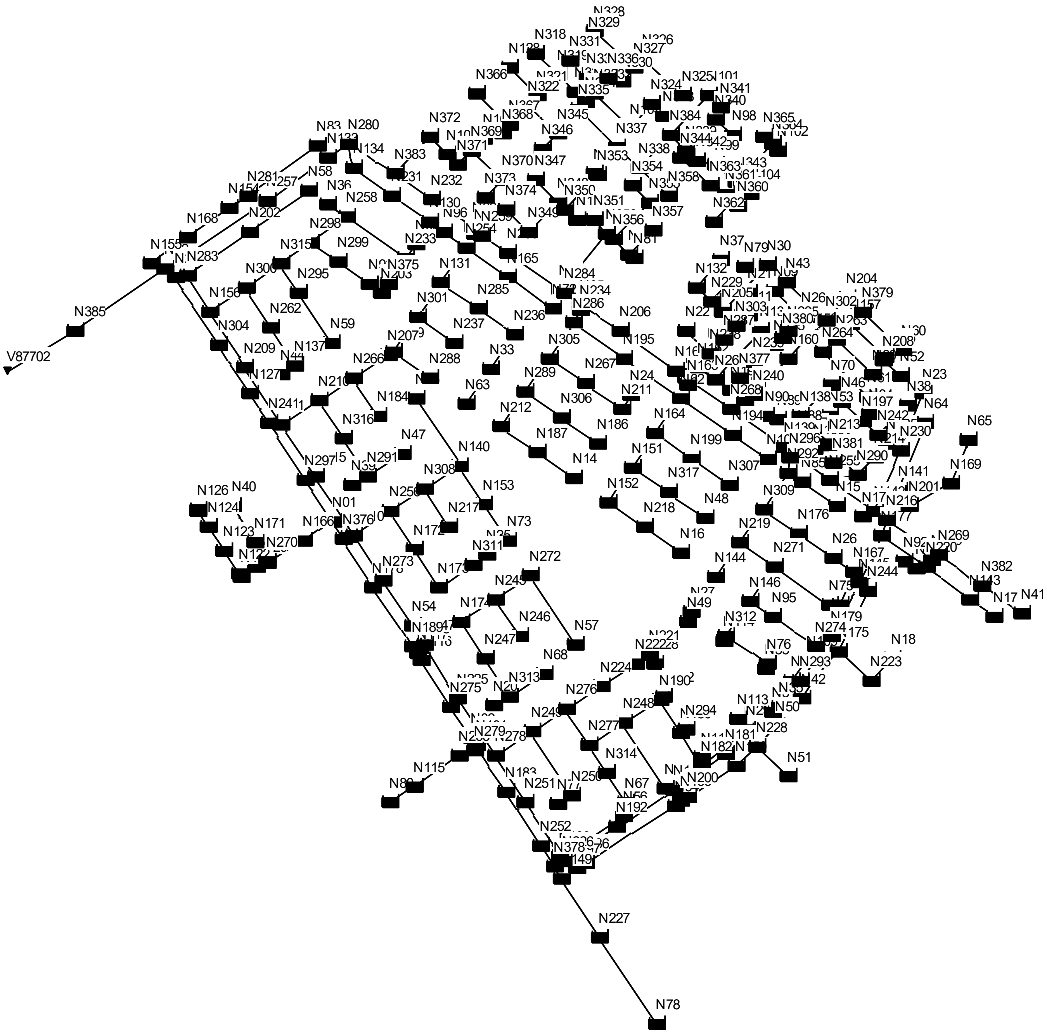


**Figure A3.4.1.** Representation of ES-N drainage network.

**Table A3.4.1.** Data for nodes and subcatchments in the ES-N network

| Node ID | Invert Elevation [m] | Max. Depth [m] | Flooding Area [m2] | Sub-catchment Area [ha] | Impervious Area [%] | Width [m] | Slope [%] |
|---|---|---|---|---|---|---|---|
| N01 | 2548.39 | 2.88 | 246.781 | 0.247 | 66.35 | 12.65 | 13.62 |
| N02 | 2548.62 | 2.88 | 160.024 | 0.160 | 63.51 | 9.64 | 22.36 |
| N03 | 2548.37 | 3.11 | 135.007 | 0.135 | 64.31 | 9.14 | 42.04 |
| N04 | 2548.45 | 3.16 | 297.522 | 0.298 | 66.40 | 13.76 | 6.95 |
| N05 | 2548.46 | 3.13 | 230.249 | 0.230 | 73.61 | 11.50 | 8.92 |
| N06 | 2548.58 | 3.68 | 33.968 | 0.034 | 62.20 | 3.97 | 24.24 |
| N07 | 2550.52 | 1.40 | 61.524 | 0.062 | 95.00 | 6.09 | 5.20 |
| N08 | 2550.04 | 1.68 | 159.264 | 0.159 | 74.17 | 8.22 | 16.39 |
| N09 | 2550.66 | 1.17 | 154.231 | 0.154 | 60.08 | 10.17 | 28.92 |
| N10 | 2550.53 | 1.13 | 242.409 | 0.242 | 81.09 | 12.98 | 22.33 |
| N11 | 2550.15 | 1.56 | 107.297 | 0.107 | 94.79 | 8.11 | 28.95 |
| N12 | 2550.08 | 1.77 | 91.358 | 0.091 | 95.00 | 7.74 | 30.01 |
| N13 | 2550.39 | 1.06 | 130.938 | 0.131 | 91.95 | 8.96 | 28.23 |
| N14 | 2550.78 | 1.18 | 613.615 | 0.614 | 38.25 | 19.03 | 14.80 |
| N15 | 2550.55 | 1.24 | 268.469 | 0.268 | 79.51 | 13.33 | 21.98 |
| N16 | 2550.89 | 1.22 | 592.549 | 0.593 | 38.78 | 17.58 | 27.97 |
| N17 | 2550.58 | 1.26 | 600.461 | 0.600 | 84.67 | 17.75 | 26.48 |
| N18 | 2550.78 | 1.32 | 785.106 | 0.785 | 93.46 | 22.49 | 24.55 |
| N19 | 2550.73 | 1.42 | 102.452 | 0.102 | 95.00 | 8.04 | 7.74 |
| N20 | 2550.52 | 1.07 | 242.729 | 0.243 | 84.07 | 12.31 | 23.18 |
| N21 | 2550.32 | 1.57 | 160.807 | 0.161 | 74.79 | 10.13 | 30.04 |
| N22 | 2550.26 | 1.79 | 420.711 | 0.421 | 72.47 | 16.92 | 38.38 |
| N23 | 2550.31 | 1.36 | 444.963 | 0.445 | 88.55 | 17.26 | 20.24 |
| N24 | 2550.8 | 1.08 | 269.901 | 0.270 | 84.44 | 13.11 | 48.78 |
| N25 | 2550.48 | 1.16 | 216.588 | 0.217 | 95.00 | 11.15 | 19.73 |
| N26 | 2550.76 | 1.65 | 358.412 | 0.358 | 87.78 | 15.37 | 21.98 |
| N27 | 2550.81 | 1.13 | 360.815 | 0.361 | 66.39 | 12.36 | 22.15 |
| N28 | 2550.331 | 1.53 | 228.442 | 0.228 | 93.87 | 11.56 | 15.56 |
| N29 | 2550.53 | 1.44 | 59.652 | 0.060 | 95.00 | 6.22 | 6.12 |
| N30 | 2550.46 | 1.62 | 420.119 | 0.420 | 64.07 | 16.17 | 64.44 |
| N31 | 2550.69 | 1.57 | 111.507 | 0.112 | 94.77 | 7.86 | 7.74 |
| N32 | 2550.7 | 1.08 | 224.679 | 0.225 | 88.53 | 10.67 | 27.11 |
| N33 | 2550.51 | 1.31 | 383.231 | 0.383 | 95.00 | 15.49 | 26.40 |
| N34 | 2550.56 | 1.17 | 96.567 | 0.097 | 81.40 | 7.35 | 27.30 |
| N35 | 2550.6 | 1.67 | 119.227 | 0.119 | 83.98 | 7.90 | 7.74 |
| N36 | 2550.53 | 1.11 | 211.952 | 0.212 | 82.10 | 11.00 | 7.88 |
| N37 | 2550.49 | 1.51 | 313.360 | 0.313 | 67.90 | 13.17 | 29.10 |
| N38 | 2550.45 | 1.50 | 173.905 | 0.174 | 67.96 | 10.95 | 28.13 |
| N39 | 2550.32 | 1.12 | 251.830 | 0.252 | 84.30 | 12.57 | 21.17 |
| N40 | 2550.4 | 1.09 | 677.749 | 0.678 | 90.00 | 21.44 | 28.41 |
| N41 | 2549.61 | 2.48 | 1150.493 | 1.150 | 78.25 | 26.79 | 48.79 |
| N42 | 2550.77 | 1.20 | 521.814 | 0.522 | 60.45 | 18.00 | 12.15 |

| Node ID | Invert Elevation [m] | Max. Depth [m] | Flooding Area [m2] | Sub-catchment Area [ha] | Impervious Area [%] | Width [m] | Slope [%] |
|---|---|---|---|---|---|---|---|
| N43 | 2550.35 | 1.40 | 399.784 | 0.400 | 74.51 | 15.97 | 40.50 |
| N44 | 2550.34 | 1.15 | 242.847 | 0.243 | 84.90 | 12.38 | 27.14 |
| N45 | 2550.48 | 1.26 | 401.502 | 0.402 | 75.87 | 15.89 | 35.47 |
| N46 | 2550.61 | 1.05 | 116.357 | 0.116 | 83.05 | 8.21 | 27.77 |
| N47 | 2550.33 | 1.25 | 463.279 | 0.463 | 95.00 | 17.33 | 25.62 |
| N48 | 2550.75 | 1.29 | 383.874 | 0.384 | 95.00 | 15.52 | 22.90 |
| N49 | 2550.75 | 1.19 | 405.799 | 0.406 | 74.00 | 12.76 | 11.36 |
| N50 | 2550.72 | 1.65 | 265.258 | 0.265 | 59.34 | 12.43 | 7.77 |
| N51 | 2550.65 | 1.31 | 831.206 | 0.831 | 62.13 | 18.45 | 17.57 |
| N52 | 2550.6 | 1.33 | 174.195 | 0.174 | 74.12 | 10.08 | 22.77 |
| N53 | 2550.46 | 1.25 | 154.851 | 0.155 | 90.16 | 9.87 | 23.16 |
| N54 | 2549.8 | 1.38 | 367.278 | 0.367 | 73.25 | 14.04 | 21.67 |
| N55 | 2551.01 | 1.10 | 250.814 | 0.251 | 95.00 | 12.64 | 7.74 |
| N56 | 2550.12 | 1.37 | 175.403 | 0.175 | 78.85 | 7.91 | 20.21 |
| N57 | 2550.42 | 1.38 | 958.174 | 0.958 | 44.01 | 25.42 | 11.95 |
| N58 | 2549.68 | 1.52 | 325.573 | 0.326 | 52.86 | 13.62 | 9.64 |
| N59 | 2550.45 | 1.24 | 553.564 | 0.554 | 52.71 | 19.63 | 43.17 |
| N60 | 2550.55 | 1.18 | 313.549 | 0.314 | 85.16 | 13.22 | 19.73 |
| N61 | 2550.37 | 1.60 | 138.940 | 0.139 | 75.21 | 8.97 | 28.23 |
| N62 | 2549.99 | 1.78 | 302.950 | 0.303 | 88.93 | 14.07 | 38.80 |
| N63 | 2550.66 | 1.24 | 469.721 | 0.470 | 53.75 | 17.36 | 43.89 |
| N64 | 2550.43 | 1.14 | 319.957 | 0.320 | 93.22 | 13.73 | 24.61 |
| N65 | 2550.14 | 1.23 | 1208.309 | 1.208 | 83.33 | 27.08 | 24.44 |
| N66 | 2550.42 | 1.22 | 287.512 | 0.288 | 95.00 | 13.61 | 17.94 |
| N67 | 2550.58 | 1.14 | 238.522 | 0.239 | 95.00 | 11.15 | 18.35 |
| N68 | 2550.48 | 1.22 | 389.188 | 0.389 | 95.00 | 15.78 | 11.99 |
| N69 | 2550.44 | 1.45 | 182.890 | 0.183 | 81.46 | 10.55 | 28.23 |
| N70 | 2550.6 | 1.16 | 251.151 | 0.251 | 95.00 | 12.66 | 28.23 |
| N71 | 2549.05 | 1.67 | 350.446 | 0.350 | 76.78 | 14.11 | 26.33 |
| N72 | 2550.2 | 1.24 | 243.593 | 0.244 | 84.35 | 12.71 | 6.60 |
| N73 | 2550.49 | 1.24 | 537.171 | 0.537 | 43.07 | 18.04 | 13.89 |
| N74 | 2551 | 1.20 | 184.103 | 0.184 | 95.00 | 9.43 | 21.98 |
| N75 | 2551 | 1.14 | 291.253 | 0.291 | 95.00 | 14.06 | 21.97 |
| N76 | 2550.8 | 1.24 | 204.840 | 0.205 | 95.00 | 11.38 | 7.74 |
| N77 | 2550.46 | 1.06 | 279.342 | 0.279 | 85.73 | 11.28 | 15.98 |
| N78 | 2549.78 | 1.64 | 2101.489 | 2.101 | 70.29 | 36.60 | 33.14 |
| N79 | 2550.38 | 1.37 | 199.247 | 0.199 | 92.80 | 10.18 | 45.67 |
| N80 | 2549.84 | 1.40 | 1719.522 | 1.720 | 78.78 | 31.51 | 9.42 |
| N81 | 2550.06 | 1.72 | 416.335 | 0.416 | 95.00 | 16.33 | 33.41 |
| N82 | 2547.49 | 4.00 | 123.223 | 0.123 | 34.93 | 6.66 | 71.36 |
| N83 | 2549.1 | 2.80 | 463.043 | 0.463 | 20.00 | 16.03 | 73.21 |
| N84 | 2550.44 | 1.56 | 240.372 | 0.240 | 61.79 | 10.71 | 23.75 |

| **Node ID** | **Invert Elevation [m]** | **Max. Depth [m]** | **Flooding Area [m2]** | **Sub-catchment Area [ha]** | **Impervious Area [%]** | **Width [m]** | **Slope [%]** |
|---|---|---|---|---|---|---|---|
| N85 | 2550.27 | 1.42 | 212.049 | 0.212 | 79.96 | 11.80 | 22.30 |
| N86 | 2549.87 | 1.63 | 505.415 | 0.505 | 86.22 | 15.57 | 19.70 |
| N87 | 2550.01 | 1.80 | 55.934 | 0.056 | 62.53 | 5.21 | 22.33 |
| N88 | 2549.97 | 2.30 | 68.080 | 0.068 | 71.60 | 6.13 | 22.33 |
| N89 | 2549.87 | 2.02 | 132.243 | 0.132 | 80.26 | 7.74 | 22.62 |
| N90 | 2549.8 | 2.08 | 144.374 | 0.144 | 73.37 | 8.52 | 22.33 |
| N91 | 2549.36 | 2.19 | 64.761 | 0.065 | 80.40 | 5.97 | 22.33 |
| N92 | 2550.33 | 1.60 | 239.371 | 0.239 | 74.74 | 11.52 | 21.98 |
| N93 | 2550.19 | 1.41 | 321.830 | 0.322 | 38.02 | 12.99 | 9.94 |
| N94 | 2550.13 | 1.69 | 889.835 | 0.890 | 87.28 | 22.59 | 15.73 |
| N95 | 2550.33 | 1.68 | 402.952 | 0.403 | 95.00 | 16.64 | 18.85 |
| N96 | 2549.5 | 1.26 | 171.545 | 0.172 | 73.95 | 9.89 | 36.85 |
| N97 | 2549.73 | 1.86 | 141.528 | 0.142 | 77.20 | 7.81 | 11.66 |
| N98 | 2550.99 | 1.28 | 221.933 | 0.222 | 73.04 | 11.22 | 49.94 |
| N99 | 2550.57 | 1.47 | 149.915 | 0.150 | 95.00 | 9.49 | 28.38 |
| N100 | 2550.1 | 1.70 | 80.255 | 0.080 | 63.26 | 6.64 | 22.33 |
| N101 | 2550.75 | 1.45 | 333.194 | 0.333 | 75.48 | 12.91 | 118.37 |
| N102 | 2551.12 | 1.30 | 960.146 | 0.960 | 79.43 | 23.88 | 41.84 |
| N103 | 2550.02 | 1.69 | 258.240 | 0.258 | 93.91 | 12.96 | 18.59 |
| N104 | 2551.13 | 1.07 | 478.429 | 0.478 | 64.60 | 16.70 | 43.61 |
| N105 | 2549.11 | 2.03 | 195.975 | 0.196 | 73.81 | 9.92 | 30.92 |
| N106 | 2550.11 | 1.33 | 232.099 | 0.232 | 95.00 | 10.85 | 38.66 |
| N107 | 2549.54 | 1.90 | 231.765 | 0.232 | 95.00 | 12.14 | 30.66 |
| N108 | 2548.98 | 1.99 | 177.155 | 0.177 | 78.04 | 9.50 | 41.00 |
| N109 | 2550.58 | 1.48 | 181.478 | 0.181 | 94.04 | 9.39 | 7.73 |
| N110 | 2549.43 | 1.97 | 33.642 | 0.034 | 67.51 | 3.93 | 42.03 |
| N111 | 2550.46 | 1.34 | 125.364 | 0.125 | 95.00 | 7.82 | 5.20 |
| N112 | 2550.7 | 1.09 | 309.201 | 0.309 | 76.20 | 13.74 | 12.22 |
| N113 | 2550.96 | 0.90 | 397.359 | 0.397 | 90.54 | 16.78 | 5.70 |
| N114 | 2550.99 | 1.13 | 402.596 | 0.403 | 83.82 | 16.46 | 6.79 |
| N115 | 2549.65 | 1.60 | 1008.510 | 1.009 | 70.61 | 22.67 | 18.70 |
| N116 | 2548.47 | 3.21 | 450.084 | 0.450 | 74.09 | 15.54 | 19.98 |
| N117 | 2548.46 | 2.85 | 97.691 | 0.098 | 81.31 | 5.29 | 14.14 |
| N118 | 2548.97 | 1.75 | 12.424 | 0.012 | 70.29 | 2.33 | 29.45 |
| N119 | 2549.31 | 1.86 | 74.128 | 0.074 | 58.48 | 5.10 | 11.17 |
| N120 | 2549.78 | 2.23 | 140.620 | 0.141 | 89.79 | 6.62 | 8.62 |
| N121 | 2549.93 | 1.74 | 559.450 | 0.559 | 61.97 | 18.32 | 8.62 |
| N122 | 2549.93 | 1.86 | 191.462 | 0.191 | 90.00 | 8.64 | 10.63 |
| N123 | 2550 | 1.45 | 386.795 | 0.387 | 90.00 | 14.18 | 19.91 |
| N124 | 2550.15 | 1.38 | 331.779 | 0.332 | 90.00 | 12.76 | 29.03 |
| N125 | 2550.42 | 0.79 | 192.705 | 0.193 | 90.00 | 8.43 | 22.86 |
| N126 | 2550.45 | 0.77 | 547.325 | 0.547 | 78.05 | 16.97 | 25.26 |

| Node ID | Invert Elevation [m] | Max. Depth [m] | Flooding Area [m2] | Sub-catchment Area [ha] | Impervious Area [%] | Width [m] | Slope [%] |
|---|---|---|---|---|---|---|---|
| N127 | 2548.16 | 3.94 | 427.281 | 0.427 | 75.76 | 15.71 | 40.92 |
| N128 | 2549.89 | 1.78 | 690.497 | 0.690 | 62.18 | 19.54 | 82.21 |
| N129 | 2550.23 | 1.95 | 79.774 | 0.080 | 57.50 | 4.60 | 24.59 |
| N130 | 2549.46 | 1.27 | 156.732 | 0.157 | 73.31 | 9.39 | 55.61 |
| N131 | 2549.84 | 1.73 | 380.734 | 0.381 | 95.00 | 15.95 | 18.21 |
| N132 | 2550.31 | 1.58 | 427.164 | 0.427 | 84.37 | 16.49 | 34.48 |
| N133 | 2547.69 | 3.96 | 157.641 | 0.158 | 37.04 | 9.67 | 20.32 |
| N134 | 2549.18 | 1.55 | 272.943 | 0.273 | 76.90 | 13.44 | 44.68 |
| N135 | 2550.15 | 1.52 | 77.342 | 1.835 | 51.01 | 34.86 | 60.84 |
| N136 | 2550.4 | 1.40 | 107.747 | 0.077 | 89.35 | 6.94 | 28.23 |
| N137 | 2550.14 | 1.33 | 272.309 | 0.108 | 72.96 | 7.33 | 19.74 |
| N138 | 2550.5 | 1.42 | 212.800 | 0.272 | 86.83 | 12.82 | 27.14 |
| N139 | 2548.6 | 4.05 | 86.450 | 0.213 | 73.52 | 11.69 | 24.18 |
| N140 | 2549.99 | 1.56 | 557.915 | 0.086 | 60.03 | 7.31 | 22.33 |
| N141 | 2550.09 | 1.79 | 242.322 | 0.558 | 64.78 | 18.93 | 29.64 |
| N142 | 2548.67 | 3.45 | 117.202 | 0.242 | 77.88 | 12.49 | 21.98 |
| N143 | 2550.21 | 1.86 | 516.425 | 0.117 | 71.88 | 8.36 | 21.98 |
| N144 | 2550.55 | 1.44 | 372.857 | 0.516 | 80.23 | 17.77 | 27.10 |
| N145 | 2550 | 2.00 | 87.641 | 0.373 | 87.74 | 15.29 | 22.07 |
| N146 | 2550.24 | 1.76 | 306.504 | 0.088 | 95.00 | 5.88 | 21.98 |
| N147 | 2549.07 | 1.73 | 152.260 | 0.307 | 95.00 | 13.82 | 22.08 |
| N148 | 2550.05 | 1.65 | 75.048 | 0.152 | 92.41 | 9.62 | 36.00 |
| N149 | 2549 | 2.30 | 568.374 | 0.075 | 95.00 | 6.16 | 10.73 |
| N150 | 2550.35 | 1.74 | 454.125 | 0.568 | 58.04 | 18.65 | 12.53 |
| N151 | 2550.28 | 0.55 | 382.326 | 0.454 | 60.73 | 15.59 | 8.99 |
| N152 | 2550.38 | 1.49 | 692.415 | 0.382 | 95.00 | 15.47 | 20.70 |
| N153 | 2550.29 | 1.35 | 551.169 | 0.692 | 33.24 | 19.93 | 14.91 |
| N154 | 2549.02 | 2.80 | 385.196 | 0.551 | 67.02 | 18.58 | 16.76 |
| N155 | 2548.97 | 2.80 | 873.015 | 0.385 | 20.08 | 15.33 | 102.93 |
| N156 | 2548.78 | 1.74 | 538.060 | 0.873 | 24.83 | 22.65 | 109.34 |
| N157 | 2550.14 | 1.69 | 141.045 | 0.538 | 71.71 | 15.23 | 58.50 |
| N158 | 2549.71 | 1.75 | 109.561 | 0.141 | 71.50 | 9.07 | 19.89 |
| N159 | 2550.3 | 1.42 | 256.446 | 0.110 | 95.00 | 8.61 | 28.23 |
| N160 | 2549.65 | 2.05 | 258.189 | 0.256 | 50.00 | 11.31 | 16.87 |
| N161 | 2548.57 | 3.48 | 249.988 | 0.258 | 89.07 | 13.84 | 28.23 |
| N162 | 2549.61 | 2.07 | 101.871 | 0.250 | 65.65 | 13.16 | 60.25 |
| N163 | 2549.74 | 1.74 | 75.841 | 0.102 | 66.74 | 7.87 | 28.51 |
| N164 | 2550.08 | 1.74 | 379.742 | 0.076 | 62.43 | 6.04 | 23.10 |
| N165 | 2550.01 | 1.38 | 374.252 | 0.380 | 95.00 | 15.66 | 53.50 |
| N166 | 2549.65 | 1.96 | 549.597 | 0.374 | 78.37 | 15.31 | 6.60 |
| N167 | 2550.89 | 1.43 | 171.322 | 0.550 | 90.00 | 17.10 | 11.69 |
| N168 | 2548.99 | 2.80 | 572.826 | 0.171 | 91.47 | 9.39 | 21.98 |

| **Node ID** | **Invert Elevation [m]** | **Max. Depth [m]** | **Flooding Area [m2]** | **Sub-catchment Area [ha]** | **Impervious Area [%]** | **Width [m]** | **Slope [%]** |
|---|---|---|---|---|---|---|---|
| N169 | 2549.96 | 1.63 | 920.693 | 0.573 | 25.06 | 18.91 | 109.31 |
| N170 | 2549.81 | 2.44 | 174.735 | 0.921 | 75.28 | 24.02 | 27.41 |
| N171 | 2550.13 | 1.36 | 306.667 | 0.175 | 72.10 | 10.10 | 21.98 |
| N172 | 2549.93 | 1.43 | 410.036 | 0.307 | 90.00 | 13.96 | 11.16 |
| N173 | 2550.07 | 1.44 | 399.768 | 0.410 | 95.00 | 16.28 | 30.67 |
| N174 | 2549.67 | 1.67 | 379.218 | 0.400 | 95.00 | 16.31 | 35.20 |
| N175 | 2550.5 | 1.50 | 302.822 | 0.379 | 95.00 | 15.63 | 38.52 |
| N176 | 2550.51 | 1.27 | 385.083 | 0.303 | 80.31 | 12.99 | 11.84 |
| N177 | 2549.79 | 2.40 | 210.855 | 0.385 | 90.92 | 16.01 | 21.98 |
| N178 | 2548.42 | 2.62 | 711.111 | 0.211 | 84.11 | 11.32 | 21.98 |
| N179 | 2550.17 | 1.83 | 169.494 | 0.711 | 73.18 | 20.61 | 12.05 |
| N180 | 2550.19 | 1.55 | 264.874 | 0.169 | 95.00 | 8.75 | 21.75 |
| N181 | 2550.36 | 1.63 | 147.584 | 0.265 | 95.00 | 13.29 | 15.86 |
| N182 | 2550.32 | 1.47 | 181.356 | 0.148 | 95.00 | 9.24 | 5.20 |
| N183 | 2548.66 | 2.66 | 616.116 | 0.181 | 91.63 | 9.70 | 5.52 |
| N184 | 2550.13 | 1.41 | 397.107 | 0.616 | 75.75 | 17.40 | 15.67 |
| N185 | 2550.2 | 1.89 | 80.549 | 0.397 | 95.00 | 15.89 | 22.15 |
| N186 | 2550.74 | 1.18 | 382.118 | 0.081 | 59.65 | 6.33 | 22.33 |
| N187 | 2550.51 | 1.34 | 556.008 | 0.382 | 92.58 | 15.47 | 16.54 |
| N188 | 2550.17 | 1.56 | 120.807 | 0.556 | 46.23 | 18.41 | 14.66 |
| N189 | 2548.44 | 2.60 | 355.912 | 0.121 | 82.14 | 4.38 | 12.42 |
| N190 | 2550 | 1.85 | 207.040 | 0.356 | 79.81 | 14.11 | 11.75 |
| N191 | 2548.64 | 2.98 | 50.373 | 0.207 | 95.00 | 11.06 | 17.71 |
| N192 | 2549.9 | 1.50 | 677.797 | 0.050 | 74.58 | 4.77 | 17.12 |
| N193 | 2549.85 | 1.45 | 133.885 | 0.678 | 85.73 | 17.60 | 20.07 |
| N194 | 2550.43 | 1.41 | 320.750 | 0.134 | 90.58 | 8.94 | 15.20 |
| N195 | 2549.65 | 1.43 | 355.718 | 0.321 | 82.03 | 14.28 | 22.33 |
| N196 | 2549.97 | 1.81 | 77.096 | 0.356 | 75.77 | 14.34 | 38.54 |
| N197 | 2550.41 | 1.14 | 125.153 | 0.077 | 83.43 | 6.54 | 22.85 |
| N198 | 2550.07 | 2.05 | 34.601 | 0.125 | 92.37 | 9.01 | 22.73 |
| N199 | 2550.36 | 1.46 | 425.959 | 0.035 | 57.50 | 3.90 | 22.33 |
| N200 | 2550.23 | 1.70 | 574.094 | 0.426 | 95.00 | 16.67 | 28.05 |
| N201 | 2549.71 | 2.40 | 295.426 | 0.574 | 60.88 | 17.10 | 11.75 |
| N202 | 2549.44 | 1.91 | 407.496 | 0.295 | 76.07 | 13.75 | 22.00 |
| N203 | 2550.3 | 1.38 | 233.422 | 0.407 | 72.57 | 16.32 | 54.76 |
| N204 | 2550.09 | 1.23 | 339.100 | 0.233 | 28.03 | 12.11 | 7.77 |
| N205 | 2550.12 | 1.78 | 100.100 | 0.339 | 83.26 | 14.26 | 25.20 |
| N206 | 2548.47 | 3.45 | 521.721 | 0.100 | 95.00 | 7.53 | 30.05 |
| N207 | 2550.16 | 1.50 | 273.484 | 0.522 | 75.99 | 17.94 | 37.38 |
| N208 | 2550.53 | 1.46 | 83.136 | 0.273 | 52.26 | 11.88 | 32.35 |
| N209 | 2548.89 | 1.45 | 312.254 | 0.083 | 57.50 | 6.07 | 23.38 |
| N210 | 2549.61 | 1.64 | 383.442 | 0.312 | 72.76 | 12.55 | 28.38 |

| Node ID | Invert Elevation [m] | Max. Depth [m] | Flooding Area [m2] | Sub-catchment Area [ha] | Impervious Area [%] | Width [m] | Slope [%] |
|---|---|---|---|---|---|---|---|
| N211 | 2550.53 | 1.30 | 267.530 | 0.383 | 94.65 | 15.73 | 26.21 |
| N212 | 2550.34 | 1.34 | 462.147 | 0.268 | 95.00 | 12.69 | 18.34 |
| N213 | 2550.15 | 2.02 | 118.647 | 0.462 | 43.90 | 16.92 | 28.12 |
| N214 | 2550.09 | 2.13 | 164.566 | 0.119 | 79.12 | 8.46 | 22.33 |
| N215 | 2549.23 | 1.43 | 253.300 | 0.165 | 72.84 | 10.01 | 22.31 |
| N216 | 2548.7 | 3.30 | 115.755 | 0.253 | 84.92 | 11.84 | 21.20 |
| N217 | 2550.02 | 1.20 | 388.098 | 0.116 | 69.66 | 7.78 | 21.98 |
| N218 | 2550.65 | 1.30 | 825.890 | 0.388 | 95.00 | 15.83 | 30.59 |
| N219 | 2550.02 | 1.88 | 374.104 | 0.826 | 31.11 | 21.98 | 19.22 |
| N220 | 2550.18 | 1.94 | 166.587 | 0.374 | 95.00 | 15.36 | 22.03 |
| N221 | 2550.271 | 1.51 | 403.570 | 0.167 | 69.59 | 8.39 | 26.81 |
| N222 | 2550.18 | 1.55 | 329.189 | 0.404 | 63.30 | 14.51 | 12.07 |
| N223 | 2550.56 | 1.54 | 646.034 | 0.329 | 92.73 | 13.09 | 12.15 |
| N224 | 2550 | 1.65 | 407.836 | 0.646 | 72.11 | 19.25 | 21.19 |
| N225 | 2549.25 | 1.42 | 251.872 | 0.408 | 95.00 | 16.14 | 12.19 |
| N226 | 2549.69 | 1.61 | 32.961 | 0.252 | 80.73 | 12.16 | 30.24 |
| N227 | 2549.25 | 2.35 | 2253.393 | 0.033 | 95.00 | 4.15 | 13.34 |
| N228 | 2550.56 | 1.44 | 185.991 | 2.253 | 64.17 | 35.44 | 13.99 |
| N229 | 2550.24 | 1.40 | 147.370 | 0.186 | 70.48 | 10.93 | 5.60 |
| N230 | 2550.06 | 1.60 | 251.282 | 0.147 | 95.00 | 9.02 | 30.86 |
| N231 | 2549.25 | 1.46 | 343.743 | 0.251 | 82.06 | 12.65 | 22.22 |
| N232 | 2548.28 | 3.04 | 298.315 | 0.344 | 83.87 | 15.11 | 56.24 |
| N233 | 2550.43 | 1.29 | 279.836 | 0.298 | 61.41 | 14.19 | 51.19 |
| N234 | 2549.41 | 1.86 | 98.610 | 0.280 | 95.00 | 12.26 | 11.16 |
| N235 | 2550.17 | 1.26 | 89.986 | 0.099 | 61.50 | 6.62 | 13.09 |
| N236 | 2550.34 | 1.37 | 403.034 | 0.090 | 81.26 | 7.07 | 28.23 |
| N237 | 2550.24 | 1.25 | 396.920 | 0.403 | 95.00 | 16.31 | 6.62 |
| N238 | 2549.8 | 1.97 | 124.361 | 0.397 | 95.00 | 15.74 | 27.11 |
| N239 | 2549.99 | 1.81 | 183.244 | 0.124 | 66.62 | 8.68 | 28.65 |
| N240 | 2549.38 | 2.13 | 149.158 | 0.183 | 90.15 | 10.81 | 28.23 |
| N241 | 2548.24 | 3.32 | 443.846 | 0.149 | 84.98 | 9.75 | 25.44 |
| N242 | 2550.26 | 1.78 | 109.076 | 0.444 | 76.21 | 14.44 | 29.13 |
| N243 | 2549.77 | 1.76 | 382.911 | 0.109 | 71.72 | 7.43 | 22.54 |
| N244 | 2550.08 | 1.92 | 378.598 | 0.383 | 80.16 | 15.10 | 11.33 |
| N245 | 2549.99 | 1.46 | 374.245 | 0.379 | 77.12 | 15.51 | 21.98 |
| N246 | 2550.08 | 1.40 | 476.201 | 0.374 | 95.00 | 15.54 | 20.48 |
| N247 | 2550.06 | 1.39 | 419.077 | 0.476 | 95.00 | 17.59 | 11.92 |
| N248 | 2549.74 | 1.90 | 452.566 | 0.419 | 95.00 | 16.69 | 31.21 |
| N249 | 2549.47 | 1.90 | 475.746 | 0.453 | 95.00 | 17.17 | 16.42 |
| N250 | 2549.96 | 1.27 | 361.942 | 0.476 | 95.00 | 18.05 | 12.63 |
| N251 | 2549.81 | 1.57 | 347.755 | 0.362 | 95.00 | 13.97 | 16.24 |
| N252 | 2548.72 | 2.36 | 572.722 | 0.348 | 73.31 | 12.39 | 15.73 |

| Node ID | Invert Elevation [m] | Max. Depth [m] | Flooding Area [m2] | Sub-catchment Area [ha] | Impervious Area [%] | Width [m] | Slope [%] |
|---|---|---|---|---|---|---|---|
| N253 | 2549.51 | 1.74 | 468.333 | 0.573 | 71.49 | 18.48 | 13.70 |
| N254 | 2549.66 | 1.85 | 229.876 | 0.468 | 88.22 | 15.93 | 21.11 |
| N255 | 2548.61 | 3.60 | 141.695 | 0.230 | 88.80 | 12.29 | 13.68 |
| N256 | 2549.59 | 1.65 | 379.040 | 0.142 | 59.60 | 9.21 | 22.31 |
| N257 | 2547.62 | 3.90 | 368.467 | 0.379 | 95.00 | 15.67 | 22.16 |
| N258 | 2550.17 | 1.38 | 386.560 | 0.368 | 39.86 | 13.87 | 23.89 |
| N259 | 2548.39 | 3.38 | 123.313 | 0.387 | 95.00 | 16.10 | 7.85 |
| N260 | 2548.41 | 3.29 | 226.278 | 0.123 | 64.46 | 8.59 | 39.01 |
| N261 | 2550.27 | 1.35 | 181.336 | 0.226 | 64.75 | 10.86 | 19.57 |
| N262 | 2549.94 | 1.37 | 440.349 | 0.181 | 83.85 | 10.50 | 26.76 |
| N263 | 2550.06 | 1.18 | 154.416 | 0.440 | 95.00 | 17.49 | 39.84 |
| N264 | 2549.89 | 1.58 | 162.087 | 0.154 | 79.11 | 9.65 | 28.23 |
| N265 | 2549.81 | 1.84 | 140.409 | 0.162 | 95.00 | 9.61 | 28.23 |
| N266 | 2549.85 | 1.57 | 384.492 | 0.140 | 70.84 | 9.09 | 25.14 |
| N267 | 2550.29 | 1.37 | 418.430 | 0.384 | 84.55 | 15.52 | 25.14 |
| N268 | 2548.59 | 4.12 | 175.521 | 0.418 | 95.00 | 16.59 | 17.40 |
| N269 | 2549.1 | 3.10 | 482.603 | 0.176 | 62.20 | 9.95 | 22.33 |
| N270 | 2549.99 | 1.50 | 71.406 | 0.483 | 77.19 | 16.78 | 26.45 |
| N271 | 2550.13 | 1.82 | 434.004 | 0.071 | 90.00 | 6.18 | 12.29 |
| N272 | 2550.08 | 1.50 | 955.513 | 0.434 | 95.00 | 17.01 | 21.98 |
| N273 | 2549.66 | 1.48 | 309.132 | 0.956 | 38.78 | 25.46 | 12.17 |
| N274 | 2550.56 | 1.45 | 173.841 | 0.309 | 82.33 | 13.56 | 13.57 |
| N275 | 2548.54 | 3.18 | 512.508 | 0.174 | 95.00 | 9.86 | 13.48 |
| N276 | 2549.53 | 1.94 | 372.711 | 0.513 | 67.57 | 16.90 | 27.52 |
| N277 | 2549.66 | 1.92 | 396.055 | 0.373 | 95.00 | 15.28 | 12.19 |
| N278 | 2549.43 | 1.94 | 288.527 | 0.396 | 95.00 | 15.92 | 13.44 |
| N279 | 2549.45 | 2.53 | 72.553 | 0.289 | 80.10 | 12.54 | 17.12 |
| N280 | 2547.72 | 4.00 | 746.596 | 0.073 | 60.59 | 5.63 | 17.12 |
| N281 | 2549.05 | 2.80 | 341.598 | 0.747 | 41.53 | 21.68 | 79.35 |
| N282 | 2548.04 | 2.66 | 411.860 | 0.342 | 20.00 | 13.37 | 94.76 |
| N283 | 2548.58 | 2.05 | 288.249 | 0.412 | 78.92 | 14.46 | 82.98 |
| N284 | 2548.45 | 3.49 | 137.432 | 0.288 | 76.78 | 13.17 | 82.90 |
| N285 | 2550.03 | 1.50 | 407.072 | 0.137 | 68.61 | 7.90 | 6.60 |
| N286 | 2549.49 | 1.83 | 246.163 | 0.407 | 95.00 | 16.11 | 11.25 |
| N287 | 2549.86 | 1.76 | 92.772 | 0.246 | 87.83 | 12.63 | 12.53 |
| N288 | 2550.43 | 1.30 | 318.737 | 0.093 | 79.98 | 7.61 | 28.24 |
| N289 | 2550.03 | 1.60 | 382.072 | 0.319 | 70.93 | 14.01 | 29.54 |
| N290 | 2549.84 | 1.99 | 200.426 | 0.382 | 94.63 | 15.46 | 20.39 |
| N291 | 2550.14 | 1.28 | 268.877 | 0.200 | 71.76 | 11.47 | 22.18 |
| N292 | 2549.75 | 1.95 | 125.761 | 0.269 | 95.00 | 12.73 | 21.37 |
| N293 | 2550.37 | 1.88 | 108.204 | 0.126 | 86.75 | 8.56 | 22.33 |
| N294 | 2550.29 | 1.76 | 251.741 | 0.108 | 84.55 | 7.02 | 7.74 |

| Node ID | Invert Elevation [m] | Max. Depth [m] | Flooding Area [m2] | Sub-catchment Area [ha] | Impervious Area [%] | Width [m] | Slope [%] |
|---|---|---|---|---|---|---|---|
| N295 | 2550.03 | 1.35 | 452.069 | 0.252 | 91.26 | 12.38 | 6.20 |
| N296 | 2549.39 | 2.75 | 73.179 | 0.452 | 51.93 | 17.43 | 52.63 |
| N297 | 2548.25 | 3.44 | 494.465 | 0.073 | 57.65 | 6.69 | 22.33 |
| N298 | 2549.78 | 1.70 | 357.175 | 0.494 | 67.79 | 18.10 | 21.12 |
| N299 | 2549.96 | 1.58 | 395.221 | 0.357 | 67.16 | 15.51 | 10.75 |
| N300 | 2549.45 | 1.74 | 471.617 | 0.395 | 44.71 | 15.15 | 9.35 |
| N301 | 2550.02 | 1.55 | 378.453 | 0.472 | 94.20 | 17.78 | 53.33 |
| N302 | 2549.92 | 1.50 | 148.663 | 0.378 | 72.48 | 15.58 | 20.79 |
| N303 | 2550 | 1.61 | 88.411 | 0.149 | 95.00 | 9.42 | 23.75 |
| N304 | 2548.05 | 3.98 | 607.617 | 0.088 | 89.30 | 7.37 | 28.74 |
| N305 | 2549.88 | 1.70 | 382.946 | 0.608 | 81.01 | 16.95 | 47.09 |
| N306 | 2550.42 | 1.33 | 394.541 | 0.383 | 93.52 | 15.71 | 11.54 |
| N307 | 2550.56 | 1.38 | 384.811 | 0.395 | 95.00 | 15.71 | 16.21 |
| N308 | 2549.82 | 1.58 | 379.274 | 0.385 | 95.00 | 16.03 | 22.33 |
| N309 | 2549.96 | 1.86 | 372.502 | 0.379 | 95.00 | 15.40 | 27.98 |
| N310 | 2549.42 | 1.77 | 232.692 | 0.373 | 95.00 | 15.80 | 22.24 |
| N311 | 2550.21 | 1.42 | 268.535 | 0.233 | 89.96 | 12.03 | 11.17 |
| N312 | 2550.55 | 1.59 | 223.667 | 0.269 | 95.00 | 12.73 | 35.59 |
| N313 | 2550.3 | 1.27 | 270.052 | 0.224 | 95.00 | 11.46 | 9.85 |
| N314 | 2550.19 | 1.44 | 369.476 | 0.270 | 95.00 | 12.74 | 12.34 |
| N315 | 2549.56 | 1.80 | 328.315 | 0.369 | 95.00 | 15.12 | 17.92 |
| N316 | 2549.93 | 1.41 | 422.317 | 0.328 | 72.16 | 14.29 | 52.63 |
| N317 | 2550.52 | 1.17 | 394.623 | 0.422 | 95.00 | 16.69 | 21.20 |
| N318 | 2550.23 | 1.37 | 805.683 | 0.395 | 92.03 | 15.71 | 40.16 |
| N319 | 2549.21 | 2.07 | 136.994 | 0.806 | 66.06 | 22.41 | 89.40 |
| N320 | 2549.32 | 1.82 | 100.677 | 0.137 | 95.00 | 9.24 | 34.72 |
| N321 | 2549.2 | 2.14 | 176.291 | 0.101 | 95.00 | 8.00 | 30.66 |
| N322 | 2549.19 | 2.21 | 183.506 | 0.176 | 92.45 | 10.36 | 31.37 |
| N323 | 2550.36 | 1.96 | 125.237 | 0.184 | 91.34 | 10.14 | 30.66 |
| N324 | 2550.28 | 2.07 | 197.328 | 0.125 | 95.00 | 8.19 | 18.47 |
| N325 | 2550.63 | 1.17 | 339.861 | 0.197 | 71.23 | 11.27 | 18.47 |
| N326 | 2550.12 | 1.43 | 603.667 | 0.340 | 85.48 | 13.10 | 65.06 |
| N327 | 2549.98 | 1.56 | 150.234 | 0.604 | 76.38 | 19.39 | 109.76 |
| N328 | 2550.5 | 1.10 | 860.644 | 0.150 | 95.00 | 8.39 | 41.96 |
| N329 | 2550.63 | 1.31 | 219.660 | 0.861 | 62.79 | 22.57 | 117.97 |
| N330 | 2549.96 | 1.55 | 144.489 | 0.220 | 0.00 | 9.53 | 82.03 |
| N331 | 2550.4 | 1.48 | 166.080 | 0.144 | 93.41 | 9.24 | 18.47 |
| N332 | 2550.07 | 1.82 | 102.927 | 0.166 | 77.48 | 9.67 | 54.61 |
| N333 | 2549.75 | 1.69 | 107.176 | 0.103 | 72.97 | 8.16 | 29.01 |
| N334 | 2549.36 | 1.75 | 80.347 | 0.107 | 95.00 | 7.89 | 24.08 |
| N335 | 2549.47 | 1.50 | 183.147 | 0.080 | 95.00 | 6.10 | 30.03 |
| N336 | 2549.84 | 1.85 | 124.073 | 0.183 | 95.00 | 10.14 | 30.66 |

| Node ID | Invert Elevation [m] | Max. Depth [m] | Flooding Area [m2] | Sub-catchment Area [ha] | Impervious Area [%] | Width [m] | Slope [%] |
|---|---|---|---|---|---|---|---|
| N337 | 2549.91 | 1.87 | 246.000 | 0.124 | 94.15 | 8.30 | 18.52 |
| N338 | 2550.1 | 1.68 | 212.950 | 0.246 | 95.00 | 12.27 | 24.22 |
| N339 | 2550.44 | 1.60 | 99.203 | 0.213 | 95.00 | 11.77 | 18.47 |
| N340 | 2550.71 | 1.28 | 170.797 | 0.191 | 95.00 | 10.63 | 18.47 |
| N341 | 2550.81 | 1.34 | 260.183 | 0.099 | 95.00 | 7.76 | 18.69 |
| N342 | 2550.48 | 1.59 | 116.046 | 0.171 | 95.00 | 10.52 | 21.95 |
| N343 | 2550.8 | 1.39 | 158.140 | 0.260 | 70.57 | 12.67 | 146.29 |
| N344 | 2550.46 | 1.42 | 144.188 | 0.116 | 95.00 | 7.62 | 22.15 |
| N345 | 2549.96 | 1.63 | 269.720 | 0.158 | 95.00 | 10.26 | 38.27 |
| N346 | 2550.19 | 1.49 | 267.854 | 0.144 | 95.00 | 9.83 | 18.63 |
| N347 | 2549.96 | 1.50 | 257.516 | 0.270 | 95.00 | 12.76 | 30.66 |
| N348 | 2549.28 | 2.01 | 199.159 | 0.268 | 69.25 | 12.54 | 30.66 |
| N349 | 2549.12 | 2.37 | 338.345 | 0.258 | 78.47 | 12.12 | 31.56 |
| N350 | 2549.37 | 1.98 | 128.750 | 0.199 | 95.00 | 10.36 | 32.98 |
| N351 | 2550.25 | 1.20 | 175.624 | 0.338 | 82.44 | 14.71 | 39.11 |
| N352 | 2549.64 | 1.88 | 180.587 | 0.129 | 95.00 | 7.48 | 34.24 |
| N353 | 2549.42 | 2.02 | 170.542 | 0.176 | 81.66 | 9.32 | 31.36 |
| N354 | 2550.66 | 1.36 | 200.109 | 0.181 | 94.99 | 8.33 | 32.97 |
| N355 | 2550.42 | 1.25 | 172.771 | 0.171 | 82.18 | 10.05 | 30.50 |
| N356 | 2549.79 | 1.82 | 194.241 | 0.200 | 79.90 | 10.93 | 21.52 |
| N357 | 2550.51 | 1.39 | 379.341 | 0.173 | 95.00 | 9.84 | 18.54 |
| N358 | 2550.47 | 1.49 | 270.360 | 0.194 | 82.29 | 8.99 | 26.26 |
| N359 | 2550.9 | 1.44 | 41.427 | 0.379 | 72.13 | 15.83 | 21.54 |
| N360 | 2551.08 | 1.34 | 181.039 | 0.270 | 92.58 | 13.47 | 20.92 |
| N361 | 2550.75 | 1.49 | 65.451 | 0.041 | 85.68 | 4.57 | 38.18 |
| N362 | 2551.25 | 1.24 | 339.401 | 0.181 | 77.30 | 10.49 | 29.56 |
| N363 | 2550.59 | 1.43 | 168.039 | 0.065 | 95.00 | 6.06 | 31.84 |
| N364 | 2551.04 | 1.24 | 121.213 | 0.339 | 67.62 | 14.58 | 25.36 |
| N365 | 2551.05 | 1.18 | 307.332 | 0.168 | 95.00 | 10.58 | 22.46 |
| N366 | 2550.32 | 1.34 | 1012.394 | 0.121 | 87.85 | 5.96 | 49.94 |
| N367 | 2549.16 | 2.11 | 173.207 | 0.307 | 76.34 | 12.67 | 84.22 |
| N368 | 2549.12 | 2.13 | 153.668 | 1.012 | 63.73 | 24.89 | 79.26 |
| N369 | 2549.06 | 2.02 | 158.299 | 0.173 | 87.28 | 9.58 | 30.66 |
| N370 | 2549.8 | 1.50 | 240.938 | 0.154 | 78.62 | 8.67 | 30.66 |
| N371 | 2549.05 | 1.89 | 183.644 | 0.158 | 89.82 | 8.66 | 31.34 |
| N372 | 2548.92 | 2.15 | 923.271 | 0.241 | 87.81 | 12.78 | 34.63 |
| N373 | 2550.1 | 1.54 | 217.700 | 0.184 | 71.82 | 10.73 | 41.87 |
| N374 | 2549.04 | 2.88 | 206.518 | 0.923 | 61.85 | 23.83 | 93.28 |
| N375 | 2550.35 | 1.26 | 172.069 | 0.218 | 62.64 | 11.99 | 42.03 |
| N376 | 2548.4 | 2.51 | 212.113 | 0.207 | 86.10 | 11.73 | 42.04 |
| N377 | 2549.98 | 1.81 | 109.398 | 0.172 | 95.00 | 9.67 | 10.13 |
| N378 | 2548.93 | 2.24 | 217.653 | 0.212 | 70.33 | 10.56 | 11.29 |

| Node ID | Invert Elevation [m] | Max. Depth [m] | Flooding Area [m2] | Sub-catchment Area [ha] | Impervious Area [%] | Width [m] | Slope [%] |
|---|---|---|---|---|---|---|---|
| N379 | 2550.21 | 1.29 | 228.645 | 0.109 | 94.63 | 8.12 | 28.11 |
| N380 | 2550.16 | 1.38 | 50.127 | 0.218 | 86.68 | 10.19 | 13.16 |
| N381 | 2550.33 | 1.66 | 115.424 | 0.229 | 78.44 | 12.03 | 19.74 |
| N382 | 2549.6 | 2.54 | 603.119 | 0.050 | 95.00 | 4.94 | 28.23 |
| N383 | 2548.16 | 3.46 | 372.686 | 0.115 | 69.40 | 7.94 | 22.33 |
| N384 | 2550.27 | 1.74 | 191.156 | 0.603 | 77.85 | 19.79 | 29.80 |
| N385 | 2547.41 | 3.00 | 1834.982 | 0.373 | 62.80 | 15.42 | 83.52 |

**Table A3.4.2.** Data for conduits in the ES-N network

| Link ID | Node 1 | Node 2 | Length [m] | Manning Roughness | Diameter [m] |
|---|---|---|---|---|---|
| P01 | N62 | N195 | 100.23 | 0.015 | 0.4 |
| P02 | N228 | N150 | 39.27 | 0.015 | 0.7 |
| P03 | N223 | N175 | 64.93 | 0.015 | 0.6 |
| P04 | N175 | N244 | 97.58 | 0.015 | 0.6 |
| P05 | N293 | N179 | 80.01 | 0.015 | 0.5 |
| P06 | N154 | N168 | 74.35 | 0.015 | 0.6 |
| P07 | N168 | N155 | 64.06 | 0.015 | 0.6 |
| P08 | N233 | N258 | 105.33 | 0.015 | 0.4 |
| P09 | N251 | N278 | 80.10 | 0.015 | 0.5 |
| P10 | N67 | N314 | 51.67 | 0.015 | 0.3 |
| P11 | N66 | N248 | 113.77 | 0.015 | 0.4 |
| P12 | N319 | N321 | 42.40 | 0.015 | 0.8 |
| P13 | N34 | N197 | 14.50 | 0.015 | 0.3 |
| P14 | N332 | N320 | 26.53 | 0.015 | 0.35 |
| P15 | N370 | N369 | 61.94 | 0.015 | 0.4 |
| P16 | N347 | N348 | 45.21 | 0.015 | 0.35 |
| P17 | N349 | N374 | 45.78 | 0.015 | 0.8 |
| P18 | N374 | N259 | 50.57 | 0.015 | 0.8 |
| P19 | N348 | N349 | 60.05 | 0.015 | 0.8 |
| P20 | N352 | N04 | 106.66 | 0.015 | 0.6 |
| P21 | N219 | N309 | 60.42 | 0.015 | 0.7 |
| P22 | N176 | N309 | 63.12 | 0.015 | 0.4 |
| P23 | N71 | N209 | 99.89 | 0.015 | 0.5 |
| P24 | N356 | N352 | 14.79 | 0.015 | 0.6 |
| P25 | N131 | N254 | 63.25 | 0.015 | 0.4 |
| P26 | N359 | N361 | 15.41 | 0.015 | 0.3 |
| P27 | N209 | N156 | 93.31 | 0.015 | 0.5 |
| P28 | N56 | N193 | 110.23 | 0.015 | 0.5 |
| P29 | N115 | N253 | 79.79 | 0.015 | 0.7 |
| P30 | N253 | N279 | 23.89 | 0.015 | 0.7 |

| Link ID | Node 1 | Node 2 | Length [m] | Manning Roughness | Diameter [m] |
|---|---|---|---|---|---|
| P31 | N33 | N236 | 60.12 | 0.015 | 0.4 |
| P32 | N225 | N147 | 91.29 | 0.015 | 0.6 |
| P33 | N375 | N203 | 17.21 | 0.015 | 0.3 |
| P34 | N229 | N205 | 21.09 | 0.015 | 0.3 |
| P35 | N152 | N151 | 61.48 | 0.015 | 0.6 |
| P36 | N37 | N132 | 52.99 | 0.015 | 0.3 |
| P37 | N289 | N305 | 60.09 | 0.015 | 0.6 |
| P38 | N308 | N256 | 58.88 | 0.015 | 0.5 |
| P39 | N274 | N95 | 77.67 | 0.015 | 0.5 |
| P40 | N102 | N364 | 12.04 | 0.015 | 0.3 |
| P41 | N101 | N384 | 81.87 | 0.015 | 0.4 |
| P42 | N339 | N384 | 32.61 | 0.015 | 0.5 |
| P43 | N325 | N326 | 79.08 | 0.015 | 0.3 |
| P44 | N295 | N315 | 50.08 | 0.015 | 0.4 |
| P45 | N203 | N93 | 23.09 | 0.015 | 0.4 |
| P46 | N365 | N364 | 15.50 | 0.015 | 0.3 |
| P47 | N324 | N103 | 46.69 | 0.015 | 0.35 |
| P48 | N103 | N333 | 73.14 | 0.015 | 0.45 |
| P49 | N357 | N08 | 50.62 | 0.015 | 0.3 |
| P50 | N81 | N08 | 8.07 | 0.015 | 0.5 |
| P51 | N19 | N109 | 36.44 | 0.015 | 0.5 |
| P52 | N194 | N62 | 93.42 | 0.015 | 0.5 |
| P53 | N238 | N162 | 27.98 | 0.015 | 0.4 |
| P54 | N89 | N90 | 17.13 | 0.015 | 0.3 |
| P55 | N341 | N101 | 24.83 | 0.015 | 0.3 |
| P56 | N153 | N140 | 64.87 | 0.015 | 0.45 |
| P57 | N140 | N308 | 61.44 | 0.015 | 0.5 |
| P58 | N93 | N299 | 54.81 | 0.015 | 0.4 |
| P59 | N279 | N191 | 6.18 | 0.015 | 0.7 |
| P60 | N380 | N135 | 15.59 | 0.015 | 0.35 |
| P61 | N72 | N165 | 79.85 | 0.015 | 0.4 |
| P62 | N331 | N332 | 35.02 | 0.015 | 0.3 |
| P63 | N230 | N142 | 95.39 | 0.015 | 0.45 |
| P64 | N235 | N380 | 12.01 | 0.015 | 0.3 |
| P65 | N181 | N148 | 92.10 | 0.015 | 0.6 |
| P66 | N329 | N331 | 39.83 | 0.015 | 0.3 |
| P67 | N73 | N153 | 65.03 | 0.015 | 0.4 |
| P68 | N192 | N226 | 94.43 | 0.015 | 0.6 |
| P69 | N174 | N147 | 63.26 | 0.015 | 0.7 |
| P70 | N47 | N291 | 59.29 | 0.015 | 0.4 |
| P71 | N78 | N227 | 151.51 | 0.015 | 0.8 |
| P72 | N288 | N159 | 65.40 | 0.015 | 0.4 |
| P73 | N63 | N33 | 61.60 | 0.015 | 0.4 |
| P74 | N373 | N370 | 33.71 | 0.015 | 0.3 |

| Link ID | Node 1 | Node 2 | Length [m] | Manning Roughness | Diameter [m] |
|---|---|---|---|---|---|
| P75 | N309 | N292 | 63.05 | 0.015 | 0.7 |
| P76 | N130 | N231 | 65.16 | 0.015 | 0.45 |
| P77 | N77 | N250 | 25.12 | 0.015 | 0.3 |
| P78 | N250 | N249 | 109.57 | 0.015 | 0.4 |
| P79 | N351 | N352 | 25.62 | 0.015 | 0.3 |
| P80 | N355 | N356 | 75.40 | 0.015 | 0.3 |
| P81 | N08 | N356 | 31.88 | 0.015 | 0.5 |
| P82 | N354 | N355 | 35.78 | 0.015 | 0.3 |
| P83 | N138 | N213 | 58.00 | 0.015 | 0.3 |
| P84 | N198 | N290 | 59.71 | 0.015 | 0.3 |
| P85 | N207 | N266 | 61.40 | 0.015 | 0.4 |
| P86 | N12 | N287 | 13.76 | 0.015 | 0.3 |
| P87 | N287 | N238 | 27.88 | 0.015 | 0.4 |
| P88 | N22 | N238 | 48.06 | 0.015 | 0.3 |
| P89 | N150 | N200 | 84.46 | 0.015 | 0.8 |
| P90 | N323 | N324 | 22.71 | 0.015 | 0.3 |
| P91 | N367 | N368 | 16.35 | 0.015 | 0.9 |
| P92 | N106 | N350 | 23.04 | 0.015 | 0.3 |
| P93 | N163 | N06 | 9.75 | 0.015 | 0.7 |
| P94 | N300 | N156 | 62.99 | 0.015 | 0.6 |
| P95 | N262 | N300 | 68.08 | 0.015 | 0.4 |
| P96 | N315 | N300 | 61.16 | 0.015 | 0.6 |
| P97 | N164 | N62 | 63.16 | 0.015 | 0.7 |
| P98 | N79 | N229 | 69.87 | 0.015 | 0.3 |
| P99 | N30 | N205 | 94.16 | 0.015 | 0.3 |
| P100 | N179 | N145 | 87.98 | 0.015 | 0.6 |
| P101 | N145 | N177 | 74.77 | 0.015 | 0.6 |
| P102 | N210 | N71 | 63.39 | 0.015 | 0.5 |
| P103 | N18 | N223 | 45.12 | 0.015 | 0.4 |
| P104 | N193 | N251 | 94.85 | 0.015 | 0.5 |
| P105 | N278 | N225 | 100.09 | 0.015 | 0.6 |
| P106 | N60 | N379 | 80.07 | 0.015 | 0.35 |
| P107 | N100 | N87 | 15.08 | 0.015 | 0.3 |
| P108 | N87 | N88 | 13.93 | 0.015 | 0.3 |
| P109 | N88 | N89 | 38.27 | 0.015 | 0.3 |
| P110 | N212 | N289 | 61.58 | 0.015 | 0.4 |
| P111 | N38 | N242 | 61.86 | 0.015 | 0.3 |
| P112 | N52 | N208 | 34.99 | 0.015 | 0.3 |
| P113 | N90 | N91 | 38.31 | 0.015 | 0.3 |
| P114 | N91 | N268 | 22.29 | 0.015 | 0.6 |
| P115 | N15 | N85 | 64.85 | 0.015 | 0.3 |
| P116 | N360 | N359 | 8.96 | 0.015 | 0.3 |
| P117 | N362 | N359 | 40.17 | 0.015 | 0.3 |
| P118 | N364 | N343 | 76.52 | 0.015 | 0.4 |

| Link ID | Node 1 | Node 2 | Length [m] | Manning Roughness | Diameter [m] |
|---|---|---|---|---|---|
| P119 | N104 | N343 | 27.12 | 0.015 | 0.3 |
| P120 | N98 | N340 | 32.82 | 0.015 | 0.3 |
| P121 | N69 | N263 | 73.67 | 0.015 | 0.3 |
| P122 | N281 | N154 | 32.44 | 0.015 | 0.6 |
| P123 | N65 | N169 | 68.03 | 0.015 | 0.45 |
| P124 | N377 | N196 | 22.44 | 0.015 | 0.35 |
| P125 | N317 | N151 | 64.99 | 0.015 | 0.35 |
| P126 | N290 | N255 | 41.46 | 0.015 | 0.45 |
| P127 | N61 | N264 | 92.55 | 0.015 | 0.3 |
| P128 | N07 | N182 | 80.44 | 0.015 | 0.5 |
| P129 | N84 | N92 | 18.55 | 0.015 | 0.3 |
| P130 | N92 | N145 | 72.50 | 0.015 | 0.3 |
| P131 | N202 | N283 | 112.00 | 0.015 | 0.6 |
| P132 | N49 | N221 | 74.43 | 0.015 | 0.35 |
| P133 | N160 | N240 | 73.14 | 0.015 | 0.6 |
| P134 | N313 | N247 | 65.15 | 0.015 | 0.4 |
| P135 | N134 | N280 | 36.30 | 0.015 | 1 |
| P136 | N318 | N319 | 44.93 | 0.015 | 0.3 |
| P137 | N333 | N334 | 16.67 | 0.015 | 0.6 |
| P138 | N335 | N334 | 15.62 | 0.015 | 0.6 |
| P139 | N336 | N333 | 30.59 | 0.015 | 0.5 |
| P140 | N330 | N336 | 19.21 | 0.015 | 0.45 |
| P141 | N321 | N322 | 19.05 | 0.015 | 0.8 |
| P142 | N128 | N321 | 58.52 | 0.015 | 0.4 |
| P143 | N310 | N215 | 100.06 | 0.015 | 0.5 |
| P144 | N144 | N219 | 61.09 | 0.015 | 0.4 |
| P145 | N222 | N224 | 60.05 | 0.015 | 0.5 |
| P146 | N28 | N221 | 12.32 | 0.015 | 0.5 |
| P147 | N379 | N204 | 30.96 | 0.015 | 0.35 |
| P148 | N76 | N312 | 73.83 | 0.015 | 0.4 |
| P149 | N197 | N242 | 29.90 | 0.015 | 0.3 |
| P150 | N316 | N210 | 65.29 | 0.015 | 0.4 |
| P151 | N215 | N71 | 91.36 | 0.015 | 0.5 |
| P152 | N266 | N210 | 60.09 | 0.015 | 0.5 |
| P153 | N113 | N07 | 19.46 | 0.015 | 0.2 |
| P154 | N132 | N229 | 29.06 | 0.015 | 0.3 |
| P155 | N13 | N265 | 96.63 | 0.015 | 0.3 |
| P156 | N196 | N265 | 27.89 | 0.015 | 0.4 |
| P157 | N345 | N322 | 59.59 | 0.015 | 0.4 |
| P158 | N96 | N130 | 27.08 | 0.015 | 0.4 |
| P159 | N83 | N281 | 123.42 | 0.015 | 0.6 |
| P160 | N17 | N143 | 42.18 | 0.015 | 0.4 |
| P161 | N172 | N256 | 64.72 | 0.015 | 0.5 |
| P162 | N54 | N273 | 77.91 | 0.015 | 0.5 |

| Link ID | Node 1 | Node 2 | Length [m] | Manning Roughness | Diameter [m] |
|---|---|---|---|---|---|
| P163 | N273 | N310 | 80.17 | 0.015 | 0.5 |
| P164 | N256 | N310 | 64.58 | 0.015 | 0.5 |
| P165 | N271 | N219 | 61.62 | 0.015 | 0.6 |
| P166 | N137 | N262 | 65.56 | 0.015 | 0.4 |
| P167 | N291 | N316 | 65.43 | 0.015 | 0.4 |
| P168 | N184 | N266 | 65.21 | 0.015 | 0.4 |
| P169 | N242 | N185 | 17.14 | 0.015 | 0.35 |
| P170 | N185 | N214 | 26.83 | 0.015 | 0.35 |
| P171 | N296 | N139 | 17.92 | 0.015 | 0.7 |
| P172 | N46 | N197 | 42.02 | 0.015 | 0.3 |
| P173 | N36 | N258 | 34.04 | 0.015 | 0.3 |
| P174 | N258 | N298 | 64.64 | 0.015 | 0.4 |
| P175 | N298 | N315 | 53.74 | 0.015 | 0.6 |
| P176 | N213 | N198 | 4.77 | 0.015 | 0.3 |
| P177 | N267 | N305 | 64.74 | 0.015 | 0.4 |
| P178 | N211 | N267 | 64.84 | 0.015 | 0.4 |
| P179 | N224 | N276 | 61.65 | 0.015 | 0.6 |
| P180 | N214 | N290 | 34.86 | 0.015 | 0.35 |
| P181 | N53 | N214 | 88.19 | 0.015 | 0.3 |
| P182 | N254 | N96 | 37.63 | 0.015 | 0.4 |
| P183 | N57 | N272 | 117.94 | 0.015 | 0.5 |
| P184 | N246 | N245 | 64.62 | 0.015 | 0.5 |
| P185 | N43 | N302 | 80.79 | 0.015 | 0.3 |
| P186 | N21 | N235 | 80.59 | 0.015 | 0.3 |
| P187 | N135 | N239 | 39.37 | 0.015 | 0.35 |
| P188 | N143 | N220 | 79.77 | 0.015 | 0.6 |
| P189 | N294 | N180 | 8.24 | 0.015 | 0.4 |
| P190 | N180 | N190 | 58.70 | 0.015 | 0.6 |
| P191 | N301 | N131 | 60.00 | 0.015 | 0.4 |
| P192 | N85 | N292 | 23.31 | 0.015 | 0.3 |
| P193 | N186 | N306 | 65.02 | 0.015 | 0.35 |
| P194 | N234 | N05 | 7.42 | 0.015 | 0.7 |
| P195 | N111 | N182 | 10.75 | 0.015 | 0.2 |
| P196 | N09 | N261 | 54.03 | 0.015 | 0.3 |
| P197 | N305 | N286 | 63.14 | 0.015 | 0.7 |
| P198 | N286 | N234 | 21.41 | 0.015 | 0.7 |
| P199 | N157 | N263 | 30.85 | 0.015 | 0.3 |
| P200 | N263 | N264 | 27.22 | 0.015 | 0.3 |
| P201 | N204 | N302 | 44.85 | 0.015 | 0.4 |
| P202 | N302 | N158 | 37.87 | 0.015 | 0.4 |
| P203 | N20 | N313 | 25.33 | 0.015 | 0.3 |
| P204 | N261 | N235 | 29.60 | 0.015 | 0.3 |
| P205 | N322 | N367 | 38.97 | 0.015 | 0.9 |
| P206 | N346 | N345 | 32.94 | 0.015 | 0.3 |

| Link ID | Node 1 | Node 2 | Length [m] | Manning Roughness | Diameter [m] |
|---|---|---|---|---|---|
| P207 | N244 | N145 | 16.56 | 0.015 | 0.6 |
| P208 | N173 | N172 | 65.79 | 0.015 | 0.5 |
| P209 | N311 | N173 | 60.04 | 0.015 | 0.5 |
| P210 | N220 | N177 | 80.11 | 0.015 | 0.6 |
| P211 | N11 | N303 | 21.86 | 0.015 | 0.3 |
| P212 | N48 | N317 | 64.92 | 0.015 | 0.35 |
| P213 | N80 | N115 | 41.99 | 0.015 | 0.5 |
| P214 | N167 | N26 | 36.12 | 0.015 | 0.4 |
| P215 | N74 | N167 | 50.22 | 0.015 | 0.4 |
| P216 | N217 | N308 | 64.67 | 0.015 | 0.4 |
| P217 | N170 | N142 | 19.19 | 0.015 | 0.5 |
| P218 | N247 | N174 | 64.67 | 0.015 | 0.4 |
| P219 | N27 | N144 | 60.26 | 0.015 | 0.3 |
| P220 | N199 | N164 | 64.82 | 0.015 | 0.45 |
| P221 | N307 | N199 | 65.18 | 0.015 | 0.4 |
| P222 | N14 | N187 | 64.32 | 0.015 | 0.4 |
| P223 | N187 | N212 | 65.50 | 0.015 | 0.4 |
| P224 | N42 | N175 | 88.31 | 0.015 | 0.6 |
| P225 | N200 | N188 | 11.23 | 0.015 | 0.8 |
| P226 | N51 | N228 | 63.78 | 0.015 | 0.6 |
| P227 | N50 | N228 | 41.37 | 0.015 | 0.7 |
| P228 | N64 | N141 | 104.64 | 0.015 | 0.4 |
| P229 | N45 | N140 | 118.04 | 0.015 | 0.4 |
| P230 | N201 | N216 | 37.95 | 0.015 | 0.6 |
| P231 | N110 | N03 | 11.10 | 0.015 | 0.7 |
| P232 | N32 | N233 | 25.02 | 0.015 | 0.3 |
| P233 | N109 | N274 | 25.32 | 0.015 | 0.5 |
| P234 | N239 | N377 | 31.04 | 0.015 | 0.35 |
| P235 | N195 | N286 | 90.33 | 0.015 | 0.5 |
| P236 | N165 | N254 | 75.14 | 0.015 | 0.4 |
| P237 | N312 | N146 | 61.50 | 0.015 | 0.4 |
| P238 | N146 | N271 | 60.10 | 0.015 | 0.5 |
| P239 | N155 | N82 | 21.27 | 0.015 | 0.6 |
| P240 | N112 | N190 | 8.47 | 0.015 | 0.25 |
| P241 | N58 | N202 | 105.02 | 0.015 | 0.5 |
| P242 | N314 | N277 | 47.46 | 0.015 | 0.35 |
| P243 | N25 | N311 | 25.25 | 0.015 | 0.3 |
| P244 | N136 | N157 | 70.75 | 0.015 | 0.3 |
| P245 | N226 | N378 | 14.02 | 0.015 | 0.7 |
| P246 | N119 | N376 | 7.94 | 0.015 | 0.7 |
| P247 | N35 | N293 | 48.95 | 0.015 | 0.4 |
| P248 | N190 | N248 | 60.79 | 0.015 | 0.6 |
| P249 | N248 | N277 | 60.70 | 0.015 | 0.6 |
| P250 | N350 | N348 | 15.61 | 0.015 | 0.8 |

| Link ID | Node 1 | Node 2 | Length [m] | Manning Roughness | Diameter [m] |
|---|---|---|---|---|---|
| P251 | N107 | N353 | 6.46 | 0.015 | 0.6 |
| P252 | N208 | N136 | 4.62 | 0.015 | 0.3 |
| P253 | N29 | N07 | 4.30 | 0.015 | 0.5 |
| P254 | N326 | N327 | 19.69 | 0.015 | 0.35 |
| P255 | N328 | N327 | 77.50 | 0.015 | 0.3 |
| P256 | N327 | N330 | 25.93 | 0.015 | 0.45 |
| P257 | N276 | N249 | 59.79 | 0.015 | 0.6 |
| P258 | N277 | N276 | 34.53 | 0.015 | 0.6 |
| P259 | N24 | N211 | 25.13 | 0.015 | 0.3 |
| P260 | N114 | N312 | 8.93 | 0.015 | 0.3 |
| P261 | N55 | N76 | 7.58 | 0.015 | 0.2 |
| P262 | N75 | N271 | 97.01 | 0.015 | 0.3 |
| P263 | N26 | N176 | 62.09 | 0.015 | 0.4 |
| P264 | N264 | N158 | 29.38 | 0.015 | 0.4 |
| P265 | N381 | N100 | 34.91 | 0.015 | 0.3 |
| P266 | N243 | N166 | 61.92 | 0.015 | 0.4 |
| P267 | N292 | N296 | 21.99 | 0.015 | 0.7 |
| P268 | N31 | N181 | 89.72 | 0.015 | 0.6 |
| P269 | N156 | N283 | 63.07 | 0.015 | 0.7 |
| P270 | N120 | N243 | 17.72 | 0.015 | 0.4 |
| P271 | N177 | N216 | 22.79 | 0.015 | 0.7 |
| P272 | N249 | N278 | 63.43 | 0.015 | 0.6 |
| P273 | N236 | N285 | 65.10 | 0.015 | 0.4 |
| P274 | N237 | N301 | 65.49 | 0.015 | 0.35 |
| P275 | N218 | N152 | 64.84 | 0.015 | 0.45 |
| P276 | N334 | N320 | 22.54 | 0.015 | 0.6 |
| P277 | N320 | N319 | 34.43 | 0.015 | 0.7 |
| P278 | N363 | N344 | 60.06 | 0.015 | 0.45 |
| P279 | N99 | N342 | 28.03 | 0.015 | 0.45 |
| P280 | N343 | N99 | 39.88 | 0.015 | 0.4 |
| P281 | N361 | N363 | 25.24 | 0.015 | 0.4 |
| P282 | N231 | N134 | 70.07 | 0.015 | 0.45 |
| P283 | N169 | N201 | 70.74 | 0.015 | 0.6 |
| P284 | N141 | N201 | 28.79 | 0.015 | 0.4 |
| P285 | N353 | N350 | 67.23 | 0.015 | 0.8 |
| P286 | N245 | N174 | 59.98 | 0.015 | 0.6 |
| P287 | N272 | N245 | 61.74 | 0.015 | 0.6 |
| P288 | N70 | N138 | 62.97 | 0.015 | 0.3 |
| P289 | N86 | N97 | 14.02 | 0.015 | 0.8 |
| P290 | N188 | N94 | 10.77 | 0.015 | 0.8 |
| P291 | N94 | N86 | 154.65 | 0.015 | 0.8 |
| P292 | N118 | N189 | 10.75 | 0.015 | 0.7 |
| P293 | N166 | N01 | 49.75 | 0.015 | 0.4 |
| P294 | N121 | N120 | 26.96 | 0.015 | 0.25 |

| Link ID | Node 1 | Node 2 | Length [m] | Manning Roughness | Diameter [m] |
|---|---|---|---|---|---|
| P295 | N23 | N230 | 90.10 | 0.015 | 0.4 |
| P296 | N151 | N164 | 60.16 | 0.015 | 0.6 |
| P297 | N39 | N291 | 25.99 | 0.015 | 0.3 |
| P298 | N221 | N222 | 22.79 | 0.015 | 0.5 |
| P299 | N108 | N372 | 34.64 | 0.015 | 0.9 |
| P300 | N372 | N383 | 73.26 | 0.015 | 0.9 |
| P301 | N366 | N367 | 66.12 | 0.015 | 0.3 |
| P302 | N368 | N105 | 27.81 | 0.015 | 0.9 |
| P303 | N105 | N369 | 26.16 | 0.015 | 0.9 |
| P304 | N337 | N335 | 79.51 | 0.015 | 0.6 |
| P305 | N338 | N337 | 43.56 | 0.015 | 0.6 |
| P306 | N358 | N338 | 59.81 | 0.015 | 0.4 |
| P307 | N265 | N162 | 31.93 | 0.015 | 0.4 |
| P308 | N162 | N161 | 31.89 | 0.015 | 0.6 |
| P309 | N306 | N289 | 64.78 | 0.015 | 0.4 |
| P310 | N148 | N192 | 98.89 | 0.015 | 0.6 |
| P311 | N44 | N137 | 24.89 | 0.015 | 0.3 |
| P312 | N285 | N131 | 65.57 | 0.015 | 0.4 |
| P313 | N299 | N298 | 49.66 | 0.015 | 0.4 |
| P314 | N59 | N295 | 85.95 | 0.015 | 0.35 |
| P315 | N283 | N282 | 17.81 | 0.015 | 0.9 |
| P316 | N240 | N91 | 15.77 | 0.015 | 0.6 |
| P317 | N158 | N160 | 41.67 | 0.015 | 0.6 |
| P318 | N344 | N339 | 13.02 | 0.015 | 0.45 |
| P319 | N342 | N339 | 20.31 | 0.015 | 0.45 |
| P320 | N340 | N339 | 61.94 | 0.015 | 0.4 |
| P321 | N95 | N146 | 39.41 | 0.015 | 0.5 |
| P322 | N303 | N287 | 27.03 | 0.015 | 0.4 |
| P323 | N369 | N371 | 27.46 | 0.015 | 0.9 |
| P324 | N371 | N108 | 21.46 | 0.015 | 0.9 |
| P325 | N159 | N301 | 61.56 | 0.015 | 0.4 |
| P326 | N205 | N303 | 30.31 | 0.015 | 0.35 |
| P327 | N122 | N121 | 4.88 | 0.015 | 0.25 |
| P328 | N123 | N122 | 38.51 | 0.015 | 0.25 |
| P329 | N68 | N313 | 60.06 | 0.015 | 0.4 |
| P330 | N124 | N123 | 41.91 | 0.015 | 0.25 |
| P331 | N126 | N125 | 4.03 | 0.015 | 0.2 |
| P332 | N129 | N269 | 13.61 | 0.015 | 0.3 |
| P333 | N97 | N149 | 28.59 | 0.015 | 0.9 |
| P334 | N40 | N171 | 63.03 | 0.015 | 0.3 |
| P335 | N171 | N270 | 32.08 | 0.015 | 0.3 |
| P336 | N270 | N243 | 3.85 | 0.015 | 0.3 |
| P337 | N16 | N218 | 65.08 | 0.015 | 0.4 |
| P338 | N182 | N180 | 54.71 | 0.015 | 0.5 |

| Link ID | Node 1 | Node 2 | Length [m] | Manning Roughness | Diameter [m] |
|---|---|---|---|---|---|
| P339 | N10 | N194 | 61.84 | 0.015 | 0.3 |
| P340 | N125 | N124 | 28.17 | 0.015 | 0.2 |
| P341 | N147 | N118 | 8.56 | 0.015 | 0.7 |
| P342 | N161 | N206 | 99.71 | 0.015 | 1.3 |
| P343 | N216 | N142 | 22.62 | 0.015 | 1.2 |
| P344 | N259 | N03 | 17.42 | 0.015 | 1.4 |
| P345 | N149 | N378 | 19.38 | 0.015 | 1.2 |
| P346 | N304 | N282 | 116.49 | 0.015 | 1.4 |
| P347 | N116 | N117 | 11.51 | 0.015 | 1.4 |
| P348 | N206 | N05 | 69.09 | 0.015 | 1.4 |
| P349 | N133 | N257 | 106.37 | 0.015 | 1.4 |
| P350 | N183 | N191 | 80.02 | 0.015 | 1.3 |
| P351 | N255 | N139 | 80.25 | 0.015 | 1.3 |
| P352 | N232 | N383 | 64.37 | 0.015 | 1.4 |
| P353 | N02 | N275 | 55.67 | 0.015 | 1.3 |
| P354 | N139 | N268 | 95.48 | 0.015 | 1.3 |
| P355 | N383 | N280 | 79.71 | 0.015 | 1.4 |
| P356 | N178 | N376 | 82.29 | 0.015 | 1.4 |
| P357 | N191 | N02 | 12.96 | 0.015 | 1.3 |
| P358 | N227 | N149 | 102.71 | 0.015 | 1.2 |
| P359 | N01 | N297 | 70.92 | 0.015 | 1.4 |
| P360 | N275 | N116 | 79.79 | 0.015 | 1.3 |
| P361 | N252 | N183 | 92.44 | 0.015 | 1.3 |
| P362 | N260 | N259 | 46.60 | 0.015 | 1.4 |
| P363 | N282 | N82 | 19.77 | 0.015 | 1.4 |
| P364 | N03 | N232 | 72.96 | 0.015 | 1.4 |
| P365 | N378 | N252 | 37.35 | 0.015 | 1.1 |
| P366 | N376 | N01 | 28.89 | 0.015 | 1.4 |
| P367 | N268 | N06 | 81.05 | 0.015 | 1.3 |
| P368 | N05 | N284 | 30.95 | 0.015 | 1.4 |
| P369 | N41 | N382 | 70.31 | 0.015 | 0.9 |
| P370 | N142 | N255 | 79.96 | 0.015 | 1.3 |
| P371 | N117 | N189 | 13.40 | 0.015 | 1.4 |
| P372 | N297 | N241 | 100.05 | 0.015 | 1.4 |
| P373 | N284 | N04 | 8.84 | 0.015 | 1.4 |
| P374 | N189 | N178 | 103.66 | 0.015 | 1.4 |
| P375 | N04 | N260 | 90.32 | 0.015 | 1.4 |
| P376 | N382 | N269 | 76.43 | 0.015 | 0.9 |
| P377 | N269 | N216 | 90.05 | 0.015 | 1.2 |
| P378 | N06 | N161 | 16.81 | 0.015 | 1.3 |
| P379 | N280 | N133 | 38.17 | 0.015 | 1.4 |
| P380 | N257 | N82 | 178.19 | 0.015 | 1.4 |
| P381 | N127 | N304 | 84.51 | 0.015 | 1.4 |
| P382 | N241 | N127 | 50.36 | 0.015 | 1.4 |

| Link ID | Node 1 | Node 2 | Length [m] | Manning Roughness | Diameter [m] |
|---|---|---|---|---|---|
| P383 | N384 | N338 | 65.07 | 0.015 | 0.6 |
| P384 | N385 | V87702 | 50.00 | 0.015 | 1.4 |
| P385 | N82 | N385 | 160.53 | 0.015 | 1.4 |

**Table A3.4.3.** Land uses in the study area of ES-N network

| Land Uses | Percentage |
|---|---|
| Restaurant | 8.17% |
| Road | 23.28% |
| General trading | 24.42% |
| Dwelling | 32.31% |
| Sports | 1.25% |
| Green Zones | 3.08% |
| Health | 1.24% |
| Office | 4.55% |
| Education | 1.12% |
| Churches | 0.58% |